

3. SUMMARY OF WESTERN NORTH PACIFIC AND NORTH INDIAN OCEAN TROPICAL CYCLONES

3.1 WESTERN NORTH PACIFIC OCEAN TROPICAL CYCLONES

The year of 1996 was busy for the Joint Typhoon Warning Center (JTWC), with a near record number of significant tropical cyclones (TCs) occurring in the western North Pacific (WNP) (Table 3-1); 43 versus 44 which was the record set in 1964 (Table 3-2).

This number was almost 40% higher than the climatological average of 31 significant TCs in the WNP for the 37-year period 1959-1995. The year of 1996 included six super typhoons, 15 lesser typhoons, 12 tropical storms and 10 tropical depressions. The calendar-year total of 33 TCs of at least tropical-storm intensity was 5 above the long-term average (Figure 3-1). The calendar-year total of 21 typhoons

Table 3-1 WESTERN NORTH PACIFIC SIGNIFICANT TROPICAL CYCLONES FOR 1996

TROPICAL CYCLONE	PERIOD OF WARNING	NUMBER OF WARNINGS ISSUED	ESTIMATED MAXIMUM SURFACE WINDS		ESTIMATED MSLP (MB)
			KT	(M/SEC)	
01W TD	29 FEB - 01 MAR	7	30	(15)	1000
02W TS ANN	02 APR - 09 APR	27	40	(21)	994
03W TD	25 APR - 26 APR	4	25	(13)	1002
04W TY BART	09 MAY - 18 MAY	39	125	(64)	916
05W TS CAM	18 MAY - 24 MAY	22	60	(31)	980
06W TY DAN	05 JUL - 12 JUL	30	75	(39)	967
07W STY EVE	13 JUL - 20 JUL	27	140	(72)	898
08W TY FRANKIE	21 JUL - 24 JUL	14	90	(46)	954
09W TY GLORIA	22 JUL - 27 JUL	22	90	(46)	954
10W STY HERB	23 JUL - 01 AUG	38	140	(72)	898
11W TS IAN	28 JUL - 31 JUL	10	40	(21)	994
12W TY JOY	29 JUL - 05 AUG	28	75	(39)	967
13W TY KIRK	03 AUG - 16 AUG	51	95	(49)	949
14W TS LISA	05 AUG - 07 AUG	8	40	(21)	994
15W TD	12 AUG - 16 AUG	9	30	(15)	1000
16W TS MARTY	13 AUG - 14 AUG	3	50	(26)	987
17W TD	14 AUG	2	30	(15)	1000
18W TY NIKI	18 AUG - 23 AUG	21	95	(49)	949
19W TY ORSON	21 AUG - 03 SEP	51	115	(69)	927
20W TY PIPER	23 AUG - 26 AUG	14	65	(33)	976
21W TD	26 AUG - 27 AUG	4	25	(13)	1002
22W TS RICK	28 AUG - 31 AUG	10	35	(18)	997
23W STY SALLY	05 SEP - 09 SEP	19	140	(72)	898
24W TS	09 SEP - 14 SEP	16	45	(23)	991
25W TY TOM	11 SEP - 20 SEP	35	75	(39)	957
26W STY VIOLET	11 SEP - 23 SEP	44	130	(67)	910
27W TY WILLIE	17 SEP - 23 SEP	22	65	(33)	976
28W STY YATES	22 SEP - 01 OCT	37	130	(67)	910
29W TY ZANE	24 SEP - 03 OCT	39	110	(57)	933
30W TS ABEL	11 OCT - 17 OCT	21	50	(26)	987
31W TD	13 OCT - 17 OCT	13	25	(13)	1002
32W TY BETH	13 OCT - 21 OCT	33	90	(46)	954
33W TY CARLO	21 OCT - 26 OCT	24	105	(54)	938
34W TD	29 OCT - 30 OCT	4	30	(15)	1000
35W TS	02 NOV - 03 NOV	6	40	(21)	994
36W STY DALE	04 NOV - 13 NOV	39	140	(72)	898
37W TS ERNIE	04 NOV - 17 NOV	48	50	(26)	987
38W TS	06 NOV - 08 NOV	5	50	(26)	992
39W TD	08 NOV - 09 NOV	3	30	(15)	1000
40W TD	25-27 NOV/29-01 DEC	15	25	(13)	1002
41W TD	14 DEC - 20 DEC	13	30	(15)	1000
42W TY FERN	21 DEC - 30 DEC	35	80	(41)	963
43W TS GREG	24 DEC - 27 DEC	10	45	(23)	991

was 3 above the long term average. Six of the typhoons became super typhoons, two over the climatological average (Figure 3-2).

Thirty-one of the 43 significant TCs in the WNP during 1996 originated in the low-latitude monsoon trough or near-equatorial trough. Eleven — Dan (06W), Eve (07W), Joy (12W), Tropical Depression (TD) 15W, TD 17W, Piper (20W), TD 21W, Rick (22W), TD 23W, Carlo (33W), and Tropical Storm

38W — formed at relatively high latitude in association with cold-core cyclonic vortices (cells) in the tropical upper-tropospheric trough (TUTT). There were no significant TCs in the WNP during 1996 which originated east of the international date line. Historically, about one TC per year numbered/named by the Central Pacific Hurricane Center or the National Hurricane Center moves into the WNP.

Table 3-2 DISTRIBUTION OF WESTERN NORTH PACIFIC TROPICAL CYCLONES FOR 1959 - 1996

YEAR	JAN	FEB	MAR	APR	MAY	JUN	JUL	AUG	SEP	OCT	NOV	DEC	TOTALS
1959	0	1	1	1	0	1	3	8	9	3	2	2	31
	000	010	010	100	000	001	111	512	423	210	200	200	17 7 7
1960	1	0	1	1	1	3	3	9	5	4	1	1	30
	001	000	001	100	010	210	210	810	041	400	100	100	19 8 3
1961	1	1	1	1	4	6	5	7	6	7	2	1	42
	010	010	100	010	211	114	320	313	510	322	101	100	20 11 11
1962	0	1	0	1	3	0	8	8	7	5	4	2	39
	000	010	000	100	201	000	512	701	313	311	301	020	24 6 9
1963	0	0	1	1	0	4	5	4	4	6	0	3	28
	000	000	001	100	000	310	311	301	220	510	000	210	19 6 3
1964	0	0	0	0	3	2	8	8	8	7	6	2	44
	000	000	000	000	201	200	611	350	521	331	420	101	26 13 5
1965	2	2	1	1	2	4	6	7	9	3	2	1	40
	110	020	010	100	101	310	411	322	531	201	110	010	21 13 6
1966	0	0	0	1	2	1	4	9	10	4	5	2	38
	000	000	000	100	200	100	310	531	532	112	122	101	20 10 8
1967	1	0	2	1	1	1	8	10	8	4	4	1	41
	010	000	110	100	010	100	332	343	530	211	400	010	20 15 6
1968	0	1	0	1	0	4	3	8	4	6	4	0	31
	000	001	000	100	000	202	120	341	400	510	400	000	20 7 4
1969	1	0	1	1	0	0	3	3	6	5	2	1	23
	100	000	010	100	000	000	210	210	204	410	110	010	13 6 4
1970	0	1	0	0	0	2	3	7	4	6	4	0	27
	000	100	000	000	000	110	021	421	220	321	130	000	12 12 3
1971	1	0	1	2	5	2	8	5	7	4	2	0	37
	010	000	010	200	230	200	620	311	511	310	110	000	24 11 2
1972	1	0	1	0	0	4	5	5	6	5	2	3	32
	100	000	001	000	000	220	410	320	411	410	200	210	22 8 2
1973	0	0	0	0	0	0	7	6	3	4	3	0	23
	000	000	000	000	000	000	430	231	201	400	030	000	12 9 2
1974	1	0	1	1	1	4	5	7	5	4	4	2	35
	010	000	010	010	100	121	230	232	320	400	220	020	15 17 3
1975	1	0	0	1	0	0	1	6	5	6	3	2	25
	100	000	000	001	000	000	010	411	410	321	210	002	14 6 5
1976	1	1	0	2	2	2	4	4	5	0	2	2	25
	100	010	000	110	200	200	220	130	410	000	110	020	14 11 0
1977	0	0	1	0	1	1	4	2	5	4	2	1	21
	000	000	010	000	001	010	301	020	230	310	200	100	11 8 2
1978	1	0	0	1	0	3	4	8	4	7	4	0	32
	010	000	000	100	000	030	310	341	310	412	121	000	15 13 4
1979	1	0	1	1	2	0	5	4	6	3	2	3	28
	100	000	100	100	011	000	221	202	330	210	110	111	14 9 5
1980	0	0	1	1	4	1	5	3	7	4	1	1	28
	000	000	001	010	220	010	311	201	511	220	100	010	15 9 4
1981	0	0	1	1	1	2	5	8	4	2	3	2	29
	000	000	100	010	010	200	230	251	400	110	210	200	16 12 1
1982	0	0	3	0	1	3	4	5	6	4	1	1	28
	000	000	210	000	100	120	220	500	321	301	100	100	19 7 2
1983	0	0	0	0	0	1	3	6	3	5	2	2	25
	000	000	000	000	000	010	300	231	111	320	320	020	12 11 2

TABLE CONTINUED ON TOP OF NEXT PAGE

Table 3-2 (CONTINUED FROM PREVIOUS PAGE)

YEAR	JAN	FEB	MAR	APR	MAY	JUN	JUL	AUG	SEP	OCT	NOV	DEC	TOTALS
1984	0	0	0	0	0	2	5	7	4	8	3	1	30
	000	000	000	000	000	020	410	232	130	521	300	100	16 11 3
1985	2	0	0	0	1	3	1	7	5	5	1	2	27
	020	000	000	000	100	201	100	520	320	410	010	110	17 9 1
1986	0	1	0	1	2	2	2	5	2	5	4	3	27
	000	100	000	100	110	110	200	410	200	320	220	210	19 8 0
1987	1	0	0	1	0	2	4	4	7	2	3	1	25
	100	000	000	010	000	110	400	310	511	200	120	100	18 6 1
1988	1	0	0	0	1	3	2	5	8	4	2	1	27
	100	000	000	000	100	111	110	230	260	400	200	010	14 12 1
1989	1	0	0	1	2	2	6	8	4	6	3	2	35
	010	000	000	100	200	110	231	332	220	600	300	101	21 10 4
1990	1	0	0	1	2	4	4	5	5	5	4	1	31
	100	000	000	010	110	211	220	500	410	230	310	100	21 9 1
1991	0	0	2	1	1	1	4	8	6	3	6	0	32
	000	000	110	100	100	100	400	332	420	300	330	000	20 10 2
1992	1	1	0	0	0	3	4	8	5	6	5	0	33
	100	010	000	000	000	210	220	440	410	510	311	000	21 11 1
1993	0	0	2	2	1	2	5	8	5	6	4	3	38
	000	000	011	002	010	101	320	611	410	321	112	300	21 9 8
1994	1	0	1	0	2	2	9	9	8	7	0	2	41
	001	000	100	000	101	020	342	630	440	511	000	110	21 15 5
1995	1	0	0	0	1	2	3	7	7	8	2	3	34
	001	000	000	000	010	020	210	421	412	512	020	012	15 11 8
1996	0	1	0	2	2	0	7	10	7	5	6	3	43
	000	001	000	011	110	000	610	433	610	212	132	111	21 12 10
(1959-1995)													
MEAN	0.6	0.3	0.6	0.8	1.3	2.2	4.7	6.6	5.9	4.9	3.0	1.5	31.4
CASES	22	10	23	27	46	79	168	238	212	177	107	54	1163

The criteria used in Table 3-2 are as follows:

- 1) If a tropical cyclone was first warned on during the last two days of a particular month and continued into the next month for longer than two days, then that system was attributed to the second month.
- 2) If a tropical cyclone was warned on prior to the last two days of a month, it was attributed to the first month, regardless of how long the system lasted.
- 3) If a tropical cyclone began on the last day of the month and ended on the first day of the next month, that system was attributed to the first month. However, if a tropical cyclone began on the last day of the month and continued into the next month for only two days, then it was attributed to the second month.

Table 3-2 Legend

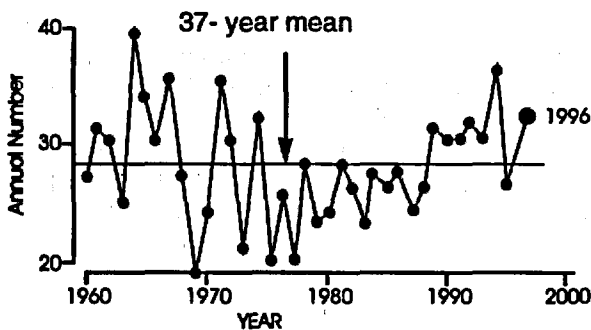
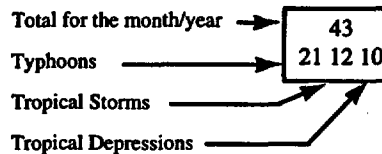


Figure 3-1 Tropical cyclones of tropical storm or greater intensity in the western North Pacific (1960-1996)

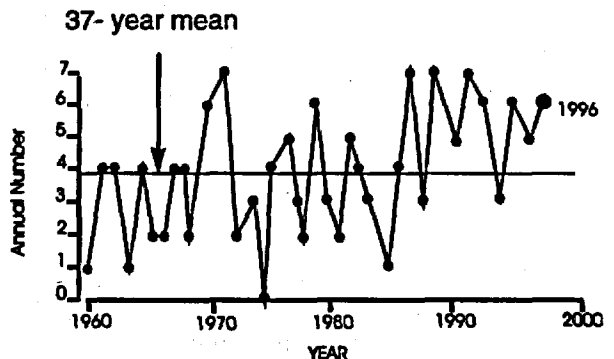


Figure 3-2 Number of western North Pacific super typhoons (1960-1996).

The 1996 year was a continuation of a weak cold phase of the El Niño/Southern Oscillation (ENSO) which began during 1995. Large-scale atmospheric and oceanic circulation anomalies during 1996 were generally as expected for a weak cold phase of ENSO (sometimes referred to as La Niña, or El Viejo). For example, the sea-surface temperature (SST) along the equator in the central and eastern Pacific was colder than normal (Figure 3-3), the Southern Oscillation Index (SOI) was positive (Figure 3-3), and low-level easterly wind anomalies persisted in the low latitudes of the WNP (Figure 3-4).

The annual mean genesis location of TCs which form in the WNP is related to the status of ENSO: it tends to be east of normal during El Niño years and west of normal during El Viejo years. Consistent with the TC distribution associated with a cold phase of ENSO, the annual mean genesis location during 1996 was west of normal (Figure 3-5a), as it was during 1995. It was also slightly north of normal. A breakdown of the genesis locations of all 1996 WNP TCs (Figure 3-5b) shows that most formed between 120°E and 160°E. Only five formed east of 160°E, while ten — six more than normal — formed in the

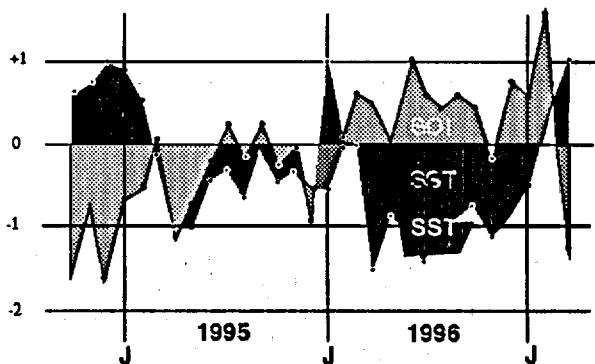


Figure 3-3 Anomalies from the monthly mean for eastern equatorial Pacific Ocean sea-surface temperature (hatched) in degrees Celsius and the Southern Oscillation Index (SOI) (shaded) for the period 1995 through 1996. (Adapted from Climate Prediction Center, 1996).

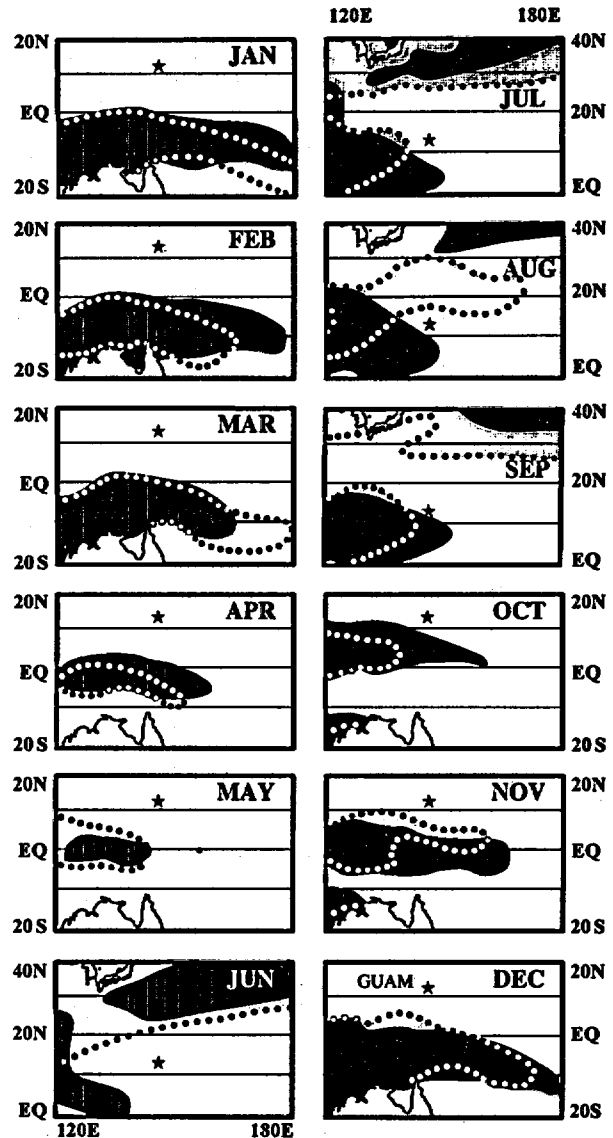


Figure 3-4 Comparison between climatological (black) and analyzed (shaded) mean monthly winds with a westerly component for the WNP in 1996. For June, July and August the area of coverage is shifted northward to include the subtropics. For reference, the star indicates the location of Guam. The outline of Australia appears in the lower left of each panel except for June, July and August and September where the Korean peninsula and Japan appear in the upper left. The climatology is adapted from Sadler, et al. (1987). The 1996 monthly mean winds were adapted from the Climate Prediction Center (1996).

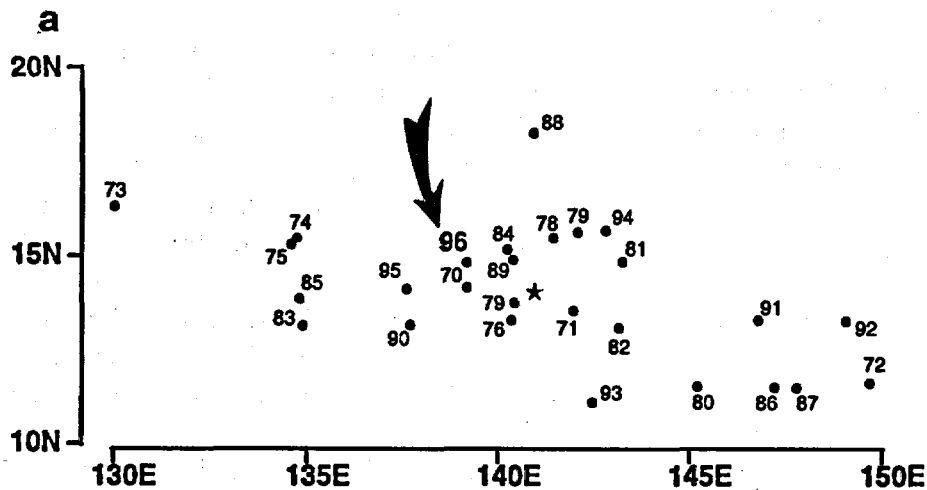


Figure 3-5a Mean annual genesis locations for the period 1970-1996. 1996's location is indicated by the arrow. The star lies at the intersection of the 27-year average latitude and longitude of genesis. For statistical purposes, genesis is defined as the first 25-kt (13-m/sec) intensity on the best track.

South China Sea, contributing to the westward displacement of the annual mean genesis location. Only one TC formed east of 160°E and south of 20°N in a region designated on Figure 3-5b as the "El Niño" box. The annual number of TCs which form in the "El Niño" box is much greater during El Niño years than during El Viejo years (Lander, 1994). During El Viejo years the few TCs which form east of 160°E tend to occur north of 20°N and are often associated with TUTT cells.

During June through October of 1996, low-level easterly wind flow was unusually persistent in the low latitudes of the WNP (Figure 3-4), and the normal southwest monsoon of the Philippine Sea (with its episodic extensions further eastward) was replaced by mean monthly easterly flow. Corresponding anomalies in the upper troposphere consisted of westerly wind anomalies over the low latitudes of the WNP. Similar large-scale wind anomalies dominated the low latitudes of the WNP during 1995, and may have been related

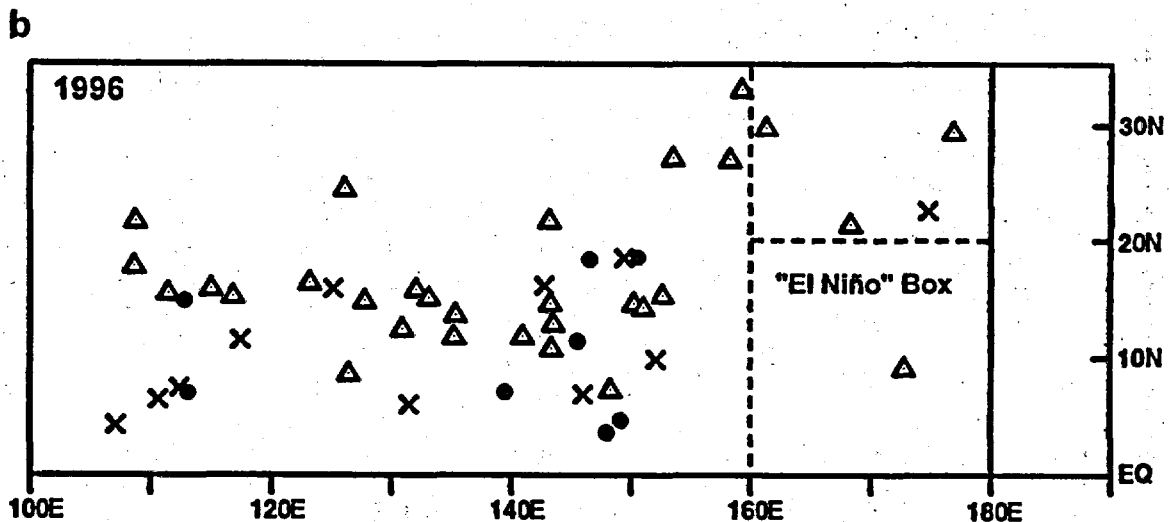


Figure 3-5b Point of formation of significant tropical cyclones in 1996 as indicated by the initial intensity of 25 kt (13 m/sec) on the best track. The symbols indicate: solid dots = 01 January to 15 July; open triangles = 16 July to 15 October; and, X = 16 October to 31 December.

to a westward displacement of the mean genesis location during that year. Despite similar wind anomalies in low latitudes, there were far more TCs during 1996 than during 1995. Some factors suggested for the enhanced number of TCs during 1996 include:

- 1) a high number of TUTT-cell related TCs during 1996;
- 2) an unusual eastward penetration of the monsoon trough at high latitudes during August of 1996 (Figure 3-6); and,
- 3) a return of near-normal monsoonal westerlies during November and December.

The most distinctive characteristic of the WNP TC distribution during 1996 was the large number of TUTT-cell related TCs. Eleven (26%) of the 43 significant TCs in the WNP during 1996 formed in association with TUTT cells. TUTT-cell related TC genesis is described in detail in Joy's (12W) summary.

Another distinctive characteristic of the TC distribution during 1996 was the formation of several TCs at high latitude in association with a displacement of the monsoon trough during August well to the north of normal. A northward-displaced monsoon trough was the site of the development of Kirk (13W), Orson (19W), Piper (20W), and Rick (22W), and TDs 15W, 17W, and 23W. Some of these TCs (e.g., Piper (20W) and Rick (22W)) also formed in association with TUTT cells.

During November and December of 1996, monsoonal westerlies returned to a near-normal distribution. Two episodes of strong low-level equatorial westerly winds (sometimes referred to as equatorial westerly wind bursts) occurred, one during early November and the other during the latter half of December. The November westerly wind burst was associated with the development of the late-season TCs

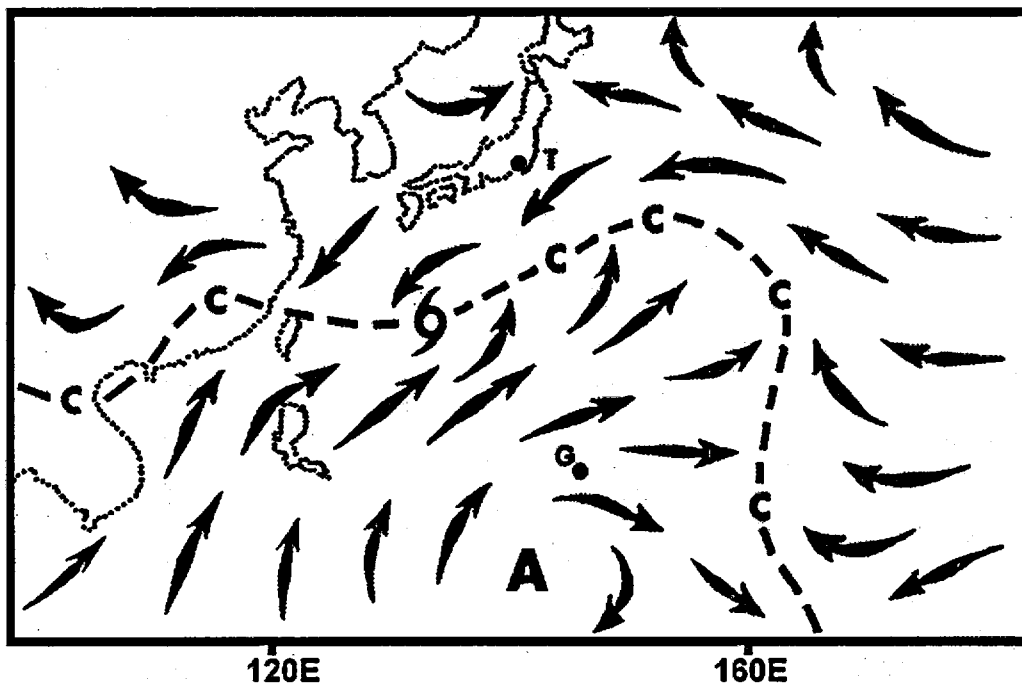


Figure 3-6 Schematic illustration of the low-level circulation pattern which dominated the WNP during August. Arrow indicates wind direction, dashed line indicates the axis of the monsoon trough, C indicates LLCCs, A = anticyclone center, G = Guam, and T = Tokyo. A TC is shown located along the trough axis.

Dale (36W) and Ernie (37W). December's episode of strong equatorial westerly wind was associated with the development of five TCs — two in the Northern Hemisphere (Fern (42W) and Greg (43W)), and three in the Southern Hemisphere (Ophelia (11S), Phil (12P), and Fergus (13P)).

The tracks of the TCs which formed in the WNP during 1996 indicate an above-normal number of TCs (10) in the South China Sea (SCS), and an above-normal number (12) of north-oriented tracks (which includes the three "S" tracks as a specific type of north-oriented motion). Of the 43 TCs, nine (21%) were straight runners, eight (19%) were recurvers, twelve (28%) moved on north-oriented tracks, and fourteen (32%) were designated as "other". Of the twelve TCs which

moved on north-oriented tracks during 1995, three underwent "S" motion. Ten of the fourteen "other" TCs remained in or near the SCS. The three "S" tracks occurred in association with a northward-displaced monsoon trough during August.

In summary, a chronology of all the TC activity in the JTWC AOR during 1996 is provided in Figure 3-7. Composite best tracks for the WNP TCs are provided for the periods: 01 January to 08 August (Figure 3-8a), 09 August to 07 October (Figure 3-8b), and 08 October to 31 December (Figure 3-8c). Table 3-3 includes: a climatology of typhoons, and tropical storms/typhoon for the WNP for the periods 1945-1959 and 1960-1996. Table 3-4 is a summary of the TCFA's for the WNP for the period 1976-1996.

Table 3-3 WESTERN NORTH PACIFIC TROPICAL CYCLONES													
<u>TYPHOONS (1945-1959)</u>													
	<u>JAN</u>	<u>FEB</u>	<u>MAR</u>	<u>APR</u>	<u>MAY</u>	<u>JUN</u>	<u>JUL</u>	<u>AUG</u>	<u>SEP</u>	<u>OCT</u>	<u>NOV</u>	<u>DEC</u>	<u>TOTALS</u>
MEAN	0.3	0.1	0.3	0.4	0.7	1	2.9	3.1	3.3	2.4	2	0.9	16.4
CASES	5	1	4	6	10	15	29	46	49	36	30	14	245
<u>TYPHOONS (1960-1996)</u>													
	<u>JAN</u>	<u>FEB</u>	<u>MAR</u>	<u>APR</u>	<u>MAY</u>	<u>JUN</u>	<u>JUL</u>	<u>AUG</u>	<u>SEP</u>	<u>OCT</u>	<u>NOV</u>	<u>DEC</u>	<u>TOTALS</u>
MEAN	0.3	0.1	0.2	0.4	0.7	1	2.8	3.4	3.4	3.2	1.7	0.7	17.9
CASES	10	2	8	15	26	38	104	126	126	120	62	25	662
<u>TROPICAL STORMS AND TYPHOONS (1945-1996)</u>													
	<u>JAN</u>	<u>FEB</u>	<u>MAR</u>	<u>APR</u>	<u>MAY</u>	<u>JUN</u>	<u>JUL</u>	<u>AUG</u>	<u>SEP</u>	<u>OCT</u>	<u>NOV</u>	<u>DEC</u>	<u>TOTALS</u>
MEAN	0.4	0.1	0.5	0.5	0.8	1.6	2.9	4	4.2	3.3	2.7	1.2	22.2
CASES	6	2	7	8	11	22	44	60	64	49	41	18	332
<u>TROPICAL STORMS AND TYPHOONS (1960-1996)</u>													
	<u>JAN</u>	<u>FEB</u>	<u>MAR</u>	<u>APR</u>	<u>MAY</u>	<u>JUN</u>	<u>JUL</u>	<u>AUG</u>	<u>SEP</u>	<u>OCT</u>	<u>NOV</u>	<u>DEC</u>	<u>TOTALS</u>
MEAN	0.5	0.2	0.5	0.6	1.1	1.8	4.3	5.6	5.1	4.3	2.7	1.2	28
CASES	19	9	17	23	41	67	159	208	189	159	100	46	1037

Table 3-4 TROPICAL CYCLONE FORMATION ALERTS FOR THE WESTERN NORTH PACIFIC OCEAN FOR 1976-1996

<u>YEAR</u>	<u>INITIAL TCFAS</u>	<u>TROPICAL CYCLONES WITH TCFAS</u>	<u>TOTAL TROPICAL CYCLONES</u>	<u>PROBABILITY OF TCFA WITHOUT WARNING*</u>	<u>PROBABILITY OF TCFA BEFORE WARNING</u>
1976	34	25	25	26%	100%
1977	26	20	21	23%	95%
1978	32	27	32	16%	84%
1979	27	23	28	15%	82%
1980	37	28	28	24%	100%
1981	29	28	29	3%	96%
1982	36	26	28	28%	93%
1983	31	25	25	19%	100%
1984	37	30	30	19%	100%
1985	39	26	27	33%	96%
1986	38	27	27	29%	100%
1987	31	24	25	23%	96%
1988	33	26	27	21%	96%
1989	51	32	35	37%	91%
1990	33	30	31	9%	97%
1991	37	29	31	22%	94%
1992	36	32	32	20%	100%
1993	50	35	38	30%	92%
1994	50	40	40	20%	100%
1995	54	33	35	39%	94%
1996	41	39	43	5%	91%
(1976-1996)					
MEAN:	37	29	30	22%	97%
TOTALS:	782	605	637		

* Percentage of initial TCFA's not followed by warnings.

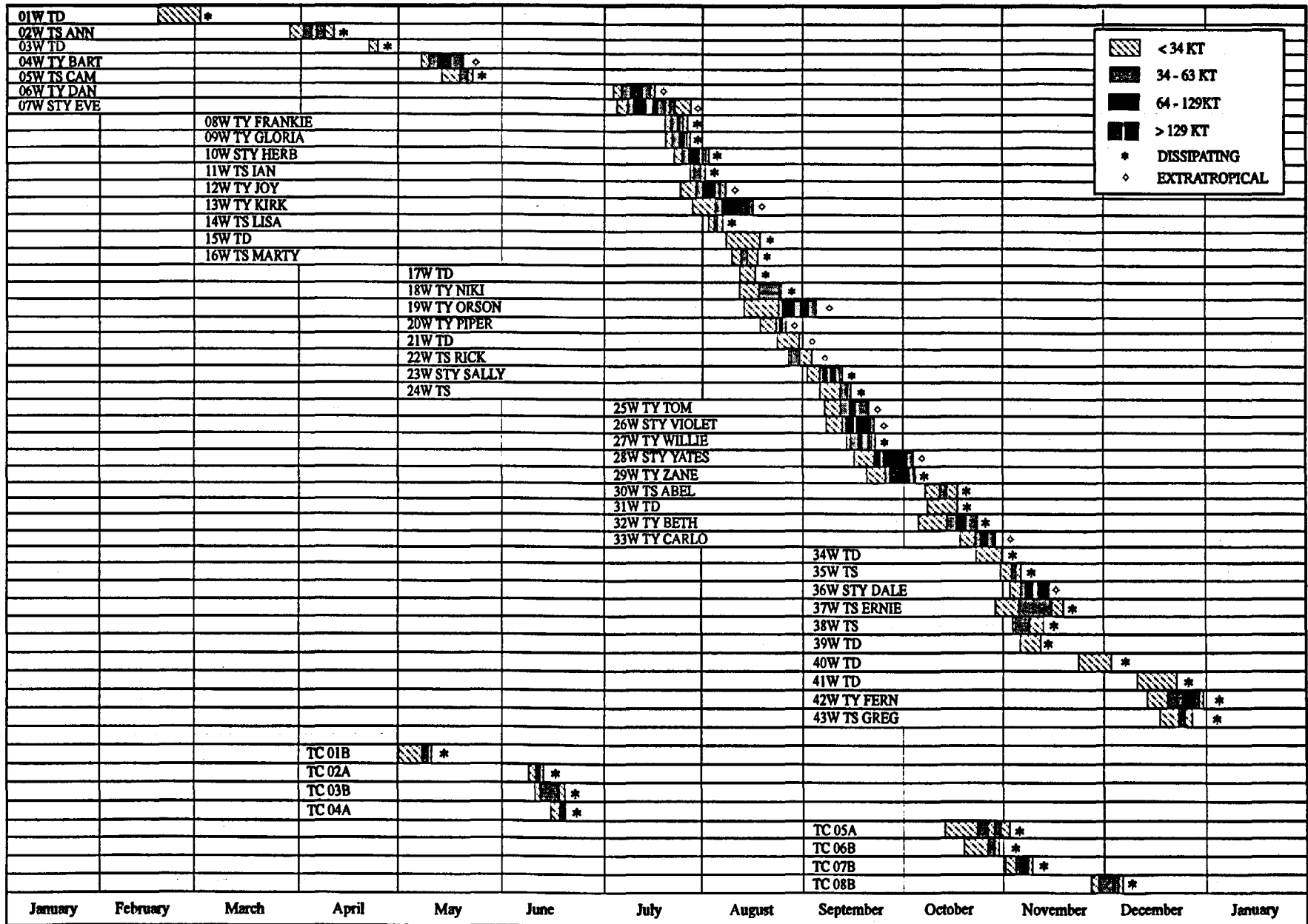


Figure 3-7 Chronology of western North Pacific and North Indian Ocean tropical cyclones for 1996.

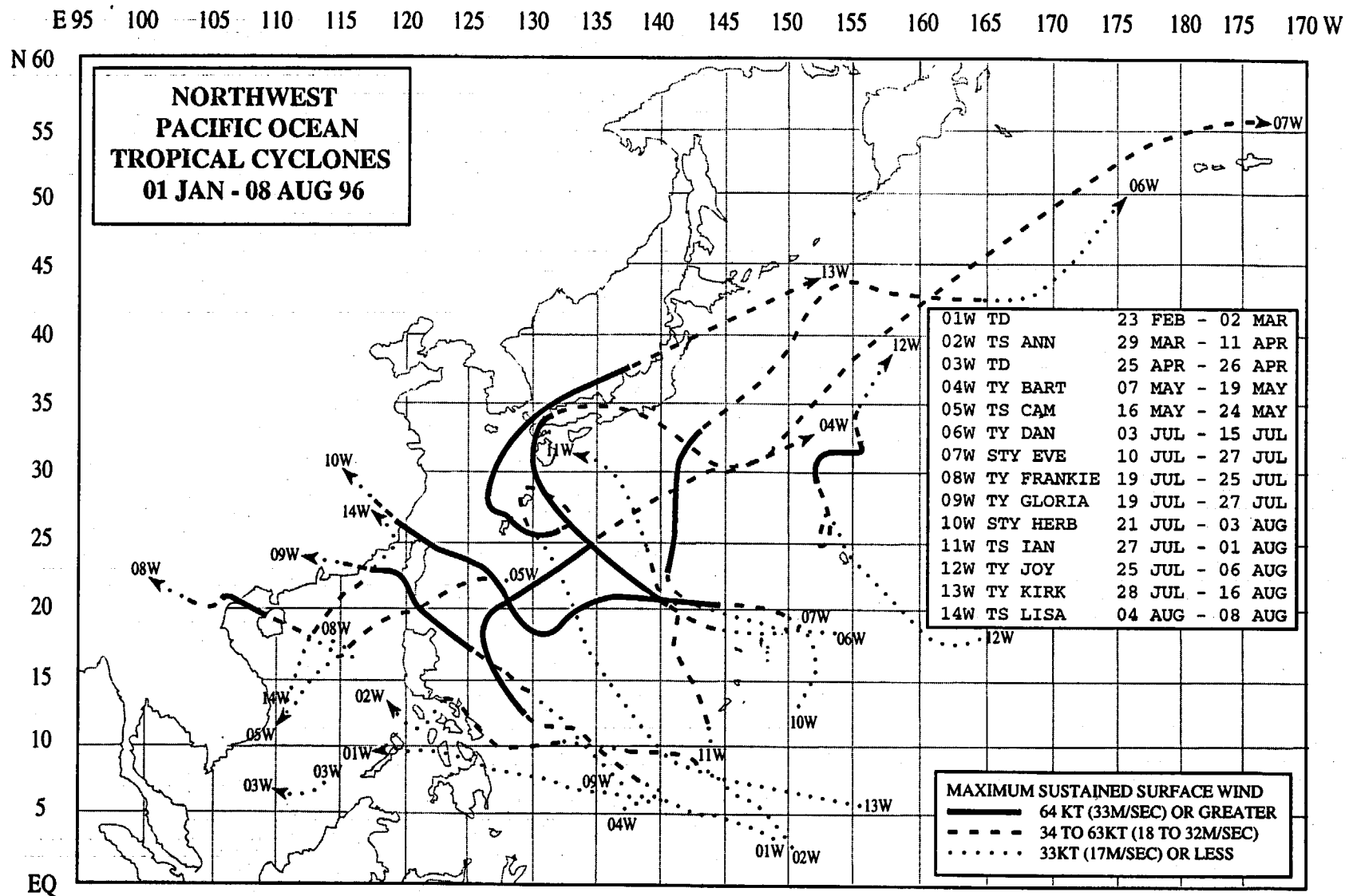


Figure 3-8a Composite best tracks for the western North Pacific Ocean tropical cyclones for the period 01 January to 08 August 1996

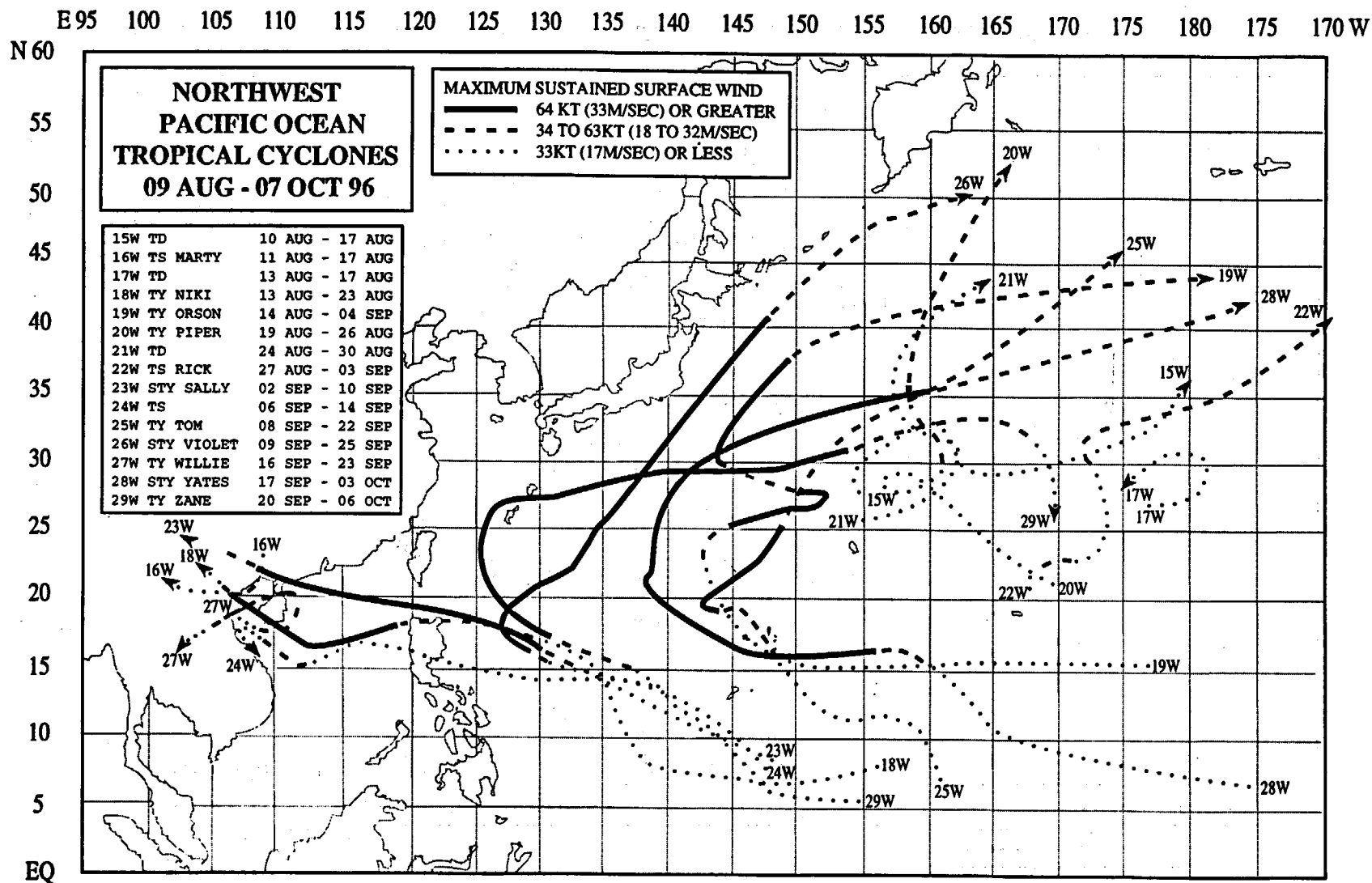


Figure 3-8b Composite best tracks for the western North Pacific Ocean tropical cyclones for the period 09 August to 07 October 1996

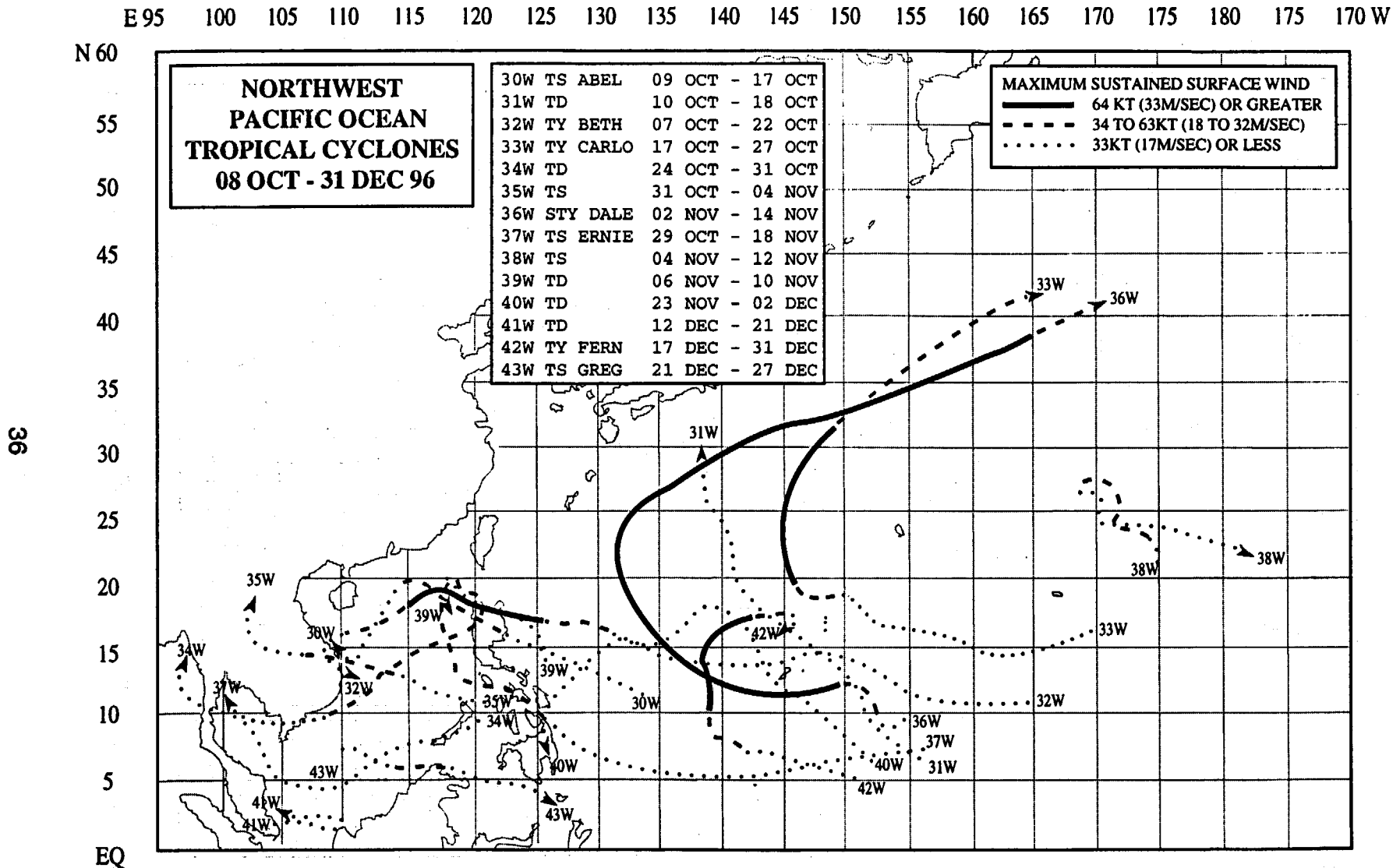


Figure 3-8c Composite best tracks for the western North Pacific Ocean tropical cyclones for the period 08 October to 31 December 1996

3.1.1 MONTHLY ACTIVITY SUMMARY

JANUARY

There were no significant TCs in the western North Pacific basin during January 1996.

FEBRUARY

For only the fourth time since 1970, a significant TC formed in the WNP during February. Toward the end of the month, **Tropical Depression (TD) 01W** formed south of Guam. It developed in a temporary near-equatorial trough over the Caroline Islands, associated with a short-lived westerly wind burst. Tropical Depression 01W moved to the west-northwest, failed to mature, and on the last day of the month it moved into the Philippine archipelago just north of Mindanao.

MARCH

During the first two days of March, TD 01W completed its passage over the Philippines, entered the SCS and dissipated. For most of the rest of March, the WNP was relatively clear, while several TCs originated within the western South Pacific (WSP). At the end of March, the WSP became quiet, and a broad, persistent area of deep convection extended westward from Hawaii to central Micronesia. On the last two days of March, the tropical disturbance which became **Ann (02W)** originated at low latitudes southeast of Guam.

APRIL

Two TCs — **Tropical Storm (TS) Ann (02W)** and **TD 03W** — were active during April. During the first week of April, Ann became the first named TC of 1996. After becoming a tropical storm while south of Guam, Ann moved westward along 10°N and made landfall in the central Philippines. On 11 April, Ann dissipated over the eastern SCS. The remainder of April was quiet until the last week when an area of persistent deep convection northwest of Borneo became **Tropical Depression 03W**. TD 03W had a very short life (30 hours).

MAY

During the first week of May, the tropics of the WNP were dominated by low-level easterly wind flow accompanied by westerly wind flow aloft. A zonally-oriented band of convection stretched east-west across Micronesia south of 10°N. By the end of the first week, an area of deep convection began to organize in the western Caroline Islands as monsoonal low-level westerly winds penetrated into the WNP eastward to 140°E and south of 5°N. This area of deep convection became **Typhoon Bart (04W)**, the first typhoon of 1996. Initially moving toward the Philippines, it turned to the north and remained at sea. Undergoing a period of rapid intensification, Bart became a very intense typhoon, peaking at 125 kt (64 m/sec) on 14 May. A day later, the intense typhoon recurved to the northeast, and on 19 May it became extratropical near 30°N 152°E.

As Bart was recurving, cloudiness began to increase in the southwesterly monsoon flow across the SCS and extended east-northeastward toward Bart. Most of the deep convection associated with this monsoon flow was located within the SCS in the form of a large ensemble of mesoscale convective systems (MCSs) which were associated with a weak low-level cyclonic circulation, and extensive cirrus outflow indicative of anticyclonic outflow aloft. These structural attributes are typical of a monsoon depression. The deep convection of this monsoon depression consolidated, and the system became **TS Cam (05W)**. Cam moved toward the east-northeast for its entire life. While at peak intensity, it passed through the Luzon Strait and then slowly weakened as it drifted eastward into the Philippine Sea and dissipated.

JUNE

There were no significant TCs in the WNP during June as amounts of deep convection were below normal, low-level winds were anomalously easterly and upper-level winds were anomalously westerly (Climate Prediction Center (CPC), 1996). While several tropical disturbances developed during the month, a

combination of stronger-than-normal low-level easterly flow with stronger-than normal upper-level westerly flow created an environment of strong vertical shear which was unfavorable for TC formation and development. Since 1959, only five other years have had no significant TCs during June.

JULY

July was a busy month in the WNP with a total of eight TCs. Early in the month, the southwest monsoon remained inactive in the WNP with large-scale wind anomalies similar to those of June. The first two TCs of the month, **Typhoon Dan (06W)** and **Super Typhoon Eve (07W)**, formed in association with TUTT cells. Typical of TC genesis in association with TUTT cells, Dan and Eve formed at relatively high latitude (Dan at 24°N, and Eve at 20°N), and both formed in low-level easterly flow. On 15 July, Eve underwent a period of explosive intensification and reached a peak of 140 kt (72 m/sec), becoming the first super typhoon in the WNP during 1996. The first TC of the year to make landfall as a typhoon, Eve passed through the northern Ryukyu Islands and made landfall in southern Japan.

In the middle of July, the monsoon began to move eastward as the axis of the monsoon trough extended into Micronesia. Extensive amounts of deep convection formed in an east-west band extending across the WNP from the coast of Southeast Asia to the Marshall Islands. By 21 July, this cloud band had consolidated into three distinct cloud clusters, all of which became named TCs — from west to east: **Typhoon Frankie (08W)**, **Typhoon Gloria (09W)**, and **Super Typhoon Herb (10W)**. Frankie originated from a monsoon depression in the SCS. It became a typhoon in the Gulf of Tonkin and went ashore in Vietnam late on 23 July. While Frankie was developing in the SCS, a monsoon depression in the Philippine Sea became Gloria. Gloria moved northwestward, became a typhoon, and affected Luzon, Taiwan, and eastern China. During the early phases of its development,

Gloria formed a very large Central Cold Cover (CCC) with a near-record cloud-top temperature of -100°C. As Frankie and Gloria moved westward, Herb formed and became the easternmost of three tropical cyclones simultaneously active along the monsoon trough. Herb became a super typhoon when east of Taiwan. A very intense TC, it was also very large — the largest TC in terms of the mean radius to its outermost closed isobar in the WNP during 1996. Herb made landfall in the southern Ryukyu Islands, Taiwan, and mainland China. Significant property damage and loss of life were attributed to Herb in these areas. On Taiwan, a brand new NEXRAD WSR-88D took a direct hit from Herb, and was severely damaged. As Herb moved westward toward Taiwan, **TS Ian (11W)** formed near Guam at the end of the monsoon trough and then moved on a north-northwestward track while embedded within the peripheral southerly flow on the eastern side of the very large Super Typhoon Herb (10W). Ian appeared to be adversely affected by Herb's upper-level outflow, and did not intensify above 40 kt (21 m/sec).

At the end of July, as Herb moved westward, a TUTT cell generated a tropical disturbance in the eastern part of the WNP basin near 20°N 165°E. This tropical disturbance became **Typhoon Joy (12W)**. Joy did not become a typhoon until 01 August when it had moved to nearly 30°N. Also by the end of July, a new monsoon trough began to form at low latitudes in Micronesia, replacing the monsoon trough which moved with Herb into China. The monsoon depression which became **Typhoon Kirk (13W)** formed south of Guam in late July, but did not become a named TC until the first week of August.

AUGUST

August was also a very busy month, with eight TCs developing during the month, and four of the July TCs — Ian (11W), Herb (10W), Joy (12W), and Kirk (12W) — carrying over into the early part of the month. On 01 August, Ian dissipated south of Japan. Herb dissipated over eastern China on 03 August.

Joy, which developed near 20°N 165°E in the last week of July, reached typhoon intensity on 01 August. It moved on a north-oriented track and merged with a frontal cloud band on 06 August. Typhoon Kirk (13W), the last of the TCs originating during July, developed from a monsoon depression at low latitude, and did not significantly intensify until reaching 27°N on 05 August. The typhoon moved on a complex north-oriented track which saw it undergo an unusual clockwise loop before passing directly over Okinawa where it took a full 12 hours for its 70-nm (130-km) diameter eye to pass. Kirk recurved near Okinawa, intensified to its peak of 95 kt (49 m/sec), moved to the northeast, and made landfall in Kyushu on 14 August.

During the period 04-17 August (as the large slow-moving Kirk tracked northward, executed its clockwise loop, and recurved), four relatively weak TCs formed elsewhere in the WNP. TS Lisa (14W) was the first TC to form during August. It originated from a monsoon depression in the SCS. Moving northeastward, the system attained only 40 kt (21 m/sec); and late on 06 August it made landfall west of Taiwan in east central China. On 12 August, TD 15W developed in the subtropics at a time when the monsoon trough was displaced far to the north of normal. Although it was located along the axis of this northward-displaced monsoon trough, the structure of the very small TD 15W was influenced by a northward-displaced TUTT, and an upper-level cut-off low to the east of Japan. The system dissipated over water on 17 August. TS Marty (16W) originated as a tropical disturbance in the monsoon trough over land in southwestern China. This disturbance moved southward into the Gulf of Tonkin and intensified to a tropical storm on 13 August. The system then turned more to the west and, after a short path over water, it made landfall about 60 nm (110 km) south of Hanoi. Marty was reported to have severely impacted Vietnamese fishing boats in the Gulf of Tonkin where 125 people were reported killed and another 107 missing. TD 17W formed to the east-southeast of TD 15W at the eastern end of the northward-displaced monsoon trough. This TD tracked eastward across the international

date line, then doubled back and crossed the date line again. On 17 August after a short life and a short track, TD 17W dissipated over water near 27°N 177°E.

During the middle of August, as TDs 15W and 17W developed along the axis of a monsoon trough which was displaced to a higher-than-normal latitude, a ridge of high pressure to its south produced easterly low-level winds across the deep tropics of the WNP. Within these low-latitude easterly winds, several tropical disturbances formed. The tropical disturbance which became Typhoon Niki (18W) can be traced to a small ensemble of MCSs which appeared in the eastern Caroline Islands on 13 August. This disturbance moved westward and slowly developed. It became a tropical storm after it crossed 130°E and before it crossed Luzon. Niki did not become a typhoon until it was in the SCS. The typhoon passed over the southern tip of Hainan Island, crossed the Gulf of Tonkin, and made landfall in northern Vietnam. The tropical disturbance which became Typhoon Orson (19W) developed within a very complex circulation pattern that can best be described as the early stages of the breakdown of the high-latitude monsoon trough within which Kirk (13W), TD 15W, and TD 17W were located. When the pre-Orson tropical disturbance formed on 15 August, Kirk (13W) was moving eastward over northern Honshu (and becoming extratropical), and TDs 15W and 17W were dissipating at high latitude (30°N) and east of 160°E. For the next four days, the pre-Orson tropical disturbance tracked westward along 15°N. On 19 August, it turned northward and intensified. Orson had a complex history, including two periods of intensification, the formation of a very large eye, and a highly erratic track.

When Orson became a typhoon while moving east-northeastward at 25°N, the monsoon trough became reestablished at a high latitude. The final three TCs of August developed at high latitude in this monsoon trough, and were also associated with TUTT cells. Typhoon Piper (20W) was another of the TCs of 1996 which originated in association with a TUTT cell. It was a very small TC — easily

the smallest typhoon in the WNP during 1996. Developing at a relatively high latitude to the east of Orson (19W), Piper was located at the eastern end of a high-latitude reverse-oriented monsoon trough. Typical of TCs associated with a reverse-oriented monsoon trough, Piper moved on a north-oriented "S"-shaped track. On 26 August, the typhoon accelerated toward the north-northeast and was absorbed into a frontal cloud band east of the Kamchatka peninsula. On 24 August, the weak low-level circulation which became TD 21W developed east of Orson and west of Piper. Sandwiched between these two TCs, TD 21W remained weak while in an environment of westerly vertical wind shear. After moving on a north-oriented "S"-shaped track, the system dissipated over water near 42°N 163°E early on 30 August. TS Rick (22W) formed after Piper and TD 21W moved out of the high-latitude monsoon trough on their north-oriented "S"-shaped tracks. The tropical disturbance which became Rick was located between Orson (19W) and a well-defined TUTT cell. In addition to its association with a TUTT cell, Rick also became part of the monsoon trough. Located at the eastern end of the high-latitude monsoon trough, it moved on a north-oriented "S"-shaped track. On 31 August, the system entered the accelerating westerlies regime north of the subtropical ridge, and by 03 September it dissipated north of 40°N and east of the international date line.

SEPTEMBER

TC activity in the WNP during September continued at a fast pace, with no break from the high levels of TC activity of July and August. The month produced seven TCs, including six typhoons (half of which became super typhoons). As the month began, two TCs — Rick and Orson — were still active from August. Rick dissipated on 03 September, and Orson became extratropical on 04 September.

As the long-lived Orson recurved at the beginning of September, the unusual monsoon flow pattern of August gave way to a pattern more in line with climatology: the maximum cloud zone and the axis of the monsoon trough

became established from the Philippines east-southeastward into Micronesia. Five TCs — Sally (23W), TS 24W, Tom (25W), Violet (26W), and Willie (27W) — formed in this monsoon trough. This very active monsoon trough moved northward, and became reverse oriented. By the final week of September, it had migrated to a relatively high latitude as TCs Tom (25W) and Violet (26W) carried the trough with them out of the tropics. As this monsoon trough exited the tropics, yet another monsoon trough formed at low latitudes, and was the site of development for the next two TCs in the WNP: Yates (28W) and Zane (29W).

Super Typhoon Sally (23W) was the first significant TC to form during September. Forming southwest of Guam, Sally moved on a relatively steady west-northwest straight-moving track. It became a super typhoon while moving through the Luzon Strait, and later, though weaker, it made landfall in southwestern China where it caused extensive damage and considerable loss of life. TS 24W (unnamed) began as a tropical disturbance located near Guam. By the morning of 09 September this disturbance became a large monsoon depression in the Philippine Sea. The system moved westward, crossed Luzon and entered the SCS. On 14 September, it moved into the Gulf of Tonkin where it dissipated. The upgrade to a tropical storm was based upon a post analysis of synoptic data which indicated that the sustained winds reached a peak of 45 kt (23 m/sec) when the TC was in the SCS.

The next two September TCs — **Typhoon Tom (25W)** and **Super Typhoon Violet (26W)** — moved in tandem along spatially-proximate recurving tracks. Although both TCs had very large circulations, their approximate 1100-nm (2050-km) separation distance was too far apart for the TCs to exhibit binary interaction. When Tom reached its peak intensity of 75 kt (39 m/sec) on 16 September, it had an unusual structure featuring a "pin-hole" eye in a small central cloud mass surrounded by extensive peripheral rain bands within a large outer wind field. By contrast, Violet (located to the west of Tom) had a size similar to Tom, and yet the structure of its core

could not have been more different: Violet's eye began small, but then became very large with a diameter on the order of 75 nm (140 km). Violet was responsible for killing seven people and injuring 44 others in southeastern Japan.

While the circulation of the large TCs Tom and Violet dominated much of the WNP, a small TC — TS Willie (27W) — developed in the Gulf of Tonkin. Never more than 90 nm (170 km) from shore, Willie circumnavigated Hainan Island while undergoing a counter-clockwise loop. Willie was a small TC, and was part of a three-TC outbreak along the monsoon trough, with the larger TCs Tom and Violet to its northeast. At one point, Tom, Violet, Willie and a subtropical (ST) low existed simultaneously along the trough axis. Due to the relative motions of these TCs (and the ST low), the trough axis became reverse oriented.

The tendency of the monsoon trough of the WNP to form and then migrate northward lends itself to a natural segregation of TCs into "families" with the commonality among the TCs within each "family" being that they were associated with the same monsoon trough. The five-TC sequence of early September — Sally, TS 24W, Tom, Violet, and Willie — all had in common an origin within the same monsoon trough. By late September, this monsoon trough moved northward, became reverse oriented, and migrated to higher latitude as TCs Tom and Violet carried it with them out of the tropics. As this monsoon trough exited the tropics, a new monsoon trough formed at low latitudes, and was the site of development for the next two TCs in the WNP: Super Typhoon Yates (28W) and Zane (29W). Like Tom and Violet before them, the final two September TCs — Yates and Zane — developed in the same monsoon trough, at approximately the same time, and recurved simultaneously along similarly shaped and spatially-proximate tracks. Yates and Zane had motion characteristics suggestive of semi-direct and indirect TC interaction. The mutual anticyclonic orbit of Yates and Zane during the period 23 to 26 September (manifested in a south-of-west track for Yates) are typical of indirect TC interaction. The periods of mutual cyclonic orbit at the beginning

and at the end of the tracks is consistent with semi-direct TC interaction. It is often difficult to differentiate between semi-direct and direct TC interaction, but one clue is often the separation distance. True mutual interaction of two TCs usually occurs when the TCs are within 780 nm (1450 km) of each other. Yates and Zane were at this threshold, and it is possible that they may have interacted directly, especially at the end of their tracks when the cyclonic orbit increased rapidly.

OCTOBER

At the beginning of October, Yates and Zane recurved and moved into the midlatitudes. During this time, for about one week, the low latitudes of the WNP became relatively free of deep convection, and there was a break in TC activity. By the end of the first week of October, amounts of deep convection began to increase in the low latitudes of the WNP, and winds throughout most of Micronesia became light and variable in association with the establishment of yet another monsoon trough. Renewed deep convection (loosely organized into discrete ensembles of MCSs) was located in an east-west zone across the low latitudes of the WNP. The first three TCs of October— Abel, TD 31W, and Typhoon Beth — developed in this cloud band over the span of three days. TS Abel (30W) originated from a monsoon depression in the Philippine Sea, crossed Luzon, and became a tropical storm in the SCS. Forced to move southwestward by the northeast monsoon, it dissipated over water while approaching the coast of southern Vietnam. Moving toward the northwest, TD 31W exhibited a shear-type cloud pattern for all of its life. On 17 October, the deep convection associated with TD 31W decreased in amount and became sheared well to the east of the LLCC as the system dissipated over water. The tropical disturbance which became Typhoon Beth (32W) was first detected in the eastern Caroline Islands. For a week, it developed very slowly, and while passing over Guam, it produced a thunderstorm with a spectacular display of cloud-to-ground lightning (an unusual event in the maritime tropics). On 16 October, Beth

became a typhoon in the Philippine Sea. The typhoon passed over Luzon where loss of life was reported. Encountering the northeast monsoon in the South China Sea, it turned to the southwest, weakened, and made landfall in central Vietnam.

On 17 October, three TCs were active in the western part of the WNP: Abel (in the South China Sea), TD 31W (east-southeast of Okinawa), and Beth (32W) (near the coast of Luzon). Elsewhere in the tropics of the WNP, amounts of deep convection were below normal and the low-level wind was predominantly from the east. The only area of deep convection considered to have a potential for TC formation was associated with a TUTT cell which was centered near 17°N 168°E. **Typhoon Carlo (33W)** formed in association with this TUTT cell. Water-vapor imagery provided detailed information on the evolution of upper-level winds, clouds, and moisture for this event. Carlo reached its peak intensity of 105 kt (54 m/sec) while moving northward after reaching its apparent "point of recurvature": a typical behavioral characteristic of TCs which move on a north-oriented track. Accelerating to a speed of 30 kt (55 km/hr), Carlo was absorbed into the frontal cloud band of an intense extratropical low on 27 October.

In late October, TC development shifted to the SCS. On 25 October, TD 34W developed just west of the Visayan Islands of the Philippines. This small and weak TC moved to the west-southwest, and as it approached the Malay peninsula, it turned toward the northwest. TD 34W passed through the Gulf of Thailand, moved across the Isthmus of Kra into the Bay of Bengal, and then dissipated over southern Myanmar on 31 October. On the last day of the month, the monsoon depression which became TS 35W formed over the Philippines at nearly the same location at which TD 34W originated. It did not become a tropical storm until early November. As a monsoon depression, TS 35W was a larger system than TD 34W. It moved across the SCS and made landfall in central Vietnam. The upgrade to tropical storm intensity was based upon post analysis of ships reports and satellite imagery.

NOVEMBER

From late October through the first day of November, the tropics of the WNP (except the SCS) was dominated by easterly low-level wind and upper-level westerly wind. Deep convection was disorganized and widely scattered. On 02 November (the same day that TS 35W became a tropical storm in the SCS), the amount of deep convection in the low latitudes of the WNP began to increase in association with lowering pressure throughout Micronesia. This was accompanied by the onset of a near-equatorial trough along 5°N. On 03 November, the deep convection consolidated into two distinct clusters: one centered near 8°N 150°E (which became Super Typhoon Dale (36W)), and the other centered near 7°N 138°E (which became TS Ernie (37W)). **Super Typhoon Dale (36W)** became a large and very intense typhoon with an extensive area of monsoon gales to its south and southwest. The equatorial westerly wind burst that preceded Dale's formation was accompanied by extremely low sea-level pressure reports along the equator. Passing 110 nm (205 km) south of Guam late on 07 November, the typhoon generated phenomenal seas and surf which pounded the island for three days. Dale recurved, and on 14 November, it transitioned into an intense extratropical cyclone. **TS Ernie (37W)** originated from a westward moving tropical disturbance first noted on 29 October in the eastern Caroline Islands. For several days the pre-Ernie tropical disturbance moved westward before showing signs of development on 03 November. The system became a tropical storm only a few hours before making landfall in northern Mindanao. Ernie crossed the Philippines and entered the SCS where it reached its peak intensity of 50 kt (26 m/sec). While undergoing a clockwise loop west of Luzon, the system merged with TD 39W, and later moved toward the west-southwest in association with a surge in the northeast monsoon to its north. On 18 November, the weakened TC dissipated in the Gulf of Thailand.

The rest of the November TCs were weak. **TS 38W (unnamed)** — the third unnamed TC of 1996 in the WNP — developed

from an unusually late-in-the-year TUTT cell located northeast of Dale. For nearly eight days (04-12 November), the system moved erratically. The TC dissipated on 12 November when it was located near 22°N 179°W, approximately 180 nm (335 km) east of where it formed late on 04 November. Late on 06 November, a tropical disturbance formed between Dale and Ernie as they were moving toward the west. This disturbance became TD 39W. Located within 200 nm (370 km) of one another, TD 39W and Ernie underwent a binary interaction that ended in merger. On 10 November, the weakened TD 39W was absorbed into the circulation of Ernie.

After Dale recurved, and Ernie and TD 39W moved into the SCS, the WNP experienced a break in TC activity associated with rising sea-level pressure (SLP) and light winds at low latitude. After a week-long lull, and although low-latitude SLP remained high, an extensive area of deep convection formed in Micronesia. On 23 November, this area of deep convection evolved into a large monsoon depression centered near Chuuk. Moving northwestward toward Guam, this monsoon depression became TD 40W. The depression moved as far north as 18°N, where it ran into a region of enhanced northeasterly low-level flow. The system then became sheared, began to drift toward the southwest, and interacted with some MCSs along its path. The weakened TC dissipated over Mindanao on 02 December.

DECEMBER

After the demise of TD 40W over the southern Philippines on 02 December, activity subsided in the WNP until 10 December when an area of deep convection formed in the SCS. On 13 December, synoptic data indicated that a weak low-level circulation center (LLCC) was located at low latitude east of the Malay peninsula in association with the deep convection in the region. The LLCC moved eastward and became TD 41W on 14 December. The depression moved eastward toward Borneo, then on December 16, as it neared the northwest coast of Borneo, it doubled back and moved west-

ward. The TC continued westward and dissipated on 21 December when located approximately 90 nm (165 km) from where it formed.

During mid-December, amounts of deep convection began to increase across Indonesia and eastward along the equator to near 160°E associated with a developing equatorial westerly wind burst (WWB). The WWB gradually strengthened and westerly winds increased to 40 kt (21 m/sec) with gusts to 50 kt (26 m/sec) extending from Indonesia to 155°E. The band of strong low-level westerly winds persisted between the axes of twin low-latitude monsoon troughs. A total of five TCs — two in the Northern Hemisphere (Fern (42W) and Greg (43W)), and three in the Southern Hemisphere (Ophelia (11S), Phil (12P), and Fergus (13P)) — formed along the respective monsoon trough axis.

Typhoon Fern (42W) formed southeast of Guam at low latitude in association with a Southern Hemisphere twin, Fergus (13P). Fern moved west-northwestward, and turned to the north on Christmas Day when it was located just west of Yap. Fern attained its maximum intensity of 80 kt (41 m/sec) on 26 December. The weakening typhoon dissipated 150 nm (280 km) northeast of Saipan on the last day of the month.

The final WNP TC of 1996, **TS Greg (43W)**, developed in the SCS mid-way between Vietnam and Borneo. Greg moved eastward at low latitude for its entire life, apparently steered by the strong westerly winds associated with the intense WWB to its south. The TC reached its peak intensity of 45 kt (23 m/sec) on Christmas Day, and the next morning made landfall in an unusual location: the northern tip of Borneo near the city of Kota Kinabalu in the East Malaysian State of Sabah. Greg was responsible for loss of life and extensive damage to property in Sabah. At least 124 lives were reported lost with another 100 reported missing primarily due to flooding from torrential rains. Greg continued its unusual east-southeastward motion and dissipated on 27 December at 3°N in the eastern Celebes Sea.

TROPICAL DEPRESSION 01W

BEST TRACK-TC 01W
23 FEB - 02 MAR 96
MAX SFC WIND 30 KT
MINIMUM SLP 1000MB

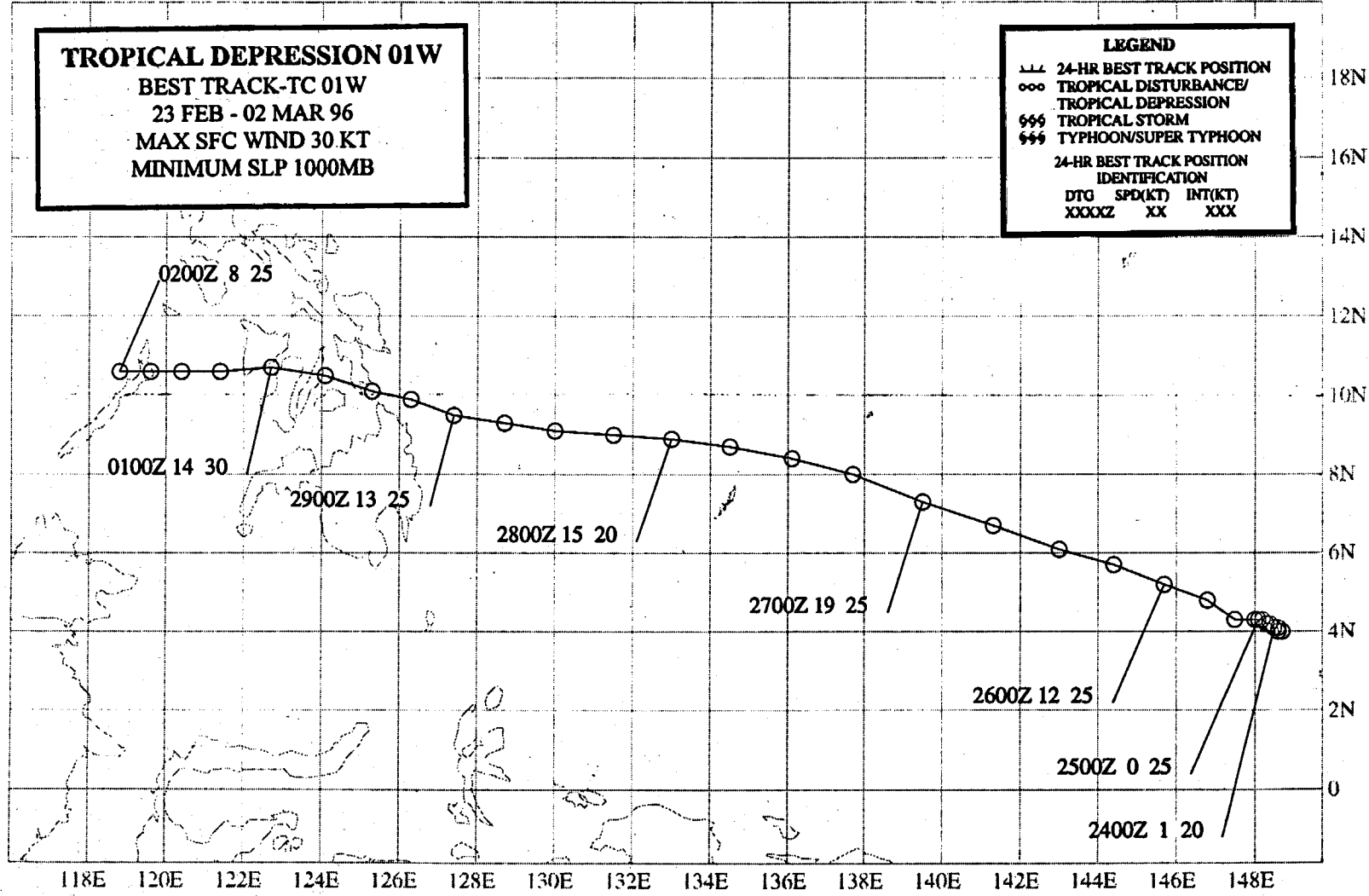
LEGEND

- 24-HR BEST TRACK POSITION
- TROPICAL DISTURBANCE/
TROPICAL DEPRESSION
- ☉ TROPICAL STORM
- ☼ TYPHOON/SUPER TYPHOON

24-HR BEST TRACK POSITION
IDENTIFICATION

DTG	SPD(KT)	INT(KT)
XXXXZ	XX	XXX

44



TROPICAL DEPRESSION 01W

The first significant tropical cyclone (TC) of 1996 in the western North Pacific (WNP), Tropical Depression (TD) 01W formed at low latitude in a near-equatorial trough associated with a surge in the monsoonal westerlies (i.e., a westerly wind burst). The tropical disturbance which became TD 01W was first mentioned on the 230600Z February Significant Tropical Weather Advisory when satellite imagery indicated that deep convection was becoming organized on the northeastern end of a monsoonal cloud band along the equator (Figure 3-01-1a). After deep convection along the equator collapsed, a weak TC consolidated in the Northern Hemisphere, and moved westward toward the Philippines (Figure 3-01-1b). Two formation alerts (one at 281300Z and the other at 290430Z) were issued prior to the first warning valid at 290600Z February. The first warning indicated that the intensity of TD 01W was 30 kt (15 m/sec). Although forecast to slowly intensify while crossing the Visayan Island group of the central Philippines, TD 01W remained at 30 kt (Figure 3-01-1c), and then weakened as it approached the South China Sea. The final warning was issued at 011800Z March. No reports of damage or injuries were received.

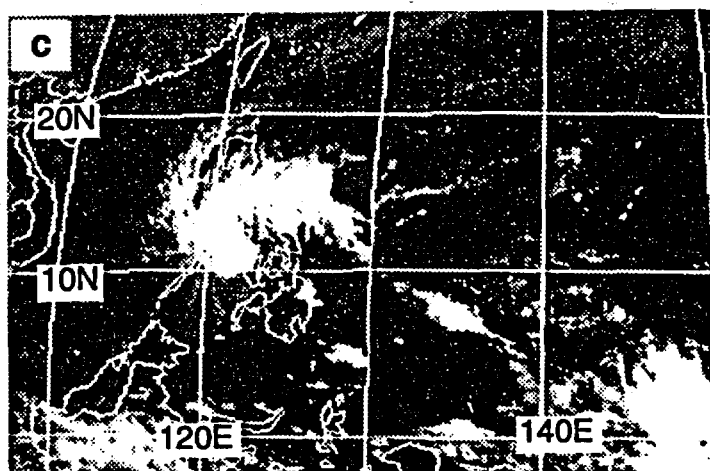
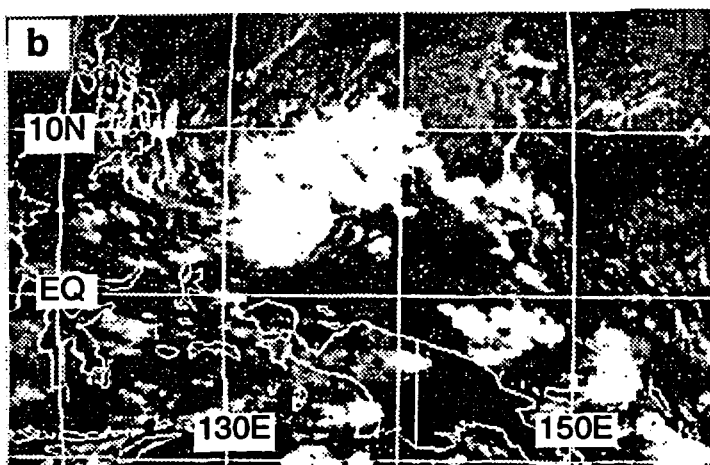
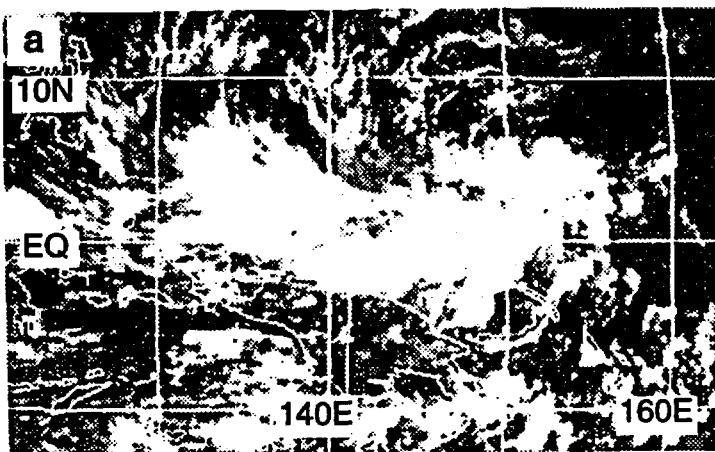


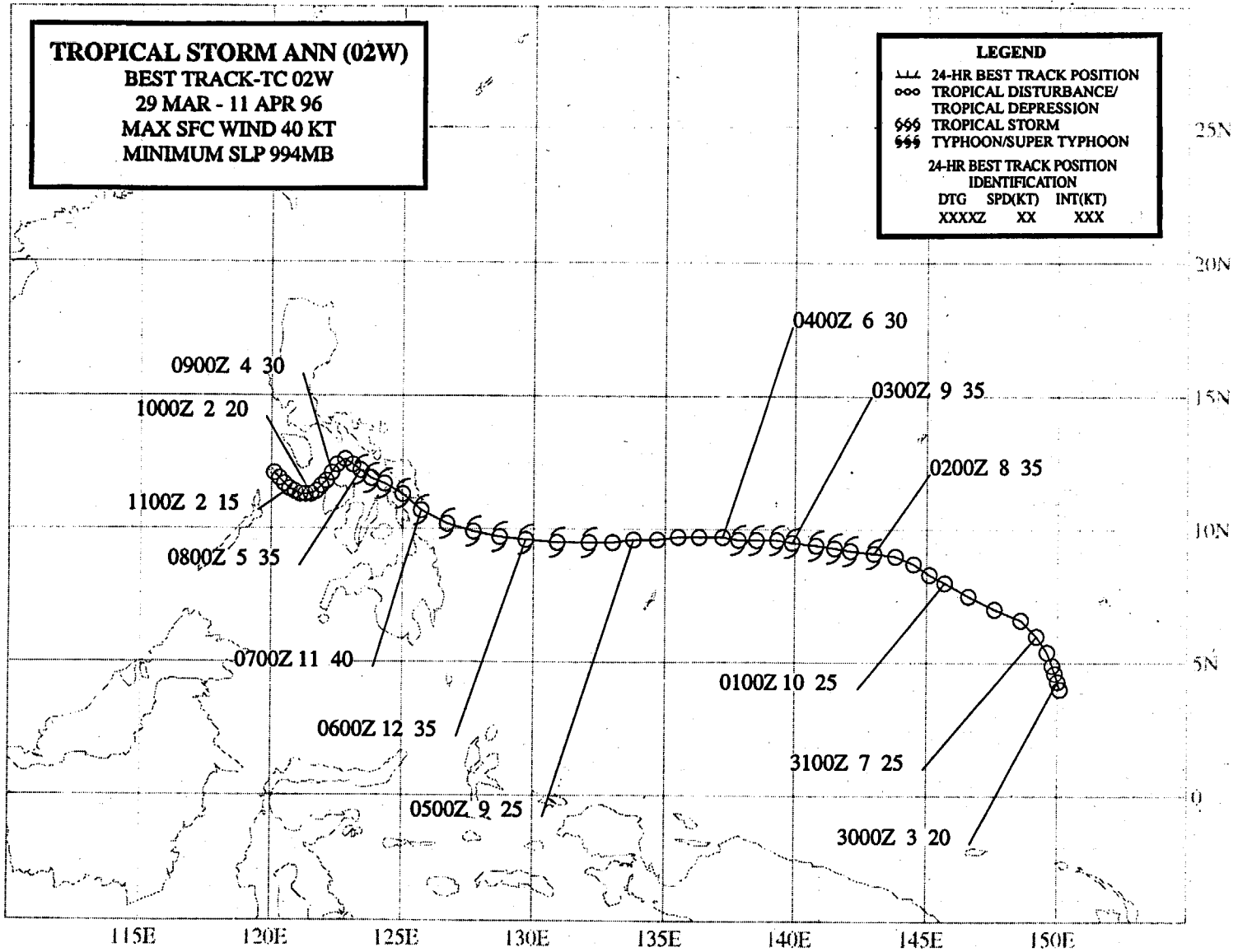
Figure 3-01-1 (a) The tropical disturbance which became TD 01W originated at the northeastern end of a monsoonal cloud band located along the equator. (b) After the equatorial deep convection collapsed, an area of deep convection consolidated at low latitude in the Philippine Sea. (c) TD 01W crosses the central Philippines at its peak intensity of 30 kt (15 m/sec) (Infrared GMS satellite imagery at 240531Z February, 261831Z February, and 010031Z March respectively).

TROPICAL STORM ANN (02W)

BEST TRACK-TC 02W
29 MAR - 11 APR 96
MAX SFC WIND 40 KT
MINIMUM SLP 994MB

LEGEND

- LLL 24-HR BEST TRACK POSITION
 - ooo TROPICAL DISTURBANCE/
TROPICAL DEPRESSION
 - 666 TROPICAL STORM
 - 999 TYPHOON/SUPER TYPHOON
- 24-HR BEST TRACK POSITION
IDENTIFICATION
DTG SPD(KT) INT(KT)
XXXXZ XX XXX



TROPICAL STORM ANN (02W)

I. HIGHLIGHTS

The first named TC of 1996 in the WNP, Ann formed in the Eastern Caroline Islands. While moving westward, Ann had two peaks of intensity, one while southwest of Guam, and the other as it went ashore in the Philippines. Deep convection associated with Ann deposited as much as five inches of rain in 24 hours on parts of Guam — the value of the monthly average rainfall for this dry-season month.

II. TRACK AND INTENSITY

The tropical disturbance that became Ann was first mentioned on the 280600Z March Significant Tropical Weather Advisory. Comments on this advisory included:

" ... An area of convection is located [in the Caroline Island group]. The area is located in a near equatorial trough with strong easterly trades to the north, while animated visible satellite imagery shows winds with a weak westerly component between the trough and the equator ..."

This disturbance moved steadily northwestward and fluctuations in the amount and organization of its deep convection prompted the JTWC to issue three Tropical Cyclone Formation Alerts (TCFA) prior to the first warning. The first TCFA was issued valid at 302000Z March when its deep convection became better organized. The second TCFA was issued, valid at 312000Z, when the disturbance failed to become better organized, but it was determined that conditions were still favorable for intensification. A third TCFA followed, valid at 012000Z April.

The first warning on Tropical Depression (TD) 02W was released, valid at 020000Z, when microwave imagery defined the low-level circulation and indicated the cyclone possessed wind speeds of 25 kt (13 m/sec). TD 02W was upgraded to Tropical Storm Ann 24 hours later based upon intensity estimates of 35 kt (18 m/sec) from both conventional satellite (i.e., infrared and visible) and microwave imagery. Ann was downgraded to a tropical depression at 040000Z when it became less organized in satellite imagery. A final warning was issued at 041200Z when it was thought that Ann was dissipating over water. The system was soon regenerated to TD 02W on the warning valid at 050000Z when the organization of its deep convection improved (Figure 3-02-1). On the warning valid at 050600Z, TD 02W was once again upgraded to Tropical Storm Ann. Traveling almost due westward along 10°N, Ann remained at minimal tropical-storm intensity until just before it passed through the Philippine archipelago where, at 061800Z, it reached its peak intensity of 40 kt (21 m/sec). Entering the central Philippines, Ann slowed its forward speed and dissipated as a significant tropical cyclone before it could cross into the South China Sea. The final warning was issued valid at 091200Z.

III. DISCUSSION

a. *Position inaccuracies*

During the five day period 010000Z through 060000Z April, the warning position (based primarily on satellite fixes) was displaced 90 to 120 nm (165 to 220 km) to the north of the final best track. The final best track for this period was placed further to the south after a careful re-examination of the synoptic data, coupled with a re-evaluation of the satellite imagery. It is not uncommon for the working best track of poorly defined, westward moving TCs at low latitude to be relocated southward in a final analysis (see the summary of Tropical Storm 35W).

b. Ann's southern twin?

As Ann moved westward toward the Philippines along 10°N, a Southern Hemisphere TC — Olivia (25S) — moved westward in near symmetry along 10°S (Figure 3-02-1). Although Ann and Olivia (25S) did not form as classical TC twins as described by Lander (1990), they were, for a short period, situated in near symmetry with respect to the equator as they both moved to the west along their respective near-equatorial trough axes. Ann later dissipated over the Philippines while Olivia recurved in the South Indian Ocean.

IV. IMPACT

No reports of damage or injuries were received. On the positive side, the peripheral rainbands of Ann contributed some much-needed dry-season rainfall to parts of the island of Guam.

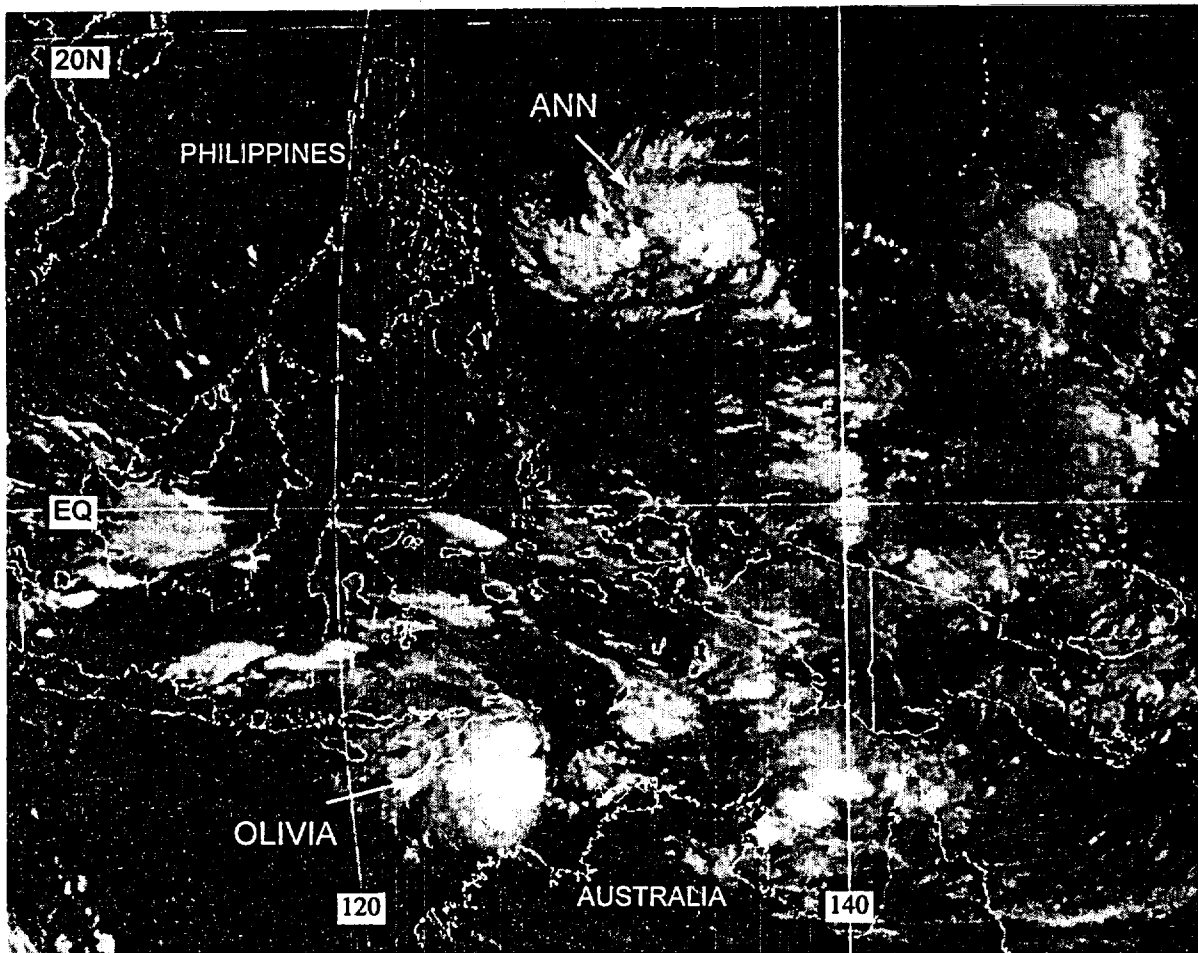
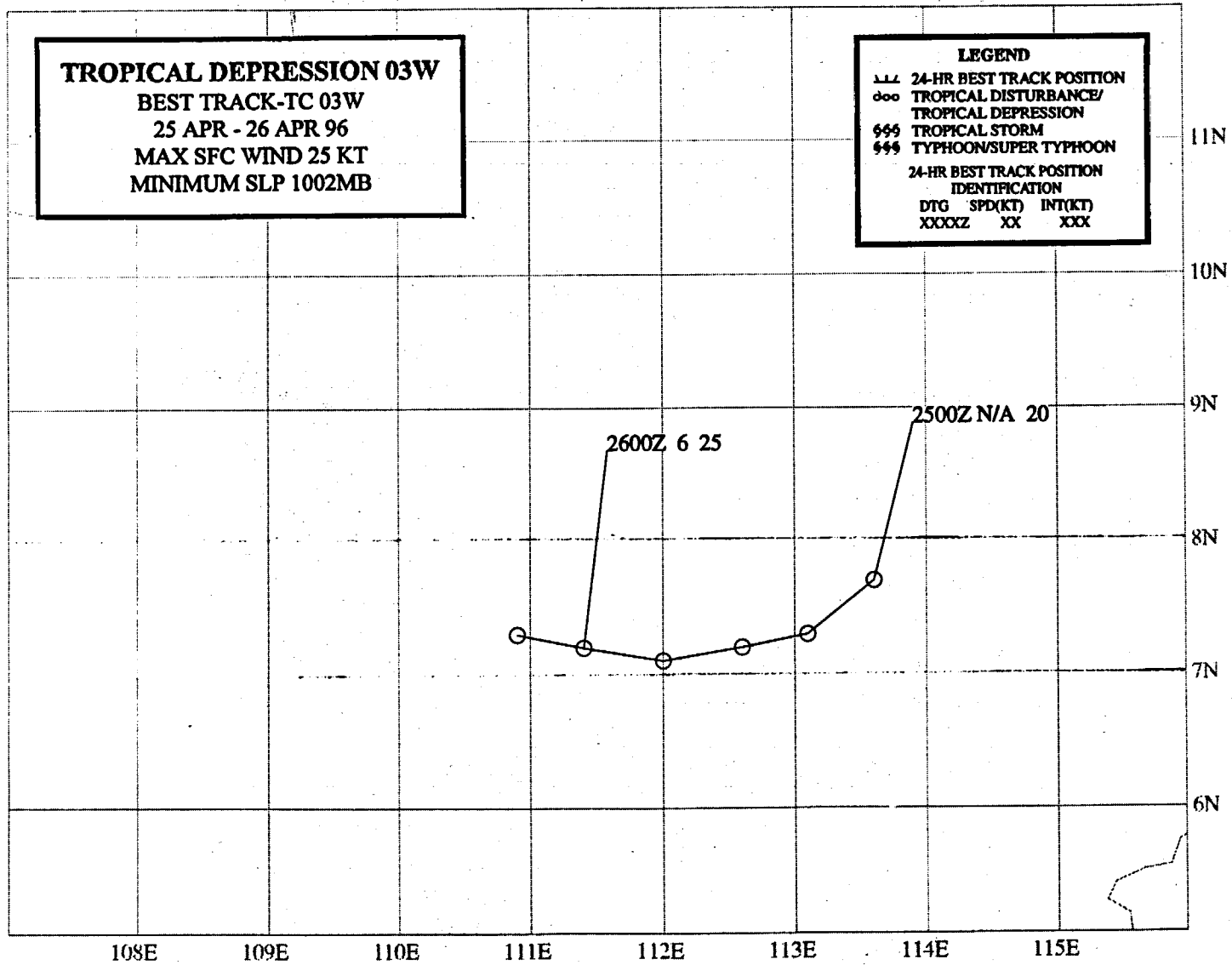


Figure 3-02-1 Tropical Storm Ann moves westward toward the Philippines in near symmetry with the westward moving TC Olivia (25S) (042224Z April infrared GMS imagery).



TROPICAL DEPRESSION 03W

Short-lived Tropical Depression (TD) 03W was first mentioned on the 250600Z April Significant Tropical Weather Advisory when satellite imagery and synoptic data showed that a low-level circulation center (LLCC) was associated with an area of persistent deep convection northwest of Borneo (Figure 3-03-1). As the persistent deep convection became better organized, and SSM/I-derived wind speeds of 30 kt (15 m/sec) were observed north and west of the LLCC, the JTWC issued a Tropical Cyclone Formation Alert, valid at 250900Z. Ship reports and satellite intensity estimates indicating wind speeds of 25 kt (15 m/sec) near the LLCC prompted the JTWC to issue the first warning on TD 03W, valid at 251200Z. TD 03W was short-lived, however, and the final warning was issued, valid at 260900Z, when the deep convection became disorganized.

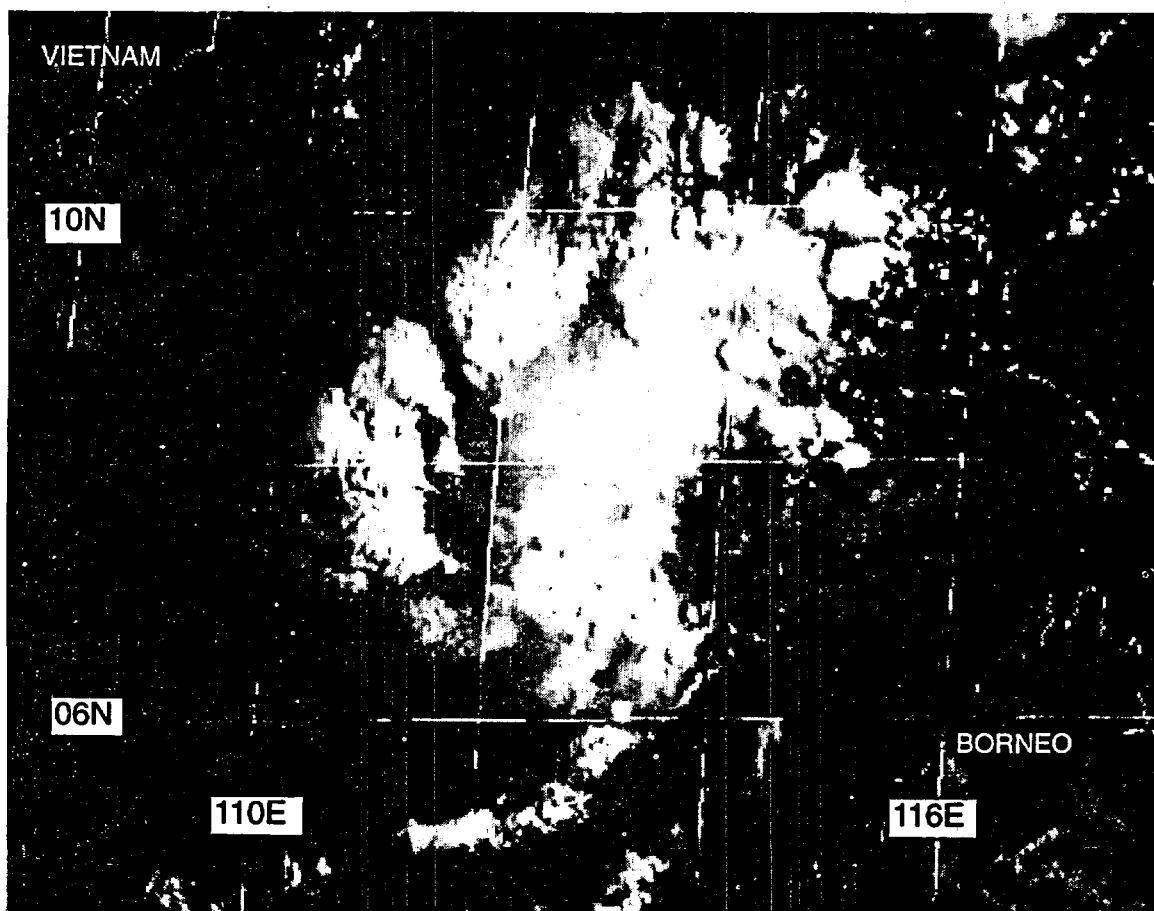
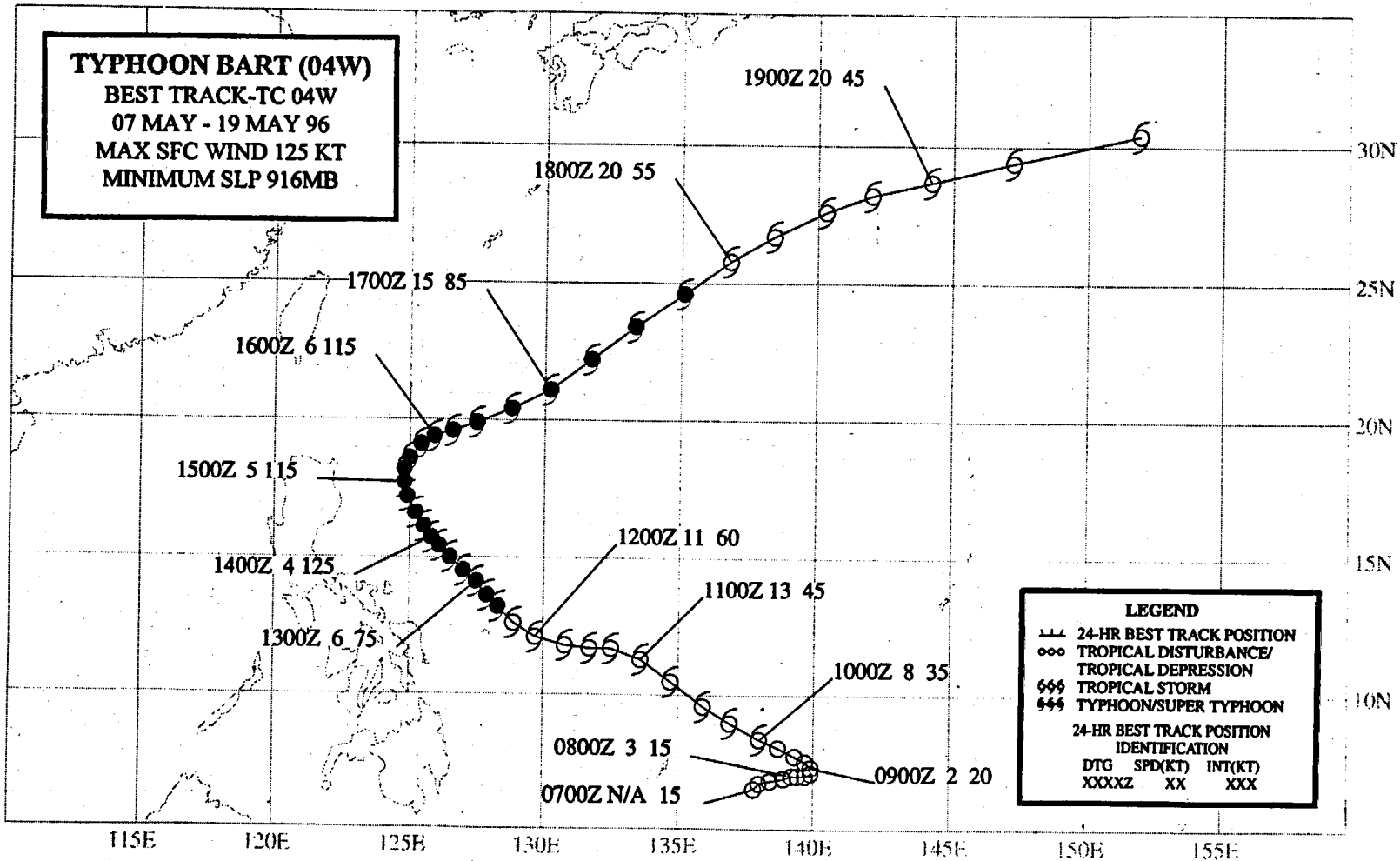


Figure 3-03-1 In the genesis stage of TD 03W, deep convection becomes loosely organized into a cyclonically curved band north and west of a partially exposed LLCC (250331Z April visible GMS imagery).



TYPHOON BART (04W)

I. HIGHLIGHTS

Bart was the first western North Pacific (WNP) TC of 1996 to reach typhoon intensity. It became a very intense typhoon, peaking at 125 kt (64 m/sec). Initially moving toward the Philippines, it turned to the north and remained at sea. Pronounced diurnal variations in Bart's central deep convection were noted.

II. TRACK AND INTENSITY

During the first week of May, the tropics of the WNP were dominated by low-level easterly wind flow accompanied by westerly wind flow aloft. A zonally-oriented band of convection stretched east-west across Micronesia south of 10°N. This convection was highly sheared from the west, and possessed a structure more characteristic of the convergence-zone cloud band that normally dominates the central North Pacific; that is, a linear band of disorganized mesoscale convective systems located along the confluence line of the northeast and southeast trades. This synoptic regime slowly changed, and by 05 May, monsoonal low-level westerly winds had penetrated into the WNP eastward to 140°E and south of 5°N. Accompanying the arrival of the monsoonal westerlies, amounts of deep convection increased in the southern portion of the Philippine Sea, and the cirrus outflow from this region became organized into a pattern indicative of an anticyclone aloft.

As amounts of deep convection began to increase in this area, the region of persistent deep convection that became Bart was first noted on the Significant Tropical Weather Advisory valid at 050600Z May. Remarks on the advisory included:

"Convective activity (near 4°N 136°E) has increased.... Visible satellite imagery and synoptic data indicate the presence of a weak circulation beneath diffluent upper-level winds. Surface and gradient level (3000 ft) analysis indicate 10-knot westerly winds along the equator enhancing surface convergence. . . . Minimum sea level pressure is estimated to be 1007 mb. . . ."

For the next four days, this disturbance — which now possessed the characteristics of a monsoon depression (see definitions section) — was slow to gain organization (e.g., well-defined low-level cloud lines, and persistent central convection). Based upon satellite imagery showing the system had acquired a small area of persistent central deep convection associated with well-defined low-level cloud lines, a Tropical Cyclone Formation Alert (TCFA) was issued valid at 090300Z May. Shortly after the TCFA was issued, cloud-top temperatures of the area of central deep convection became colder on infrared satellite imagery, and the first warning on Tropical Depression (TD) 04W was issued valid at 090600Z. Based upon indication of some shearing from the east, and implications of the structure of the system (i.e., a monsoon depression), a slower than normal rate of intensification was forecast.

Eighteen hours later (100000Z), TD 04W was upgraded to Tropical Storm Bart, based upon an improved satellite signature (an increase in the areal extent of very cold central convection), and upon the indication of 35-kt (18-m/sec) surface wind speeds from microwave imagery. A gradual turn from a westward motion to a more northward track was indicated on this warning — a track that would now spare the Philippines a landfall. With relatively low environmental shear, Bart was now forecast to intensify at a normal rate and become a typhoon in 48 hours (i.e., at 120000Z).

Evolving a classic banding-type eye (Dvorak, 1984) (see definitions section), Bart was upgraded to a typhoon at 121200Z. After becoming a typhoon, Bart began to intensify more rapidly, and reached its peak intensity of 125 kt (64 m/sec) at 140000Z (Figure 3-04-1). The estimated fall

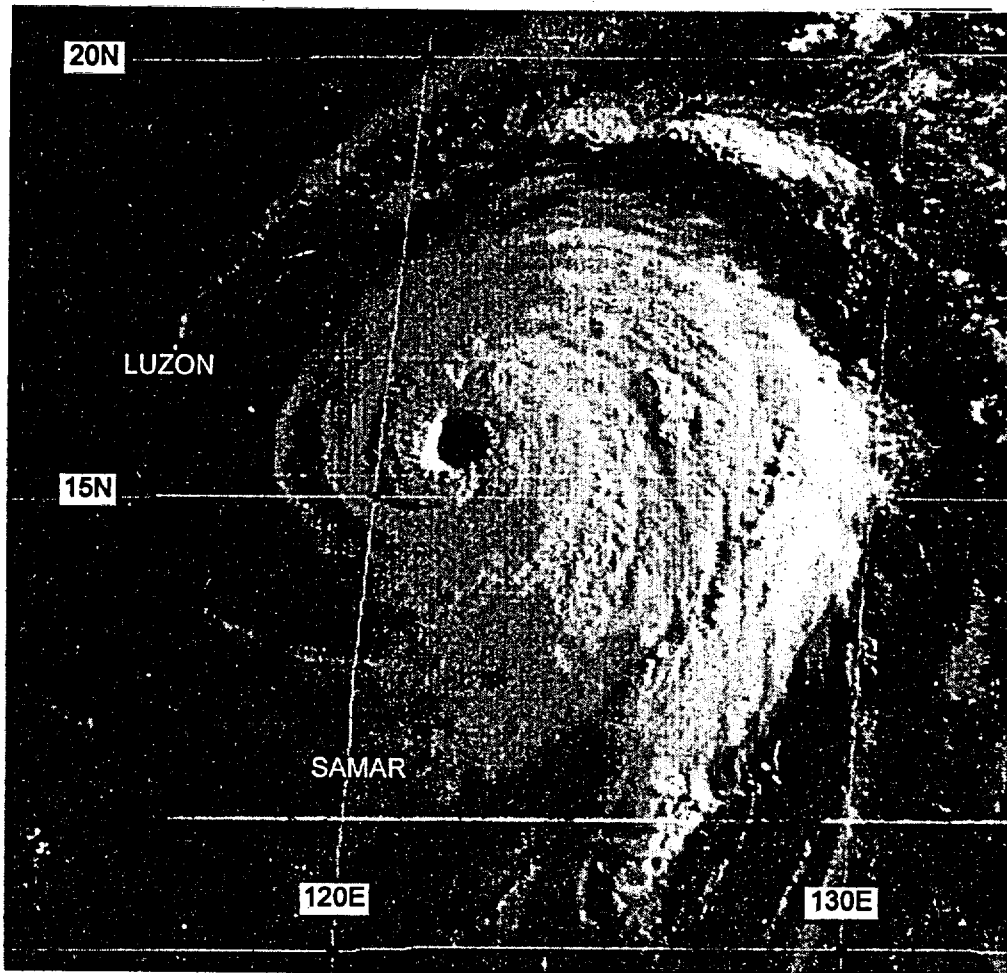


Figure 3-04-1 Bart reaches its peak intensity (132131Z May GMS visible imagery).

of central pressure of 52 mb during the 24-hour period, 130000Z to 140000Z, was sufficient to be classified as rapid intensification (Holliday and Thompson, 1979) (see definitions section).

Twenty-four hours after reaching peak intensity (i.e., at 150000Z), Bart reached its point of recurvature at 18°N, which is the climatological mean latitude of recurvature during May (Shanghai Typhoon Institute, 1990). Following recurvature at 150000Z, Bart did not begin to significantly accelerate until after 170000Z. Also during this period of slow east-northeast motion, its intensity fell only gradually. As Bart began to accelerate on 17 May, its intensity began to decrease — falling below typhoon intensity after 171800Z. On 18 May, its speed of forward motion increased to 20 kt (37 km/hr), and Bart began to shear while undergoing extratropical transition. The final warning was issued valid at 181800Z as Bart lost all its central deep convection and completed its extratropical transition.

III. DISCUSSION

Use of digital Dvorak (DD) numbers

One of the utilities installed in the MIDDAS satellite image processing equipment is an automated routine for computing Dvorak "T" numbers for TCs that possess eyes. The routine, developed by Zehr (personal communication) and programmed by Schaeffer (personal communication), adapts the rules of the Dvorak technique as subjectively applied to enhanced-infrared imagery (Dvorak, 1984) in order to arrive at an objective T number, or "digital Dvorak" T number (hereafter

referred to as DD numbers). Infrared imagery is available hourly from the GMS satellite, and hourly DD numbers were calculated for all of the typhoons of 1996.

The DD numbers presented herein are experimental, and methods for incorporating them into operational practice are being explored. In some cases, the DD numbers differ substantially from the warning intensity and also from the subjectively determined T numbers obtained from application of Dvorak's technique. The output of the DD algorithm, when performed hourly, often undergoes rapid and large fluctuations. The fluctuations of the DD numbers may lay the ground work for future modifications to the current methods of estimating tropical cyclone intensity from satellite imagery. The discussion of the behavior of the time series of the DD numbers for Bart, and for some of the other typhoons of 1996, is intended to highlight certain aspects of the DD time series that may prove to have important research and/or warning implications.

In Dvorak's 1975 and 1984 papers, he advises that the intensity estimation from satellite imagery be made at 24-hour intervals in order to remove any possible diurnal cycles that the TC might be undergoing. Dvorak further claims that the intensity of a TC is not influenced by diurnal changes in the central convection. Diurnal variations of convection reported to occur in TCs are similar to those reported to occur over the marine tropics in general: a peak in the amount of very cold cloud tops during the early morning hours with warmer cloud-top temperatures during the afternoon (Dvorak, 1985; Zehr, 1992). Observations by Black and collaborators (e.g., Black, 1983;

Black et al., 1986; Black and Marks, 1987) show that major cold convective eruptions in TCs tend to be initiated in the early morning.

Bart is one of only a few cases during the past two years in which a strong diurnal cycle can be found in the time series of its DD numbers (Figure 3-04-2). Although the DD number is based upon both the cloud-top temperature of the eye-wall cloud and the temperature within the eye, the strong diurnal cycle in Bart's DD time series (Figure 3-04-3) is certainly linked to a diurnal cycle of the eye-wall cloud-top temperatures. The DD time series of Bart has an unusually strong diurnal cycle when compared with those of other typhoons of 1996 and with those typhoons of 1995 for which the DD time series was compiled (see the 1995 ATCR). Consistent with Dvorak's rules, Bart's warning and best track intensities do not contain the large diurnal fluctuations that appear in its DD time series.

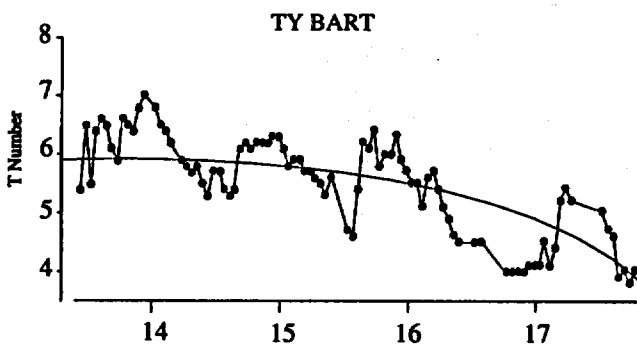


Figure 3-04-2 Bart's DD time series for the period 131030Z May through 171530Z May.

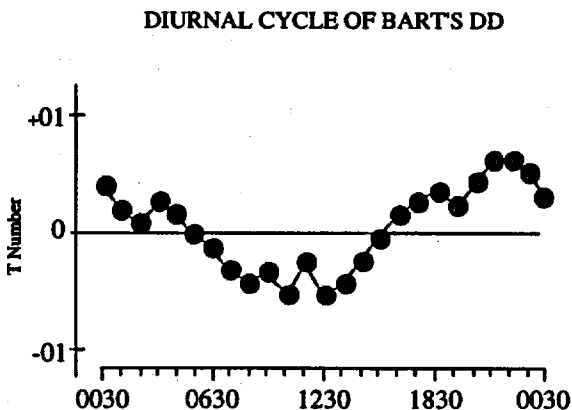
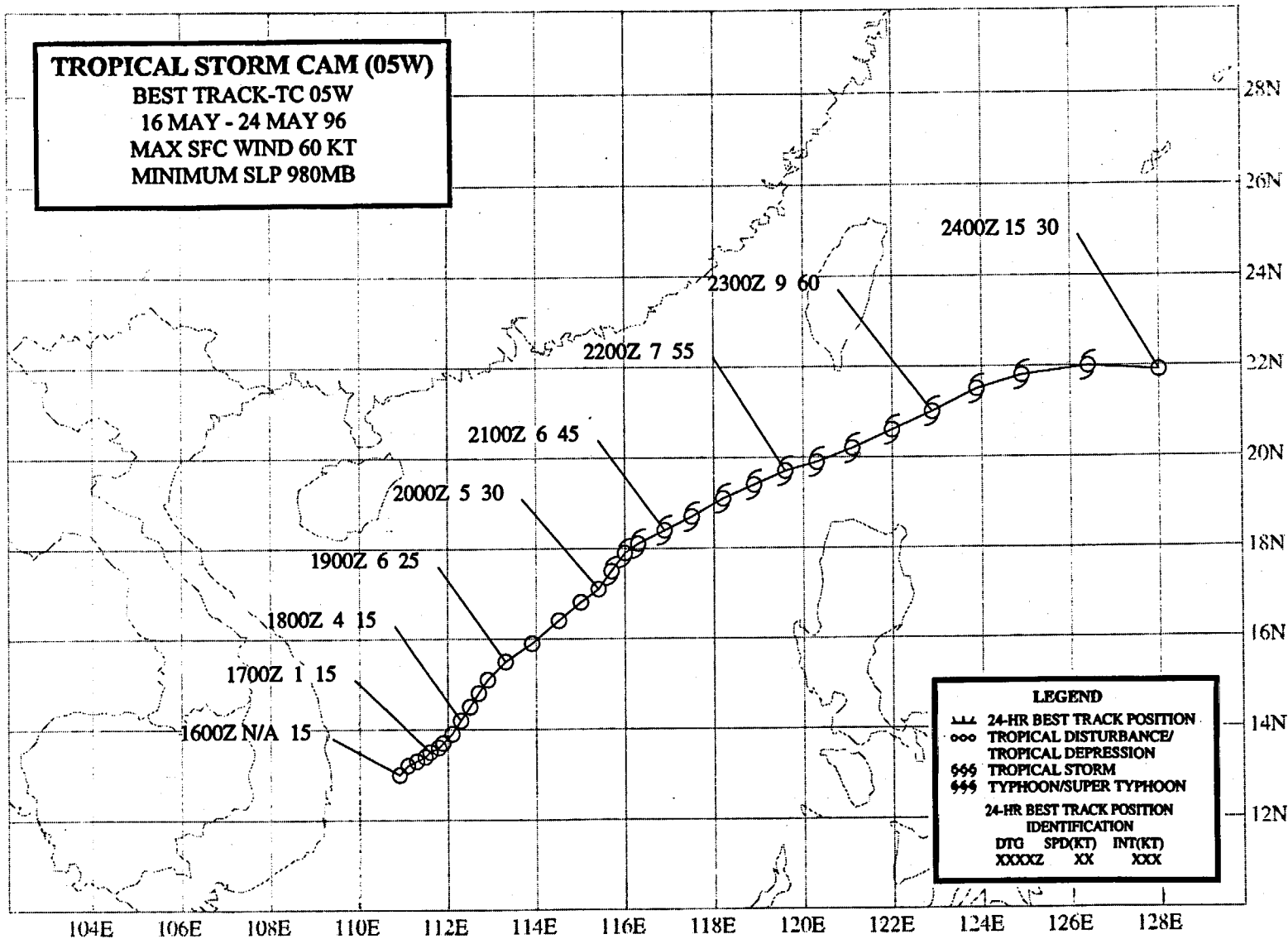


Figure 3-04-3 The diurnal cycle of Bart's DD time series as obtained by averaging the DD numbers at each hour during the period 131030Z May through 160930Z.

IV. IMPACT

No reports of significant damage or injuries were received at the JTWC.



TROPICAL STORM CAM (05W)

I. HIGHLIGHTS

Originating from a monsoon depression in the South China Sea (SCS), Cam moved toward the east-northeast for its entire life. While at peak intensity, it passed through the Luzon Strait and then slowly weakened as it drifted eastward into the Philippine Sea and dissipated.

II. TRACK AND INTENSITY

As Typhoon Bart (04W) was moving eastward while located south of Japan, cloudiness began to increase in the southwesterly monsoon flow across the SCS and extended east-northeastward toward Bart. Most of the deep convection associated with this monsoon flow was located within the SCS in the form of a large ensemble of mesoscale convective systems (MCS). The ensemble of MCSs showed some signs of low-level organization around a weak low-level cyclonic circulation, and extensive cirrus outflow indicative of anticyclonic outflow aloft. These structural attributes are typical of a monsoon depression (see Appendix A and the Discussion). The system was first mentioned on the Significant Tropical Weather Advisory valid at 170600Z May. Remarks on this advisory included:

" . . . An area of convection is located [in the South China Sea]. . . . Satellite imagery and synoptic data indicate an area of strong convergence being driven by monsoon flow in a sharp trough. . . ."

The organization of the deep convection within this monsoon depression slowly improved, and a Tropical Cyclone Formation Alert was issued valid at 181630Z. The broad circulation center of this system, as defined by low-level cloud lines and by the center of symmetry of the extensive cirrus outflow, appeared to be drifting very slowly toward the northeast.

Further improvements in the low-level organization coupled with a consolidation of persistent convection closer to the low-level circulation center (Figure 3-05-1) prompted the JTWC to upgrade the system to Tropical Depression (TD) 05W on the warning valid at 181800Z. Slow northeastward motion was occurring (and was forecast to continue), as deep southwesterly monsoonal flow dominated the steering.

During the daylight hours of 20 May, the convection near the center of TD 05W increased and deepened (i.e., expanded and became colder on infrared satellite imagery). The primary and peripheral cloud bands became more tightly curved and better organized around the low-level circulation center (LLCC) (Figure 3-05-2). Given these improvements in the satellite signature, TD 05W was upgraded to Tropical Storm Cam on the warning valid at 200600Z. Motion continued toward the northeast under the influence of southwesterly steering that was dominated by strong monsoon southwest winds to the south of the system.

Continuing on a relatively slow east-northeast track, Cam intensified. The peak intensity of 60 kt (31 m/sec) occurred as Cam moved through the Luzon Strait on the morning of 23 May. At this time, infrared satellite imagery (Figure 3-05-03a) indicated a tightly wound primary cloud band, and visible satellite imagery (Figure 3-05-03b) indicated the presence of a ragged eye.

After passing through the Luzon Strait, Cam accelerated eastward within deep westerly flow in the subtropics. It also weakened under the influence of westerly shear. The final warning was issued valid at 240000Z as the remnants of Cam entered the mei-yu front (which stretched eastward from Taiwan) and dissipated.

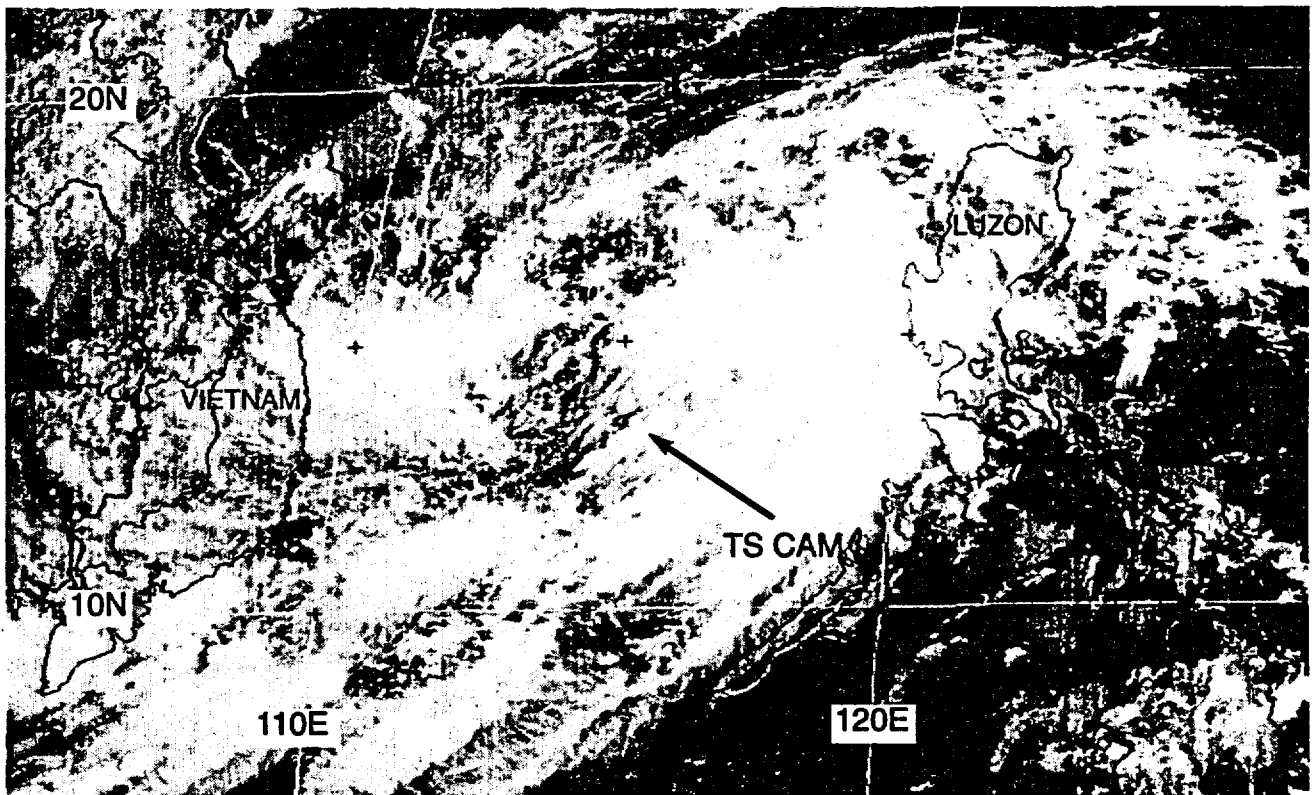


Figure 3-05-1 Near the time of the first warning, the disturbance that became Cam is organized as a monsoon depression (182331Z May visible GMS imagery).

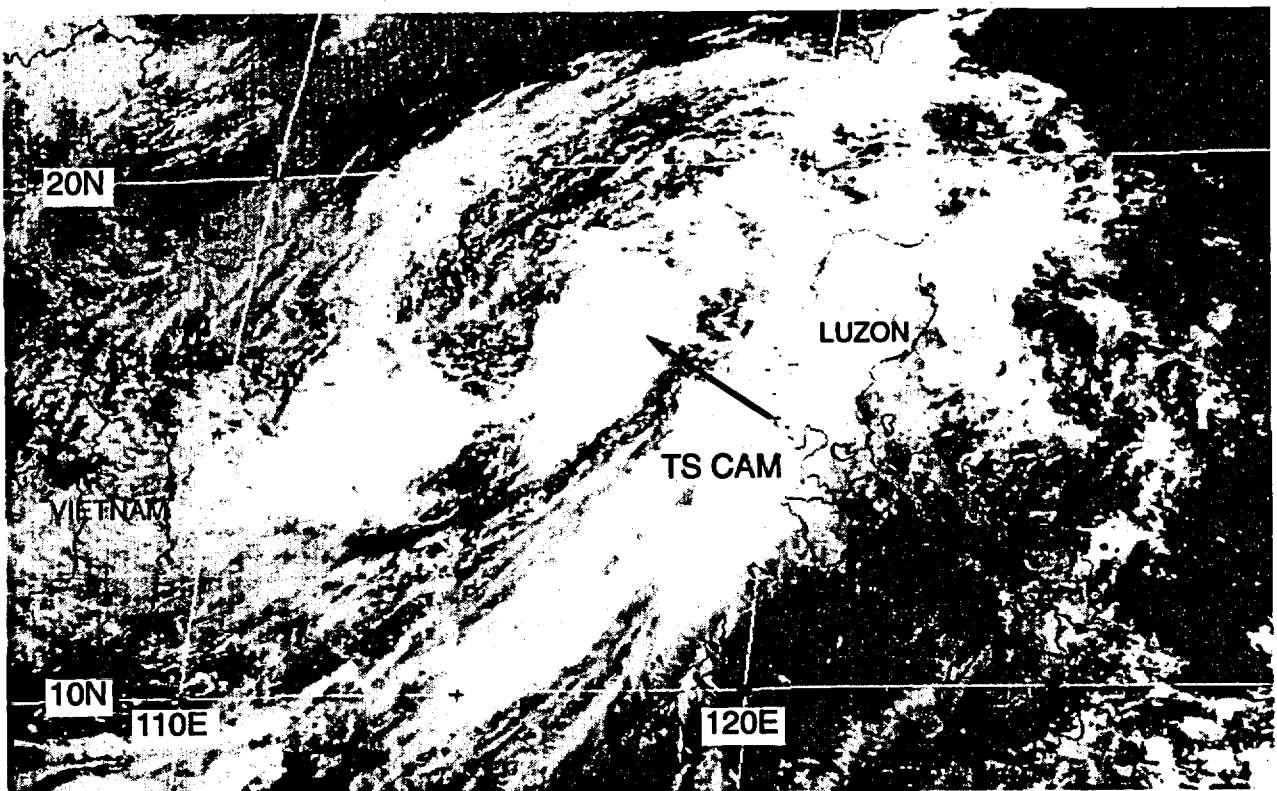


Figure 3-05-2 Deep convection has consolidated near the low-level circulation center marking the transition of the pre-Cam monsoon depression into a tropical storm (192331Z May visible GMS imagery).

III. DISCUSSION

a. *The Monsoon Depression*

Dvorak (1975, 1984) developed techniques for estimating the intensity of TCs from satellite imagery. His techniques are now used worldwide. The TC pattern types identified by Dvorak will be referred to as conventional TCs. In the Dvorak classification scheme, persistent deep convection must be located near the LLCC in order to initiate classification. The intensity of the TC is determined by several properties of the deep convection (e.g., the proximity of the low-level circulation center to the deep convection, the size of the central dense overcast, the cloud-top temperatures and

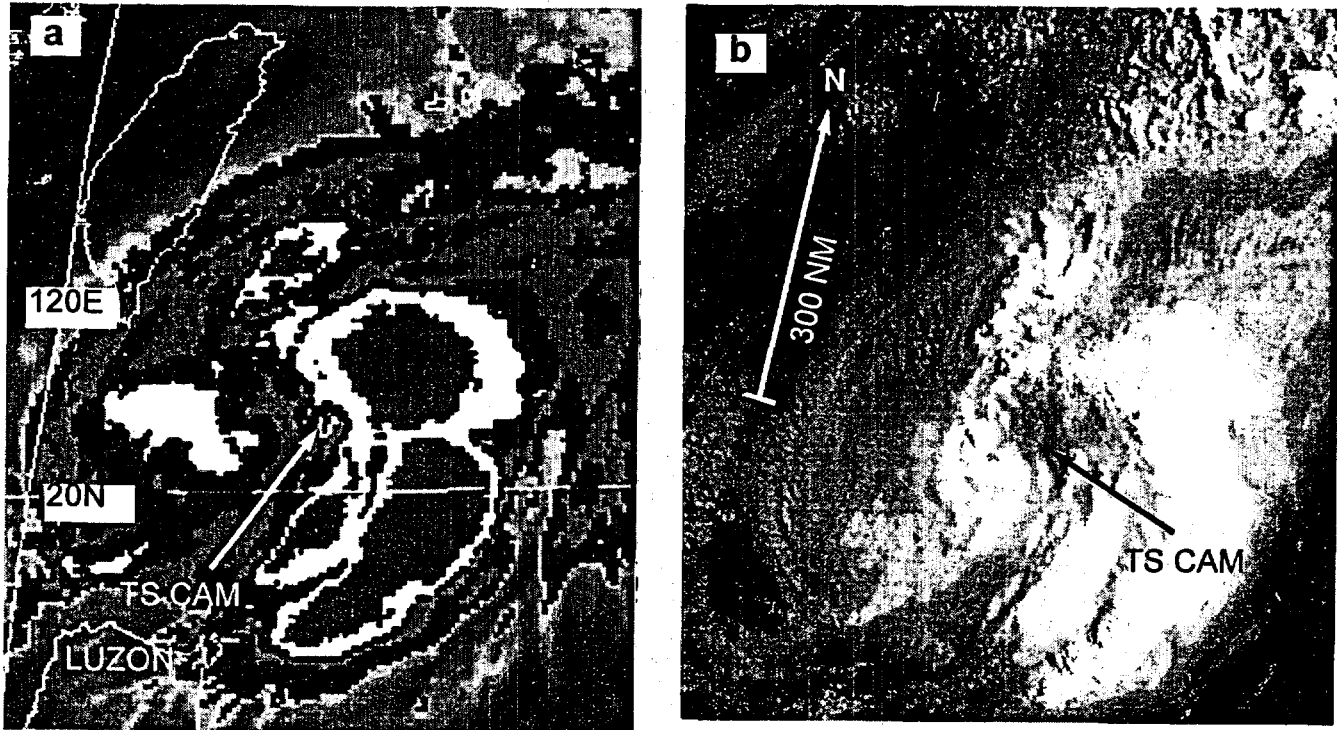


Figure 3-05-3 Cam at peak intensity: (a) 222331Z May enhanced infrared GMS imagery, and (b) 222331Z May visible GMS imagery.

horizontal width of the eye wall cloud, the width and extent of peripheral banding features). The basic TC data types identified by Dvorak are:

- 1) the "curved band" pattern (Figure 3-05-4a, b);
- 2) the "shear" pattern (Figure 3-05-4c, d);
- 3) the "central dense overcast" pattern (Figure 3-05-4e, f); and,
- 4) the "eye" pattern (Figure 3-04-4g, h).

This set of basic TC data types comprise the suite of conventional TCs.

Some conventional TCs that form in the WNP start out as monsoon depressions. The monsoon depression is a type of cyclone in the tropics that differs in several ways from the conventional types of TCs as described in Dvorak's work. The canonical monsoon depression forms over the northern Bay of Bengal in summer, and tracks west-northwestward across northeastern India (Ramage, 1971). These monsoon depressions have been studied for decades (e.g., Ramanathan and Ramakrishnan, 1932; Desai and Koteswaram, 1951; and Ramaswamy, 1969). Later, it was realized that monsoon depressions with structures similar to those of the Indian monsoon depressions occur in the Australian tropical region (Davidson and Holland, 1987), in the tropics of the western North

Pacific (JTWC, 1993), and over the deep tropics of Africa. The monsoon depression differs from conventional TCs in some respects:

- 1) very large size (the outer-most closed isobar may have a diameter on the order of 1000 km);
- 2) a lack of persistent deep convection near the LLCC (most of the deep convection in monsoon depressions is loosely organized in clusters or bands displaced from a few to several hundred kilometers from the low-level circulation center); and,
- 3) a low-level wind distribution that features a 200-km diameter light-wind core which may be partially surrounded by areas of gales or even storm force winds.

Because of the structure of monsoon depressions (e.g., their lack of persistent central deep convection), the use of Dvorak's techniques to estimate their intensity may be a misapplication. When applied to monsoon depressions, Dvorak's techniques yield intensities which are below the maximum winds that are usually present in areas displaced a few hundred kilometers from the LLCC. The intensity estimates yielded by Dvorak's techniques for monsoon depressions may, however, be representative of the lighter winds near their LLCCs.

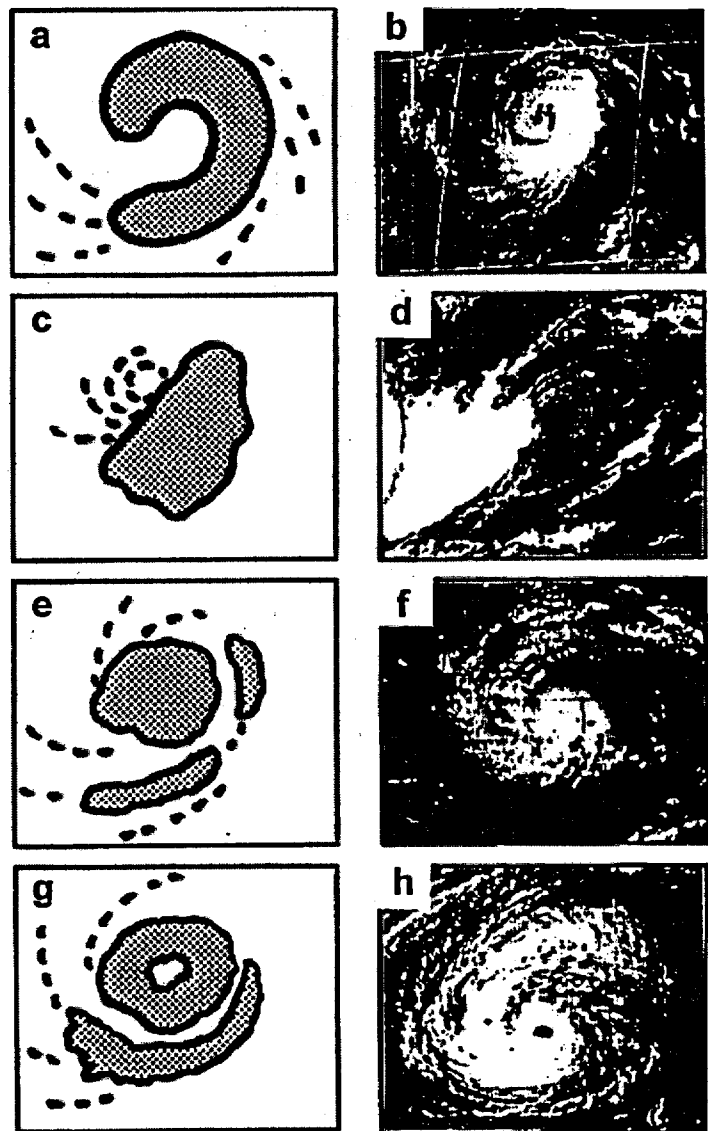


Figure 3-05-4 Schematic illustration (left column) and representative satellite imagery (right column) of Dvorak's (1975) basic tropical cyclone data types: (a,b) the "curved band" pattern; (c,d) the "shear" pattern; (e,f) the "central dense overcast" pattern; and, (g,h) the "eye" pattern.

Monsoon depressions can evolve into conventional TCs. As they slowly intensify, many monsoon depressions observed over the WNP eventually acquire persistent central deep convection and become conventional TCs. An unresolved question remains concerning the transition of a monsoon depression into a conventional TC: does the monsoon depression become the conventional TC, or does a conventional TC form within the circulation of the monsoon depression?

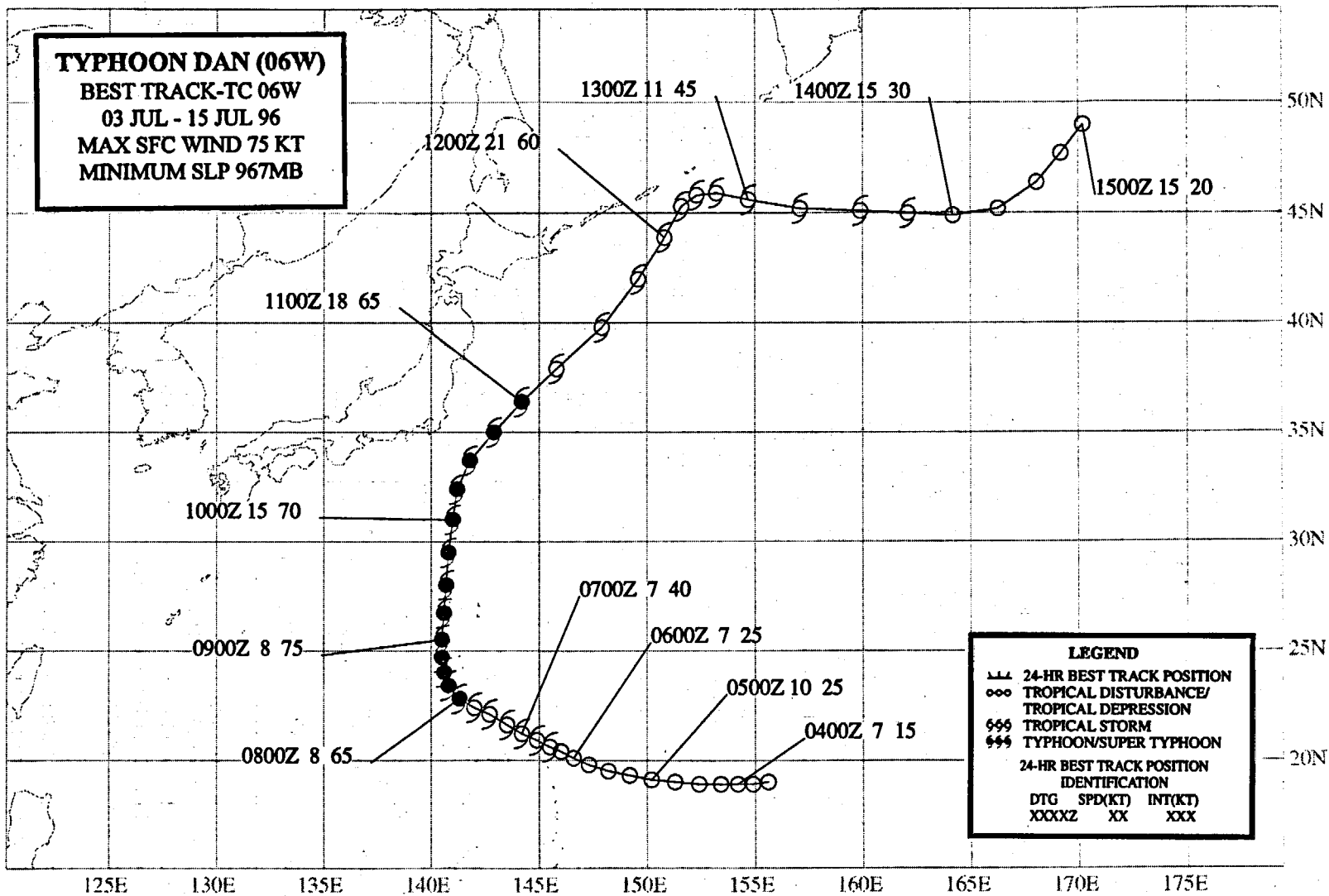
Cam began as a monsoon depression in the South China Sea. Initially it was a large ensemble of mesoscale convective systems embedded within a region of lowered sea-level pressure. It lacked persistent central deep convection, and the maximum winds in the system were displaced outward from the low-level circulation center, particularly to the south where monsoonal flow was strong. Eventually, as the system moved toward the northeast, circulation intensified and persistent central deep convection became established, marking its transition to a conventional TC.

b. *Unusual motion*

Persistent eastward motion of a TC at low latitude is unusual. Cam moved eastward for its entire track: forming near 13°N in the South China Sea it moved slowly toward the east-northeast for its entire track and eventually dissipated in the subtropics at 22°N. Most cases of eastward motion of a TC at low latitude in the WNP can be attributed to the influence of the monsoon circulation on the steering flow. In Cam's case, the deep southwesterly monsoon flow to its south was, for much of its track, the dominant flow asymmetry responsible for its northeastward motion. Monsoonal influences on TC motion form an important part of Carr and Elsberry's "Systematic and Integrated Approach" to TC forecasting (see Chapter 1).

IV. IMPACT

No reports of significant damage or injuries were received at the JTWC.



TYPHOON DAN 06W

I. HIGHLIGHTS

After Cam (05W) dissipated in the mei-yu front during the last week of May, there were no significant TCs in the WNP until early July when Dan formed. The tropical disturbance which became Dan was associated with the tropical upper-tropospheric trough (TUTT) and with cyclonic circulations (TUTT cells) within it. Scatterometer data received on 07 July resulted in JTWC doubling the radius of gales on the warning, and ship reports of 60 kt (31 m/sec) provided crucial ground truth for the intensity after Dan recurved and was becoming extratropical.

II. TRACK AND INTENSITY

During June, the WNP tropics were inactive. There were no significant TCs, amounts of deep convection were below normal, low-level winds were anomalously easterly and upper-level winds were anomalously westerly (Climate Prediction Center (CPC), 1996). In early July, the Southwest Monsoon remained inactive in the WNP with large-scale climatic wind anomalies similar to those of June. The tropical disturbance which became Dan was associated with the TUTT (see the discussion section), and first appeared as an inverted trough in the low-level easterly flow (Figure 3-06-1a, b). This disturbance was first mentioned on the 031700Z July Significant Tropical Weather Advisory. This advisory included the comments:

"... An area of convection is located near 21N 155E. Satellite imagery and synoptic data indicate a closed circulation exists within a... TUTT. Animated infrared satellite imagery indicates the circulation of this TUTT cell has likely built down to the mid-levels of the atmosphere. Convection near the center of the TUTT cell has improved over the past 6 to 12 hours..."

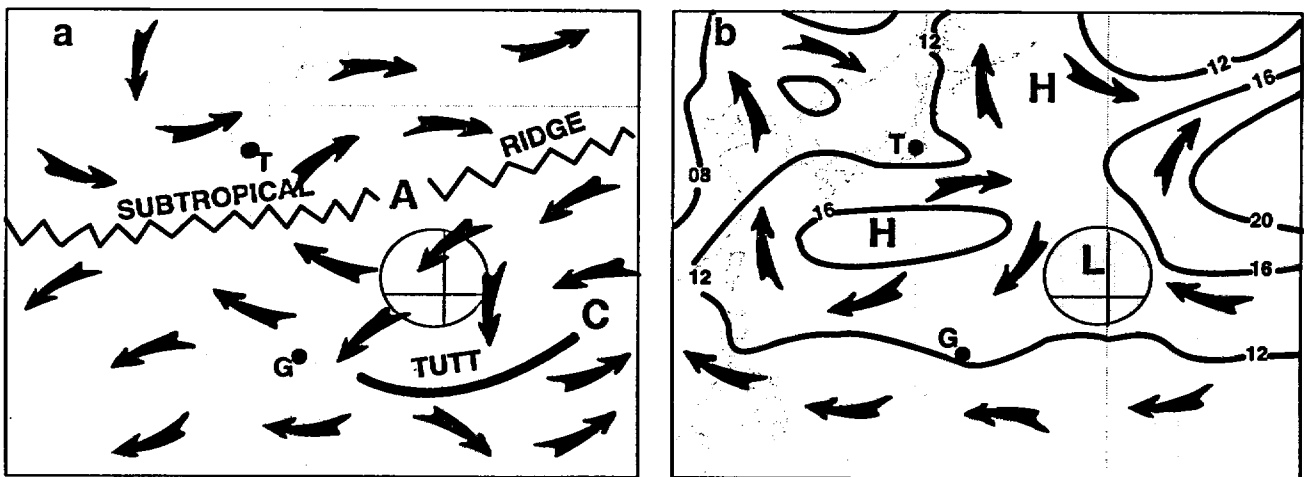


Figure 3-06-1 (a) An area of deep convection (shaded circle) forms in the diffluent northeasterly flow between the axis of the TUTT and the subtropical ridge at 200 mb. (b) At the surface, the area of deep convection (shaded circle) is associated with an inverted trough in the easterly flow southwest of a subtropical high. Arrows depict wind direction, A = anticyclone, C = TUTT cell, L = low pressure, G = Guam, and T = Tokyo. Analyses are adapted from the 021200Z July NOGAPS 200-mb and SLP products.

When synoptic data showed that a low-level cyclonic circulation was located beneath an area of organized deep convection, the JTWC issued a Tropical Cyclone Formation Alert, valid at 041951Z. At this time, the LLCC and most of the deep convection were located to the northeast of

a TUTT cell. The first warning on Tropical Depression (TD) 06W was issued, valid at 050000Z, based upon satellite intensity estimates of 25 kt (13 m/sec).

Dan intensified to a tropical storm at 061200Z, and at 080000Z became a typhoon (Figure 3-06-2). A scatterometer pass over the cyclone at 071304Z (Figure 3-06-3) resulted in a large increase in the radius of gales reported on the warning valid at 071800Z (see the discussion). After becoming a typhoon, Dan turned toward the north and reached its peak intensity of 75 kt (39 m/sec). Moving on a poleward-oriented track, Dan's intensity changed very little for three days following the peak: at 100000Z the intensity was 70 kt (36 m/sec), at 110000Z it was 65 kt (33 m/sec), and at 120600Z it was still at 60 kt (31 m/sec) despite reaching 45°N.

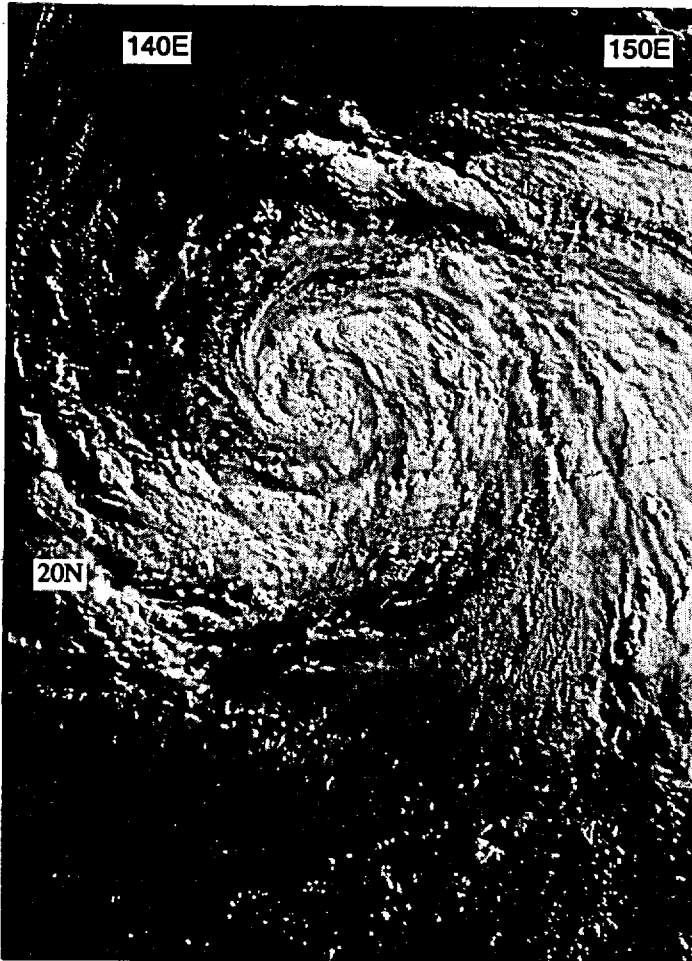


Figure 3-06-2 Dan becomes a typhoon (072040Z July visible DMSP imagery).

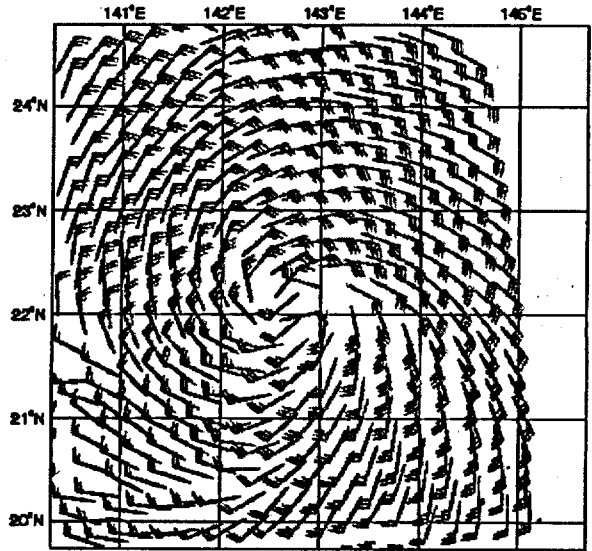


Figure 3-06-3 Scatterometer-derived wind speeds in a swath that passed over Dan (071304Z July ERS-2 scatterometer-derived marine surface wind speeds). This product was used in real time to expand the area of gales on the TC warning.

After 111200Z, satellite intensity estimates began to fall. Based on synoptic data, intensity estimates of Dan after 111200Z were kept significantly higher than satellite intensity estimates (Table 3-06-1). The problem of dropping the satellite intensity estimates far too low as a TC becomes extratropical is long-standing. During 1996, JTWC

satellite analysts developed and implemented a new technique for estimating the intensity of TCs which are undergoing extratropical transition (Miller and Lander, 1996) (see the discussion). The JTWC issued the final warning on Dan, valid at 120600Z, as the system moved eastward and completed its extratropical transition.

III. DISCUSSION

a. *TUTT-related genesis*

Dan (06W) originated and developed in association with a TUTT cell. Typical of TCs which develop in association with TUTT cells, Dan formed at a relatively high latitude (20°N), and as Figure 3-06-1 indicates, the system developed in the low-level easterly flow on the southwest flank of a subtropical high. For a more complete discussion of TUTT-related TC genesis, see Carlo's (33W) summary. In Carlo's (33W) case, and also in the case of Joy (12W), water-vapor imagery very clearly depicted the process of TC genesis associated with a TUTT cell. The formation of Dan (and also of Eve (07W)) in association with TUTT cells was more complicated than that of Carlo (33W) or Joy (12W), and its description is beyond the scope of this summary.

b. *Scatterometer aids diagnosis of wind distribution*

On the warning valid at 071800Z, the radius of 35-kt (18-m/sec) wind was nearly doubled from its value on the warning valid at 071200Z. This large change in the wind radius was based upon scatterometer data from the European Remote Sensing Satellite-2 (ERS-2) (Figure 3-06-3). Comments on the 071800Z warning included:

"... The most significant change in this warning compared to the previous warning is the sudden change of wind radii, which is based on satellite scatterometry data from an overhead pass of the European ERS-2 polar orbiter..."

The JTWC has access to scatterometer wind data, and has used it to help determine the position, intensity and wind distribution of TCs. Some drawbacks of the scatterometer data are its small swath width, 180° directional ambiguity, relatively coarse resolution, an upper limit on the wind speeds that it can accurately detect, and a low-speed bias. For a more detailed discussion of scatterometer data, see Rick's (22W) summary.

c. *On the intensity of TCs undergoing extratropical transition: the "XT" technique*

For many years, the JTWC has had a problem diagnosing the intensity of TCs as they undergo extratropical transition. In general, the application of Dvorak's techniques to these systems has resulted in intensity estimates that are significantly lower than what is reported by ships or land stations. An extreme example of this problem occurred during the approach of Seth (1994) to Korea which is highlighted in Seth's summary in the 1994 ATCR. Dan provided another good example of this problem: as it was becoming extratropical (Figure 3-06-4), the satellite intensity estimates fell to values that were later proven to be far too low when compared to ship reports (Table 3-06-1). Attempts to apply Hebert and Poteat's (1975) techniques for estimating the intensity of subtropical cyclones to these systems were not successful.

In order to address the problem of underestimating the intensity of TCs undergoing extratropical transition, satellite analysts at the JTWC in conjunction with ONR-supported researchers at the University of Guam devised a technique (Miller and Lander, 1996) for estimating the intensity of TCs undergoing extratropical transition. This technique yields XT (for extratropical transition) numbers that equate to wind speeds identical to Dvorak's T numbers of the same magnitude. The technique also defines the completion of extratropical transition. On the few independent cases for which it was applied during 1996 the technique appears to have worked well. Though operational, the technique may be refined as more cases are examined. Specific details are beyond the scope of this summary, and those interested are invited to request a copy of the Miller and Lander (1996) technique.

IV. IMPACT

Skirting east of Japan, Dan drenched the Tokyo metropolitan area with over 5 inches of rain, and over twice that much in the adjoining Chiba prefecture. High water stalled trains and flooded streets. In Chiba prefecture, 29 houses were evacuated and at least 200 were reported damaged by flooding.

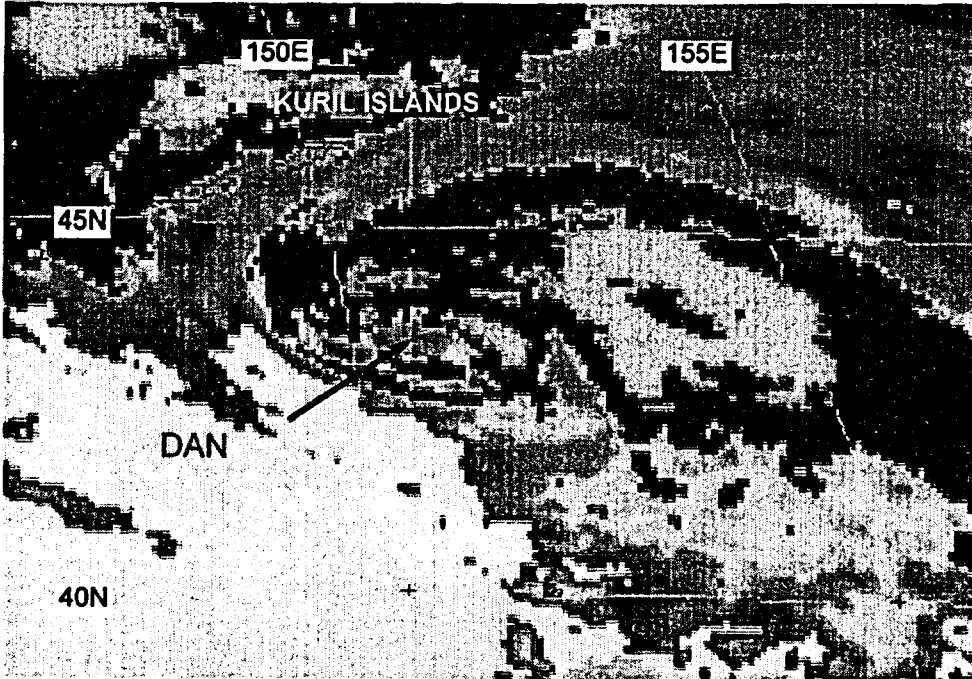
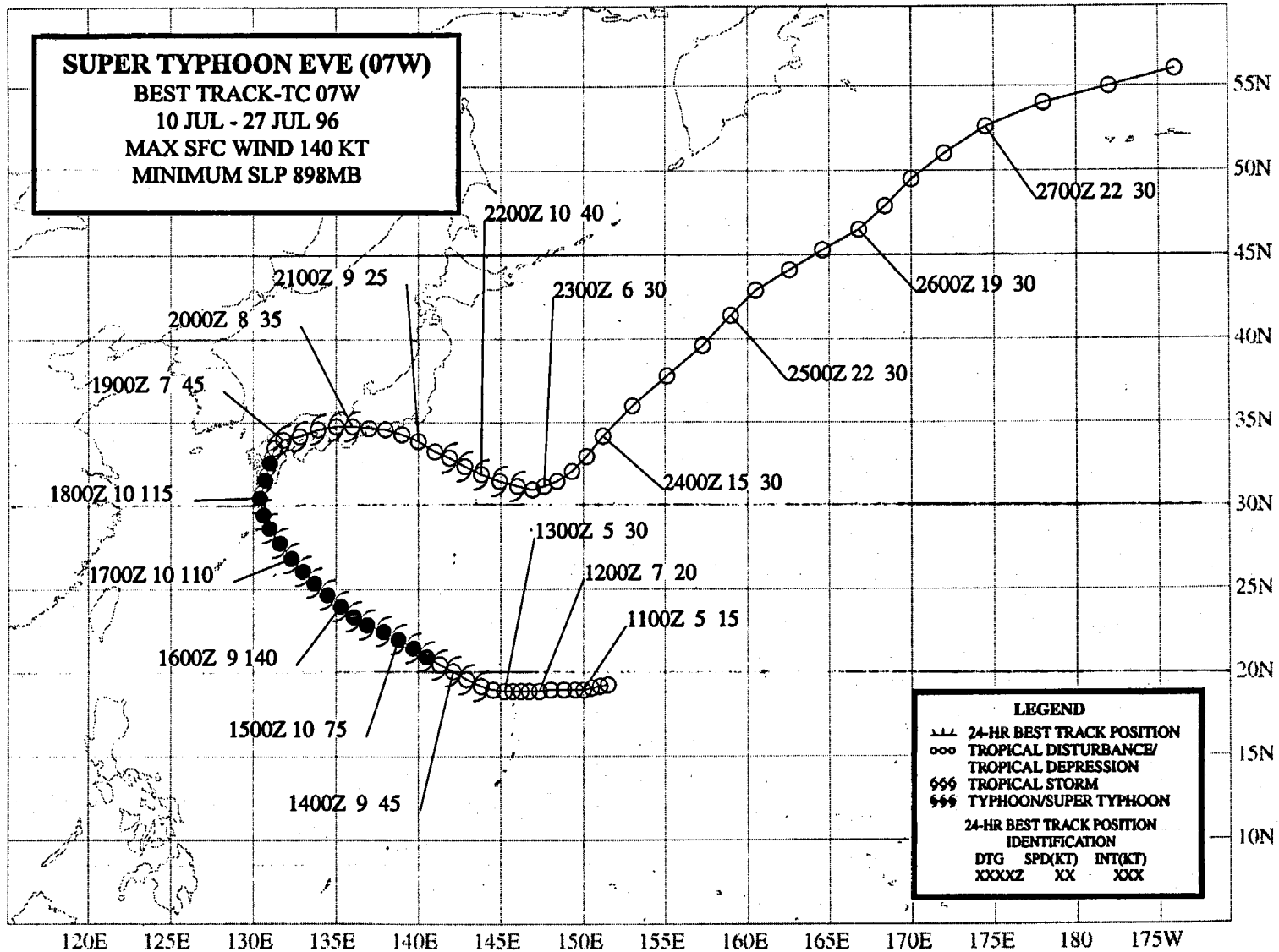


Figure 3-06-4 Dan begins its extratropical transition. Satellite intensity estimates as low as 35 kt (18 m/sec) at this time were far lower than ship reports of 60 kt (31 m/sec) used to support the best-track intensity (112031Z July enhanced infrared GMS imagery).

Table 3-06-1 Intensity estimates derived from satellite imagery during Dan's extratropical transition. In the code, T = Dvorak tropical numbers, ST = Hebert and Poteat subtropical numbers, and the number that follows the "/" is the current intensity which is always held higher when the TC is weakening over water.

Time (Z)	Code	Intensity (kt)	Best Track Intensity (kt)
101430	T 2.5/3.5	55	65
101432	T 2.5/3.5	55	65
101730	T 2.5/3.0	45	65
102014	T 2.5/3.0	45	65
102032	T 2.0/3.0	45	65
102330	T 2.5/3.5	55	65
110230	T 2.0/3.0	45	65
110407	T 2.5/3.0	45	60
110530	T 2.5/3.5	55	60
110717	T 2.5/3.0	45	60
110830	T 2.5/3.5	55	60
110832	T 1.5/2.5	35	60
111130	T 2.5/3.0	45	60
111432	T 2.0/2.5	35	60
112030	T 2.0/2.5	35	60
112002	ST 2.5/2.5	35	60
112032	T 2.0/2.0	30	60
112330	ST 3.0/3.0	45	60
120530	ST 3.0/3.0	45	60
120703	T 0.5/1.0	25	60
120830	ST 3.0/3.0	45	60



SUPER TYPHOON EVE (07W)

I. HIGHLIGHTS

Eve, like Dan (06W) which preceded it, originated in association with a TUTT cell. After undergoing explosive deepening, Eve became the first WNP super typhoon of 1996. The typhoon passed through the northern Ryukyu Islands and made landfall in southern Japan. Moving eastward over Japan, the system weakened before intensifying to tropical storm intensity after moving offshore.

II. TRACK AND INTENSITY

As Dan was recurving to the east of Japan, a TUTT cell formed to its southeast. A band of deep convection formed a "U" shape to the south of this TUTT cell (Figure 3-07-1). Although not mentioned until 120600Z July on the Significant Tropical Weather Advisory, the disturbance which

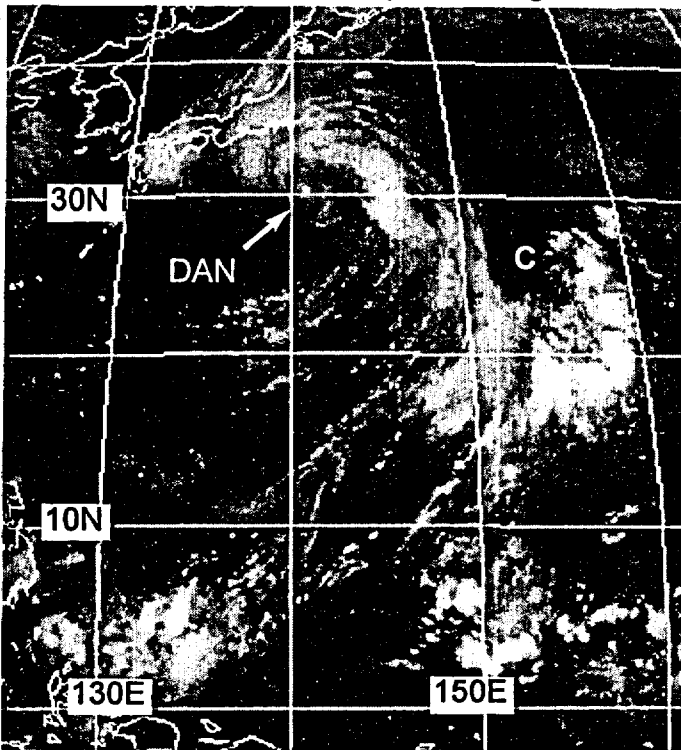


Figure 3-07-1 The tropical disturbance that became Eve originated from an area of deep convection to the south of a TUTT cell (C). This TUTT cell was, in turn, located to the southeast of the recurving Dan (06W) (091831Z July infrared GMS imagery).

at 160000Z it reached its peak intensity of 140 kt (72 m/sec) (Figure 3-07-3). Forming concentric wall clouds (Figure 3-07-4), the intensity decreased to 100 kt (51 m/sec) by 170600Z. Just prior to making landfalling at Kyushu, Japan, on 18 July, the eye once again became small and well defined, and the intensity increased to 115 kt (59 m/sec). The system made landfall at approximately 180300Z and began to weaken over the mountainous terrain of Kyushu. The system was downgraded to a tropical storm at 191200Z, and the final warning was issued, valid at 200000Z, as the system moved eastward over the main Japanese island of Honshu and weakened.

became Eve was tracked in post analysis back to the place where, at 100600Z, it consolidated in the TUTT-related area of deep convection. On 13 July, an area of persistent deep convection located about 300 nm (550 km) to the north of Guam, began to show signs of increasing organization. Synoptic data indicated that a low-level cyclonic circulation was located within this area of deep convection, and the JTWC issued a Tropical Cyclone Formation Alert valid at 130800Z July. During the night of 13 July, the persistent area of deep convection became well-organized, and satellite intensity estimates of 25 kt (13 m/sec) (later adjusted to 35 kt (18 m/sec) in post analysis) prompted the JTWC to issue the first warning on Tropical Depression (TD) 07W, valid at 131200Z.

When Eve formed a beautiful banding eye on the morning of 15 July (Figure 3-07-2), it was upgraded to a typhoon on the warning valid at 150000Z. From 150000Z to 160000Z, Eve underwent a period of explosive deepening (see the discussion section). At 151800Z, it became a super typhoon, and

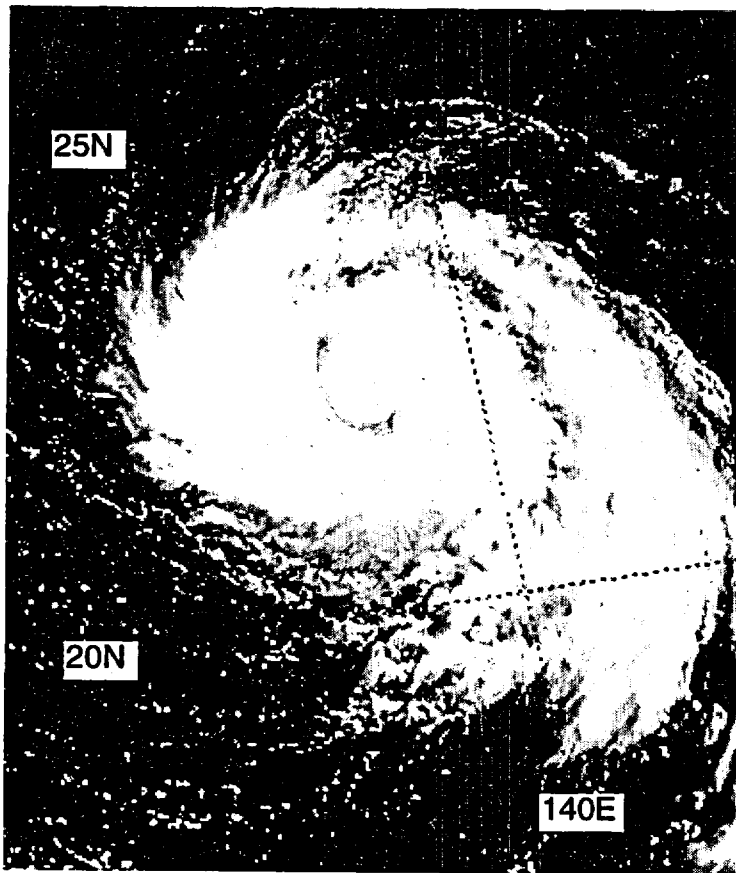
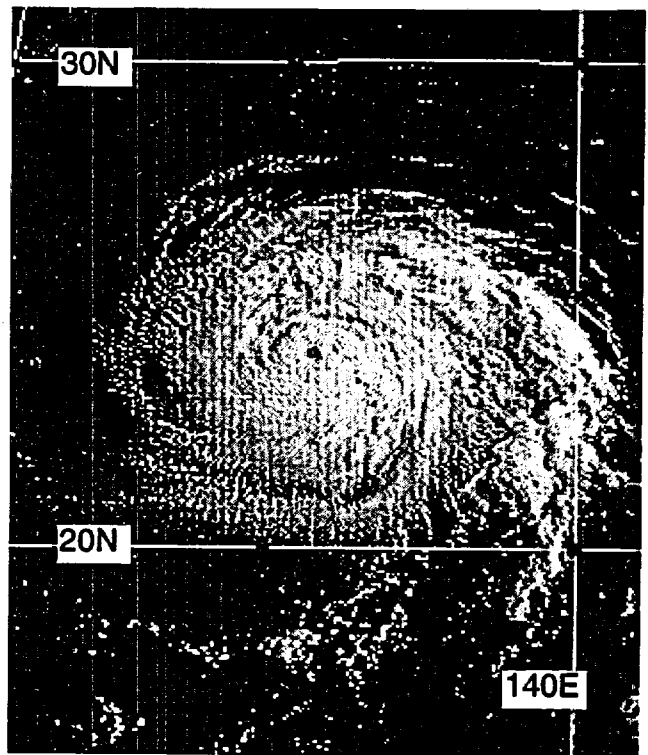


Figure 3-07-2 Eve forms a text-book quality banding eye pattern (150019Z July visible DMSP imagery).

Figure 3-07-3 Eve at its peak intensity 140 kt (72 m/sec) (152131Z July visible GMS imagery).



When the system moved over water to the east of Japan, it regenerated. A post analysis of synoptic data, and a reanalysis of satellite imagery (e.g., Figure 3-07-5), supported a regeneration to tropical-storm intensity for the 24-hour period 211200Z to 221200Z, with a maximum intensity of 40 kt (21 m/sec) at 211800Z. After 251200Z, all deep convection was sheared away from the LLCC, marking the completion of extratropical transition. The system was identifiable on satellite imagery as it tracked all the way to the Aleutian Island chain where hourly data from Shemya (WMO 70414) indicated a small pressure fall and a wind shift attributable to the remnants of Eve passing to the southeast on 27 July.

III. DISCUSSION

a. TUTT-related genesis

Eve, like Dan (06W) which preceded it by a week, originated in association with a TUTT cell. Typical of TCs which develop in association with TUTT cells, Eve formed at a relatively high latitude (20°N), and it formed in the cloud-minimum region north of the cloudiness associated with the monsoon trough. For a more complete discussion of TUTT-related TC genesis, see Carlo's (33W) summary. In Carlo's (33W) case, and also in the case of Joy (12W), water-vapor imagery very clearly depicted the process of TC genesis from a TUTT cell.

b. Explosive deepening

Between 150000Z and 160000Z July, Eve's intensity increased from 75 kt (39 m/sec) to 140 kt (72 m/sec). The equivalent 24-hour pressure fall (using Atkinson and Holliday's (1977) wind-pressure relationship) was 70 mb, resulting in an average decrease of 2.92 mb/hr. This rate of pressure fall easily qualifies as a case of explosive deepening which is described by Dunnavan (1981) as a decrease in the minimum sea-level pressure of a TC of 2.5 mb/hr for at least 12 hours or 5 mb/hr for at least six hours. If one honors the digital Dvorak (DD) time series at this time (Figure 3-07-6), the rate of intensity increase is even more remarkable: the DD numbers at 150000Z were on the order of T 4.5, and then rose to their peak of approximately T 7.5 at 151800Z. The equivalent pressure fall using the DD

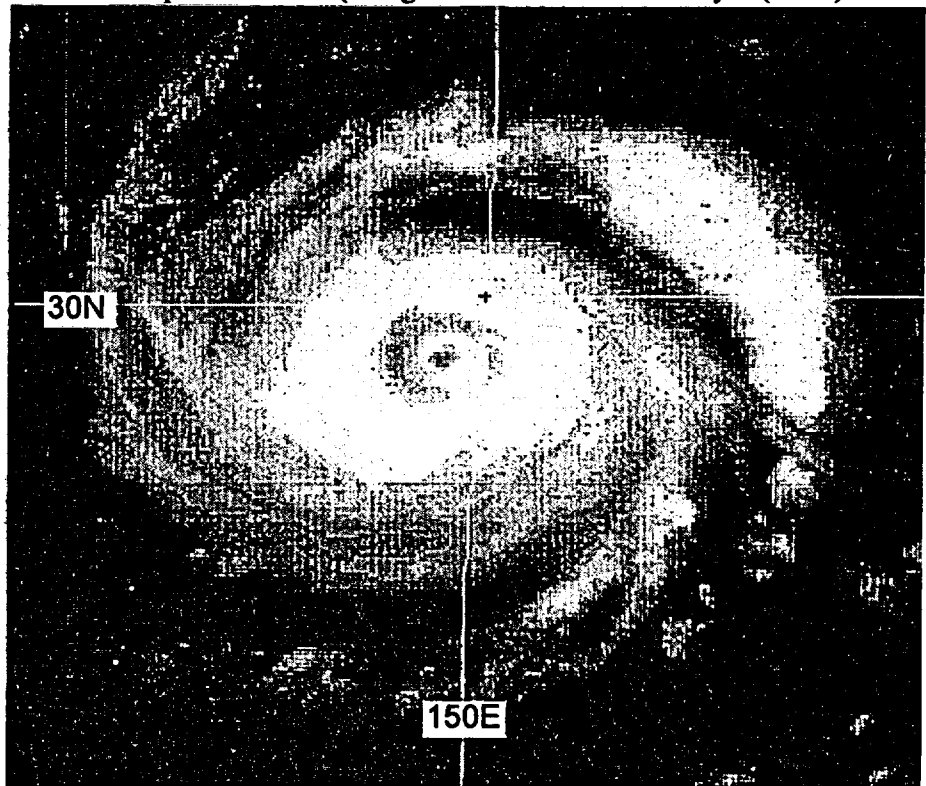


Figure 3-07-4 Shortly after reaching its peak intensity, Eve formed concentric eye walls. The relatively cloud-free moat between the eye walls resulted in a substantial drop in the default values of the DD number (160331Z July visible GMS imagery).

intensity estimates was 87 mb in 18 hours, resulting in an average decrease of 4.8 mb/hr. The explosive deepening was not anticipated, and 24-hour and 48-hour forecasts of Eve's intensity fell short by as much as 70 kt (36 m/sec) and 90 kt (46 m/sec) respectively during the two days prior to the event.

c. A discussion of Eve's DD time series

Infrared imagery is available hourly from the GMS satellite, and hourly DD numbers were calculated for all of the typhoons of 1996 (see Bart's (04W) summary for a detailed description of the DD algorithm installed on the JTWC's satellite image processing equipment). The discussion of the behavior of the time series of the DD numbers for Eve, and for some of the other typhoons of 1996, is intended to highlight certain aspects of the DD time series that may prove to have important research and/or warning implications.

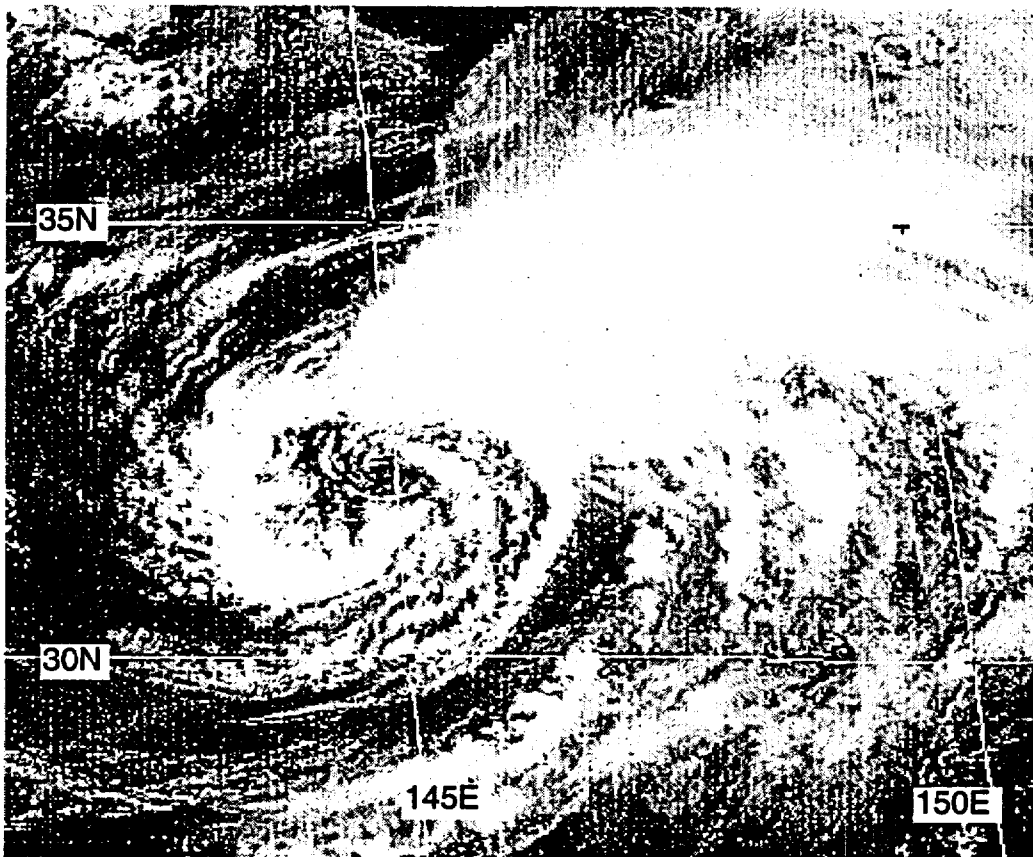


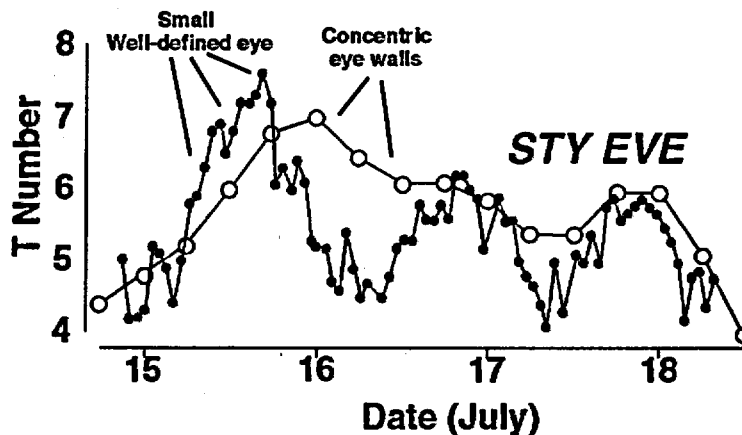
Figure 3-07-5
Exhibiting a Dvorak "shear" pattern type, Eve has regenerated and reached tropical-storm intensity after moving back over water to the east of Japan (220231Z July visible GMS imagery).

Eve is one of only a few cases during the past two years in which a strong diurnal cycle can be found in the time series of its DD numbers (Figure 3-04-6): higher DD numbers occur in the early morning hours (around 1800Z), and lower DD numbers occur in the late afternoon (around 0600Z). Although the DD number is based upon both the cloud-top temperature of the eye-wall cloud and the temperature within the eye, the apparently cyclical fluctuations in Eve's DD time series are linked more to major structural changes of the TC rather than fluctuations in the cloud-top temperatures of an otherwise stable cloud pattern. During the rise to the first DD peak during 15 July, Eve's eye evolved from a banding eye to a well-defined small eye. The fall of the DD numbers on 16 July is predominantly a manifestation of the formation of concentric eye walls. The default radius used to define the eye wall cloud-top temperature in the DD algorithm is 30 nm. When Eve

possessed concentric eye walls, this radius fell in the relatively cloud-free moat between the inner and outer wall clouds, and resulted in the period of low DD values after the first peak. The radius used to define the eye-wall cloud-top temperature is an adjustable parameter on the MIDDAS system, and when set to 10 nm it was able to measure Eve's intensity based on the cloud-top temperature of the inner eye wall. This resulted in DD numbers approximately one T number higher than those computed using the default radius when Eve possessed concentric eye walls.

Thus, while diurnal fluctuations of the intensity estimate of a TC may be the result of the general observation that cloud-top temperatures of deep convection in the tropics tend to be coldest in the early morning, the diurnal fluctuations of Eve's DD time series can be linked to major structural changes of the eye which may have only coincidentally occurred at the diurnal time scale. A similar sharp rise of the DD time series to a peak of over T 7.0 followed by a drop to near T 5.0 (due to the formation of concentric wall clouds) occurred with Dale (36W). In the case of Dale (36W), the timing of the rise and fall of the DD time series was 180° out of phase with that of Eve and with the generally observed diurnal cycle of tropical cloud-top temperatures.

Figure 3-07-6 The time series of Eve's hourly DD numbers (small black dots connected by thin solid line). For comparison, the final best track intensity at six-hour intervals (converted to a T number) is superimposed (open circles connected by thin solid line).



IV. IMPACT

Strong winds and heavy rains affected the Japanese island of Kyushu, disrupting sea and air transport. Nine people were reported injured. The eye of Eve passed directly over the island of Yaku Jima (WMO 47836) in the northern Ryukyus where reports of wind gusts to 83 kt (43 m/sec) were received at the JTWC.

TYPHOON FRANKIE (08W)

BEST TRACK-TC 08W

19 JUL - 25 JUL 96

MAX SFC WIND 90 KT

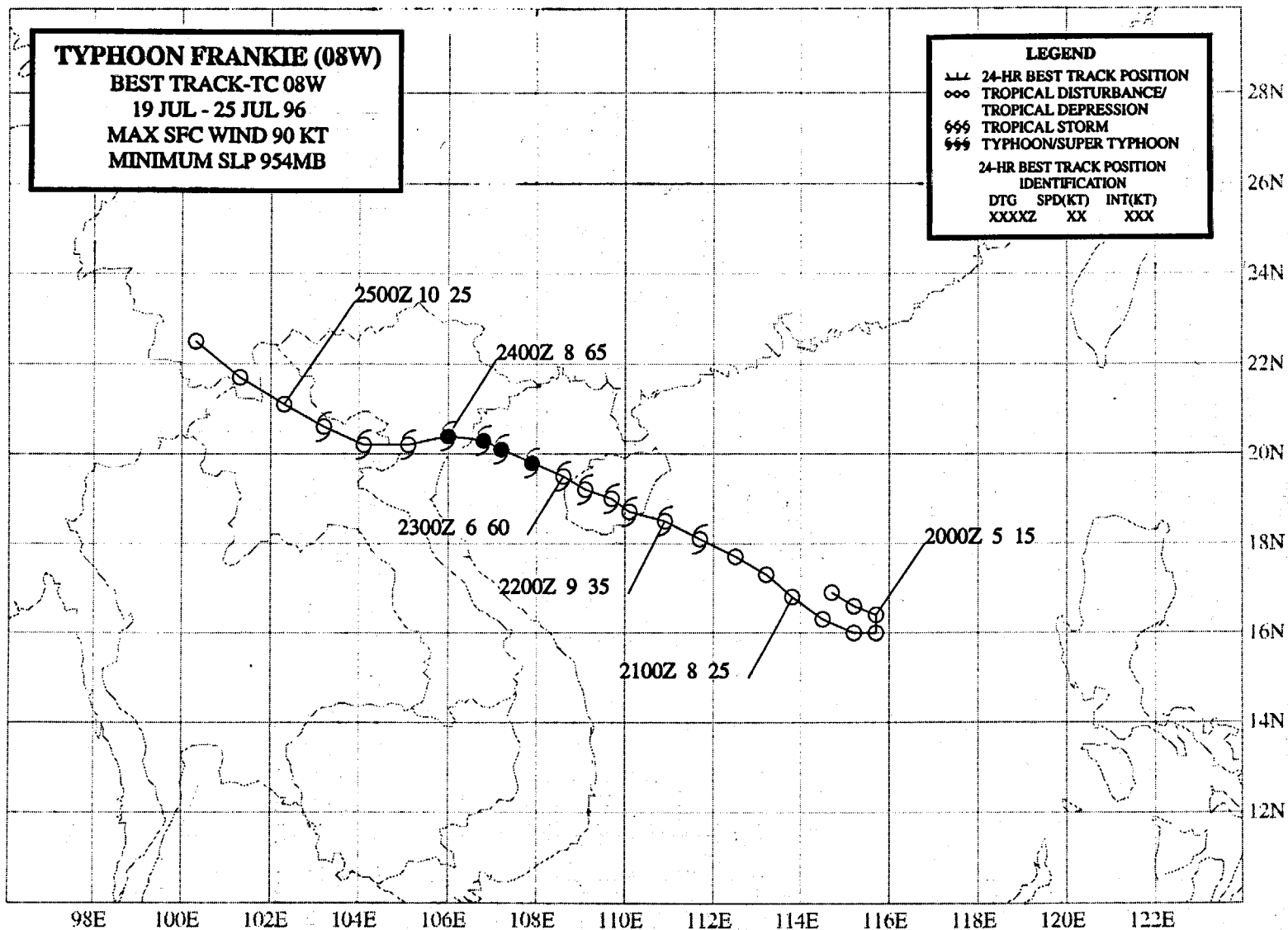
MINIMUM SLP 954MB

LEGEND

- 24-HR BEST TRACK POSITION
- TROPICAL DISTURBANCE/
TROPICAL DEPRESSION
- ⊖ TROPICAL STORM
- ⊕ TYPHOON/SUPER TYPHOON

**24-HR BEST TRACK POSITION
IDENTIFICATION**

DTG	SPD(KT)	INT(KT)
XXXXZ	XX	XXX



TYPHOON FRANKIE (08W)

I. HIGHLIGHTS

During late July, the monsoon trough became established across the northern half of the South China Sea and extended east-southeastward into Micronesia. Three TCs formed in this trough — Frankie, Gloria (09W), and Herb (10W). The westernmost of these three, Frankie originated from a monsoon depression in the South China Sea tracked to the west-northwest, and made landfall in northern Vietnam.

II. TRACK AND INTENSITY

During June and the first half of July, the monsoon trough was either very weak or absent from the tropics of the WNP. Easterly winds prevailed, and TC formation occurred at relatively high latitude (20°N) in association with disturbances in the TUTT. During the latter half of July, the first major penetration of the monsoon trough into Micronesia occurred. Inevitably, the monsoon cloud band consolidated into discrete areas of deep convection (in this case, three of them). The westernmost of the three areas of deep convection along the monsoon trough became a monsoon depression in the South China Sea (see the discussion section). It was first mentioned on the 180600Z July Significant Tropical Weather Advisory. A small well-defined LLCC (Figure 3-08-1) embedded within this monsoon depression became Frankie. A Tropical Cyclone Formation Alert was issued valid at 201100Z when deep convection continued to consolidate around the LLCC shown in Figure 3-08-1. Rapid development of a CDO pattern type with well-defined peripheral low-level cloud lines (Figure 3-08-2) prompted the JTWC to issue the first warning on Tropical Depression (TD) 08W, valid at 210000Z. During the early morning of 22 July, TD 08W formed a large CCC (Figure 3-08-3) prompting its upgrade to Tropical Storm Frankie on the warning valid at

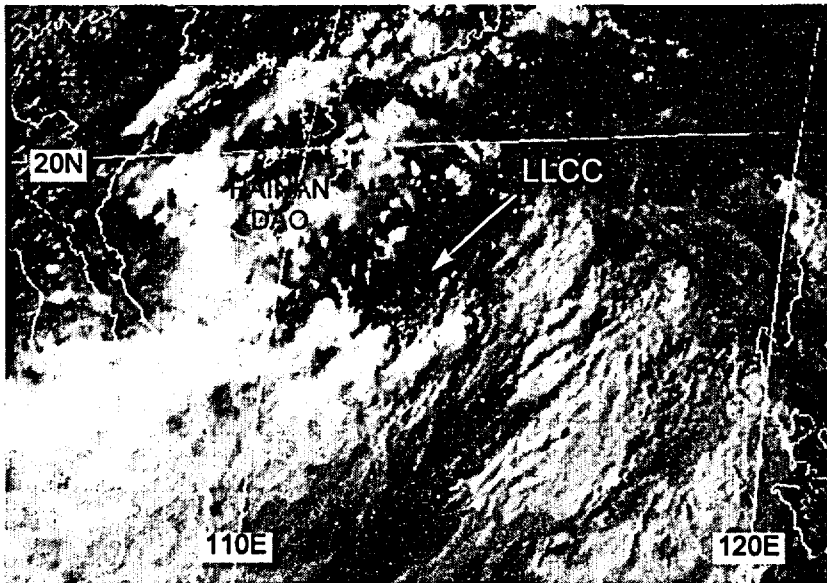


Figure 3-08-1 A small well-defined LLCC is present near the center of a monsoon depression. This LLCC became Frankie (210731Z July visible GMS imagery).

211800Z. After becoming a tropical storm, Frankie passed over the island of Hainan and continued to intensify. After clearing the west coast of Hainan, Frankie developed a ragged eye (Figure 3-08-4). Over the Gulf of Tonkin, the eye became better defined and Frankie was upgraded to a typhoon on the warning valid at 230600Z. The intensity peaked at 90 kt (46 m/sec) at 231200Z, and remained at that intensity until it crossed the coast of northern Vietnam at approximately 232200Z July. Thereafter, the system weakened, and the final warning was issued, valid at 240600Z.

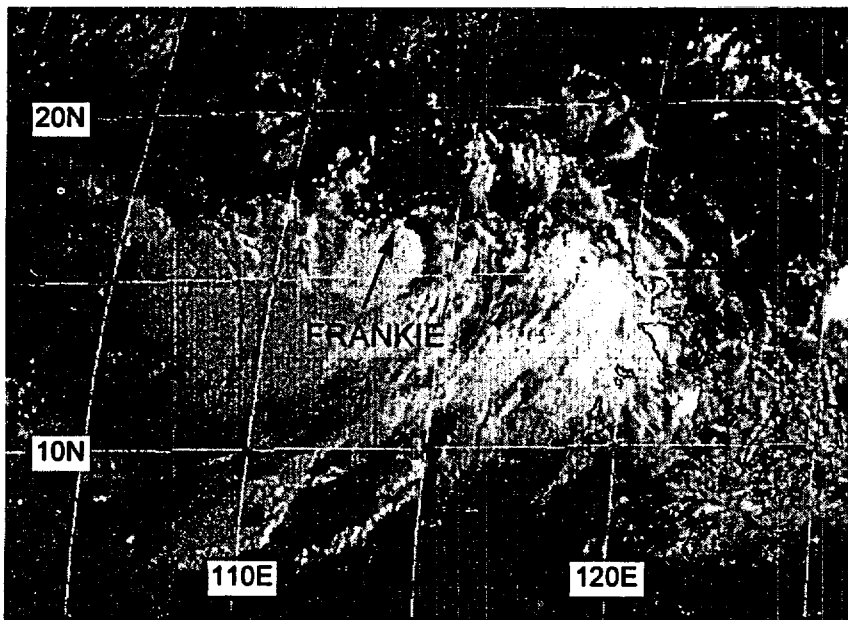


Figure 3-08-2 Deep convection becomes established over the LLCC shown in Figure 3-08-1 (202331Z July visible GMS imagery).

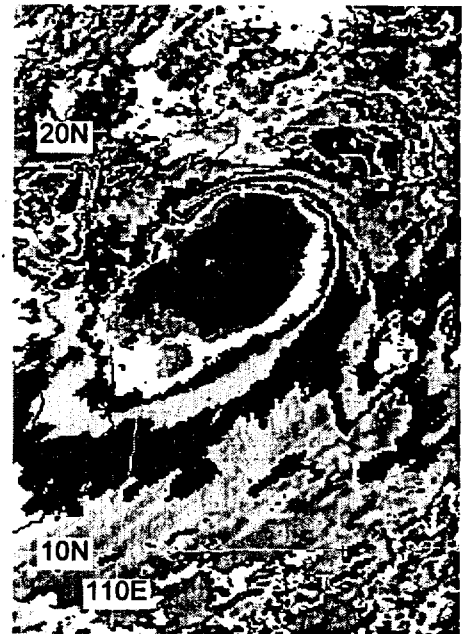


Figure 3-08-3 A large CCC erupts over the LLCC of Frankie. Coldest cloud-top temperature was -97°C (indicated by the arrow) (212224Z July enhanced infrared GMS imagery).

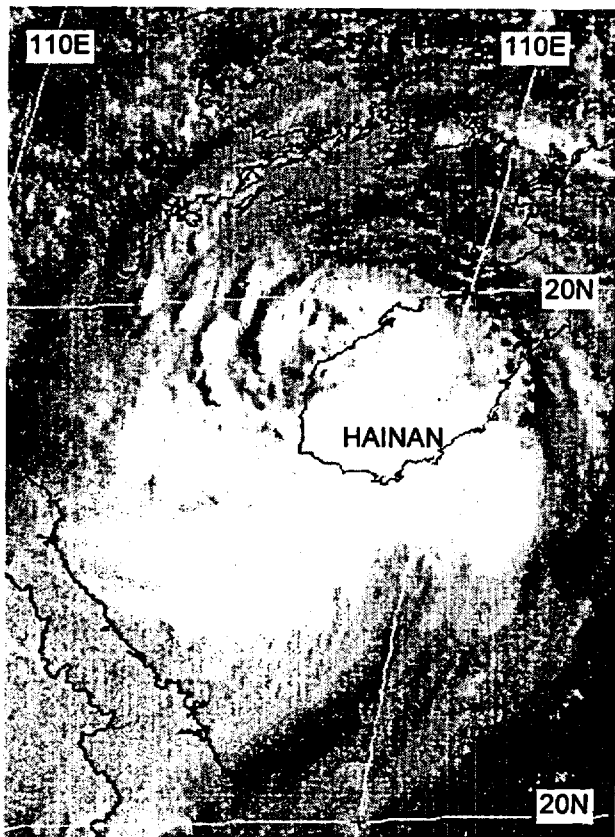


Figure 3-08-4 Frankie acquires a ragged eye as it clears the coast of Hainan island (230031Z July visible GMS imagery).

III. DISCUSSION

a. *The transformation of a monsoon depression into a typhoon*

Frankie originated from a monsoon depression — a common genesis pathway for TCs in the WNP (see Appendix A for a detailed description of monsoon depressions in the WNP). An unresolved question remains concerning the transition of a monsoon depression into a conventional TC: does the monsoon depression become the conventional TC, or does a conventional TC form within the circulation of the monsoon depression? In Frankie's case, it can be argued that the conventional TC (Frankie) formed within the preexisting circulation of the monsoon depression. The well-defined exposed LLCC (Figure 3-08-1) that became the focus of Frankie's deep convection was surrounded by an area of gales (Figure 3-08-5) before the core winds increased. When persistent deep convection appeared in the core of the monsoon depression, it quickly became a CDO-type conventional TC. Soon after the formation of Frankie's CDO, the peripheral cloudiness in the monsoon depression was suppressed and the areal extent and amount of

deep convection in the system became much smaller. TCs in the WNP that develop from monsoon depressions tend to be large, and Frankie's small size is somewhat unusual. Perhaps the geomorphology of the Gulf of Tonkin contributed to the evolution of this monsoon depression into a small TC. Many TCs which move into the Gulf of Tonkin become smaller.

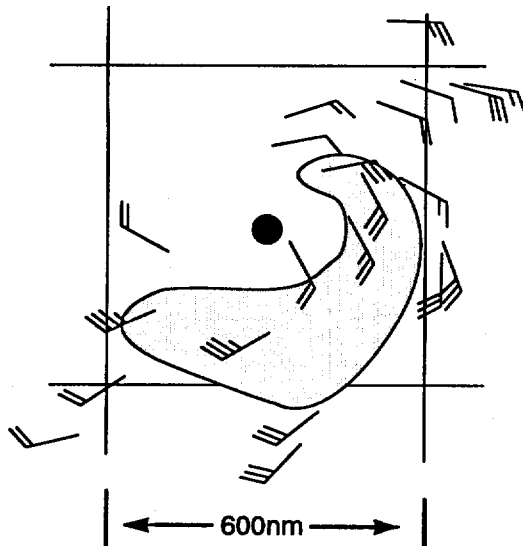


Figure 3-08-5 An area of gales existed in the monsoon depression before deep convection grew in its center (black dot) and the system became a conventional tropical cyclone. Wind reports are a center-relative composite of ship observations at 201200Z, 210000Z and 211200Z July.

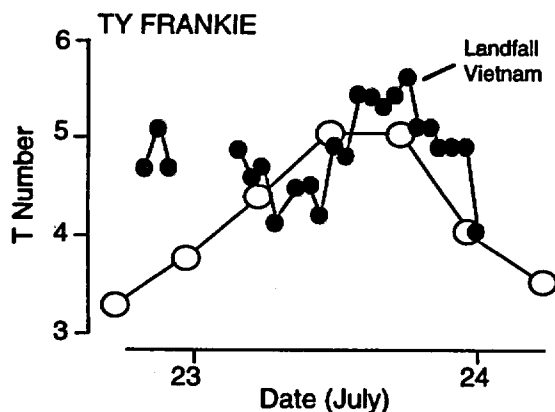


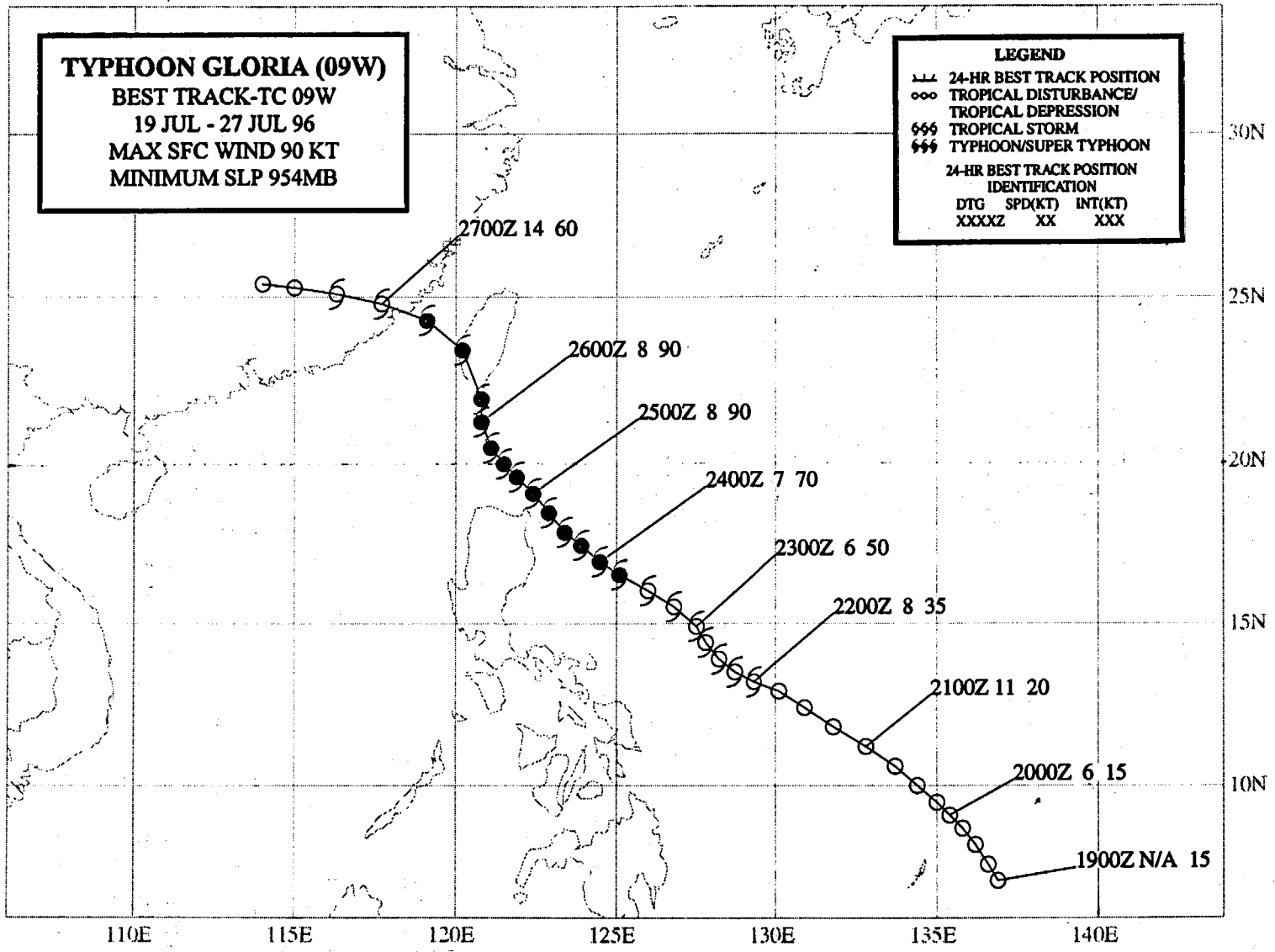
Figure 3-08-6 A time series of Frankie's intensity as it crossed the Gulf of Tonkin and made landfall in Vietnam. The hourly DD time series is indicated by black dots, and the six-hourly best-track intensity (converted to a T number) is indicated by the open circles.

b. Frankie's intensity time series

Upon entering the Gulf of Tonkin, Frankie acquired an eye and intensified from 50 kt (26 m/sec) to 90 kt (46 m/sec) in a period of 24 hours (Figure 3-08-6). The equivalent pressure drop of 33 mb in 24 hours was below the criteria for rapid deepening, defined as a decrease of 42 mb in 24 hours (Holliday and Thompson, 1979). The intensity increase did, however, qualify as "fast" in terms of its rise of more than 1.5 Dvorak T numbers in 24 hours. Dvorak classifies the rate of intensification of a TC as "slow", "normal", or "fast" if the 24-hour rise in its T-number estimate is 0.5, 1.0, and 1.5 respectively. Another aspect of Frankie's intensification over the Gulf of Tonkin concerns the timing of its peak. The best track indicates it reached its peak intensity approximately eight hours prior to landfall, while the DD numbers (Figure 3-08-6) continued to rise until the western eye-wall cloud made landfall. The discussion of the behavior of the time series of the DD numbers for Frankie, and for some of the other typhoons of 1996, is intended to highlight certain aspects of the DD time series that may prove to have important research and/or warning implications. Differences between the DD numbers and the best-track intensity are expected, and substantial disagreements are curiosities that lack ground-truth verification.

IV. IMPACT

Frankie caused extensive property damage and loss of life in the northern provinces of Vietnam. There were 104 people reported dead or missing, and 466 were reported injured. Total economic losses were estimated at over US \$200 million.



TYPHOON GLORIA (09W)

I. HIGHLIGHTS

Developing from a monsoon depression in the Philippine Sea, Gloria moved northwestward, became a typhoon, and affected Luzon, Taiwan, and eastern China. During the early phases of its development, Gloria formed a very large Central Cold Cover (CCC) with a near-record cloud-top temperature of -100°C .

II. TRACK AND INTENSITY

During the latter half of July, extensive amounts of deep convection formed in an east-west band extending across the WNP from the coast of Southeast Asia to the Marshall Islands. By 21 July, this cloud band had consolidated into three distinct cloud clusters (see Figure 3-10-1 in Herb's (10W) summary), all of which became named tropical cyclones — from west to east: Frankie (08W), Gloria, and Herb (10W). The tropical disturbance which became Gloria was first mentioned on the 170600Z July Significant Tropical Weather Advisory when synoptic data from Koror (WMO 91408) indicated the presence of a weak cyclonic circulation associated with a region of enhanced deep convection along the monsoon trough. Over the course of the next few days this disturbance moved slowly westward without much sign of increased organization in the deep convection or the surface wind field.

Early on 21 July, convection in the pre-Gloria disturbance became more organized and the first of two Tropical Cyclone Formation Alerts (TCFA) was issued valid at 201830Z. The areal extent of deep convection in this disturbance increased markedly, and the system acquired the structure of a monsoon depression. Although the cloud system appeared to be well organized, synoptic data still indicated that the winds were weak, and most of the deep convection had not yet consolidated near the low-level circulation center (LLCC). Thus, a second TCFA was issued valid at 211830Z, containing a caution stating deep convection had begun to develop near the LLCC (Figure 3-09-1), and formation of a significant tropical cyclone was anticipated within 6 to 12 hours. Indeed, when synoptic reports were received which indicated the wind speed had reached 30 kt (15 m/sec) in the broad circulation, the first warning on Tropical Depression 09W was issued valid at 220000Z. Steering flow was dominated by a strong subtropical ridge to its north, and Gloria was forecast to move on a steady west-northwest track towards Luzon.

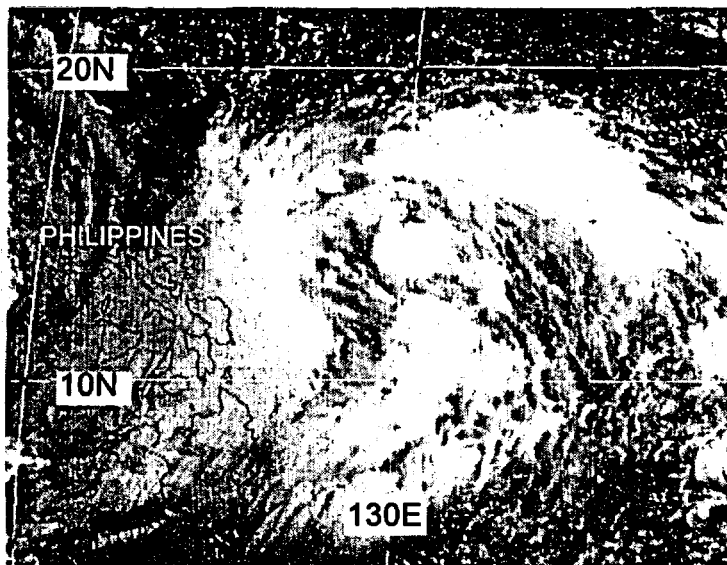


Figure 3-09-1 The mesoscale convective systems within the pre-Gloria monsoon depression show signs of increased organization and consolidation toward the LLCC, prompting the first warning (212224Z July visible GMS imagery).

Based upon synoptic reports of gales within the large circulation, TD 09W was upgraded to Tropical Storm Gloria on the warning valid at 221200Z. During the night, following its upgrade to tropical-storm intensity, and subsequent increase to 55 kt (28 m/sec), Gloria underwent a profound structural change: a very large Central Cold Cover (CCC) formed (see the discussion section). This CCC persisted from the late evening of 23 July to the morning of 24 July. As the CCC began to dissipate, Gloria became a typhoon. By the afternoon of 24 July, the cirrus debris of the CCC had largely cleared away revealing that Gloria had acquired a visible eye.

Tracking on a more northwestward course than forecast, Gloria brushed by Luzon and entered the Luzon Strait. It is here, during the afternoon of 26 August that Gloria made an abrupt jog to the north to make landfall on the southern tip of Taiwan. The typhoon then made a quick jump to the western coast of Taiwan, where it then turned to the west, crossed the Taiwan Strait and went inland in southeastern China. The peak intensity of 90 kt (46 m/sec) was maintained from 241200Z to 260600Z as Gloria moved across the Luzon Strait and made landfall in Taiwan. After landfall in Taiwan, its intensity dropped to the typhoon threshold, and having little time to recover during its passage across the Taiwan Strait, it entered mainland China as a minimal typhoon and quickly dissipated over land. The final warning was issued at 270600Z.

III. DISCUSSION

a. *An unusually large Central Cold Cover*

Dvorak (1984) noted that the use of enhanced IR imagery required the introduction of a new concept — the central cold cover (CCC) — in order to deal with the occurrence of a sudden spreading of cold clouds over the central features of a TC. When a CCC persists, it signals an interruption in the development of the TC. Specific details of the CCC pattern are found in Dvorak (1984):

"The CCC pattern is defined when a more or less round, cold overcast mass of clouds covers the storm center or comma head obscuring the expected signs of pattern evolution. The outer curved bands and lines usually weaken with the onset of CCC. When using VIS pictures, substitute the word 'dense' for 'cold'. It is only rarely that the CCC pattern is used with VIS pictures since the CDO [central dense overcast] or curved lines are usually visible through the thin cirrus clouds. When the CCC persists . . . , development has been arrested until signs of development or weakening once again appear in the cloud features. Care should be exercised under the following conditions:

"1) Do not confuse a CCC pattern with a very cold comma pattern. A very cold (usually white [i.e., a gray-shade enhancement on the BD curve that is indicative of temperatures between -70 to -75°C]) pattern is indicated by a very cold (very smooth texture) comma tail and head with some indication of a wedge in between. Curved cirrus lines or boundaries usually appear around the [very] cold [comma] pattern and not around the CCC pattern. The very cold [comma] pattern for T-numbers of T3 or less warrant an additional 1/2 number in intensity estimate and often indicates rapid growth.

"2) Do not assume weakening in a CCC pattern when the comma tail begins to decrease in size. It is common to observe the tail decreasing in size at the onset of the CCC. Also, the CCC often warms as the eye of the T4 pattern begins to be carved out by a warm incursion into the side of the cold overcast. This signals the resumption of pattern evolution (intensification) even though some warming is evident."

In the WNP, the CCC pattern is observed every year in the developmental process of several of the named TCs. One major difference between the CCC pattern observed in the WNP versus the North Atlantic (where Dvorak obtained most of the data for the development of his techniques) is that the cloud-top temperature of the CCC tends to be at least 10°C to 15°C colder in the WNP. Another difference between the CCC patterns observed in the WNP versus those observed in the Atlantic is the very large size of some of the CCC patterns observed in the WNP.

Prior to the formation of its CCC, Gloria had been developing as a monsoon depression. During the evening hours of 23 July, a cluster of small cold-topped MCSs began to grow near the estimated center position of Gloria. During a six-hour period, this cluster of MCSs mushroomed into an enormous CCC (Figure 3-09-2a-e). By local midnight, the average diameter of the area within which the cloud-top temperature was at or below -70°C was approximately 700 km (Figure 3-09-3). Roughly half of this area was colder than -90°C. The coldest IR pixel, with an equivalent black-body temperature of -100°C, was located near the geometric center of the CCC. This is an extremely cold cloud-top temperature which is rarely seen. It is only 2°C shy of the record cold cloud-top temperature of -102°C reported by Ebert and Holland (1992) in the deep convection associated with a TC near Australia.

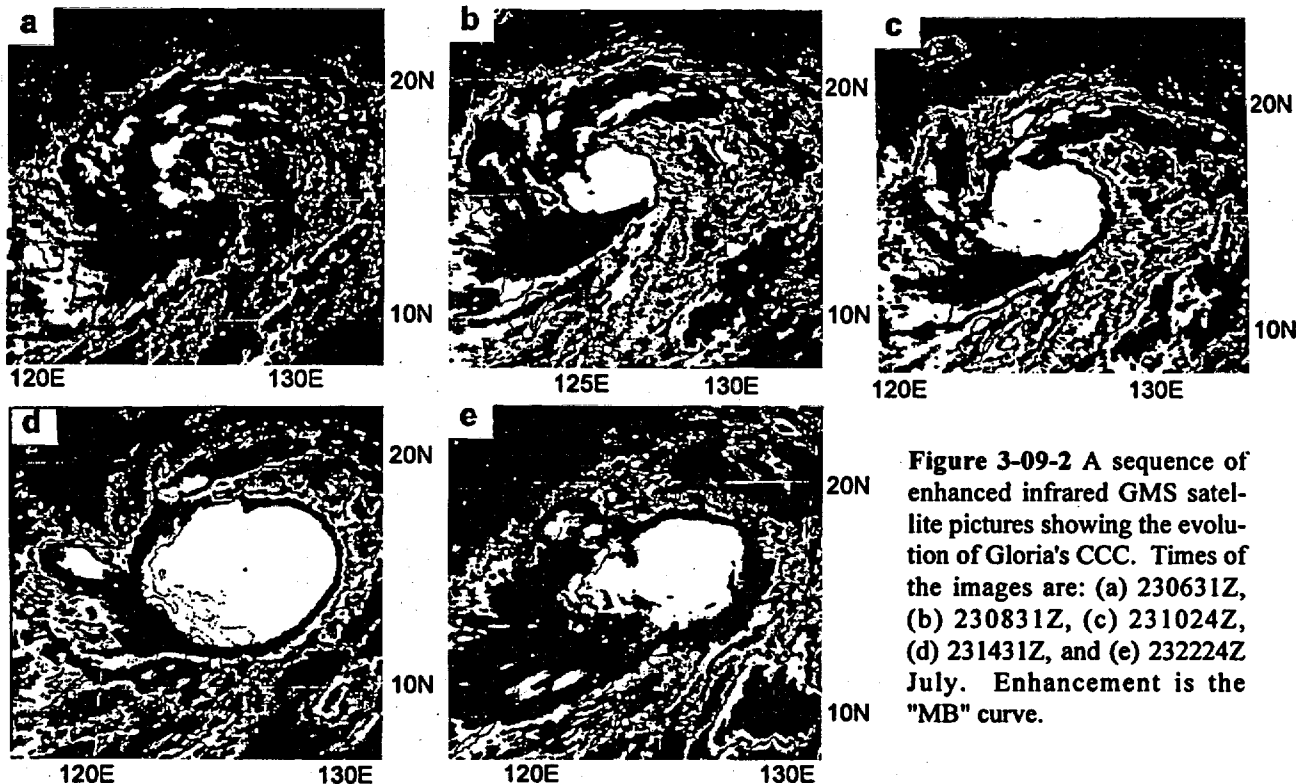


Figure 3-09-2 A sequence of enhanced infrared GMS satellite pictures showing the evolution of Gloria's CCC. Times of the images are: (a) 230631Z, (b) 230831Z, (c) 231024Z, (d) 231431Z, and (e) 232224Z July. Enhancement is the "MB" curve.

By the early daylight hours of 24 July, the periphery of the CCC began to warm on IR imagery, and a new smaller CCC mushroomed into the preexisting cold cirrus canopy (Figure 3-09-4). As the day progressed, the underlying structure of Gloria gradually emerged in VIS imagery as the supporting convection of the CCC ended, and the large cirrus canopy of the CCC thinned. By mid-afternoon, the cold cirrus of the CCC became nearly transparent, and the eye, wall cloud, and peripheral convective cloud bands of the intensifying Gloria were then plainly seen (Figure 3-09-5).

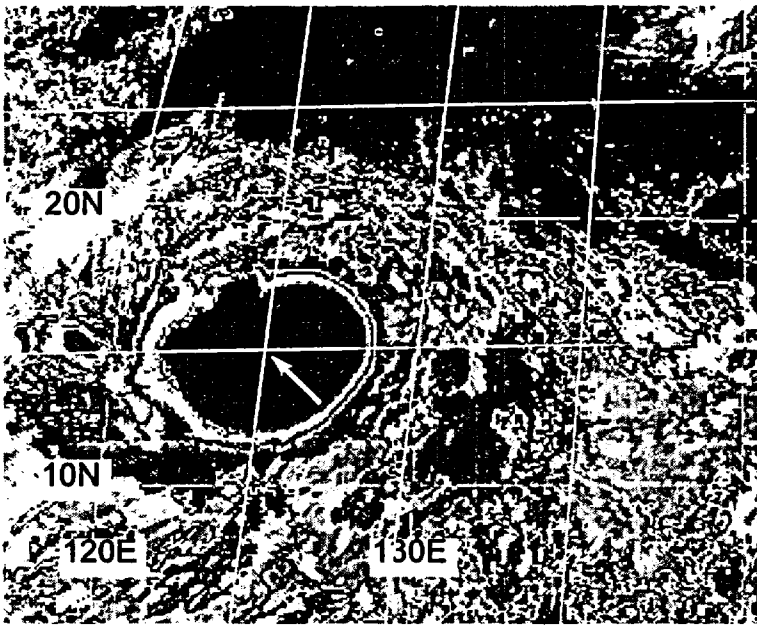


Figure 3-09-3 Gloria's CCC reaches its maximum areal extent, and registers its coldest temperatures. The location of the coldest temperature of -100°C is indicated by the arrow. Enhancement is the basic Dvorak, or "BD", curve applied to the 231431Z July infrared GMS imagery.

In the 24-hour period encompassing the full evolution of Gloria's CCC, the estimated intensity increased from 55 kt to 75 kt; hardly a remarkable change considering the extreme changes in the cloud pattern. This is consistent with Dvorak's findings that the appearance of a CCC signals arrested (or at least slowed) development which is renewed as the eye pattern of the T4 (minimal typhoon intensity) emerges beneath the thinning cirrus. Additional observations made during the occurrence of the CCC pattern in WNP TCs include the following:

1) the CCC usually begins to form at local sunset (this is at some variance with observations by Black and collaborators (e.g., Black, 1983; Black, et al., 1986; Black and Marks, 1987) who

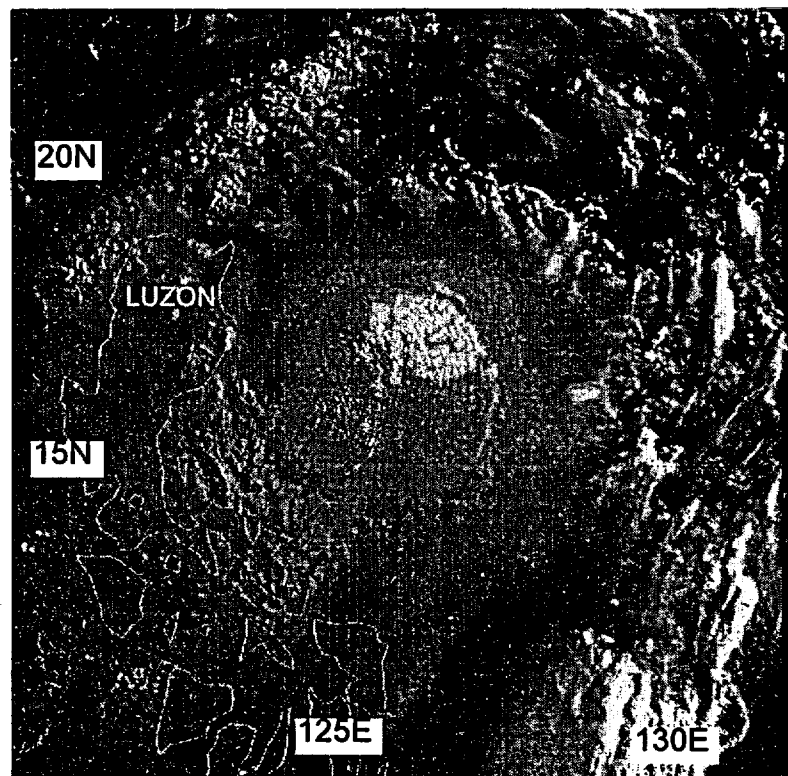


Figure 3-09-4 The appearance of Gloria's CCC by the early local daylight hours of 24 July: another pulse of dense cirrus is mushrooming into the thinning remains of earlier cold cirrus (232224Z July visible GMS imagery).

show that major cold convective eruptions in TCs tend to be initiated in the early morning);

2) the CCC reaches its greatest size and coldest temperature between local midnight and predawn; and,

3) the CCC pattern is most commonly observed to occur in weaker TCs that are at intensities of between T3 to T4 (45 - 65 kt) (this is consistent with observations of the aforementioned Black and collaborators; it is not consistent with guidance in Dvorak's 1984 report wherein it is stated that the CCC could occur at any stage of development of the TC and last for several hours to several days).

b. The influence of Taiwan on the motion of tropical cyclones

As Gloria was moving slowly to the northwest in the Luzon Strait, it made an abrupt turn to the north, and made landfall on the extreme southern tip of Taiwan. It then made an abrupt jump to the west coast of Taiwan before resuming a westward track toward mainland China. It is offered as a hypothesis that this abrupt meander in Gloria's track was induced by the island of Taiwan. Research by the Taiwan Central Weather Bureau (CWB) (1982) has demonstrated that the island of Taiwan can significantly alter the tracks of typhoons that approach it. The effects differ depending upon the angle of approach. The track changes noted during Gloria's approach to Taiwan are consistent with the track changes noted by the CWB which occur when a typhoon approaches Taiwan from the south or southeast.

IV. IMPACT

In the Philippines, Gloria was reported to have killed at least 20 people and caused nearly US \$40 million in property damage. Hardest hit were the northeastern provinces of Luzon, where the eye of Gloria approached to within 60 nm (110 km) of the northeastern tip of the island. Gloria also passed to within 60 nm (110 km) of some of the smaller islands in the Luzon Strait where, although there were reports of typhoon force winds, the JTWC received no reports of any damage or injuries. On Taiwan, three people were reported killed: a child by a falling tree, an adult as he was blown from his motorcycle into a creek, and another adult as he fell from a roof. Rock slides disrupted traffic along Taiwan's east coast, and heavy rains flooded fields and caused several rivers to overflow their banks.

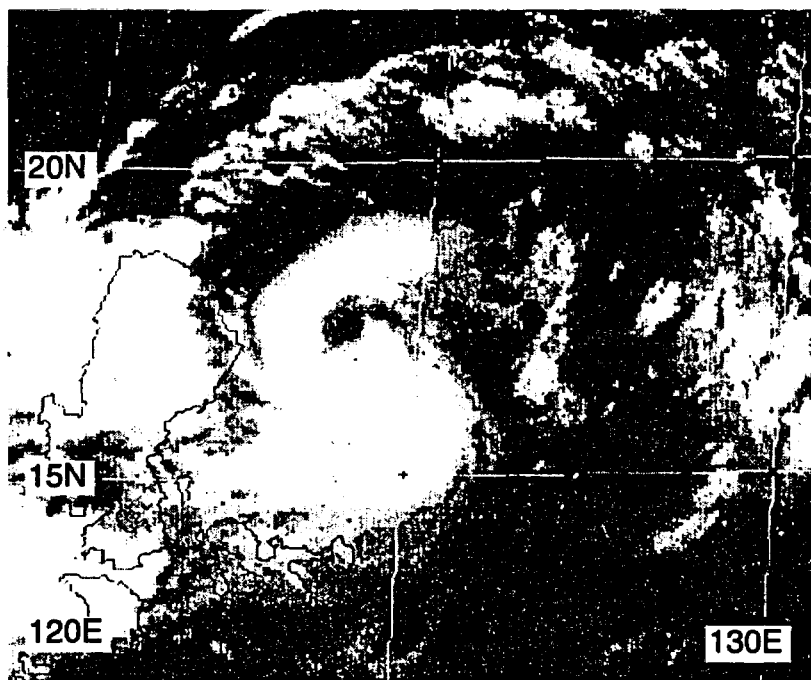


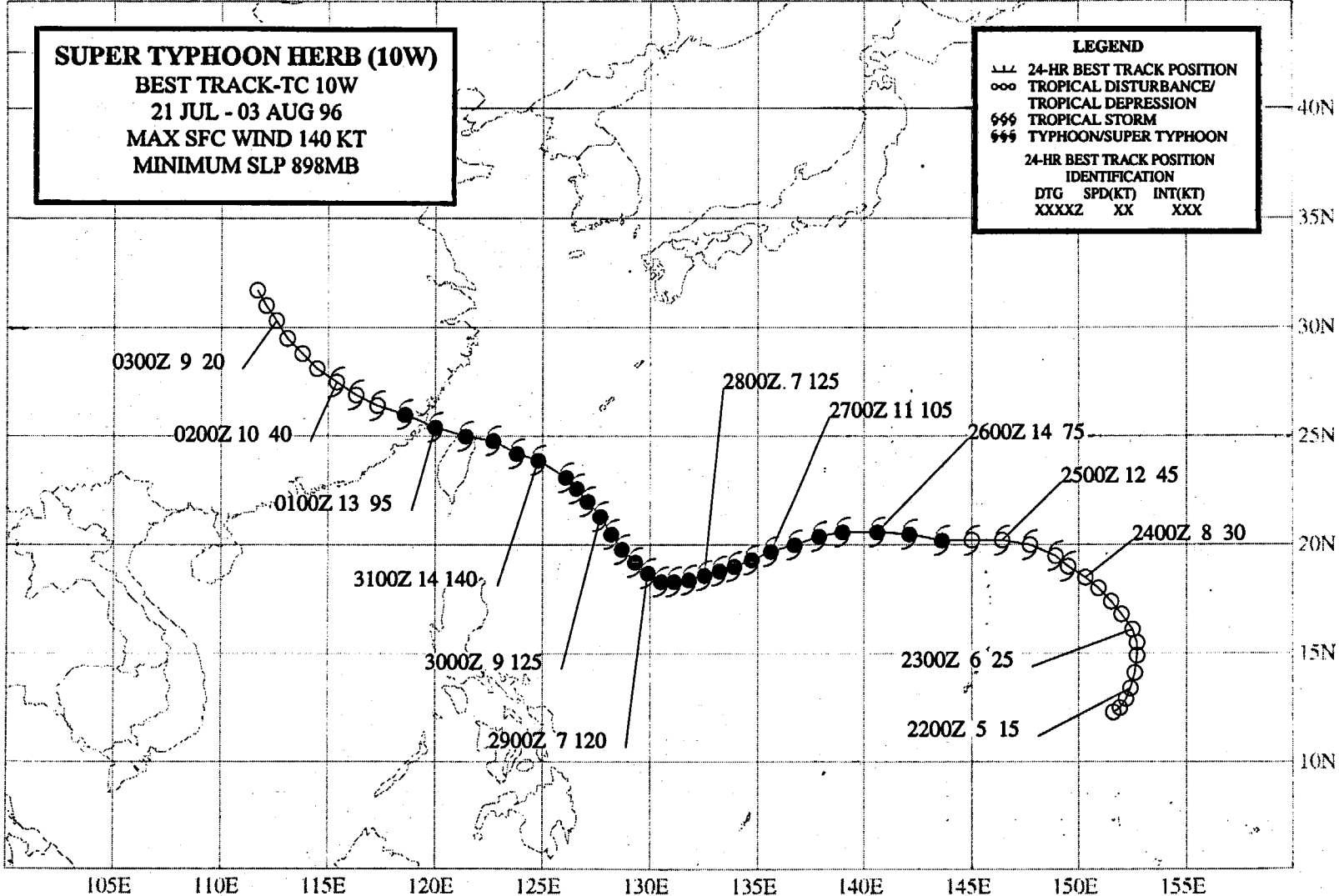
Figure 3-09-5 The eye, wall cloud, and peripheral rainbands of Gloria are plainly visible after the cirrus overcast of the CCC cleared away (240531Z visible GMS imagery).

SUPER TYPHOON HERB (10W)
BEST TRACK-TC 10W
21 JUL - 03 AUG 96
MAX SFC WIND 140 KT
MINIMUM SLP 898MB

LEGEND

- 24-HR BEST TRACK POSITION
- ooo TROPICAL DISTURBANCE/
TROPICAL DEPRESSION
- 666 TROPICAL STORM
- 999 TYPHOON/SUPER TYPHOON

24-HR BEST TRACK POSITION
IDENTIFICATION
DTG SPD(KT) INT(KT)
XXXXZ XX XXX



SUPER TYPHOON HERB (10W)

I. HIGHLIGHTS

When Herb formed, it became the easternmost of three tropical cyclones simultaneously active along the monsoon trough — the other two were Frankie (08W) and Gloria (09W). Herb's mode of formation was somewhat unusual: the cloud cluster from which it developed became organized into a "fishhook" cloud pattern. While moving generally westward toward China, Herb peaked twice in intensity. As the tropical cyclone neared its second peak intensity, it possessed a large eye. In addition, Herb was also a very large tropical cyclone; the largest tropical cyclone in terms of the mean Radius of Outermost Closed Isobar (ROCI) in the WNP during 1996. Herb made landfall in the southern Ryukyu Islands, Taiwan, and mainland China. Significant property damage and loss of life were attributed to Herb in these areas. On Taiwan, a new NEXRAD WSR 88D took a direct hit from Herb, and was severely damaged.

II. TRACK AND INTENSITY

During the latter half of July, extensive amounts of deep convection formed in an east-west band extending across the WNP from the coast of Southeast Asia to the Marshall Islands. By 21 July, this cloud band had consolidated into three distinct cloud clusters (Figure 3-10-1), all of which became named tropical cyclones — from west to east: Frankie (08W), Gloria (09W), and Herb.

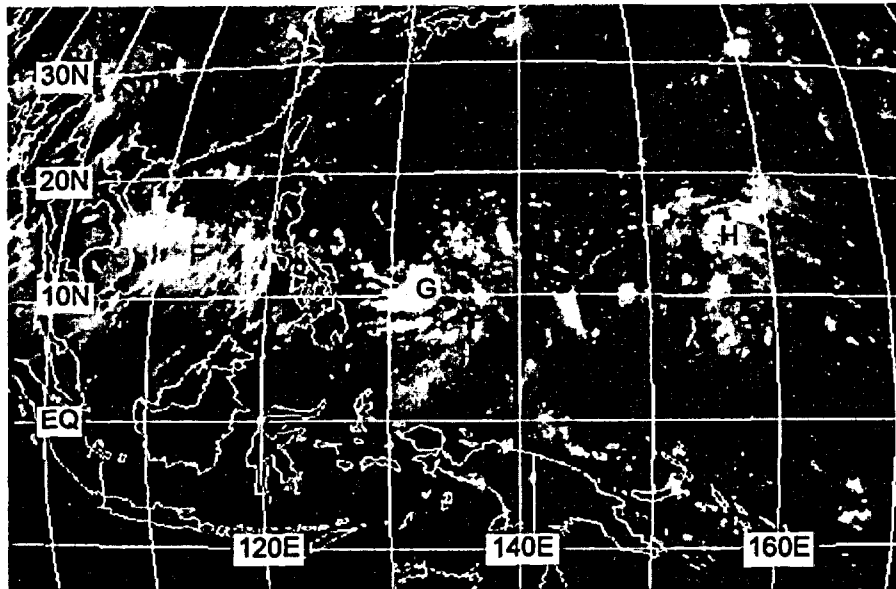


Figure 3-10-1 The cloudiness associated with the monsoon trough consolidates into three distinct cloud clusters that will soon become Frankie (08W), Gloria (09W), and Herb (201831Z July Infrared GMS imagery).

Based upon 24-hours of persistent deep convection, and synoptic data indicating the presence of an associated weak low-level cyclone beneath upper-level anticyclonic flow, the tropical disturbance that became Herb was first mentioned on the 210600Z July Significant Tropical Weather Advisory. Convection in this disturbance remained poorly organized until the morning of 23 July, when deep convection consolidated within a smaller area, and microwave imager data and visible satellite imagery indicated improved

organization of the low-level circulation center (LLCC). This prompted the JTWC to issue a TCFA valid at 230000Z. Continued improvements in the organization of low-level cloud lines accompanying a persistent area of deep convection near the LLCC led to the first warning on Tropical Depression (TD) 10W valid at 230600Z.

Based upon satellite intensity estimates, TD 10W was upgraded to Tropical Storm Herb on the warning valid at 240600Z. After becoming a tropical storm, Herb's central deep convection began to detach from the peripheral monsoon cloudiness to form a fishhook pattern (Figure 3-10-2).

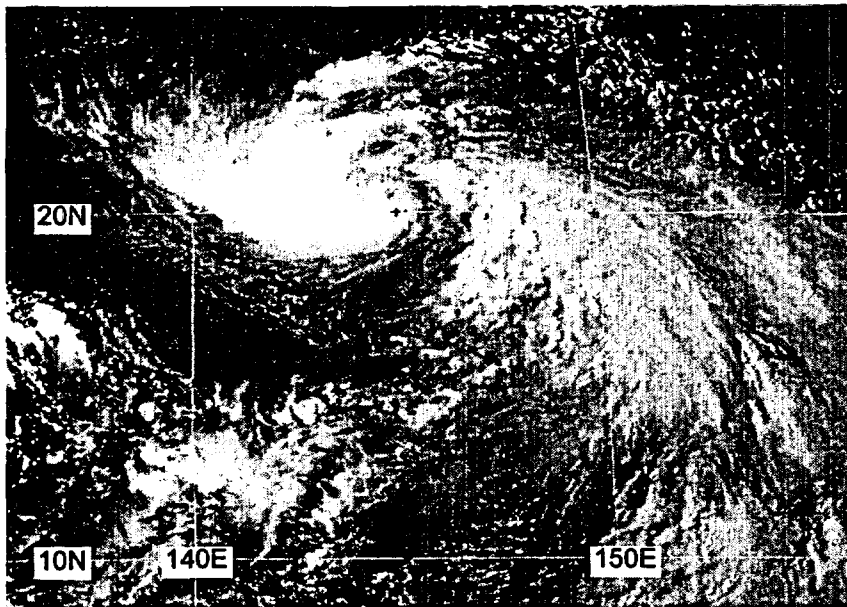


Figure 3-10-2 Herb's central deep convection begins to detach from the end of a fishhook shaped cloud pattern (250631Z July visible GMS imagery).

As the cloud system center moved to the head of the fishhook cloud pattern, Herb's motion became more westward. On a westward heading, Herb began to intensify and grow in size. Herb became a typhoon at 251200Z, and 48 hours later it reached 125 kt (64 m/sec) (Figure 3-10-3a,b); the first of two intensity maxima. At this time, Herb was moving in an unusual west-southwestward direction. This unusual motion may have been the result of an indirect interaction with Typhoon Gloria (09W) (the various types of direct and indirect interactions between two tropical cyclones

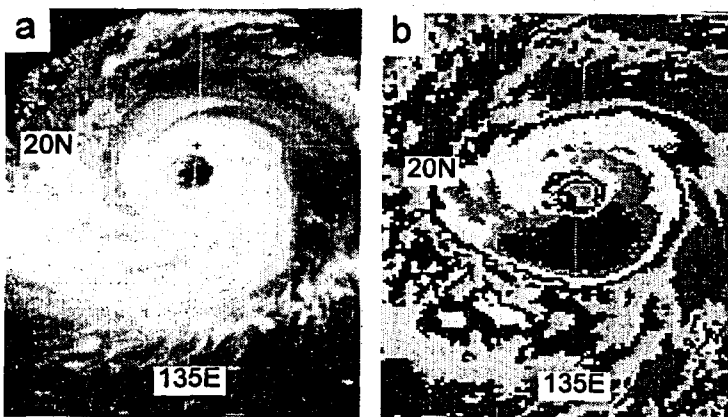


Figure 3-10-3 Herb nears its first of two intensity maxima: (a) 270331Z July visible GMS imagery and (b) 270331Z July enhanced infrared GMS imagery.

are discussed in detail by Carr and Elsberry (1994)).

On 29 July, Herb began to weaken with its intensity falling to 115 kt (59 m/sec) at 290600Z. While the typhoon weakened, the system made a gradual track change from a west-southwestward heading during 28 July to a northwestward heading during 29 July. Although weakened slightly, Herb had become a very large tropical cyclone with a mean ROCI of approximately 8.5° of great-circle arc (Figure 3-10-4). Early on 30 July, Herb began to intensify once again, reaching a peak of 140 kt (72 m/sec) at

301800Z (Figure 3-10-5). After reaching its peak intensity, Herb took a more westward course which brought it ashore on the northeast tip of Taiwan at approximately 311600Z with a landfall intensity of 130 kt (67 m/sec). Passing over Taiwan, Herb lost its eye, but then regained a ragged eye during its short passage across the Taiwan Strait. It quickly lost its eye over land in China. The final warning was issued valid at 011200Z August as the system moved farther inland and dissipated.

III: DISCUSSION

a. Unusual genesis

While Herb was forming in the monsoon trough, it followed an unusual developmental pathway: the deep convection associated with Herb's LLCC moved on a backwards "C" shaped trajectory

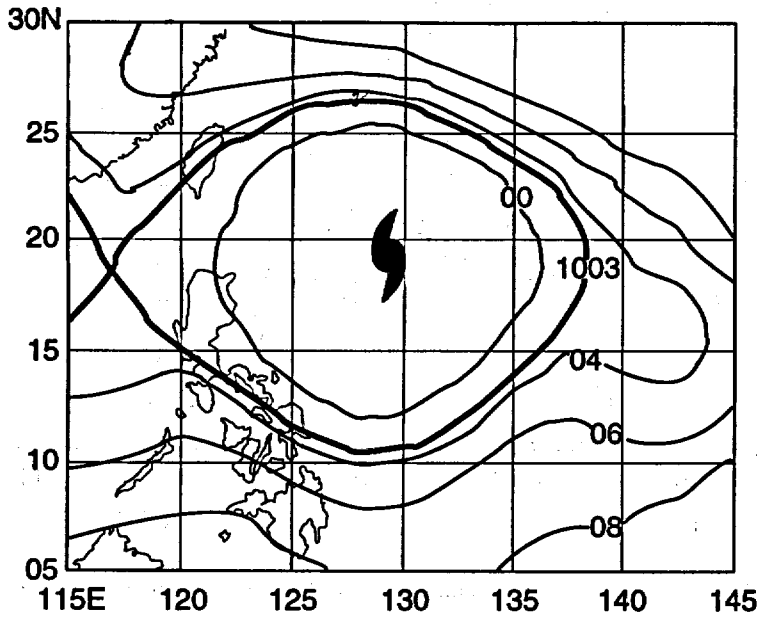


Figure 3-10-4 Herb became a very large tropical cyclone, the largest of 1996 in the WNP. As a measure of its size, the average radius of the outermost closed isobar is over 8.5° of great circle arc at 290000Z July. (290000Z July NOGAPS SLP analysis).

ry and gradually detached from the peripheral monsoon cloudiness to form a fishhook pattern (Figure 3-10-2). When the monsoon trough becomes organized as a monsoon gyre (Lander 1994) (see Appendix A), the large-scale monsoon cloud band often becomes organized into a large fishhook cloud pattern. One, or more, tropical cyclones may traverse the eastern periphery of the monsoon gyre (in a cyclonic orbit of the gyre) and emerge from the end of the fishhook. Although smaller in scale than the monsoon gyres cited by Lander (1994), the process of organization of the monsoon cloud pattern into a fishhook, and the backwards "C" motion of Herb as the fishhook evolved, are consistent with the cloud evolution and behavior of tropical cyclones associated with larger monsoon gyres.

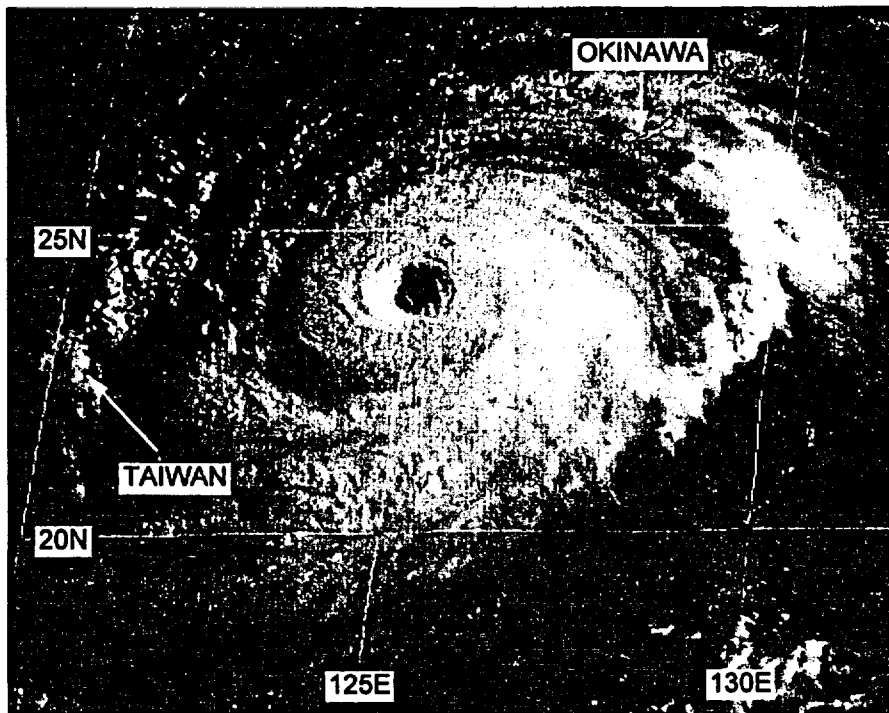


Figure 3-10-5 Herb at peak intensity of 140 kt (72 m/sec) (302224Z July visible GMS imagery).

b. *Three periods of intensification*

The time series of the DD numbers obtained for Herb (Figure 3-10-6) indicate three maxima: one maximum at approximately 270000Z, a second at approximately 281800Z, and a third sustained maximum during 30 July. The first maximum indicated by the DD algorithm occurred a little bit ahead of the first maximum in the final best track intensity. The best track intensity does not reflect the fall and rise of the DD time series to its second maximum. One reason for this, is that as the T-number falls, the Dvorak

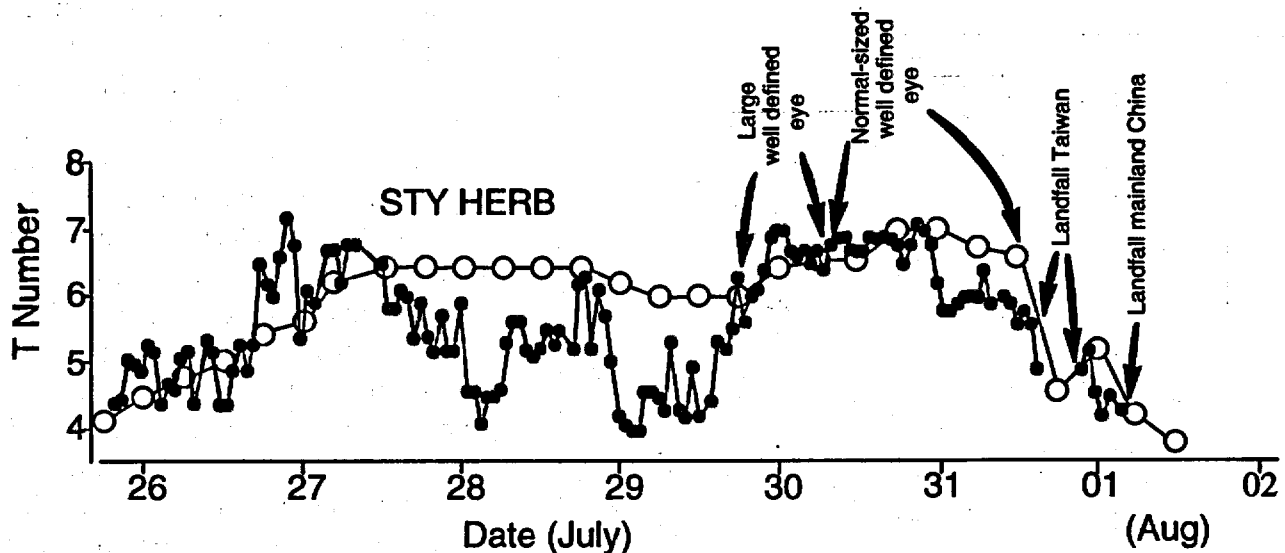


Figure 3-10-6 The time series of Herb's Digital Dvorak "DD" numbers (small dark circles) with the final best track intensity superimposed (large open circles).

technique requires that the current intensity be held one-half to one number higher than the T-number for at least 12 hours. For the most part, this is true of a comparison of Herb's DD time series with its final best track intensities (Figure 3-10-6). The second drop of intensity indicated on the DD time series was reflected by a slight drop in the warning and best track intensity before both rose once again to the peak that occurred on 30 July. Note that the DD time series contains some rather large fluctuations that do not appear in the final best track intensity time series. It is not known to what extent the fluctuations in the DD time series may represent actual short term changes in the intensity of tropical cyclones (see Bart's (04W) summary for a discussion of the DD algorithm).

c. Largest tropical cyclone of 1996

Super Typhoon Herb was the largest tropical cyclone of 1996. Using the mean ROCI as a measure of Herb's size, the system surpassed the threshold of the "very large" size category used by the JTWC (see Appendix A). At its largest, the mean ROCI of Herb was about 8.5° of great-circle arc (GCA) (Figure 3-10-4).

Tropical cyclone size is a very difficult parameter to objectively measure. Merrill (1984) classified a tropical cyclone as "small" if the mean ROCI was three degrees (180 nm, 335 km) GCA, or smaller; as "medium" if the mean ROCI was between three to five degrees GCA (180 nm (335 km) to 300 nm (555 km)), and as "large" if the mean ROCI was greater than five degrees GCA (greater than 300 nm). The Japan Meteorological Agency (JMA) recognizes two additional size categories — "very small" and "ultra large" — that mesh neatly with Merrill's scheme. The definitions of size used herein (see Appendix A) have been adapted by a mesh of the JMA size categories with those of Merrill.

d. Eyewall mesocyclonic vortices as seen by Taiwan's NEXRAD

Eyewall mesocyclonic vortices (EMs) were first detected and documented in airborne Doppler radar data by Marks and Houze (1984) and also with aircraft inertial navigation equipment as noted by Black and Marks (1991). Stewart and Lyons (1996) identified EMs with the Guam

NEXRAD in association with the passage of Super Typhoon Ed (1993). Until the implementation of the NEXRAD radar network in the United States during the early 1990s, only chance encounters with EMs have occurred during reconnaissance aircraft penetrations. However, now that Doppler velocity data are available, strong mesocyclones associated with TC outer convective bands and eyewall convection are frequently detected.

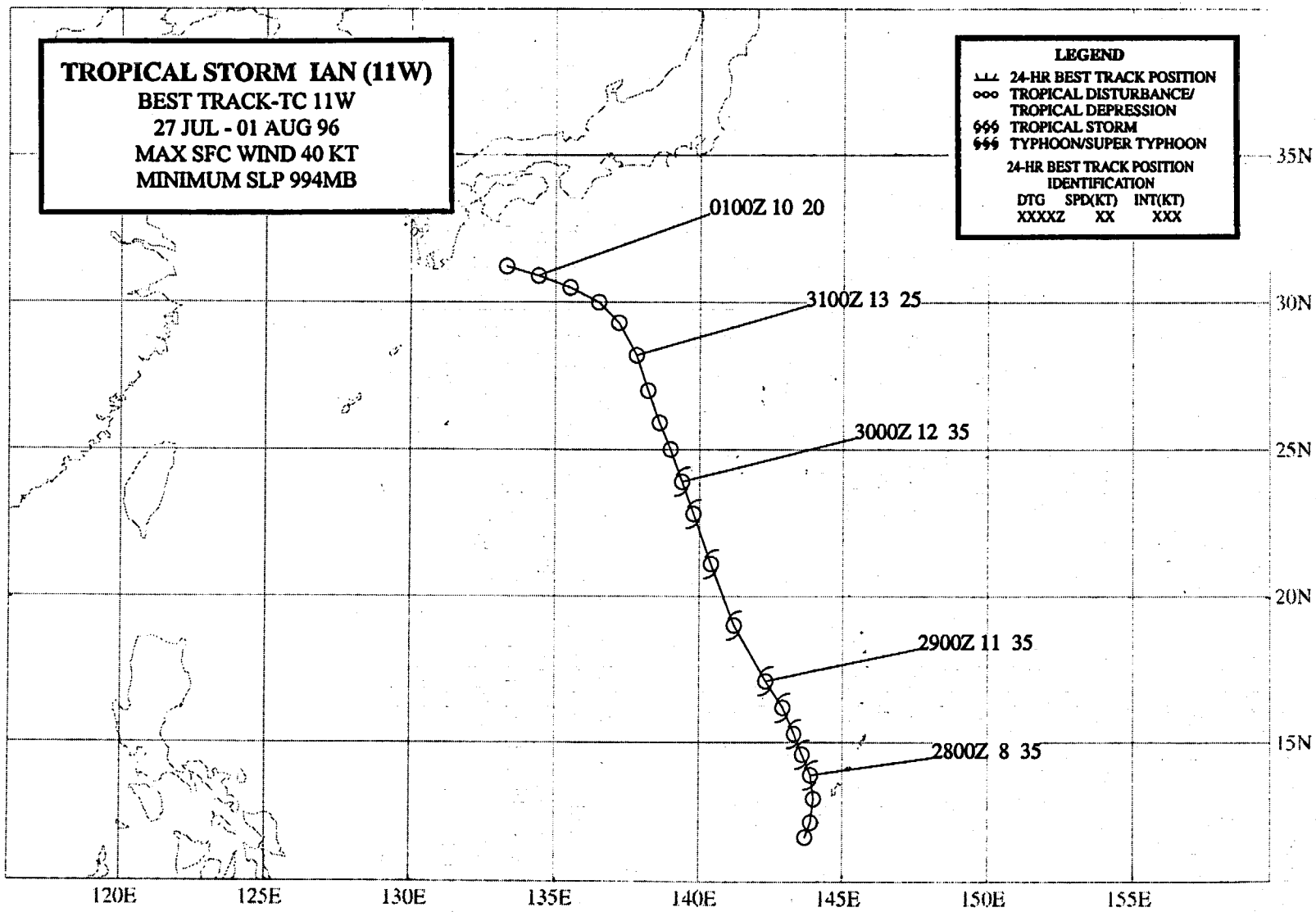
Stewart et al. (1997) used NEXRAD data to show that EMs in the wall clouds of TC eyes may be a mechanism for TC intensification and for extreme wind bursts in TCs as noted with Hurricane Andrew damage (Wakimoto and Black 1993). In three cases (including Herb), the TC underwent a period of rapid intensification during which time several vertically deep, EMs formed prior to the occurrence of rapid intensification and persisted for several hours while rapid deepening was occurring. Comments from Stewart et al. (1996) include:

"Approximately three hours prior to landfall in Taiwan, satellite imagery indicated Herb had weakened . . . In contrast, the [Taiwan NEXRAD] indicated that Herb was actually intensifying . . . As early as 310656Z July, [the NEXRAD] indicated intense EMs had begun to develop and this trend continued until the last available data at 311350Z [when the data record ended because of damage to the radar by high wind.] . . . Although the [Taiwan NEXRAD] detected several EMs (as many as 6 EMs occurred simultaneously in the eyewall), one particular EM became quite intense and persisted for more than 1.5 hours just prior to Herb's landfall . . . This particular EM peaked at 311314Z with a rotational shear of 0.075/sec which is more than triple the [NEXRAD] criteria for a Tornadic Vortex Signature . . ."

Based on observations of EMs in TCs (including Herb), Stewart et al. (1997) conclude that the EMs appear to have a positive feedback on TC intensification.

IV. IMPACT

In addition to the destruction of Taiwan's NEXRAD, Herb caused extensive damage to property and agriculture in Taiwan and China. At least 51 lives were lost and 22 missing in Taiwan. Twenty-four of these lives were lost in the city of Nantou, 120 miles south of Taipei, due to rock-slides and flooding. Daily rain totals of nearly 40 inches (1000 mm) were reported over the central mountain range. An estimated US \$5 billion dollars of damage to crops, roads and power equipment was reported in Taiwan. In China, rains from Herb contributed to flooding that killed upwards of 250 people. In Fujian Province, 950 miles south of Beijing, at least 233 people were reported killed and 284 missing when flooding destroyed 70,000 homes.



TROPICAL STORM IAN (11W)

I. HIGHLIGHTS

Ian formed at the end of the monsoon trough and then moved on a north-northwestward track while embedded within the peripheral southerly flow on the eastern side of the very large Super Typhoon Herb (10W). The initial warnings on Ian were based primarily on synoptic reports from the islands of Guam and Saipan because the circulation was poorly organized on satellite imagery.

II. TRACK AND INTENSITY

During the final week of July, Super Typhoon Herb (10W) grew in size and came to dominate much of the flow of the WNP. On 27 July, a large area of deep convection became established in the monsoon flow to the south and east of Herb (Figure 3-11-1). The possibility of tropical cyclogenesis occurring in association with this area of deep convection was first mentioned on the 271800Z Significant Tropical Weather Advisory. Comments on this advisory included:

"... An area of convection is located [southeast of Guam] ... within the monsoon trough. Sounding data from Guam indicates falling heights throughout the lower troposphere. Additionally, northerly winds at Guam suggest a circulation center southeast of the island. As Typhoon Herb moves westward, this region becomes an increasingly favorable genesis area ..."

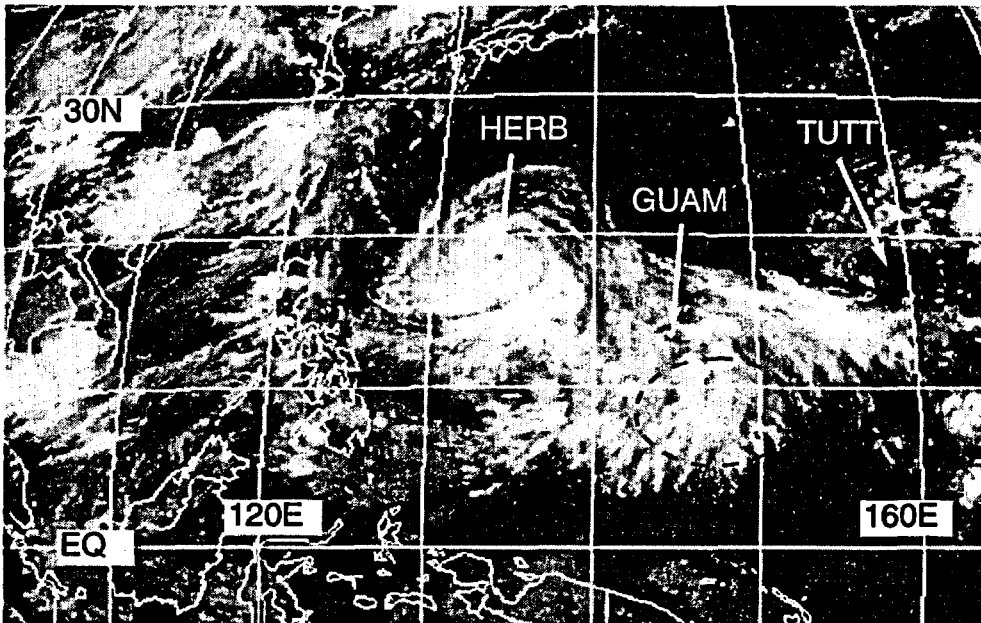


Figure 3-11-1 A large ensemble of mesoscale convective systems develops in monsoon flow to the southeast of Herb (dashed circular area) (271331Z July infrared GMS imagery).

Based upon reports of increasing winds and falling pressures on Guam and Saipan, a Tropical Cyclone Formation Alert was issued valid at 280430Z. The circulation center was then estimated to have been approximately 50 nm (90 km) to the west of Guam, and drifting slowly northward. Later that day, two ships moored at Saipan reported to the JTWC that they were experiencing gales and had to put to sea. Based upon these ship reports, and from high winds (20 to 30 kt) and low pressure (1003 mb) experienced on Guam and Saipan, the first warning on Tropical Depression (TD) 11W was released valid at 281200Z. When an area of persistent deep convection became established near the estimated center location, TD 11W was upgraded to Tropical Storm Ian on the warning valid at 290000Z. In post analysis, based upon data recorded in the logs of the

aforementioned ships which had to depart Saipan, and upon indications on microwave imagery (Figure 3-11-2) that the organization of the deep convection was better than indicated on conventional visible (Figure 3-11-3) and infrared satellite imagery, TD 11W was increased to a tropical storm at 280000Z.

On 29 July, a third TC — TD 12W formed within a TUTT cell to the northeast of Ian (see Joy's (12W) summary and figure 3-11-1) to create a reverse-oriented monsoon trough that stretched northeastward from Herb (10W). Embedded in this trough, and also embedded in the large circulation of Herb (10W), Ian moved northward, as anticipated. Strong upper-level northwesterly winds, which were part of Herb's extensive outflow, exerted shear on Ian, and the system failed to mature. Instead, the low-level circulation center (LLCC) became displaced to the north of Ian's deep convection, and the system was downgraded to a tropical depression on the warning valid at 300600Z. On 31 July, deep convection was completely sheared away from Ian's LLCC, and the final warning was issued valid at 310600Z as the exposed LLCC slowly dissipated over water to the south of Japan.

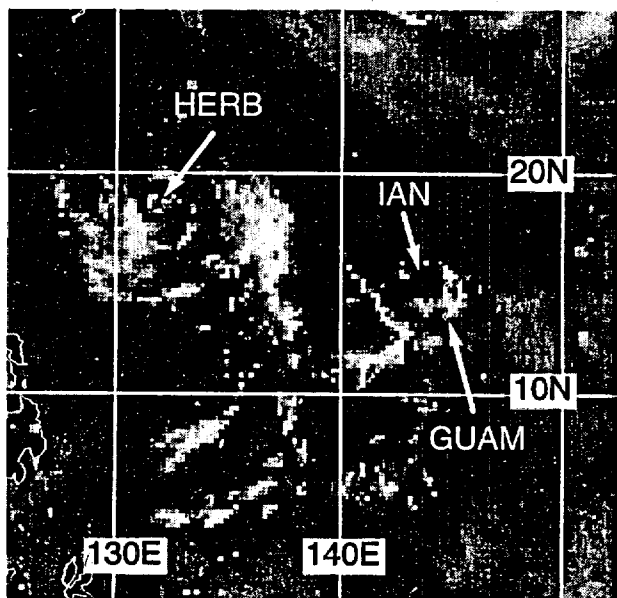
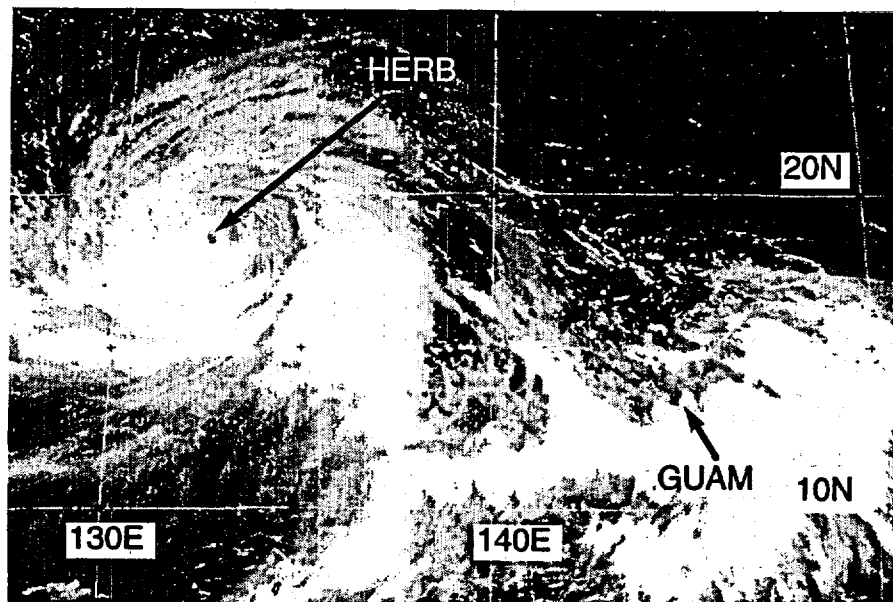


Figure 3-11-2 Deep convection associated with Ian is organized into cyclonically-curved bands (280914Z July 85 GHz microwave DMSPI imagery).

Figure 3-11-3 Although the deep convection appears to be poorly organized, a low pressure area associated with over-water gales has developed near Guam and Saipan. In post analysis, Ian became a tropical storm at this time (272331Z July visible GMS imagery).



III. DISCUSSION

a. Unusual structure

As Ian moved northward in a cyclonically-curved track around the eastern periphery of the larger circulation of Herb (10W), it was often difficult to establish whether it was an independent cyclonic circulation, vice a cusp or a wave. Synoptic data indicated for most of its life, Ian took the form of a cusp, with a region of gales on its eastern side and a zero velocity singularity at the center (or at most, a very small region of northerly winds on its western side) (Figure 3-11-4). When Ian passed Guam and Saipan, it was at first thought the high winds were associated with a surge (or squall line) in the monsoon. The drop of pressure to 1003 mb at its closest point of approach, the day-long duration of high wind, and a subsequent 24-hour pressure rise of 8 mb in 24 hours at Guam, however, were more consistent with the passage of a tropical cyclone.

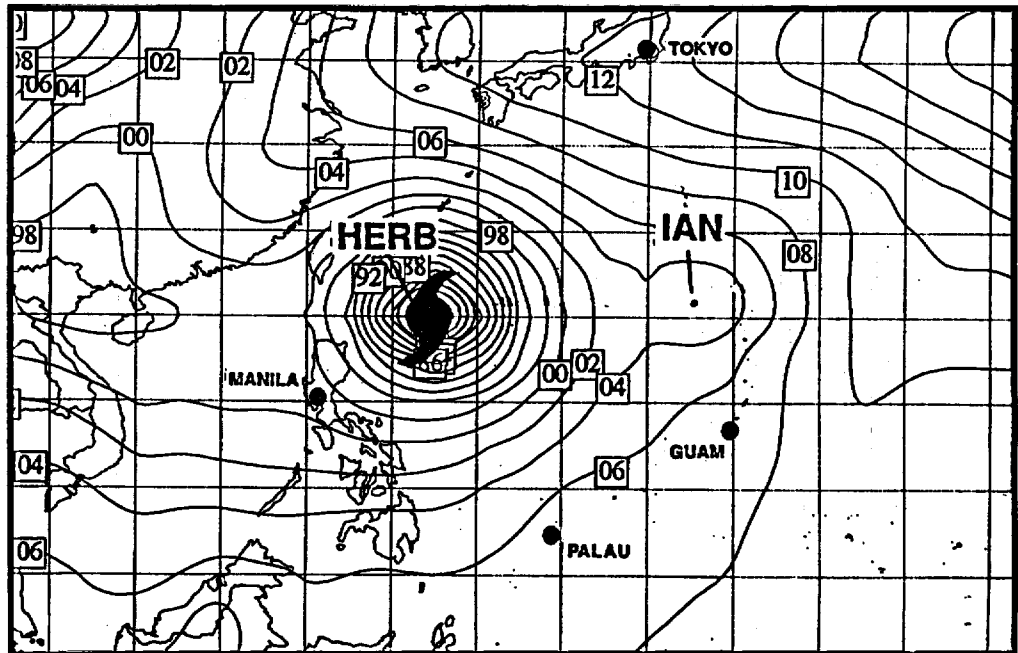
b. Ian as a "satellite" of Herb (10W)

Occasionally, small TCs are observed to develop in the peripheral flow of very large TCs in the WNP. These small TCs tend to be weak, have short life spans, and are advected around the larger TC. These small TCs which form and orbit in the peripheral flow of very large TCs will herein be called "satellite" TCs, based upon the astronomical analogy of a small object (i.e., a satellite) in orbit of a much larger object. Very large TCs in recent years which have had smaller "satellite" TCs in their peripheral circulation include Abby (1983) which had two "satellites" (Ben and Carmen), and Hal (1988) which also had two "satellites" (Jeff and Irma). Ian was a "satellite" TC of the very large Herb (10W), and was closely analogous with respect to its cloud signature and relative position to Hal's "satellite", Irma (1988).

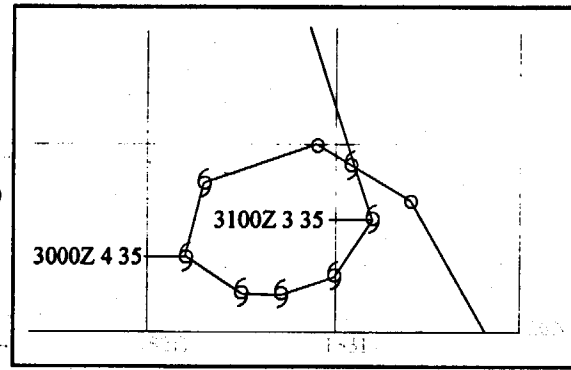
IV. IMPACT

Much of the northern half of Saipan lost power when high winds associated with Ian caused power lines to short out against tree branches. Some similar spot power outages occurred on Guam. Also on Saipan, some ships at anchor were forced to put to sea. No other reports of significant damage or injuries attributable to Ian were received by the JTWC.

Figure 3-11-4
Ian, which is embedded within the strong southerly flow on the eastern side of Herb, is difficult to "close-off" (290000Z July NOGAPS sea-level pressure analysis).



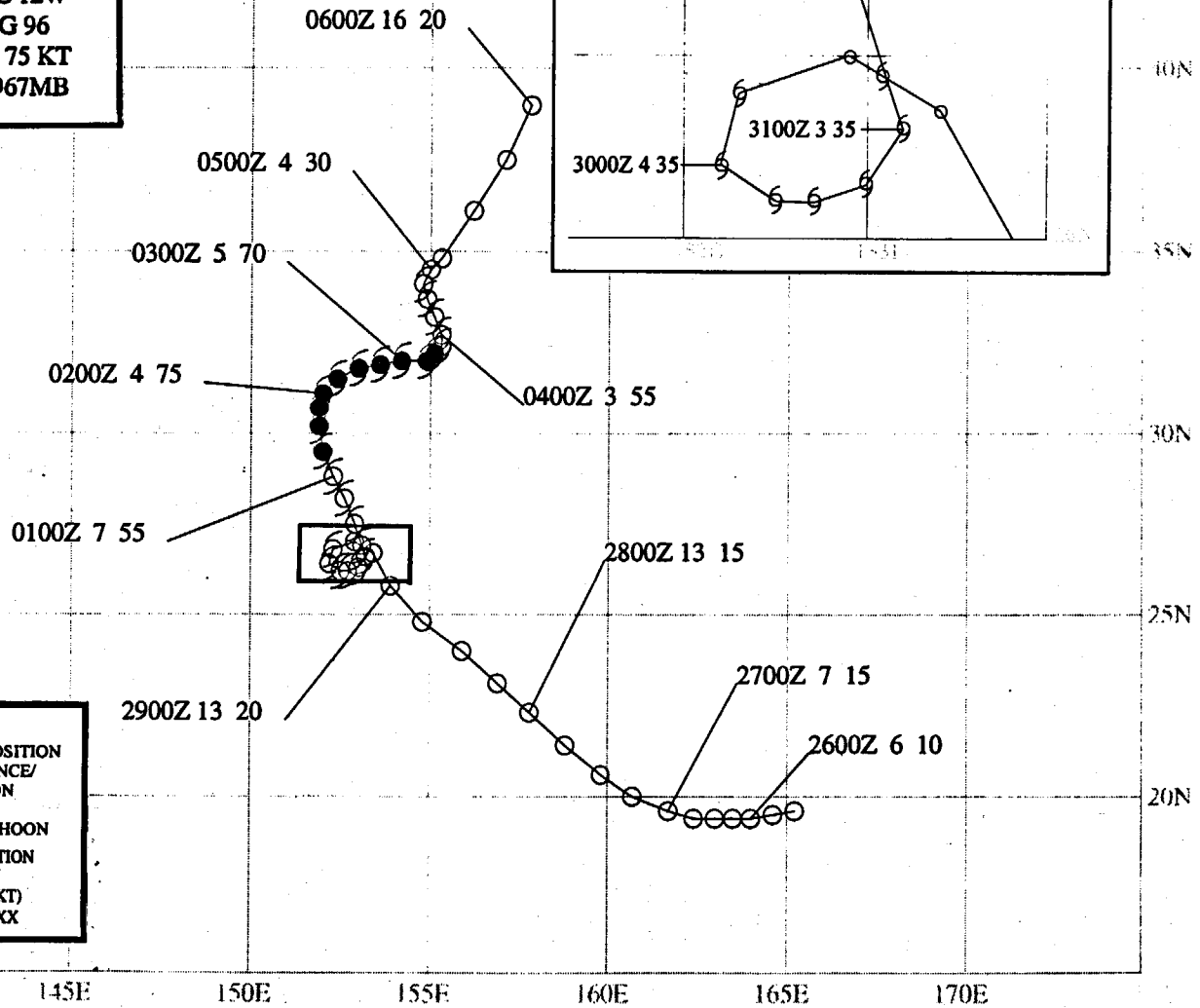
TYPHOON JOY (12W)
BEST TRACK-TC 12W
25 JUL - 06 AUG 96
MAX SFC WIND 75 KT
MINIMUM SLP 967MB



LEGEND

- 24-HR BEST TRACK POSITION
- ooo TROPICAL DISTURBANCE/
TROPICAL DEPRESSION
- 666 TROPICAL STORM
- \$\$\$ TYPHOON/SUPER TYPHOON

24-HR BEST TRACK POSITION
IDENTIFICATION
DTG SPD(KT) INT(KT)
XXXXZ XX XXX



TYPHOON JOY (12W)

I. HIGHLIGHTS

Joy formed at a relatively high latitude in direct association with a TUTT cell, and did not become a typhoon until it had moved to nearly 30°N. Prevented from recurving by a blocking high, the system moved slowly on a meandering north-oriented track.

II. TRACK AND INTENSITY

During the final week of July, a monsoon trough became established across the WNP, and three tropical cyclones formed simultaneously in this trough — Frankie (08W), Gloria (09W), and Herb (10W). Several days later, Ian (11W) and Kirk (13W) also formed at the eastern end of this monsoon trough. During the time this activity was occurring in the monsoon trough, a TUTT cell (that was first detected near the international date line), was moving slowly westward along 20°N. The tropical disturbance which became Joy originated directly from deep convection associated with this TUTT cell (see the discussion section for more details). On 27 July, deep convection associated with this TUTT cell increased, cirrus outflow became organized into a well-defined anticyclonic pattern, and visible satellite imagery indicated that a low-level circulation had formed, which led to its inclusion on the 270600Z July Significant Tropical Weather Advisory. Comments on this advisory included:

"... An area of convection is located near 21N 160E. Visible satellite imagery indicates the presence of a low-level cyclonic circulation beneath well-defined anticyclonic flow aloft. Water vapor imagery also indicates that a [TUTT] cell is located to the south of the disturbance. ..."

The TUTT cell continued its westward motion for the next two days, and the convection located to its north remained poorly organized until 29 July when a small area of deep convection persisted near the estimated low-level circulation center. The first warning on Tropical Depression (TD) 12W was issued valid at 290600Z based on a satellite intensity estimate of 25 kt (13 m/sec).

Upgrade of TD 12W to Tropical Storm Joy occurred on the warning valid at 300000Z, based upon a satellite intensity estimate of 35 kt (18 m/sec).

Between 29 and 30 July, Joy remained nearly stationary in weak steering before intensifying as it began moving slowly toward the north-northwest on 31 July. During the daylight hours of 01 August, Joy became well-organized, and its primary band of deep convection became tightly coiled to form a banding-type eye (Figure 3-12-1). This prompted the JTWC to upgrade Joy to a typhoon on the warning valid at 010600Z September.

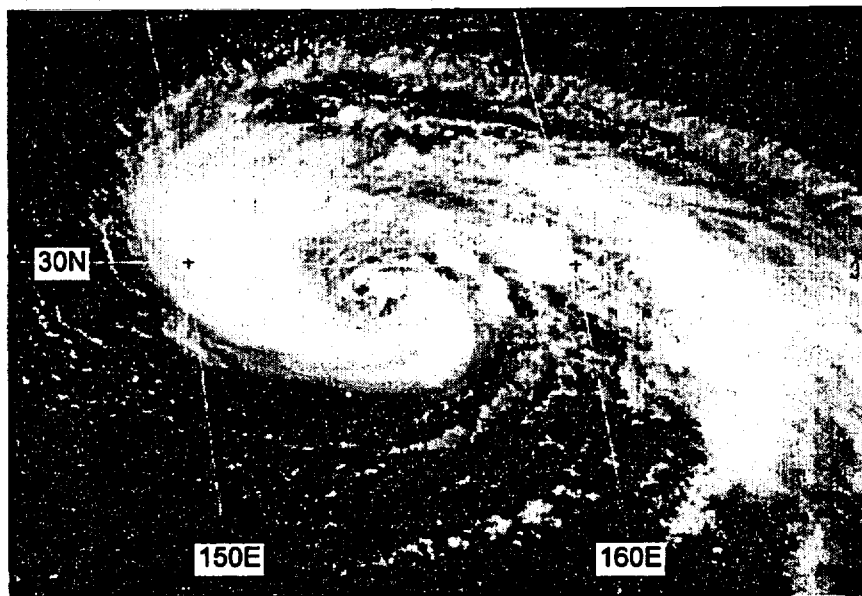


Figure 3-12-1 Joy's primary band of deep convection coils into a banding-type eye (010331Z August visible GMS imagery).

Meandering slowly northward, Joy reached its peak intensity of 75 kt (39 m/sec) at 011800Z (Figure 3-12-2).

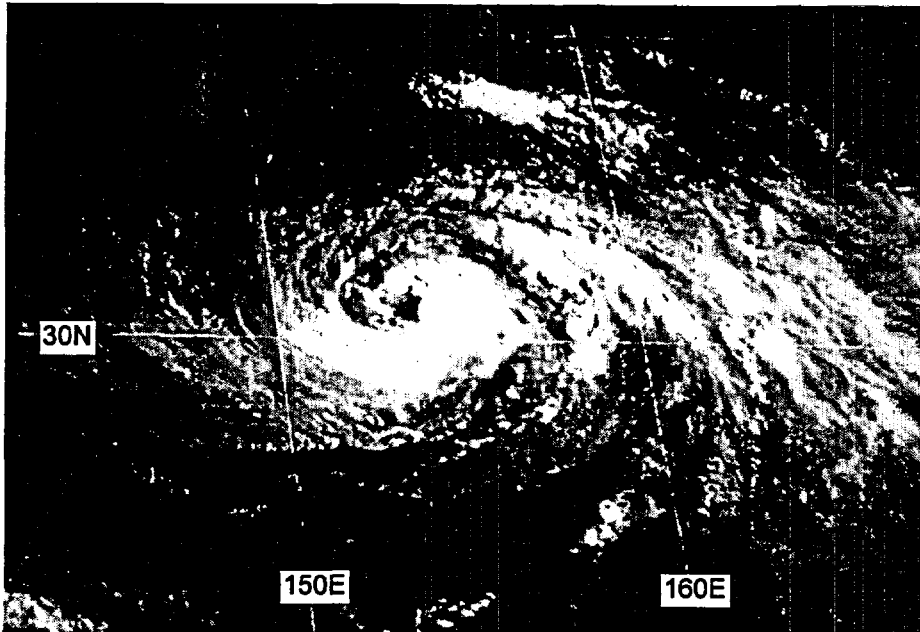


Figure 3-12-2 Joy at its peak intensity of 75 kt (39 m/sec) (012131Z August visible GMS imagery).

Continuing its slow northward drift, Joy began to shear on 04 August. On 05 August, Joy still had some deep convection located to the east of its exposed LLCC, but it had begun to accelerate toward the north-northeast as it interacted with a slow moving north-south oriented frontal cloud band. Expecting Joy to merge with the frontal cloud band and become extratropical, the JTWC issued the final warning valid at 050600Z.

III. DISCUSSION

Tropical cyclogenesis induced by a TUTT cell

A persistent feature of the upper-tropospheric flow over the tropics of the WNP and North Atlantic oceans during the summer is the tropical upper-tropospheric trough (TUTT) (Sadler, 1975). In the mean, the axis of the TUTT overlies low-level easterly trade wind flow approximately midway between the axis of the subtropical ridge and the axis of the monsoon trough.

In synoptic analyses, the TUTT is commonly observed to consist of a chain of westward moving synoptic-scale cyclonic vortices called "TUTT cells" in the WNP ("upper cold lows" in the Atlantic). The typical distribution of clouds associated with a TUTT cell features a relatively small region of isolated cumulonimbi (CB) or small mesoscale convective systems (MCS) within (or very near) its core. Sometimes extensive multi-layered clouds with embedded CB and MCSs are found to its south and east. The cloudiness to the south and east of a TUTT cell in the WNP is often associated with the monsoon trough, and the TUTT cell (or a chain of TUTT cells) acts to modulate the distribution of cloudiness along the axis of the trough, and also acts to produce an accentuated sinusoidal pattern to the outflow cirrus on the northern side of the monsoon cloud band.

Sadler (1967) proposed that the TUTT (with its embedded TUTT cells) was the primary source for disturbances (e.g., inverted troughs, isolated clusters of CB, etc.) in the trade wind flow. Sadler (1967) also credits TUTT cells with the capacity to induce TC genesis. TUTT-induced TC genesis was envisioned by Sadler to be the result of the distal penetration of the TUTT cell cyclonic circulation to the lower levels, thereby initiating deep convection which, through the release of latent heat, gradually converted the TUTT cell into a warm-core low (i.e., a TC). In two later papers (Sadler 1976, 1978), the role of the TUTT (and of TUTT cells within it) is relegated to one of contributing to the development of a TC by providing a region of persistent upper-level divergence to

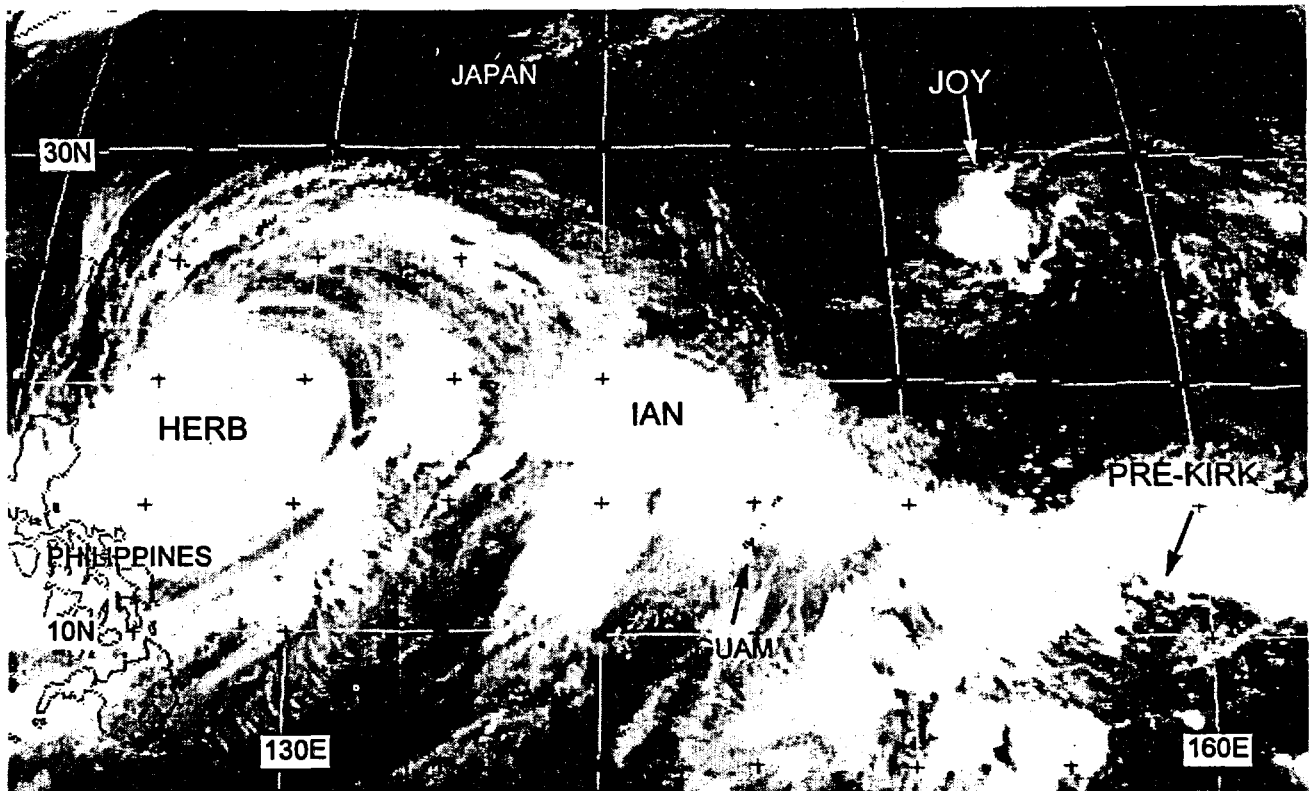


Figure 3-12-3 A characteristic typical of TUTT-induced tropical cyclones, Joy is isolated in the relatively cloud-free region of easterly low-level wind flow to the north of the monsoon cloud band (291331Z July infrared GMS imagery).

initiate and maintain deep convection. The TUTT cell also creates an efficient outflow channel for the incipient TC. In this scenario, the TC is usually located to the south or southeast of the TUTT, or a TUTT cell that propagates in tandem with it.

In our investigations of the role of the TUTT — and in particular, TUTT cells — in TC formation in the WNP, we have observed a process whereby a TC forms (sometimes rapidly) near the core of a TUTT cell. This process is similar to Sadler's (1967) distal mechanism of TUTT-cell induced TC formation. Careful observation has shown that the isolated convective cloud cluster (i.e., a mesoscale convective system) that forms a TC near the TUTT cell, does so not directly in the core of the TUTT cell, but usually within 200 to 400 km to the east through north of the upper-level circulation center of the TUTT cell where the upper-level flow is diffluent and anticyclonically curved. Also, it is here, on the northern side of the TUTT cell, that both the upper-level and lower-level flow is easterly resulting in a region of low vertical wind shear. Another typical characteristic of these TUTT-induced tropical cyclones is their isolation in the cloud minimum region of easterly wind flow to the north of the monsoon cloud band (e.g., Figure 3-12-3). The origin of Joy from a TUTT cell is well illustrated by water-vapor imagery (Figure 3-12-4a-g).

IV. IMPACT

No reports of injuries or damage were received at the JTWC.

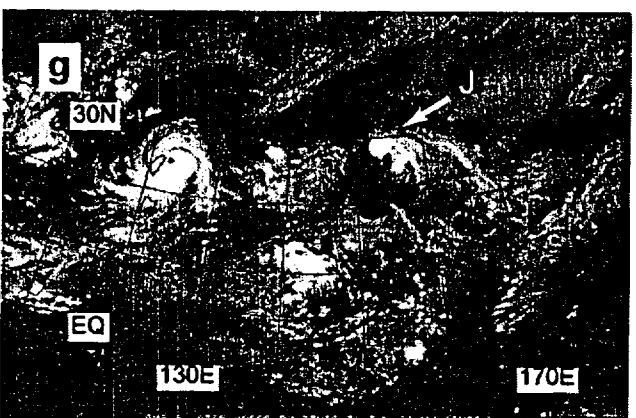
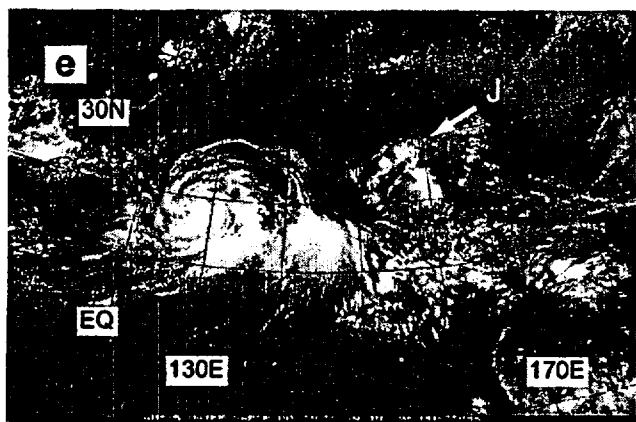
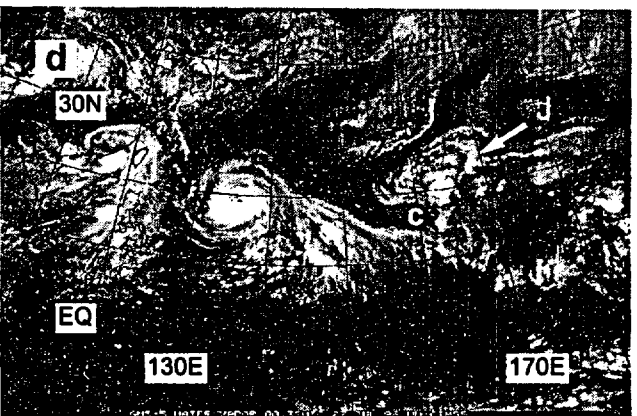
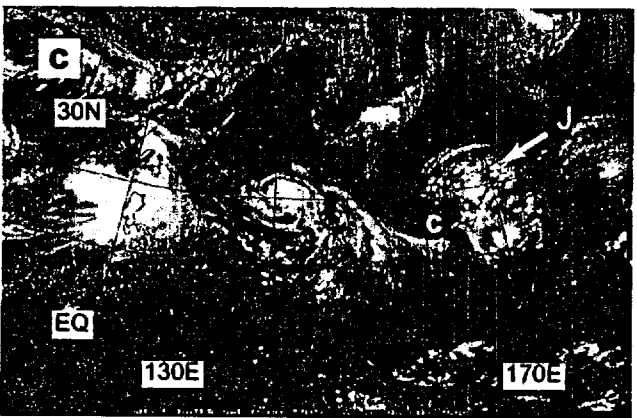
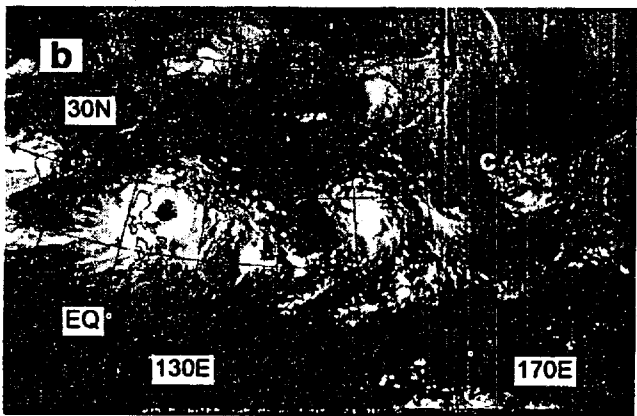
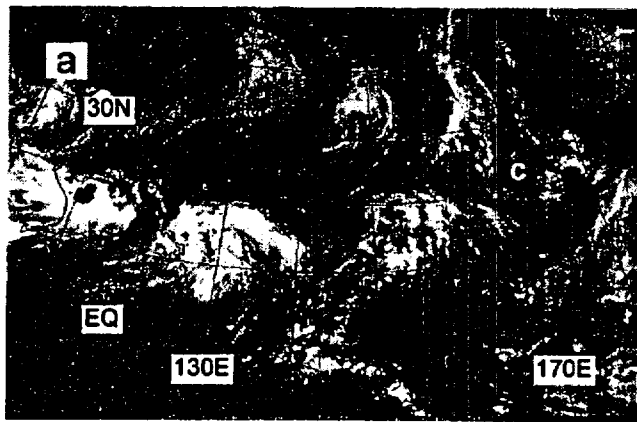
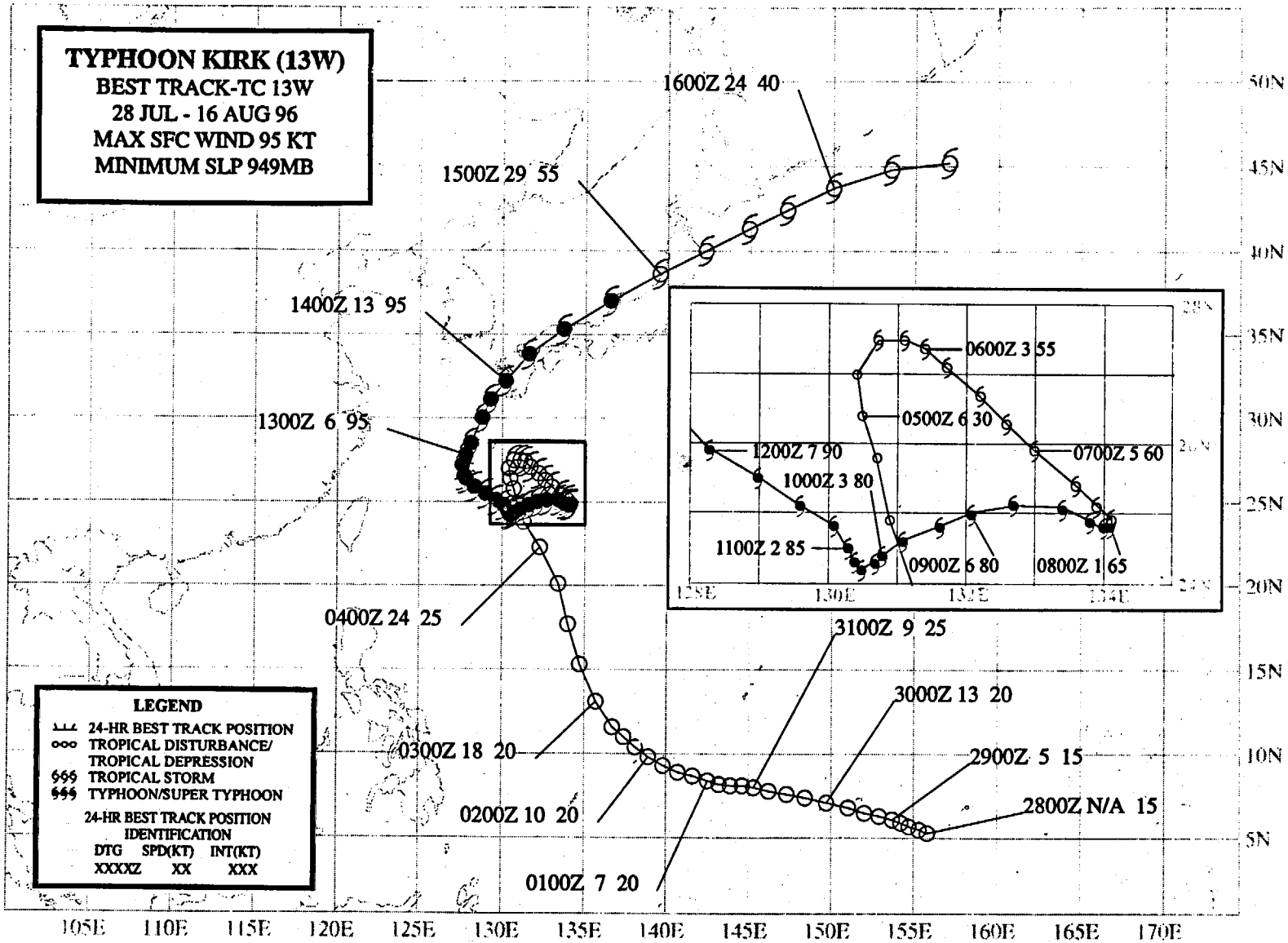


Figure 3-12-4 A TUTT cell (C) moves westward along 20°N in the WNP and induces the formation of Joy (J): (a) 212331Z July, (b) 240031Z, (c) 260031Z, (d) 270031Z, (e) 290031Z, (f) 300031Z, and (g) 310931Z July water-vapor GMS imagery.



TYPHOON KIRK (13W)

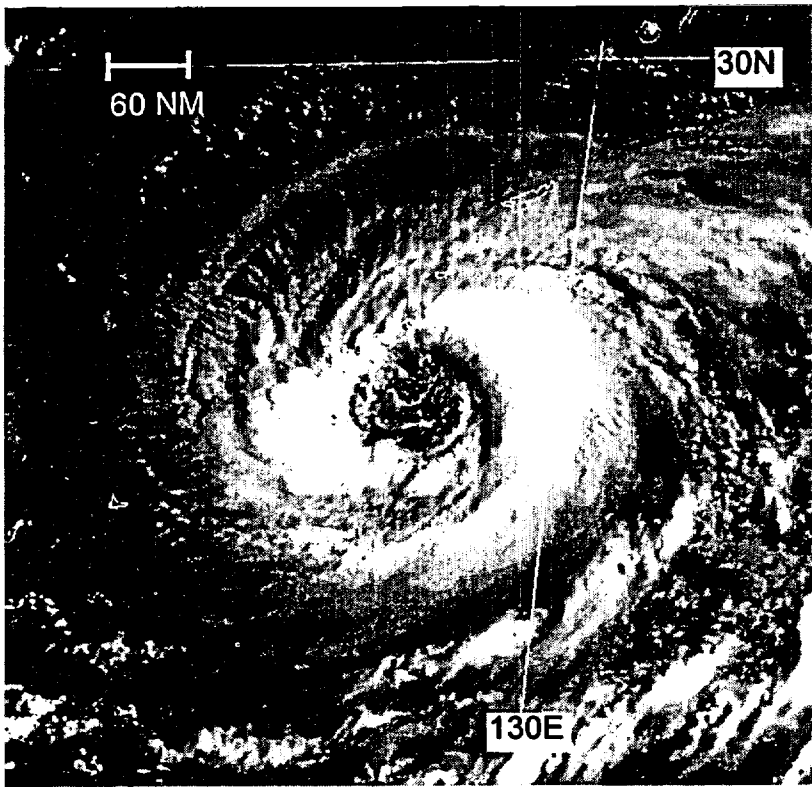


Figure 3-13-1 Kirk exhibits a very large eye as it approaches Okinawa (112331Z August visible GMS imagery).

I. HIGHLIGHTS

Forming from a monsoon depression in the Philippine Sea, Kirk moved on a complex north-oriented track which saw it undergo an unusual anticyclonic loop before passing directly over Okinawa. Kirk was the first of three TCs during 1996 to acquire a very large eye (Figure 3-13-1) — it took a full 12 hours for Kirk's 70-nm (130-km) diameter eye to pass over Okinawa. The NEXRAD Doppler radar at Kadena AB afforded a rare chance to investigate a typhoon with a ground-based radar from within the eye. After passing over Okinawa, Kirk moved north and passed over southern Japan where extensive property damage and loss of life were reported.

II. TRACK AND INTENSITY

During the final days of July, the tropical disturbance which became Kirk formed at the end of the monsoon trough to the southeast of Guam while both Herb (10W) and Joy (12W) were still active. During the first few days of August, Herb moved into China, Joy moved into the midlatitudes, and the pre-Kirk tropical disturbance was subsumed by a larger monsoon depression that formed in the Philippine Sea (Figure 3-13-2). Slow to consolidate (and undergoing a major structural change), the pre-Kirk disturbance received a total of five Tropical Cyclone Formation Alerts (TCFA) prior to the issuance of the first warning.

The tropical disturbance which became Kirk was first mentioned on the Significant Tropical Weather Advisory valid at 290600Z July, when synoptic data showed that a weak low-level circulation accompanied an area of convection near Chuuk. The first TCFA was issued valid at 292100Z when amounts of deep convection increased near the persistent low-level circulation center (LLCC). The second TCFA was issued valid at 300730Z to reposition the alert box for the continued west-northwestward motion of the pre-Kirk disturbance. This disturbance was undergoing large fluctuations in the amounts and organization of its deep convection which consisted of an ensemble of mesoscale convective systems (MCS), a hallmark characteristic of a monsoon depression. At 310300Z, the second TCFA was canceled when convection became more poorly organized. On 01 August, extensive amounts of deep convection formed in the Philippine Sea — disorganized bands and small clusters of MCSs occupied an area within a box bounded by 5°N to 25°N and 130°E to 150°E. On 02 August, this large area of deep convection became organized as a large monsoon depression (Figure 3-13-2) comprised of an enormous ensemble of MCSs associated with a large, but weak, cyclonic circulation and extensive cirrus outflow organized into an anticyclonic pattern. A third TCFA was issued valid at 020030Z August when scatterometer data indicated the presence of an LLCC with monsoon gales located to its southeast. Remarks on this TCFA include:

"... A disturbance resembling a monsoon depression is located within the monsoon trough. Scatterometer data [from an earlier pass of the ERS-1 satellite] supports the presence of a closed low-level circulation center, with gale force winds located 180 nm to the southeast of the circulation. These winds are associated with a surge in the monsoon. . . ."

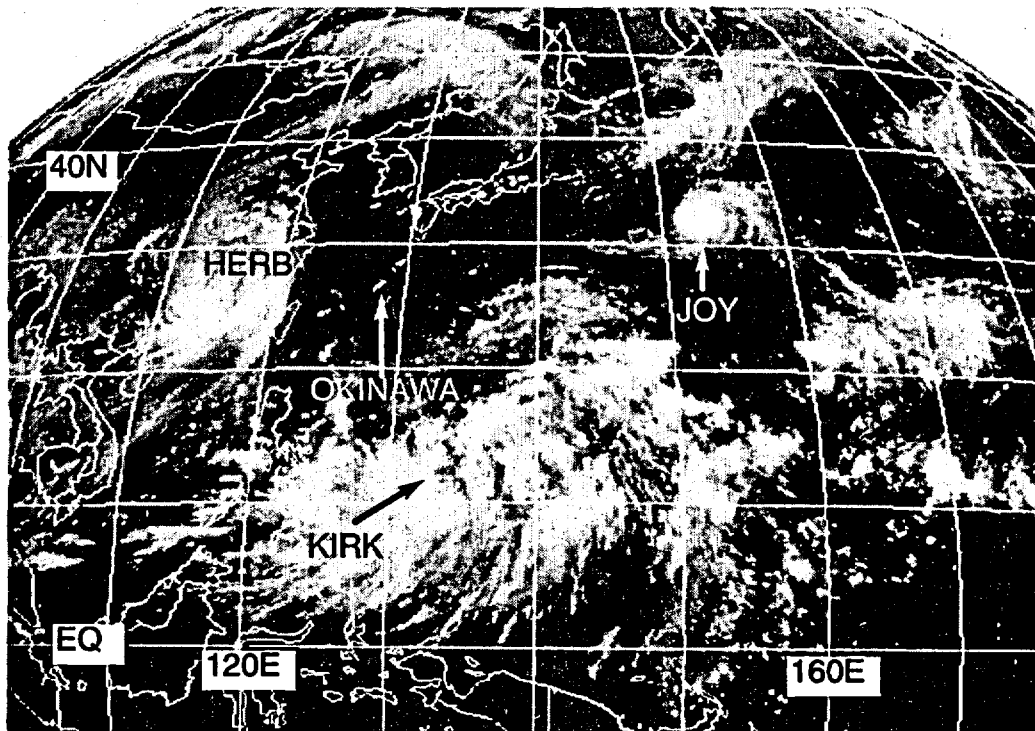


Figure 3-13-2 The monsoon depression in the Philippine Sea from which Kirk developed (020631Z August infrared GMS imagery).

As is often the case with TCs originating from a monsoon depression, the extensive ensemble of MCSs associated with the monsoon depression fluctuated greatly, and were slow to consolidate near a well-defined LLCC. Thus a fourth TCFA was issued valid at 030030Z when satellite

imagery could not confirm the presence of a well-defined LLCC, and deep convection was still widely distributed and not showing signs of consolidation. The fifth, and last, TCFA was issued valid at 031100Z in order to reposition the alert box to encompass an area of deep convection that was becoming organized outside the alert box specified by the fourth TCFA. This area of deep convection increased in organization near the LLCC, and the first warning on Tropical Depression (TD) 13W was issued valid at 031800Z.

Moving on a north-oriented track within a monsoon trough which had become reverse oriented (see Appendix A), TD 13W gradually slowed its forward speed, and on 06 August, it turned toward the southeast as it began an anticyclonic loop in its track. On the warning valid at 060000Z, TD 13W was upgraded to Tropical Storm Kirk.

While executing its anticyclonic loop, Kirk intensified and became a typhoon at 080000Z. At this time, it began to move on a generally westward heading toward Okinawa. Before reaching Okinawa on 12 August, Kirk's eye became extremely large (see Discussion section). Radar and satellite measurements of its eye diameter exceeded 60 and 70 nm respectively during most of 12 August (Table 3-13-1).

After passing over Okinawa, Kirk turned toward the north, its eye diameter decreased, and the system reached its peak intensity of 95 kt (49 m/sec) (Figure 3-13-3) while accelerating along a recurving track that brought it across southern Japan and into the Sea-of-Japan. Kirk dropped below typhoon intensity as it skirted northeastward along the coast line on the Sea of Japan side of Honshu. On 15 August, Kirk crossed the northern end of Honshu from west to east and entered the Pacific. The system then accelerated within the midlatitude westerlies, became extratropical, and the final warning was issued valid at 160600Z August.

Table 3-13-1 EYE DIAMETER OF KIRK FROM NEXRAD AND SATELLITE DURING PASSAGE OVER OKINAWA.

DTG (Z)	NEXRAD eye diameter (nm)	Satellite eye diameter (nm)
120501	—	76
120530	—	70
120630	—	70
120640	70	—
120830	—	67
120930	61	71
120942	—	70
121030	63	74
121130	—	77
121151	63	—
121230	55	70
121240	—	65
121330	53	70
121430	51	68
121530	60	68
121630	66	67
121730	53	70
121815	58	—

III. DISCUSSION

a) Unusual motion: a synoptic-scale anticyclonic loop

It is well known that TCs tend to meander or oscillate about a mean path. These oscillations cover a wide range of scales and can take on several forms, including small-amplitude and short-period trochoidal oscillations around an otherwise smooth track, larger-scale and longer-period meanders, more erratic and nonperiodic meanders (occasionally including stalling, or small loops), or highly-erratic wandering with no well-defined track. A wide range of scales are involved as the meanders vary in period from a few days to less than an hour and have amplitudes up to a few hundred kilometers.

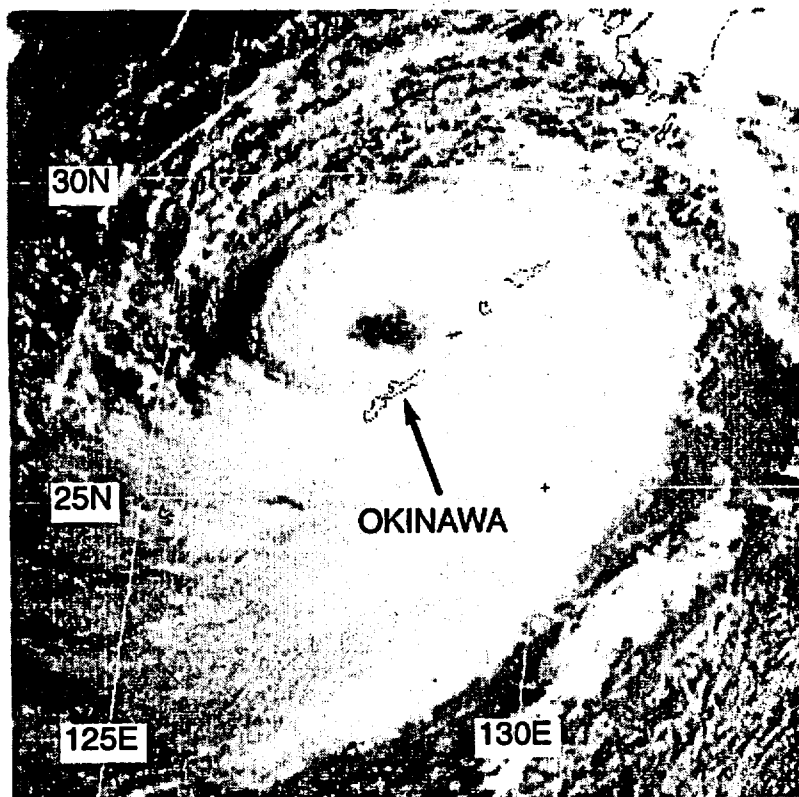


Figure 3-13-3 Kirk reaches its peak intensity of 95 kt (49 m/sec) (122131Z August visible GMS imagery).

During the two days prior to passing over the island of Okinawa, Kirk executed an anticyclonic loop with a diameter of approximately 300 nm (550 km). Well-defined looping of a TC, whereby the looping motion results in the TC recrossing its track, is unusual. According to Holland and Lander (1993), medium-scale meanders with period greater than one day and amplitude of several tens to hundreds of kilometers tend to have an equal distribution of cyclonic and anticyclonic rotation. There is a strong tendency toward exclusively cyclonic rotation at shorter periods as confirmed by an examination of 17 radar tracks of TCs provided by Meighen (1987): seven of these had no clearly discernible oscillation, and the remainder contained 23 small-scale meanders, all of which were cyclonic.

Potential mechanisms for the larger meanders include interactions with surrounding weather systems such as other TCs, TUTT cells, and synoptic-scale troughs and ridges in the subtropics or midlatitudes. During the period of its anticyclonic meander, Kirk probably interacted with other circulations in the monsoon trough and with a high-pressure system to its north. While Kirk was executing its anticyclonic loop, the monsoon trough had lifted to a very high latitude (Figure 3-13-4) and had become reverse-oriented along the portion of it that contained Kirk. Reverse orientation of the monsoon trough is often associated with north-oriented motion of its associated TCs (Lander, 1996). While this may be a satisfactory explanation for Kirk's overall northward drift, it does not offer much insight on the slow anticyclonic loop Kirk made during the period 050000Z through 120000Z. Possible explanations for this loop include an interaction of Kirk with other low-pressure systems along the reverse-oriented monsoon trough, and the affects of a midlevel anticyclone which passed slowly to Kirk's north during this time period. Once the midlevel high moved eastward into the Pacific, Kirk recurved and entered the midlatitude westerlies.

b) *Extremely large eye*

In Dvorak's analysis techniques (Dvorak 1975, 1984), the eye of a TC is considered to be small if its satellite-observed diameter is less than 30 nm (55 km), average if between 30 nm and 45 nm (55 km and 85 km), and large if greater than 45 nm (85 km). Kirk's satellite-observed eye diameter was in excess of 70 nm (150 km) during much of 12 August (the day it passed over Okinawa). This very large eye required 12 full hours to pass directly across Okinawa. Kirk was one of three TCs during 1996 — the others were Orson (19W) and Violet (26W) — which possessed, at some time during their evolution, an eye with an exceptionally large diameter (on the order of 75 nm).

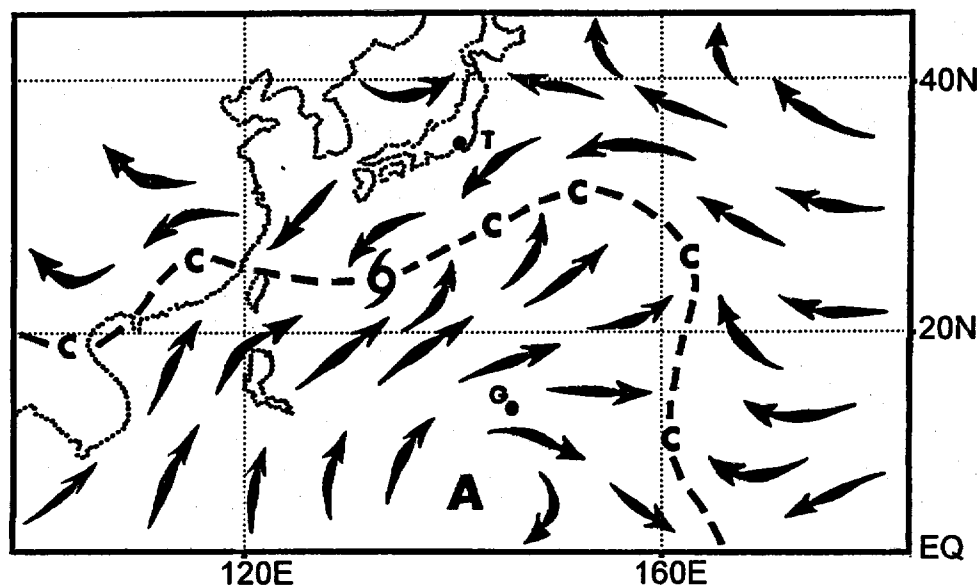
Eye diameters on the order of 75 nm, or greater, are not common. None were observed during 1995. One of the TCM-90 TCs — Abe — possessed an eye with an exceptionally large diameter of about 80 nm. The unusual form of these TCs on satellite imagery led to their being called "truck tires" by JTWC satellite analysts and forecasters.

In a survey of past ATCRs, the largest eye diameter ever reported was that of Typhoon Carmen (1960). By strange coincidence, Carmen, like Kirk, passed directly over Okinawa. Carmen's eye diameter, as measured by the weather radar at Kadena was 200 statute miles (175 nm ; 325 km). Comments in the 1960 Annual Typhoon Report include:

" . . . Another feature quite unusual about this typhoon was the diameter of its eye. Reconnaissance aircraft frequently reported eye diameters of 100 mi, using as the basis of measurement, surface winds and pressure gradient. However, with respect to wall clouds surrounding the eye, radar photographs taken from the CPS-9 at Kadena AB show quite clearly that on 20 August, the eye had a diameter of approximately 200 mi . . . The eye diameter of Carmen was probably one of the largest ever reported . . ."

Kirk, like Carmen, was also viewed by a radar at Kadena: this time a new NEXRAD.

Figure 3-13-4
Schematic illustration of the monsoon circulation which became organized in an unusual pattern as Kirk underwent its anticyclonic loop along its north-oriented track (illustration based on 090000Z August JTWC surface analysis).



c) Kirk's passage over Kadena's NEXRAD

One of only four NEXRAD radar units to be installed in the WNP (the others are on Guam and in Korea), the NEXRAD installed on Okinawa affords an excellent opportunity to gather data on the TCs which frequently pass near or over this island. When Kirk passed directly over Okinawa, it was continuously under surveillance by NEXRAD. The NEXRAD support provided to the JTWC by Kadena base weather personnel was superb. They provided timely, thorough information on center positions, wind distribution and intensity. The most striking aspect of Kirk's radar signature was its large eye. During 12 August, as Kirk passed over the radar site from east to west the eye diameter was reported to have been consistently on the order of 60 nm (110 km) (Figure 3-13-5). This is about 10 to 15 nm less than the eye diameters as derived from satellite imagery during this time (Table 3-13-1). It is common for the eye diameter as observed from satellite to be larger than the radar-observed eye diameter due to the general outward sloping with height of the eye-wall cloud.

Another fascinating aspect of the radar coverage occurred when the radar was exactly in the center of the eye: the Doppler velocity product indicated almost zero velocity along all radials. This is certainly what might be expected, but it may be the first time it has actually been observed. Another feature of the velocity product at this time was a slight asymmetry in the radial velocity which were mostly light inbound to the east-southeast and light outbound toward the west-northwest (i.e., indicative of the motion of the typhoon at that time).

d) *Fog in the eye, and other ground observations*

In recent years, there has been much debate concerning the possible effects of warmer sea-surface temperatures (SST) on the annual numbers and the potential peak intensities of TCs under conditions of a warmer climate. Emanuel (1988) set the theoretical ground work for this problem when he introduced his method for calculating the potential peak intensity of TCs. The potential peak intensity of a TC, in his framework, is largely a function of the difference between the warm SST and the colder temperatures of the upper-level outflow layer. Observationally, there is a relationship between the SST and the upper bound of TC intensity.

Granting for sake of argument that the climate will soon become warmer, and that the SST may become on the order of 1°C higher, a question arose as to the affects of this on TC distribution and intensity. This question was addressed in a special symposium at the third International Workshop on Tropical Cyclones (held in Huatulco, Mexico in 1993). The findings of this symposium (published in Lighthill, et al., 1994) were that any effects of a warmer world would likely be masked by the natural variability in TC distribution and intensity and the natural large-scale factors that govern TC formation and development.

A crucial part of this argument hinges on the physical processes which limit the intensity of a TC. As the intensity of a TC increases, frictional drag and evaporative cooling of sea spray have been suggested as brakes on the continued intensification of the TC. Other limiting factors on intensity may be the efficiency of the deep convection in the eye wall to evacuate the mass of the low-level inflow.

The thermodynamics of the TC are not fully understood. The relative contributions to the energy available to the TC by latent heat release and sensible heat fluxes from the ocean are not fully known. The cooling effects of sea spray which is produced at higher wind speeds has been introduced as an important factor in the energetics of the TC (Kepert and Fairall, 1993).

A tangential sidelight which may have important implications on the debate on the role of sea-surface fluxes on the energetics of TCs is the frequent observation of fog within the eye of TCs. During all TCs which have passed over Guam during recent years, ground fog has been reported in the eye. Observations from Kadena indicate fog was present in the eye of Kirk for the first three hours within the eye. Ramage (1974) discusses the occurrence of fog reported at sea by a ship in the eye of a typhoon (this was under the special condition of the SST having been significantly cooled by the recent passage over the same location by another typhoon). Simpson (personal communication, 1996) indicates ground fog was often reported in the eye of landfalling hurricanes in the United States. The suggested mechanism was sensible cooling of the air within the eye as it passes over land chilled by the rain and wind of the eye wall. Fog in the eye at ground or sea level could have relevance to the thermodynamic arguments concerning TC intensity (e.g., rates of sea-spray evaporation in the inflow layer, and extent of subsidence of warm dry air within the eye).

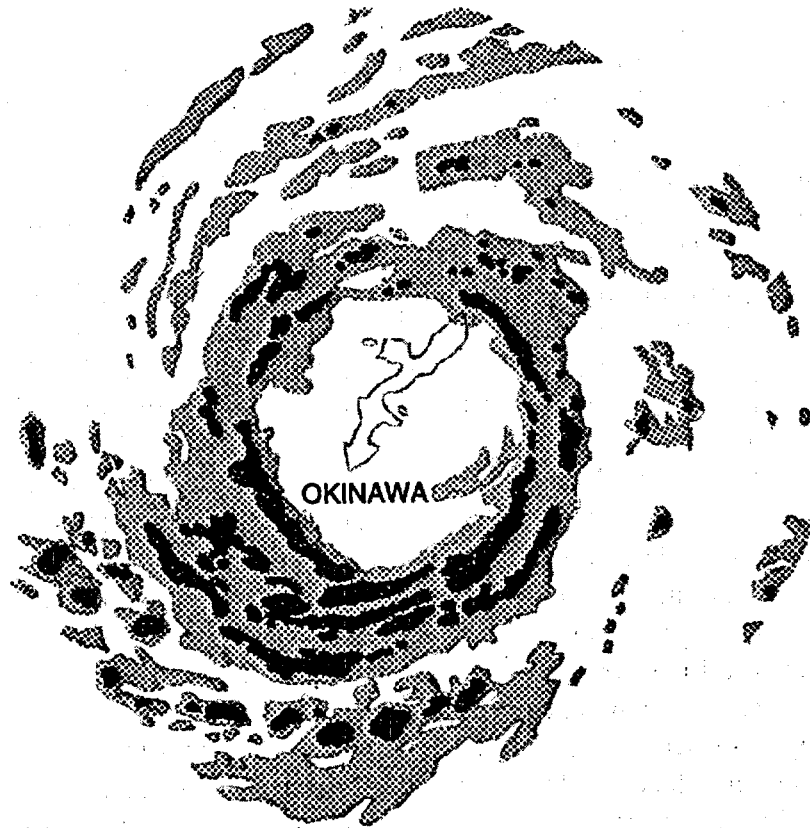
IV. IMPACT

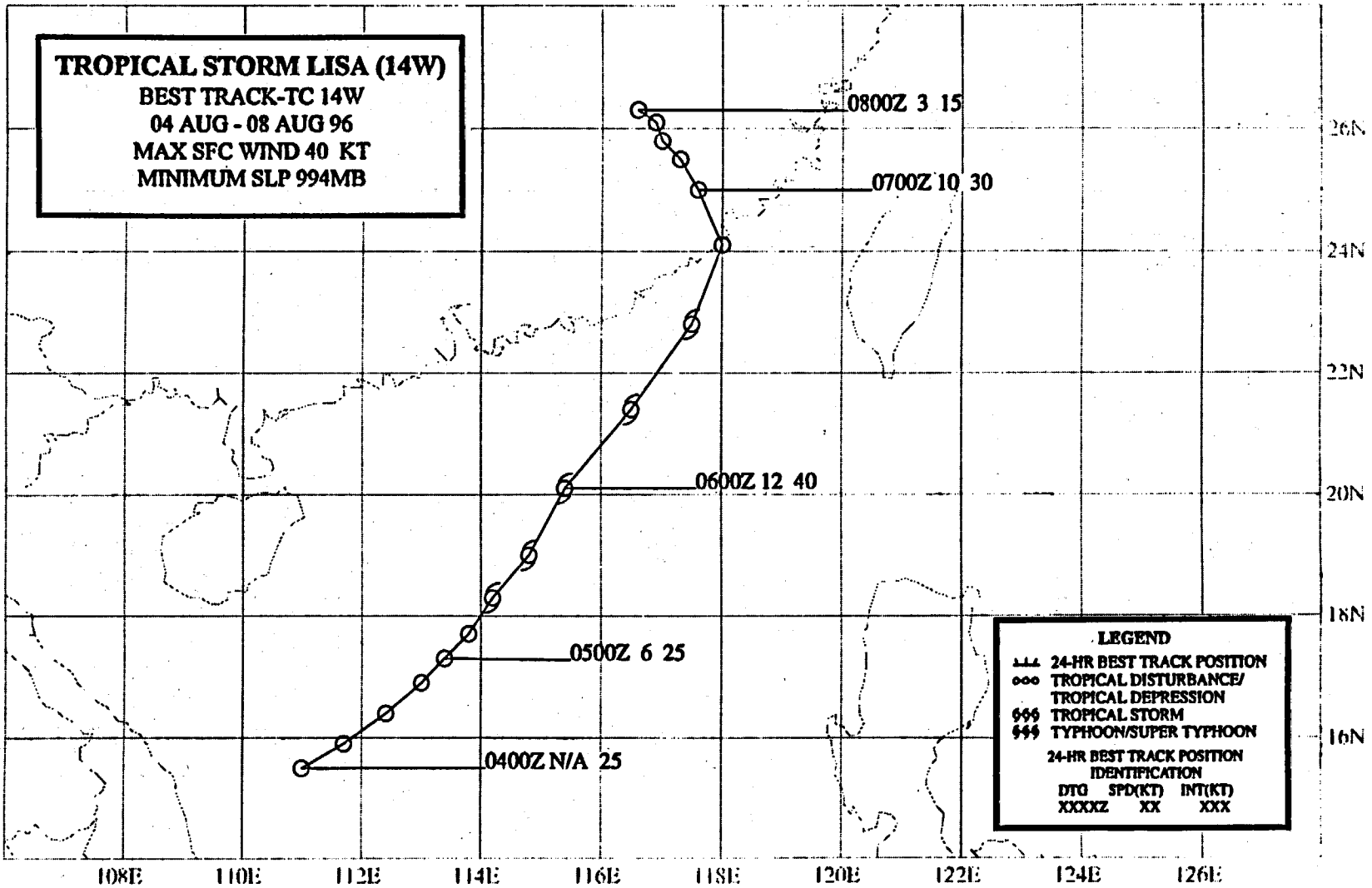
Kirk's impact on Okinawa was largely superficial with many trees blown down, street signs broken, decorative wooden fences knocked over, and street light fixtures twisted or damaged. Some local flooding was reported. Some economic losses were incurred due to the cancellation of normal air service, the closing of shops, and a halting of an oil refinery.

Damage was more extensive, and loss of life was reported, as Kirk moved into southern Japan. There, at least two people were reported killed (a Japanese woman and a U.S. Navy serviceman were swept out to sea by high surf) and 15 injured. Over 100,000 homes were left without electricity.

At the Navy base at Sasebo, superficial damage was reported on some ships, while several other ships dragged anchor. Numerous trees were reported down on the main base, as well as a brief loss of power. At Misawa AB, some aircraft were evacuated and some others secured in hangars, but the effects of Kirk there were minimal, and no damage was reported.

Figure 3-13-5 A radar depiction of Kirk while it was centered over Kadena. Shaded regions indicate reflectivity values of at least 30 dBZ, and the black regions indicate reflectivity values of at least 40 dBZ. (Depiction based upon the 120611Z NEXRAD composite reflectivity product).





TROPICAL STORM LISA (14W)

In early August, as Herb (10W) moved into China, and Joy (12W) recurved into the midlatitudes, deep convection began to increase in the monsoon trough which stretched across the Philippines into the Philippine Sea. On 02 August, deep convection consolidated within two regions, one (which became Kirk (13W)) in the Philippine Sea, and the other (which became Lisa) over the Philippines. The area of deep convection in the Philippine Sea became a monsoon depression and moved north, while the area of convection over the Philippines moved westward and became a monsoon depression in the South China Sea (SCS). Indications of organization of the deep convection over the SCS were first mentioned on the 040600Z Significant Tropical Weather Advisory. When satellite imagery and synoptic data indicated the presence of a low-level cyclonic circulation within an area of persistent deep convection (Figure 3-14-1a), the JTWC issued a Tropical Cyclone Formation Alert, valid at 050430Z. The first warning on Tropical Depression (TD) 14W soon followed (valid time 050600Z) based on satellite intensity estimates of 25 kt (13 m/sec). With Kirk (13W) east of Okinawa, the axis of the monsoon trough became reverse oriented, and TD 14W moved northeastward toward Taiwan. The upgrade of TD 14W to Tropical Storm Lisa at 060000Z was based upon synoptic reports of gales near the LLCC at a time when the satellite signature was not well-organized. Late in the day on 06 August, the persistent deep convection associated with Lisa moved over land in southeastern China. Microwave imagery (Figure 3-14-1b), however, indicated that the LLCC was sheared to the east of this convection and remained offshore through the night. On the morning of 07 August, synoptic data indicated the LLCC of Lisa had moved ashore in China, and the final warning was issued valid at 070000Z.

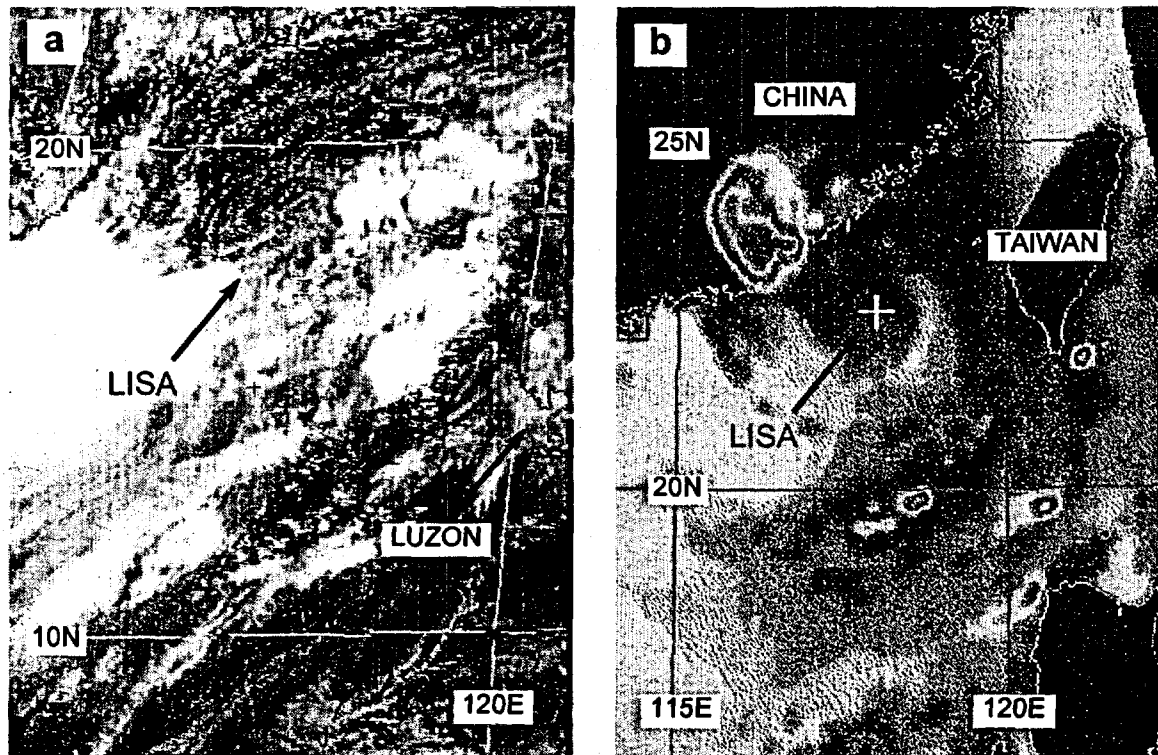
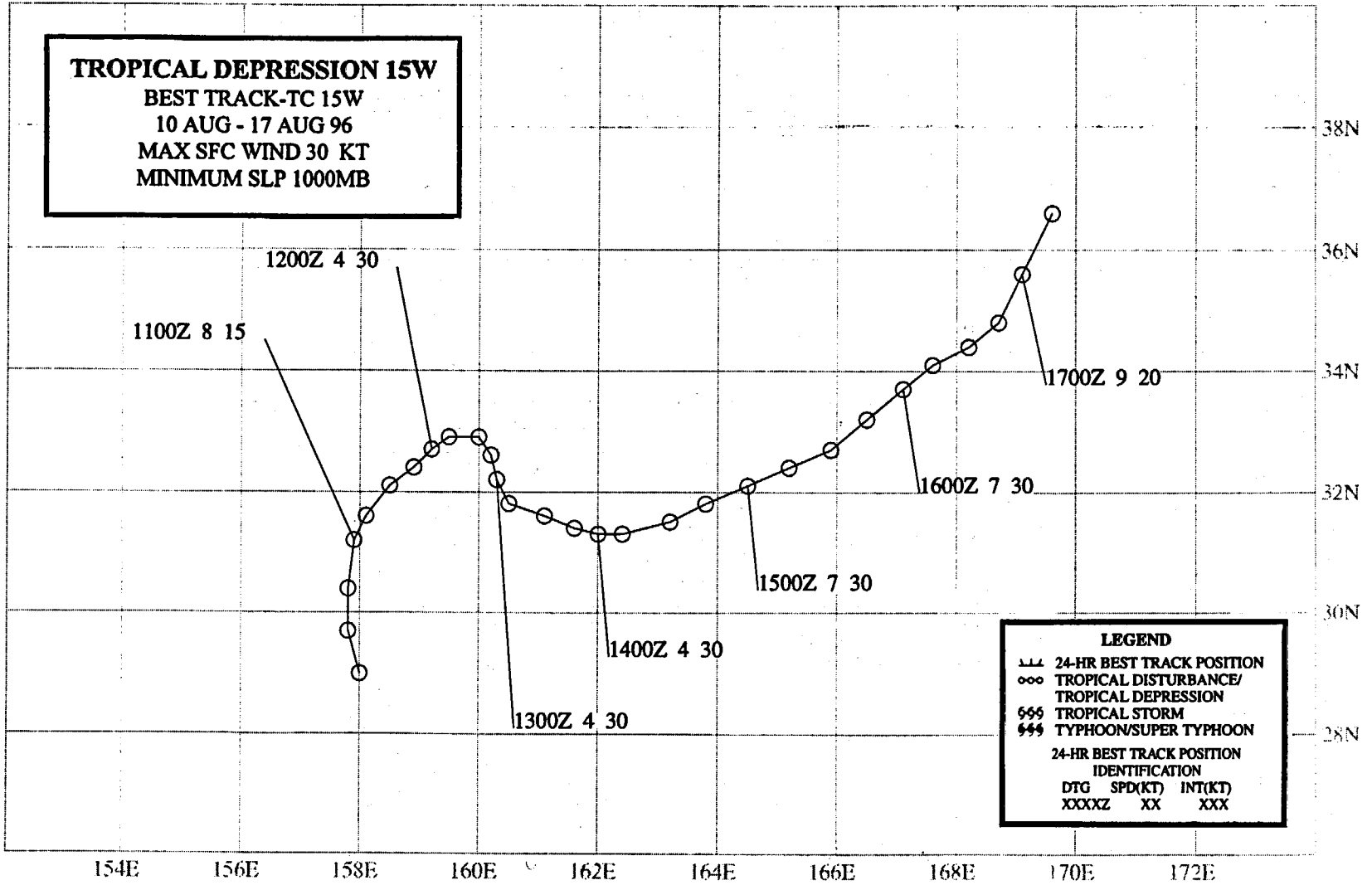


Figure 3-14-1 (a) A well defined LLCC is exposed amidst the ensemble of MSCs associated with a monsoon depression in the SCS (050031Z August visible GMS imagery). (b) Lisa's LLCC is clearly located over water to the southeast of the deep convection in microwave imagery (061415Z August 85 GHz horizontally-polarized microwave DMSP imagery).



TROPICAL DEPRESSION 15W

Tropical Depression (TD) 15W originated in the subtropics at a time when the monsoon trough was displaced far to the north of normal (see Figure 3-13-4 in Kirk's summary for a graphic depiction of this unusual low-level flow pattern). TD 15W had an unusual structure comprised of an extensive region of low-level cloud lines surrounding a small area of deep convection (Figure 3-15-1a). First identified on the 100600Z August Significant Tropical Weather Advisory, the system drifted slowly northward and became better organized. Based on satellite intensity estimates of 25 kt (13 m/sec), the first warning was issued, valid at 120600Z. Moving generally toward the east-northeast, the system maintained its unusual cloud pattern. The peak intensity of 30 kt (15 m/sec) — as estimated from satellite imagery, and confirmed by a scatterometer pass (Figure 3-15-1b) — was maintained for several days. When the system lost its deep convection, and the extent and organization of the low-level cloud lines decreased, the final warning was issued valid at 160600Z.

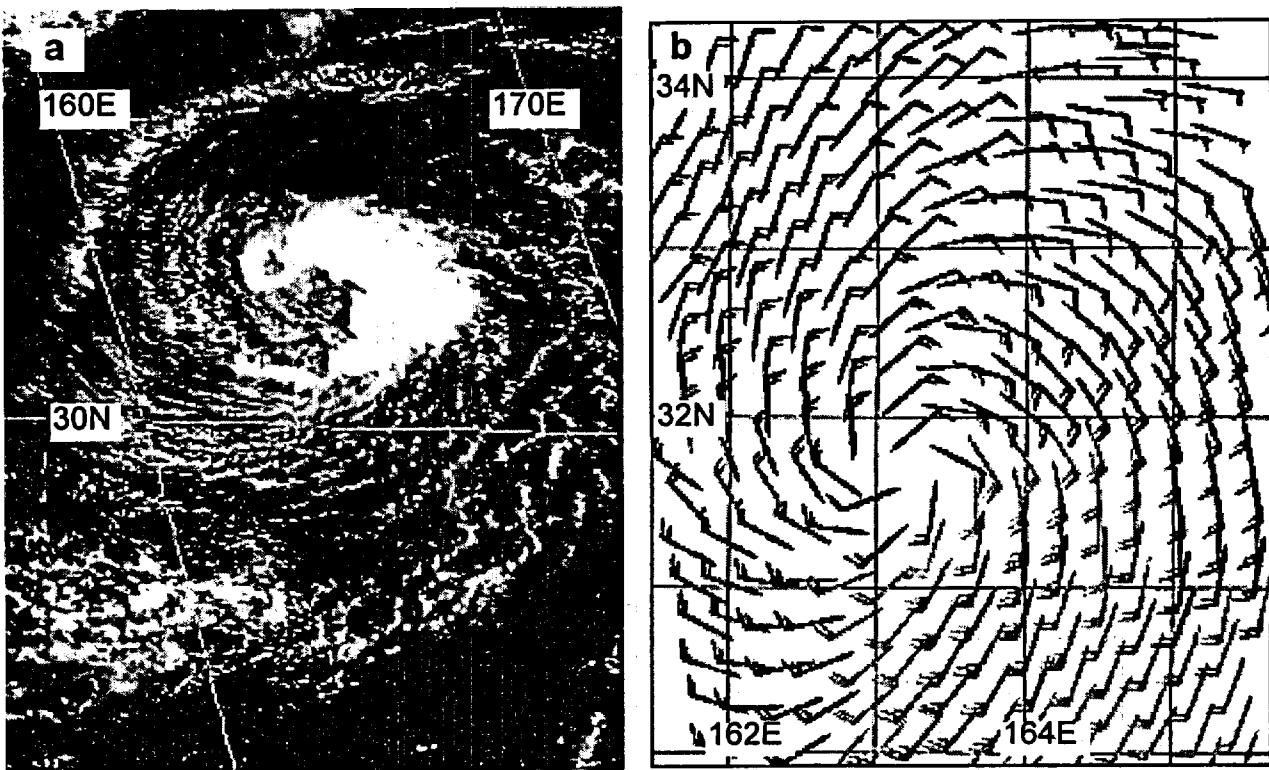


Figure 3-15-1 (a) Well-defined low-level cloud lines coil tightly around a poorly organized area of deep convection (132331Z August visible GMS imagery). (b) A region of 25- to 30-kt (13- to 15-m/sec) winds was detected by scatterometry in the southeastern quadrant of TD 15W (141132Z August ERS-2 scatterometer-derived marine surface winds).

TROPICAL STORM MARTY (16W)

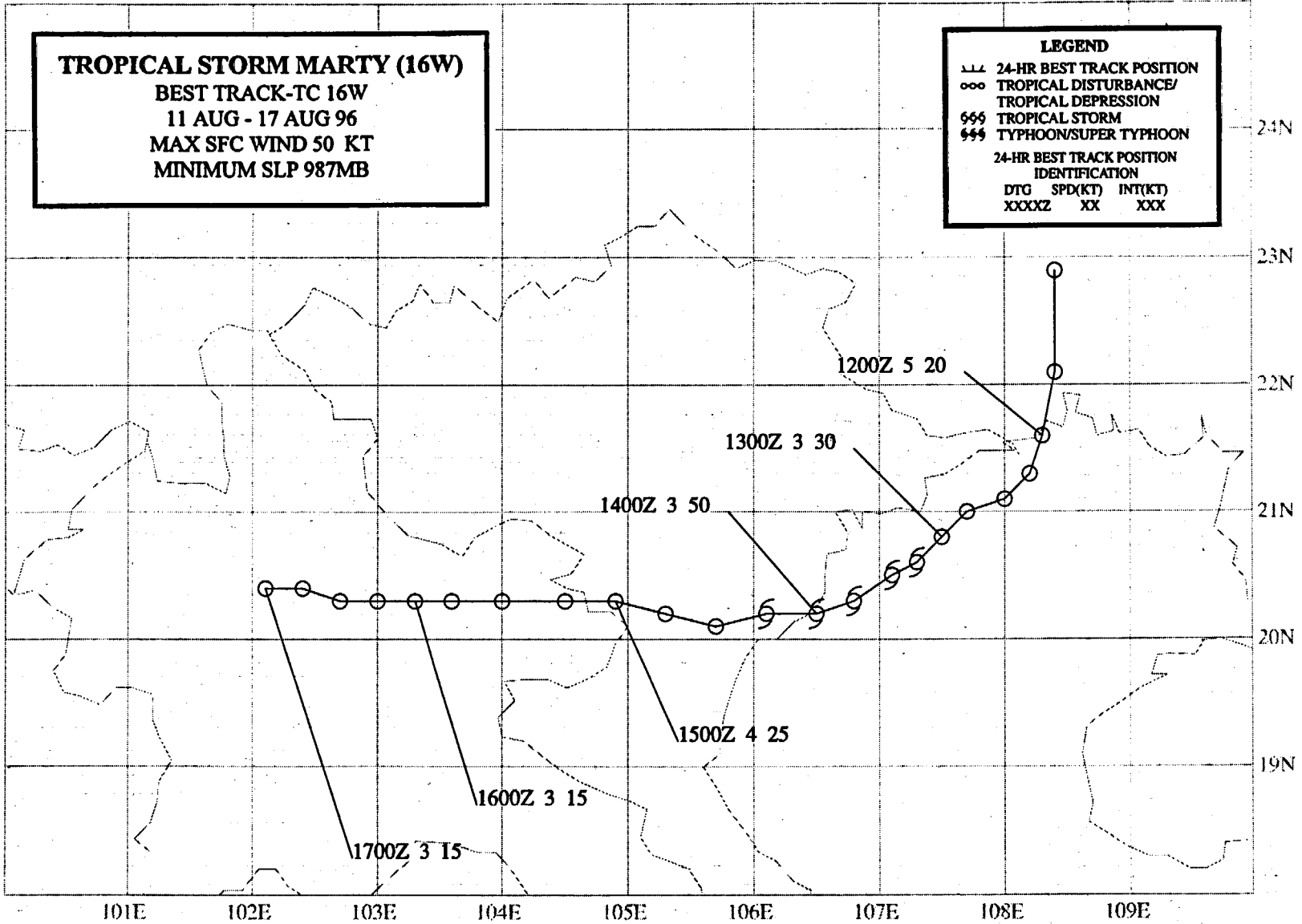
**BEST TRACK-TC 16W
11 AUG - 17 AUG 96
MAX SFC WIND 50 KT
MINIMUM SLP 987MB**

LEGEND

- 24-HR BEST TRACK POSITION
- ooo TROPICAL DISTURBANCE/
TROPICAL DEPRESSION
- 666 TROPICAL STORM
- 666 TYPHOON/SUPER TYPHOON

24-HR BEST TRACK POSITION
IDENTIFICATION
DTG SPD(KT) INT(KT)
XXXXZ XX XXX

109



TROPICAL STORM MARTY (16W)

I. HIGHLIGHTS

Developing in the Gulf of Tonkin, Marty was a very small tropical cyclone. In real time, satellite intensity analyses did not agree with synoptic data and with news reports of the devastation of Vietnamese fishing boats in the Gulf of Tonkin where 125 people were reported killed and another 107 missing. Marty was upgraded to a tropical storm after it had crossed the coast because synoptic data indicated that gales were present along the coast and over waters to the east. The final best track increases Marty to a tropical storm while it was over the Gulf of Tonkin and raises its peak intensity from 35 to 50 kt.

II. TRACK AND INTENSITY

Marty originated in the monsoon trough over land in southwestern China. Though first mentioned on the 130600Z August Significant Tropical Weather Advisory, the area of deep convection that became Marty could be identified (in post analysis) as early as 11 August (Figure 3-16-1). The pre-Marty disturbance moved southward into the Gulf of Tonkin and intensified. Based on indications from satellite and synoptic data that the system had moved over water, the first warning (valid at 130600Z August) was issued on Tropical Depression (TD) 16W. The TD then turned more to the west, and shortly after 140000Z (after a short path over water) it made landfall about 60 nm (110 km) south of Hanoi. Although over land at 140600Z, TD 16W was upgraded to Tropical Storm Marty when synoptic data indicated that gales were occurring along the coast and over water to the east. The upgrade to a tropical storm after the system made landfall is unusual, but it was realized the intensity of Marty had been underestimated. Ironically, the warning that upgraded Marty to a tropical storm was also the final warning, since the system was then weakening over land.

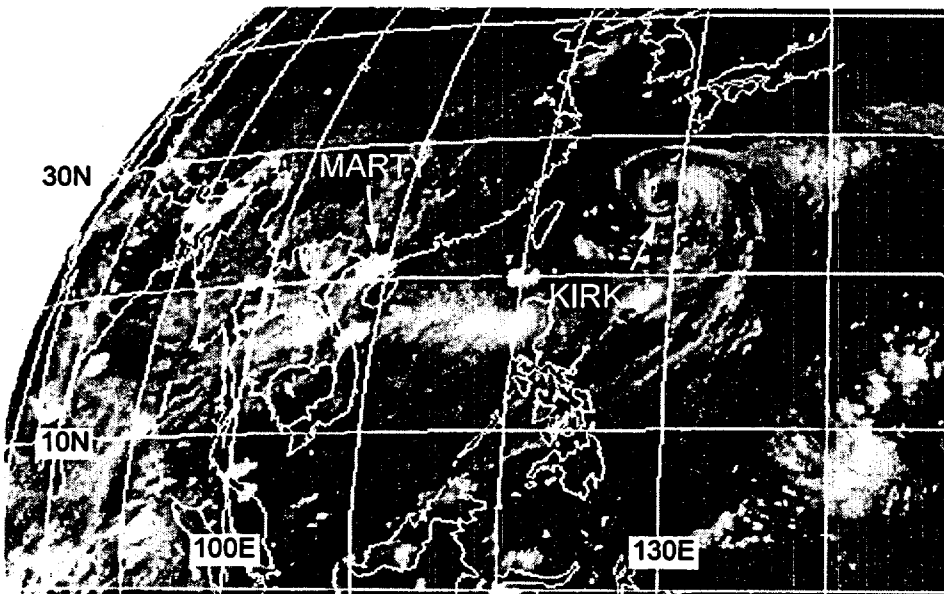


Figure 3-16-1 The disturbance that became Marty formed in southwestern China along the axis of the monsoon trough (111831Z August infrared GMS imagery).

III. DISCUSSION

The importance of post analysis

A comprehensive post analysis provides insight into the behavior of a TC in a specific situation. The goal of such an analysis is to produce a more exact, definitive product from the usually vague, imprecise, and often incomplete real-time data input. In the case of Marty, there was very lit-

the synoptic data available in the region. When the TC made landfall in Vietnam, crucial synoptic data (including a scatterometer pass) became available which indicated Marty was more intense than

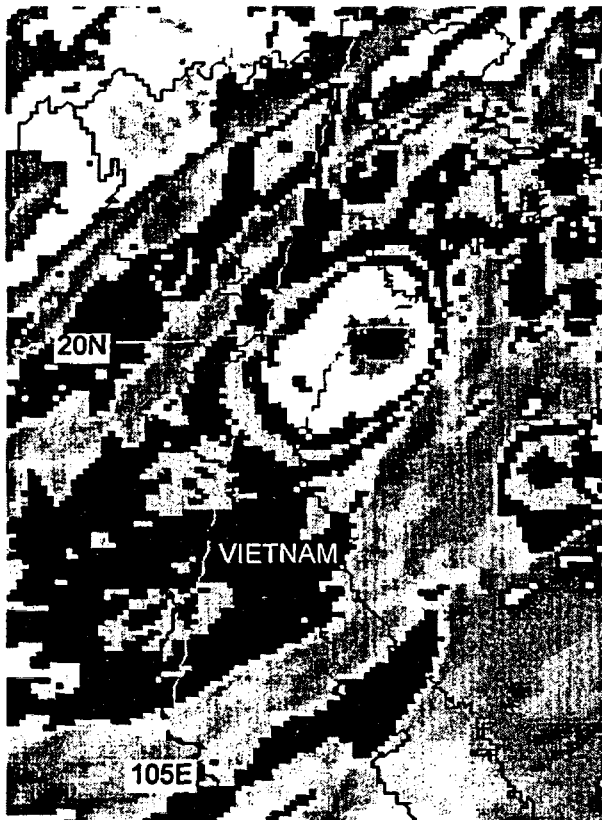


Figure 3-16-2 Exhibiting a CDO pattern, the very small Marty attains its peak intensity of 50 kt (26 m/sec) while over the Gulf of Tonkin (132131Z August enhanced infrared GMS imagery).

thought. Also hindering an accurate assessment of Marty's intensity was its small size (Figure 3-16-2) which biased the satellite intensity estimates on the low side. A careful review of Marty was conducted and it included a reassessment of intensity estimates from satellite imagery (Table 3-16-1). Concerning Marty's intensity, the following was noted by the reassessment team:

"TS Marty was close to a midget in size. Dvorak [satellite intensity estimates] did not appear to coincide with synoptic data and news reports of 'whirlwind destroying numerous fishing boats with the loss of from 125 to 232 people'. All T number [intensity estimates] . . . were 0.0 [less than 25 kt] except for a T2.0 . . . at 13/1730Z just before it went on shore in Vietnam. Pressures were below 997 mb within 60 nm of the circulation center — lots of room for greater intensity of the cyclone if it was 'truly' a midget".

Figure 3-16-3 is satellite imagery on 13 August originally thought to indicate wind speeds less than 25 kt (13 m/sec), but in post analysis was considered to be indicative of 30 kt (15 m/sec). Figure 3-16-2 (and later visible imagery — not shown) was reassessed to be indicative of an intensity of 50 kt (26 m/sec).

IV. IMPACT

News out of Vietnam claimed that a "whirlwind" capsized fishing boats along the northern Vietnamese coast, killing at least 125 people with another 107 missing and feared dead.

DTG	New T Number	Intensity (kt)	Old T Number	Intensity (kt)
12/03Z	1.0	25	0.0	<25
13/03Z	2.0	30	0.0	<25
13/09Z	2.5	35	0.0	<25
13/21Z	3.5	55	2.0	30

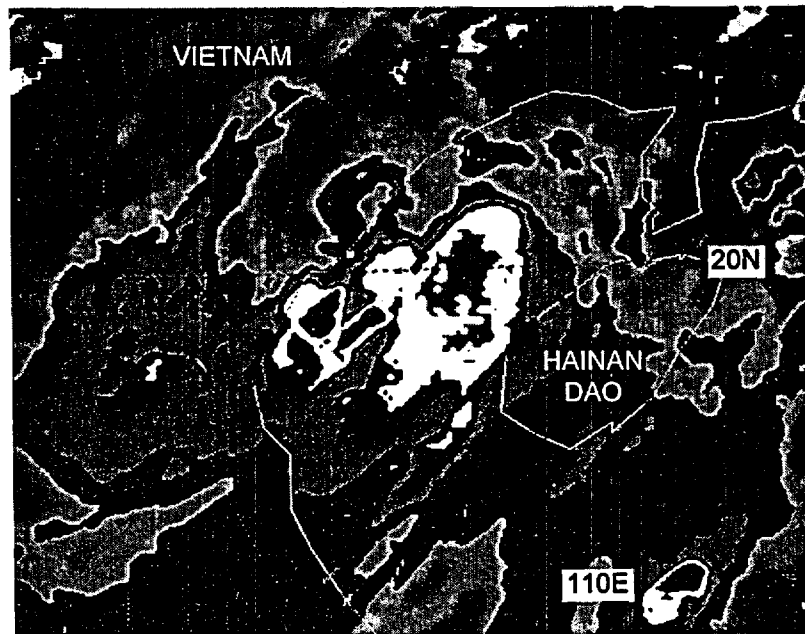
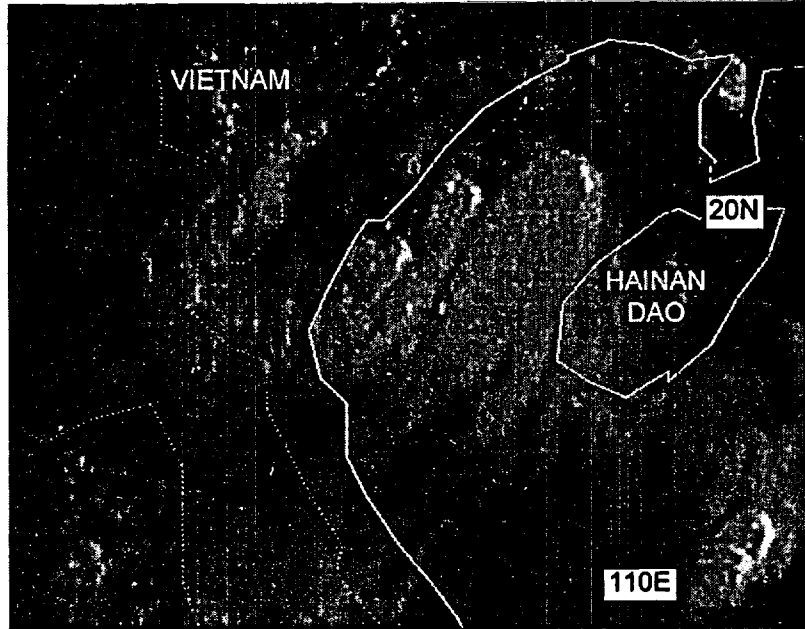


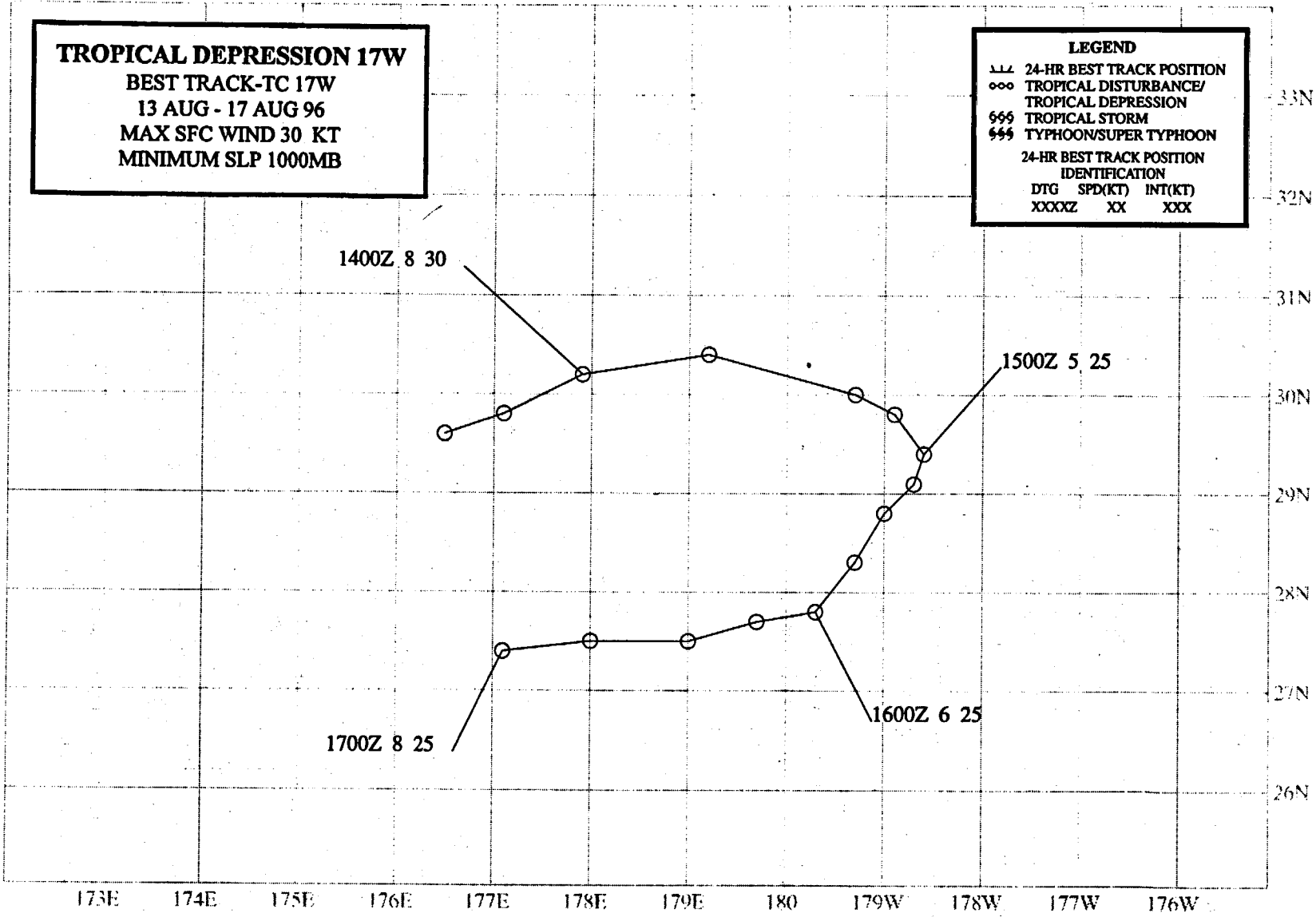
Figure 3-16-3 This satellite imagery of the tropical disturbance that became Marty was reassessed to be indicative of 30 kt (15 m/sec) intensity instead of the original diagnosis of less than 25 kt (13 m/sec) ((a) 130031Z August visible GMS imagery, and (b) 130031Z enhanced infrared GMS imagery).

TROPICAL DEPRESSION 17W
BEST TRACK-TC 17W
13 AUG - 17 AUG 96
MAX SFC WIND 30 KT
MINIMUM SLP 1000MB

LEGEND

LLL 24-HR BEST TRACK POSITION
 ooo TROPICAL DISTURBANCE/
 TROPICAL DEPRESSION
 666 TROPICAL STORM
 888 TYPHOON/SUPER TYPHOON

24-HR BEST TRACK POSITION
 IDENTIFICATION
 DTG SPD(KT) INT(KT)
 XXXXZ XX XXX



TROPICAL DEPRESSION 17W

Tropical Depression (TD) 17W originated in the subtropics at a time when the monsoon trough was displaced far to the north of normal (see Figure 3-13-4 in Kirk's summary for a graphic depiction of this unusual low-level flow pattern). TD 17W and Tropical Depression 15W formed and developed in this trough simultaneously (Figure 3-17-1). First identified on the 110600Z August Significant Tropical Weather Advisory, the area of deep convection which became TD 17W drifted slowly eastward and became better organized. The first warning was issued, valid at 140000Z when visible satellite imagery revealed a well-defined LLCC to the north of an area of persistent deep convection on the morning of 14 August (Figure 3-17-1). Whereas TD 15W drifted east-northeastward into higher latitudes, TD 17W executed an anticyclonic oval-shaped loop (centered at 29°N 179°E) with an average diameter of approximately 200 nm (370 km). After 141200Z, TD 17W moved across the international date line, and the JTWC passed warning responsibility to the Central Pacific Hurricane Center (CPHC). The depression continued east and came within 90 nm (170 km) of Midway Island (WMO 91066) (Figure 3-17-2) and began to weaken. The CPHC issued the final warning valid at 150000Z. At Midway, gusty winds and showers persisted for several days: the automatic remote collector there recorded a peak gust of 35 kt (18 m/sec) and approximately 2.5 inches (64 mm) of rain. TD 17W turned back to the west, recrossing the international date line on 16 August, and dissipated on 17 August.

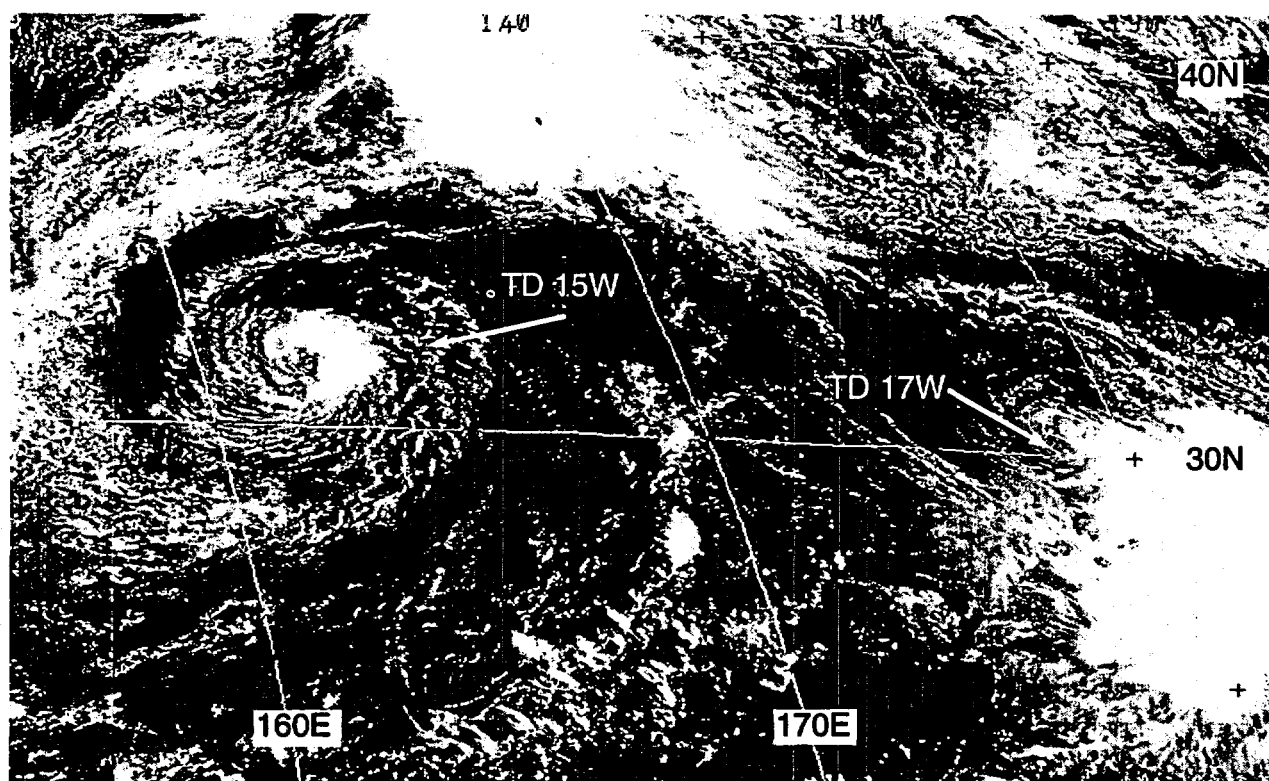


Figure 3-17-1 TD 17W and TD 15W both formed in subtropical latitudes within a monsoon trough which had moved far to the north and east of normal (132331Z August visible GMS imagery).

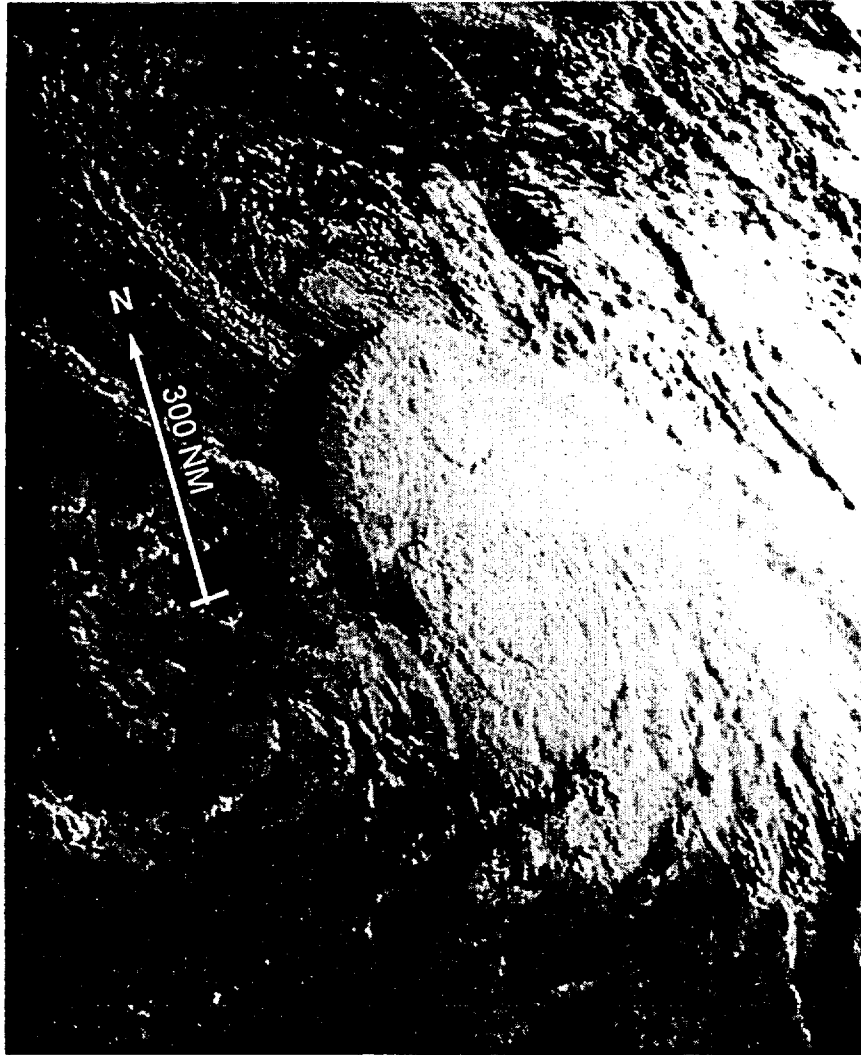


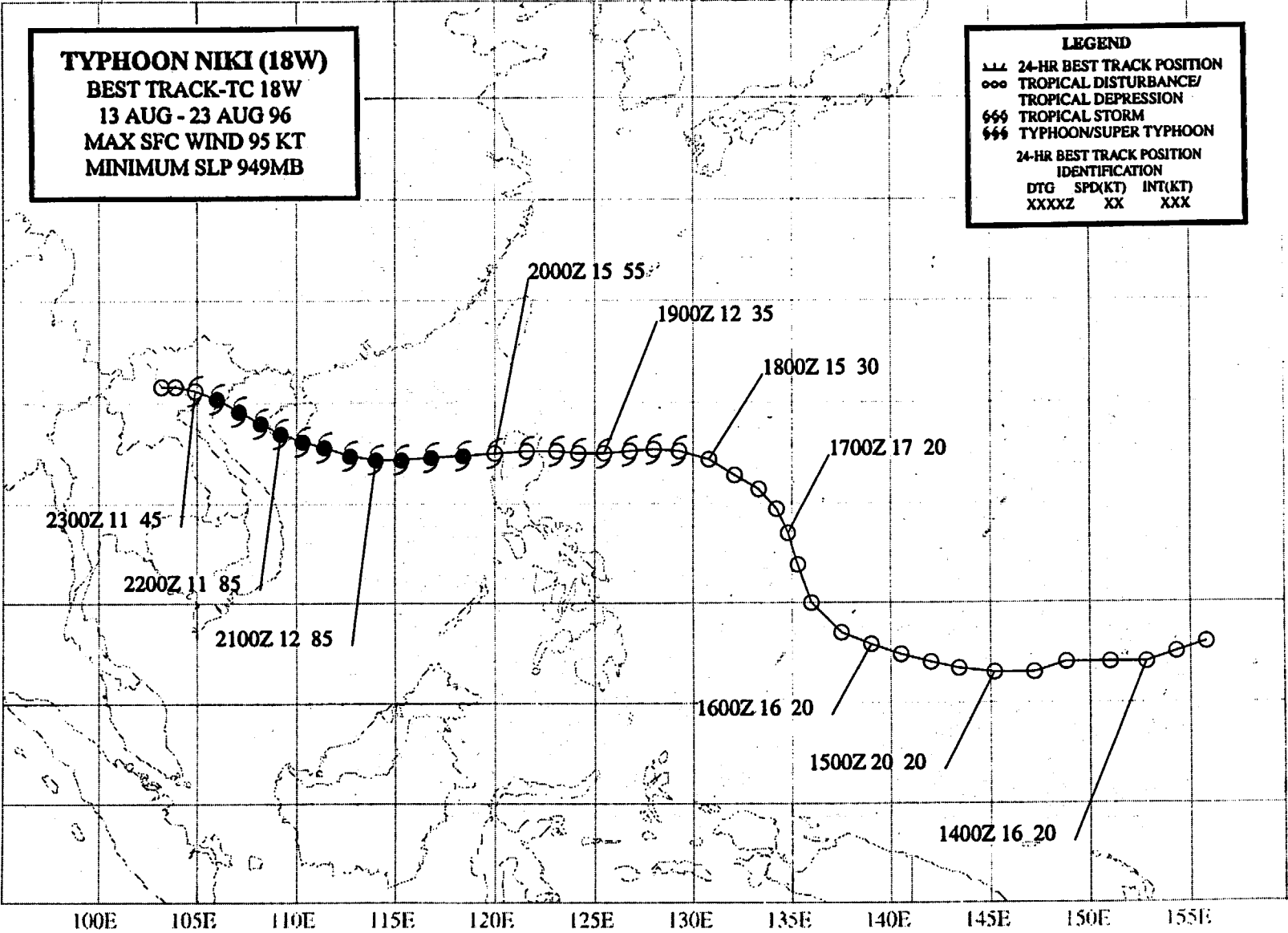
Figure 3-17-2 TD 17W exhibits a classical Dvorak "shear" type cloud pattern after crossing to the east side of the international date line (141830Z August visible GMS imagery).

TYPHOON NIKI (18W)
BEST TRACK-TC 18W
13 AUG - 23 AUG 96
MAX SFC WIND 95 KT
MINIMUM SLP 949MB

LEGEND

- 24-HR BEST TRACK POSITION
- TROPICAL DISTURBANCE/
TROPICAL DEPRESSION
- ⊖ TROPICAL STORM
- ⊕ TYPHOON/SUPER TYPHOON

24-HR BEST TRACK POSITION
 IDENTIFICATION
 DTG SPD(KT) INT(KT)
 XXXXZ XX XXX



TYPHOON NIKI (18W)

I. HIGHLIGHTS

Niki persisted as a weak tropical disturbance for several days as it moved toward the west at low latitude in Micronesia. It did not intensify until it reached the Philippine Sea east of Luzon. Crossing Luzon, it became a typhoon in the South China Sea (SCS) where it crossed the southern tip of Hainan island, and later made landfall in Vietnam south of Haiphong. Early in its life, satellite fixes were consistently north of the synoptic fixes. In the Philippine Sea, a circular exhaust cloud formed near Niki's center.

II. TRACK AND INTENSITY

During the middle of August, the monsoon trough moved to a very high latitude, and a ridge of high pressure to its south produced easterly low-level winds across the deep tropics of the WNP. Within these low-latitude easterly winds, several tropical disturbances formed. The tropical disturbance that became Niki can be traced to a small ensemble of MCSs which appeared in the eastern Caroline Islands on 13 August. This disturbance moved westward (south of 10°N) and, though first mentioned on the 130600Z August Significant Tropical Weather Advisory, there was no definitive evidence that it possessed a LLCC until 15 August when the system had moved due south of Guam. The JTWC issued a Tropical Cyclone Formation Alert (TCFA) at 170600Z August when, according to remarks on the alert:

"Convection surrounding a low-level circulation center has become better organized over the past 6 hours. Water vapor winds courtesy of the University of Wisconsin and synoptic data indicate the presence of an upper-level anticyclone over the LLCC which is enhancing the convective signature. . . ."

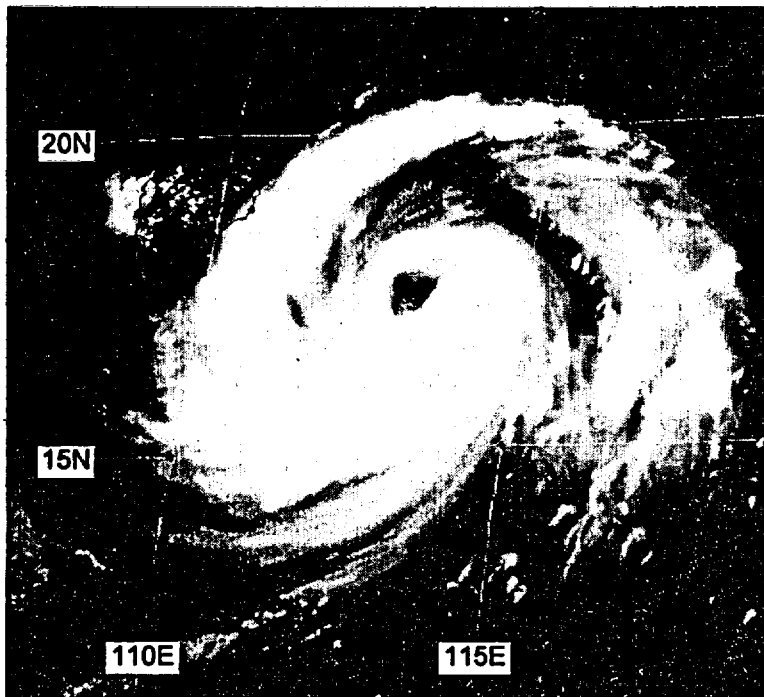


Figure 3-18-1 Typhoon Niki intensifies to 90 kt (46 m/sec) in its track across the South China Sea toward Hainan Island (210424Z August visible GMS imagery).

A second TCFA was issued at 172330Z August (primarily to reposition the TCFA box). The first warning on Tropical Depression (TD) 18W soon followed (valid at 180000Z) based on satellite intensity estimates of 30 kt (15 m/sec). TD 18W was upgraded to Tropical Storm Niki on the warning valid at 190000Z (post analysis pushed this back to 180600Z). Moving nearly due west, Niki passed across the northern end of Luzon during the six-hour period 191600Z to 192200Z. Northern Luzon had very little effect upon Niki's intensity, and as soon as it moved into the SCS, an eye began to form and Niki became a typhoon at 200600Z. The typhoon continued to intensify as it moved across the SCS (Figure 3-18-1), and reached a peak intensity of 95 kt (49 m/sec) at 211800Z just as the sys-

tem made landfall on the southern end of Hainan Island. Niki's eye became large and ragged as it passed from Hainan into the Gulf of Tonkin. Intensity estimates slowly fell, and the system (at minimal typhoon intensity) made landfall approximately 50 nm (95 km) south of Haiphong on the coast of Vietnam at 221800Z. The final warning was issued valid at 23000Z as the system weakened over land.

III. DISCUSSION

a. Common fix errors for low-latitude tropical depressions

When TCs form at low latitude (i.e., between 5° and 10°N) it is common that the satellite fixes tend to be located to the north of the synoptic fixes (Figure 3-18-2), especially when the TC is very weak and poorly defined. At such times, the satellite fix is often based upon the point of symmetry of anticyclonic cirrus outflow, and the curvature of poorly defined and transient bands of deep convection. A careful post analysis of the synoptic data indicated that the satellite fixes were too far north during the period 13 to 17 August.

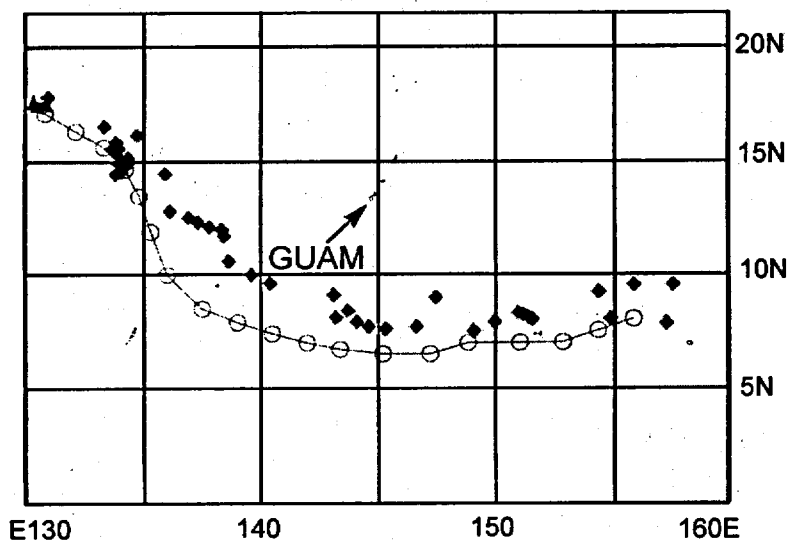


Figure 3-18-2 Based on a reanalysis of synoptic data, Niki's best track (small circles connected by thin line) was moved approximately 100 nm (185 km) to the south of the satellite fixes (black diamonds) during the period 13 to 17 August.

b. The circular exhaust cloud

In the early days of satellite reconnaissance, a peculiar structural feature was sometimes observed during the intensification phase of some TCs: the circular exhaust cloud. The term (coined by Fujita) was used to describe the emergence — in a developing TC — of an extremely tall, nearly circular, and sharply delineated cirrus canopy possessing an overshooting top surrounded by overlapping concentric rings and radial spokes (in visible imagery) which are the manifestation of gravity waves. On the morning of 19 August, a circular exhaust cloud formed near the center of Niki (Figure 3-18-3).

Originally thought to represent the center of the TC (in the context of a small CDO), it was later revealed by aircraft reconnaissance (Black, personal communication ; Black, et al., 1986), that the circular exhaust cloud was a "hurricane supercell" with its roots in the primary rainband (or developing wall cloud). Thus, its centroid did not lie over the TC center (Figure 3-18-4). In his work with infrared imagery, Dvorak (1984) noted that the use of IR imagery required the introduction of a new concept — the central cold cover (CCC) — in order to deal with the occurrence of a sudden spreading of cold clouds over the central features of a TC. The circular exhaust cloud may be a particular form of the general phenomenon of the CCC, however, the term "circular exhaust cloud" has fallen into disuse. See Gloria's (09W) summary for a more complete description of the concept of the CCC.

IV. IMPACT

When Niki made landfall in Vietnam, a total of 61 people were reported dead or missing with another 161 injured. Total economic losses were reported to be US \$66 million.

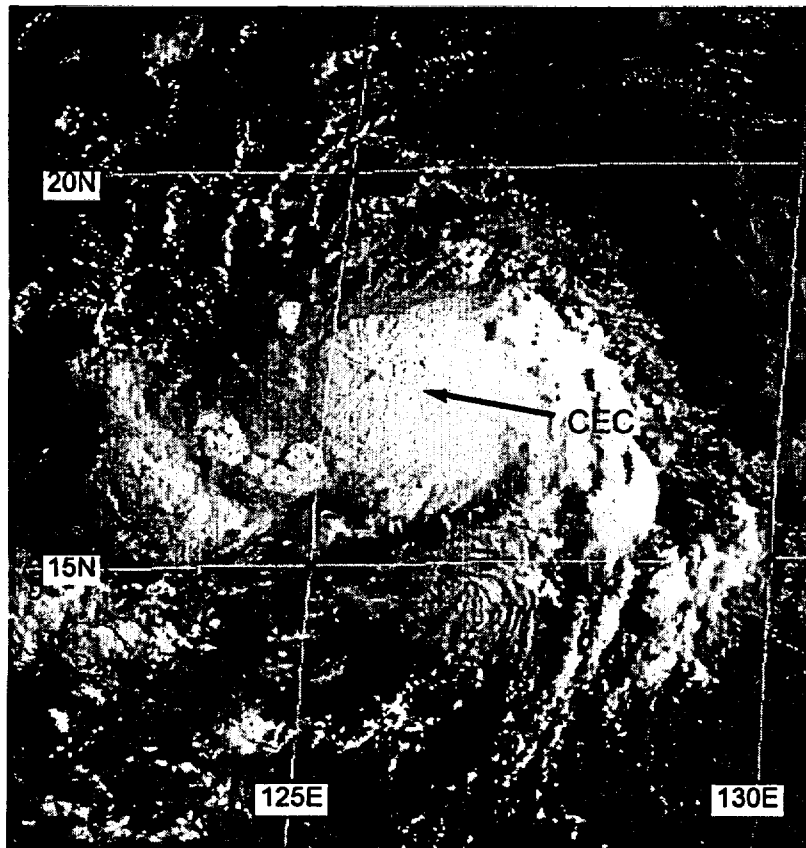


Figure 3-18-3 A circular exhaust cloud (CEC) appears within Niki's CDO (182224Z visible GMS imagery).

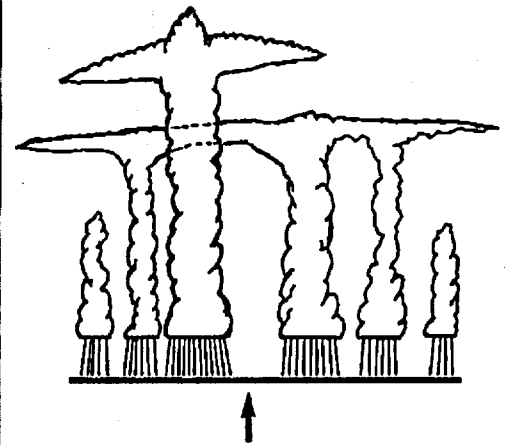
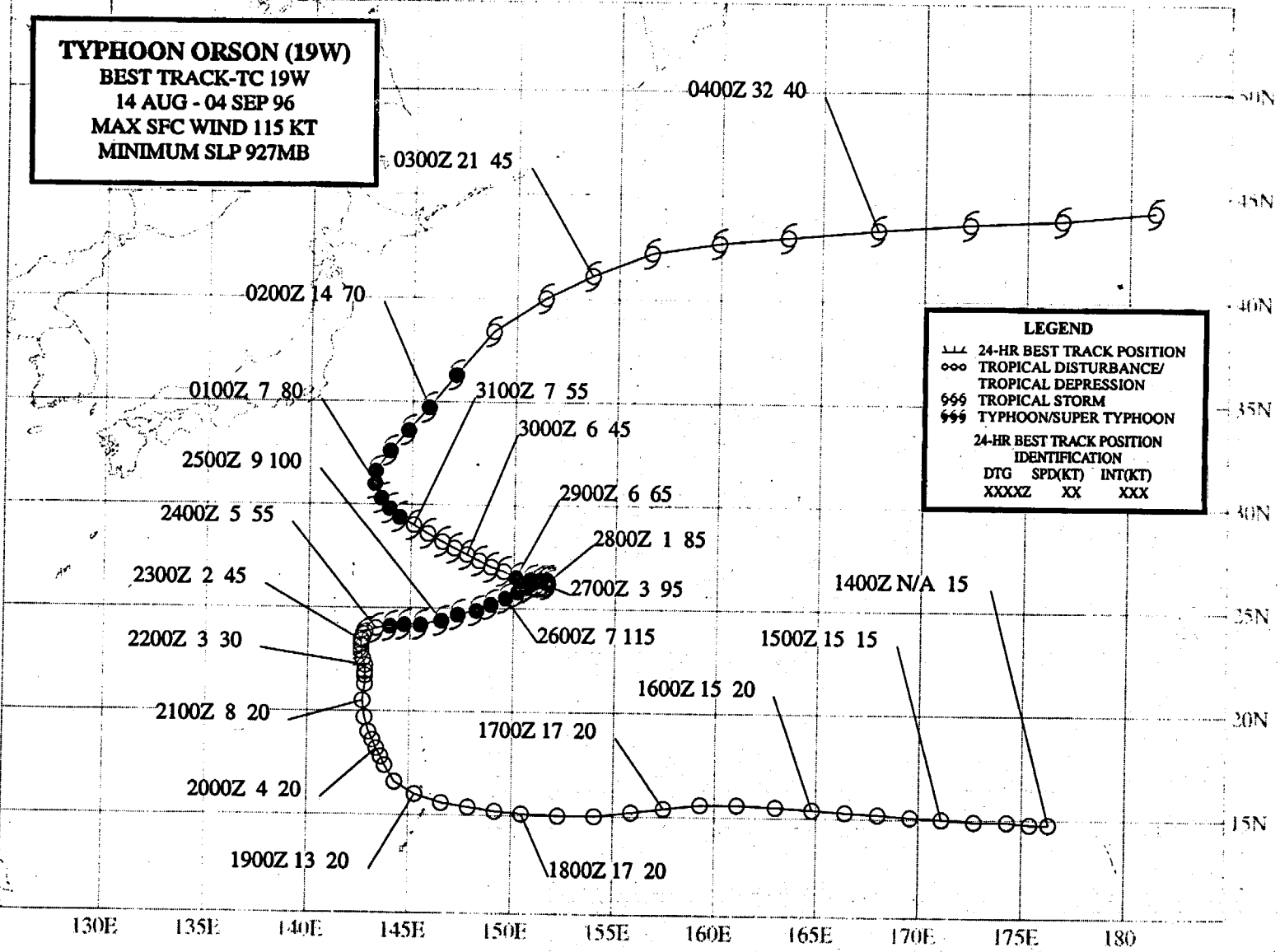


Figure 3-18-4 A schematic illustration of the vertical structure of the circular exhaust cloud.

TYPHOON ORSON (19W)
BEST TRACK-TC 19W
14 AUG - 04 SEP 96
MAX SFC WIND 115 KT
MINIMUM SLP 927MB

LEGEND
 --- 24-HR BEST TRACK POSITION
 ○○○ TROPICAL DISTURBANCE/
 TROPICAL DEPRESSION
 666 TROPICAL STORM
 999 TYPHOON/SUPER TYPHOON
 24-HR BEST TRACK POSITION
 IDENTIFICATION
 DTG SPD(KT) INT(KT)
 XXXXZ XX XXX



TYPHOON ORSON (19W)

I. HIGHLIGHTS

Tracing its origins to a mesoscale convective system (MCS) which formed on the northeastern side of a TUTT cell, Orson had a complex developmental history including two periods of intensification, the formation of an enormous eye, and a highly erratic track.

II. TRACK AND INTENSITY

The tropical disturbance that became Orson was first noted on the 150600Z Significant Tropical Weather Advisory near 15°N 170°E within a very complex circulation pattern that can best be described as the early stages of the breakdown of the very high latitude monsoon trough within

which Kirk (13W), TD 15W, and TD 17W were located. When the Pre-Orson tropical disturbance formed on 15 August, Kirk (13W) was moving eastward over northern Honshu (and becoming extratropical), and TDs 15W and 17W were dissipating at high latitude (30°N) and east of 160°E. After Kirk became an extratropical low, a ridge of high pressure became established along 27°N. To the south of this ridge the pre-Orson tropical disturbance moved westward, accompanied by a westward moving TUTT cell aloft and to its southwest (Figure 3-19-1). As this disturbance neared the Mariana Island chain, its organization improved and the first of three Tropical Cyclone Formation Alerts (TCFA) was issued at 172230Z August. The second TCFA was issued at 180930Z primarily to move the alert box westward to accommodate the rapid (20 kt) westward translation of the disturbance. At 190330Z, the second TCFA was canceled when much of the deep convection associated with

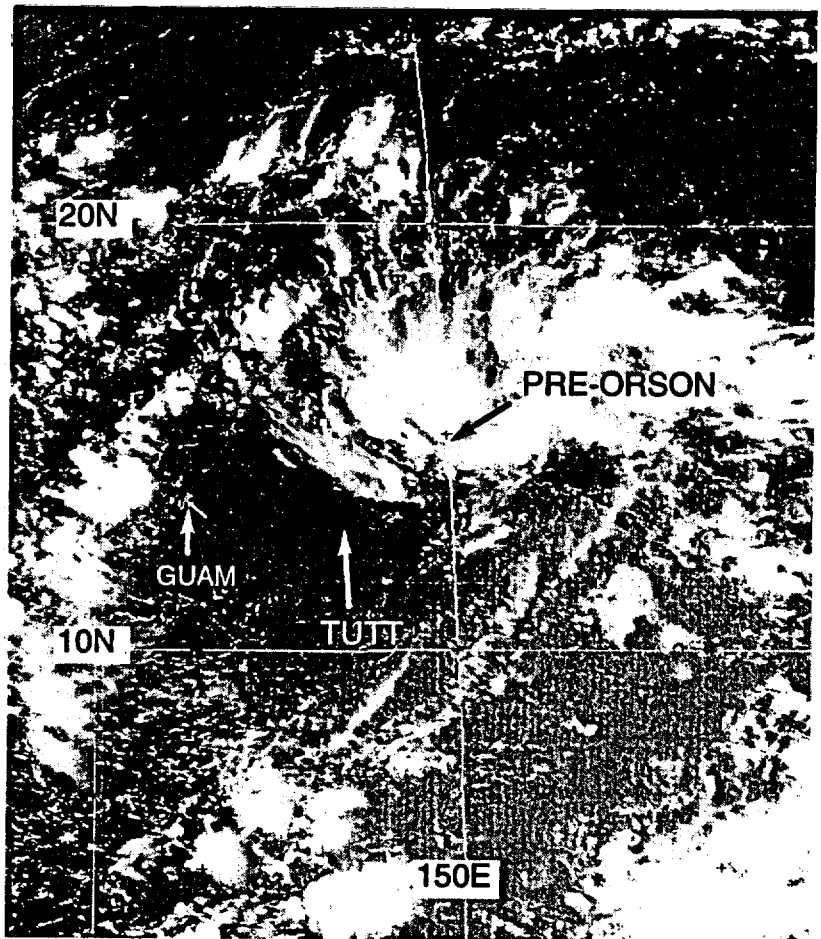


Figure 3-19-1 The tropical disturbance that became Orson was accompanied by a TUTT cell (180031Z August visible GMS imagery).

the system collapsed and became disorganized. During the night of 19 August a large area of deep convection developed over Guam (Figure 3-19-2). This area of convection collapsed, and on the morning of 21 August, a smaller MCS was located north of the collapse region (Figure 3-19-3). Synoptic data indicated the presence of a low-level cyclonic circulation center beneath this MCS, so a TCFA was issued at 202300Z August. Drifting slowly northward, the deep convection persisted,

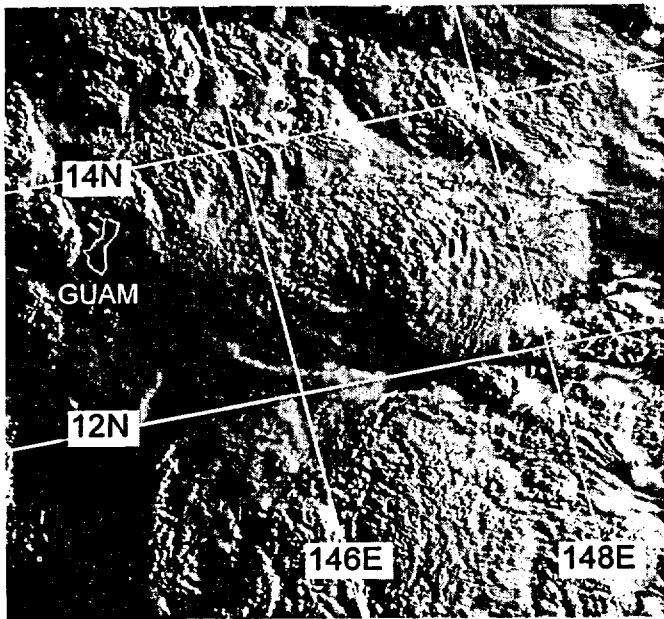


Figure 3-19-2 A very high-resolution image of the cloud-top topography of deep convection that developed near Guam as the pre-Orson tropical disturbance passed to the north (192026Z August high resolution visible DMSP imagery).

and on the night of 21 August, based upon a satellite intensity estimate of 25 kt (13 m/sec), the first warning on Tropical Depression (TD) 19W was issued valid at 211800Z. As TD 19W drifted very slowly to the north it slowly intensified and was upgraded to Tropical Storm Orson at 221200Z. At this time another TC — Piper (20W) — was developing northeast of Orson. With the development of Piper (20W), the monsoon trough became reverse oriented (Figure 3-19-4), and Orson began to move slowly toward the east-northeast along the axis of this trough. Orson intensified while moving east-northeast; becoming a typhoon at 240600Z and reaching a peak intensity of 115 kt (59 m/sec) at 250600Z (Figure 3-19-5). Thereafter, the system weakened as concentric (but ragged) eye walls formed, and the forward motion slowed as high pressure built to the north and east of the typhoon. On the morning of 29 August, the system lost its eye, and it was downgraded to a tropical storm on the warning valid at 290600Z. Under the influence of a ridge to its north, Orson began to track toward the northwest. While on this leg of its erratic track, the system underwent a remarkable structural evolution: several distinct MCSs began to orbit a large (100 nm diameter) central cloud-minimum area (Figure 3-19-6a, b). Its intensity estimate had bottomed out at 45 kt (23 m/sec) at this time. As the MCSs consolidated into a more contiguous cloud band around the very large ragged eye (Figure 3-19-7), the system once again rose to typhoon intensity, and reached a second relative intensity maximum of 80 kt (41 m/sec) at 311800Z. After reaching its second peak of intensity, Orson recurved and entered the accelerating westerly steering flow north of the subtropical ridge. The final warning was issued valid at 030600Z September as the system transitioned into an extratropical low.

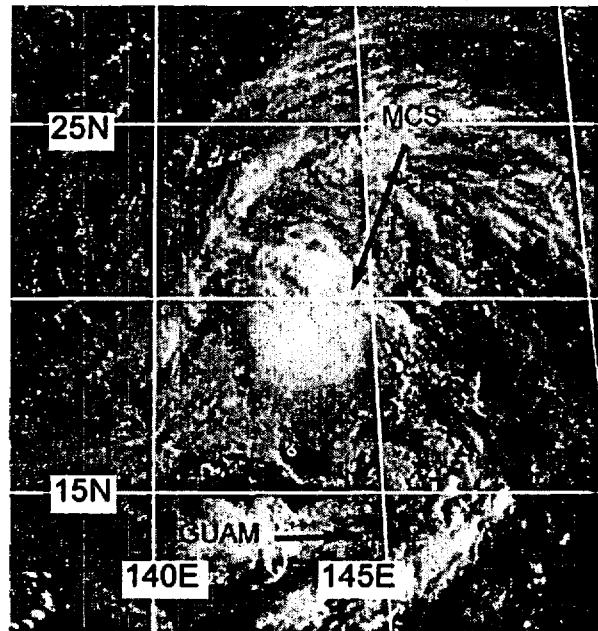


Figure 3-19-3 After the area of deep convection near Guam collapsed, a new MCS (accompanied by a LLCC) developed further to the north (202131Z August visible GMS imagery).

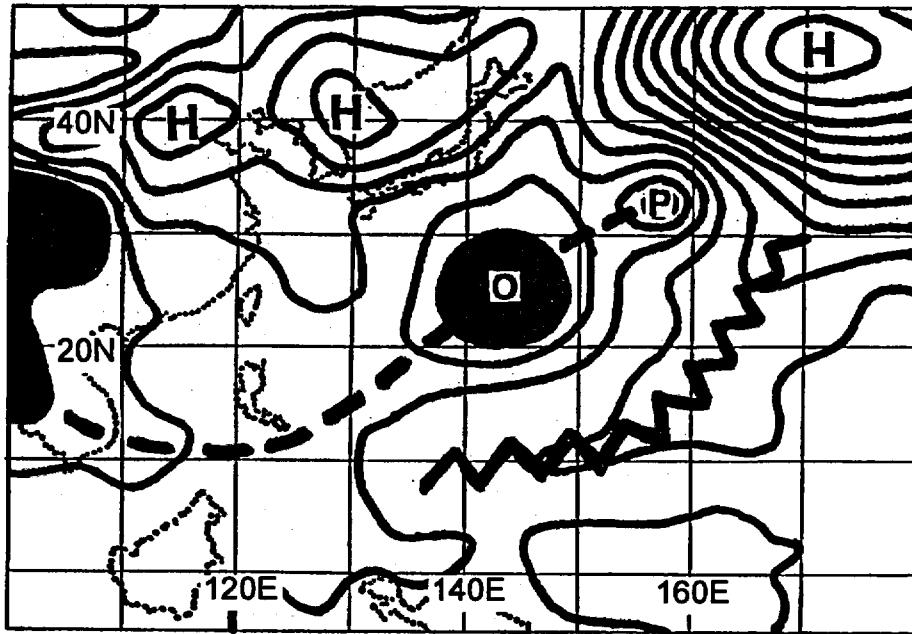


Figure 3-19-4 With the formation of Piper (20W) (P), it was clear that the monsoon trough (thick dashed line) had become reverse oriented. Influenced by the southwest monsoon flow between the trough axis and a ridge (bold zigzag line) which had become established in low latitude, Orson began to move to the east-northeast on the first leg of its "S" track (isobars at 2 mb intervals adapted from the 241200Z August NOGAPS SLP analysis).

III. DISCUSSION

a. Unusual motion

Orson's erratic motion can be described as a special variant of the north-oriented track type: the "S" track. The north-oriented track was first recognized by the Japan Meteorological Agency (JMA) (1976). Carr and Elsberry (1996) renamed this track type as "poleward oriented" to make the term appropriate for both the Northern and Southern hemispheres. Lander (1996) further elaborated on the characteristics of north-oriented tracks, with a special emphasis on "S"-shaped tracks. "S" motion is poleward-oriented motion of a Northern Hemisphere TC that features eastward motion at low latitude, a later bend to the north or northwest, and then eventually northeastward motion as the TC enters the mid-latitude westerlies. Most cases of "S" motion (including that of Orson) occur when a TC is located along the axis of a reverse-oriented monsoon trough. Surprisingly, the Navy's dynamic models often handle "S" motion (and poleward-oriented motion in general) quite well (Carr, personal communication). Indeed, NOGAPS and GFDN did a good job in predicting the erratic motion of Orson.

b. Very large eye

Orson was one of three TCs during that acquired very large eyes during 1996 — the other two were Kirk (13W) and Violet (26W). Once the large ragged clearing within the ring of MCSs was interpreted as an eye, its diameter on satellite imagery ranged from 70 nm (130 km) to 102 nm (190 km) (Table 3-19-1).

IV. IMPACT

No reports of damage or injuries were received.

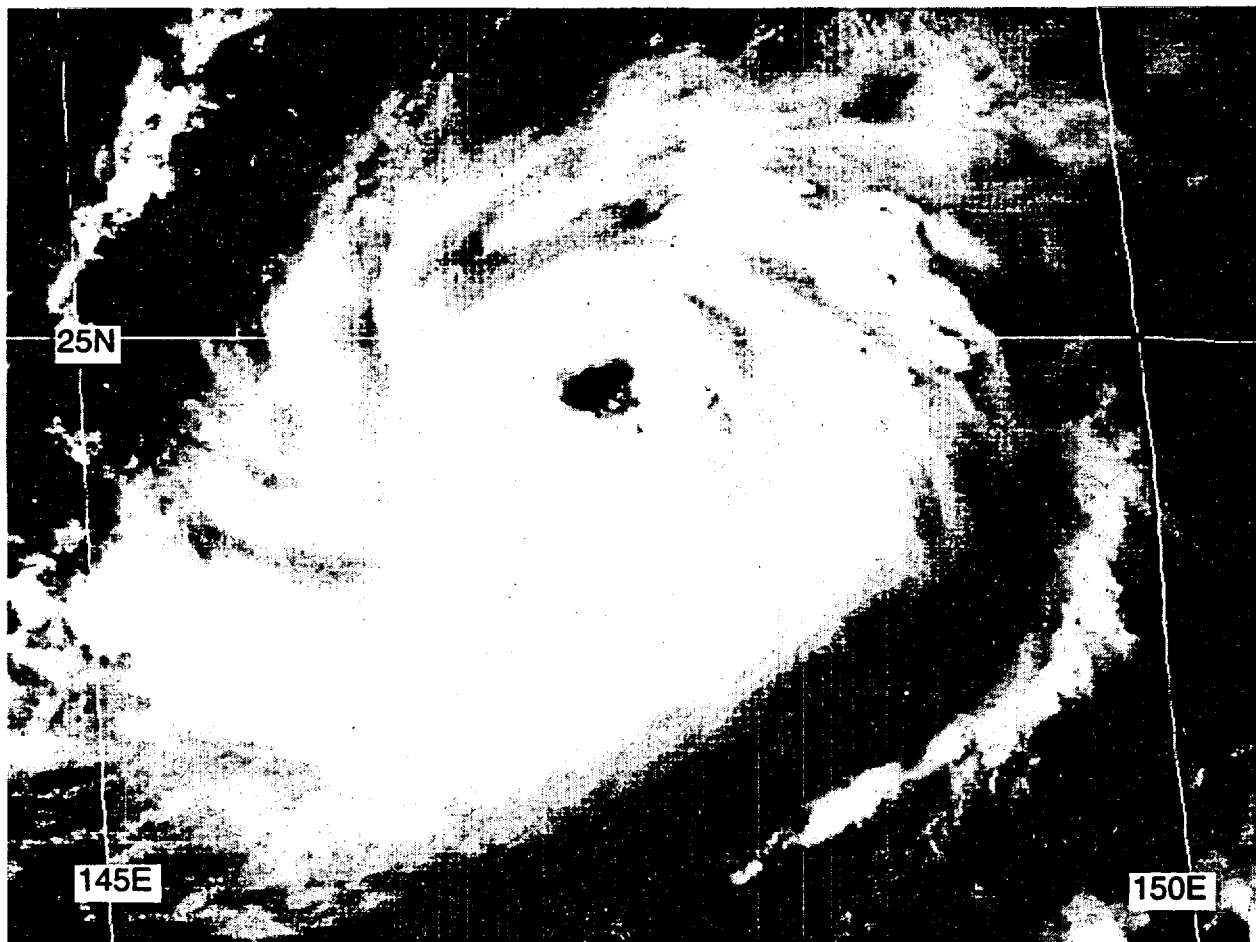


Figure 3-19-5 Orson at its peak of 115 kt (59 m/sec) (250531Z August visible GMS imagery).

Table 3-19-1 EYE DIAMETER OF ORSON FROM SATELLITE DURING ITS SECOND PERIOD OF INTENSIFICATION.

DTG (Z)	T Number	Satellite eye diameter (nm)
301042	3.5	98
301130	3.5	84
301610	3.5	81
301730	3.5	75
310530	4.0	75
310830	---	74
311130	4.0	84
311559	4.0	70
312030	---	77
312330	4.5	90
010230	---	102
010530	4.0	94
010830	---	98

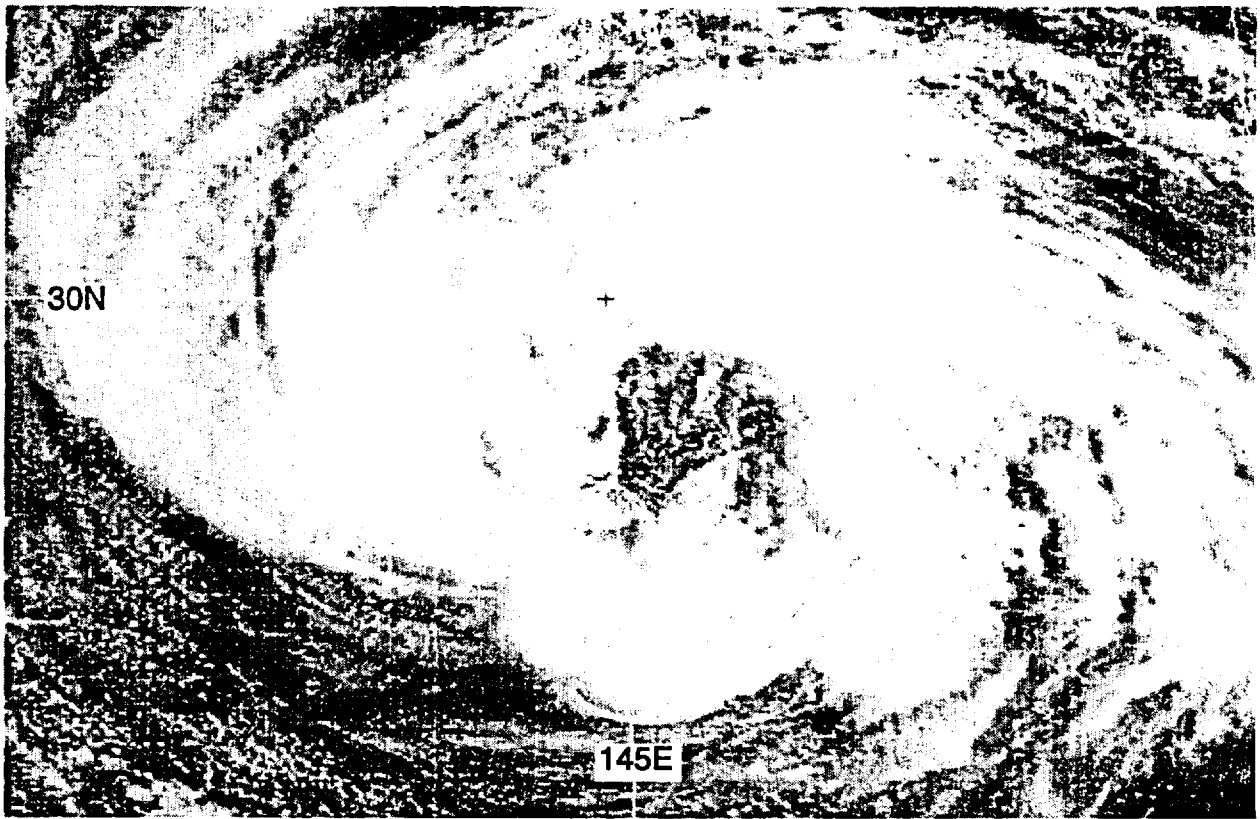
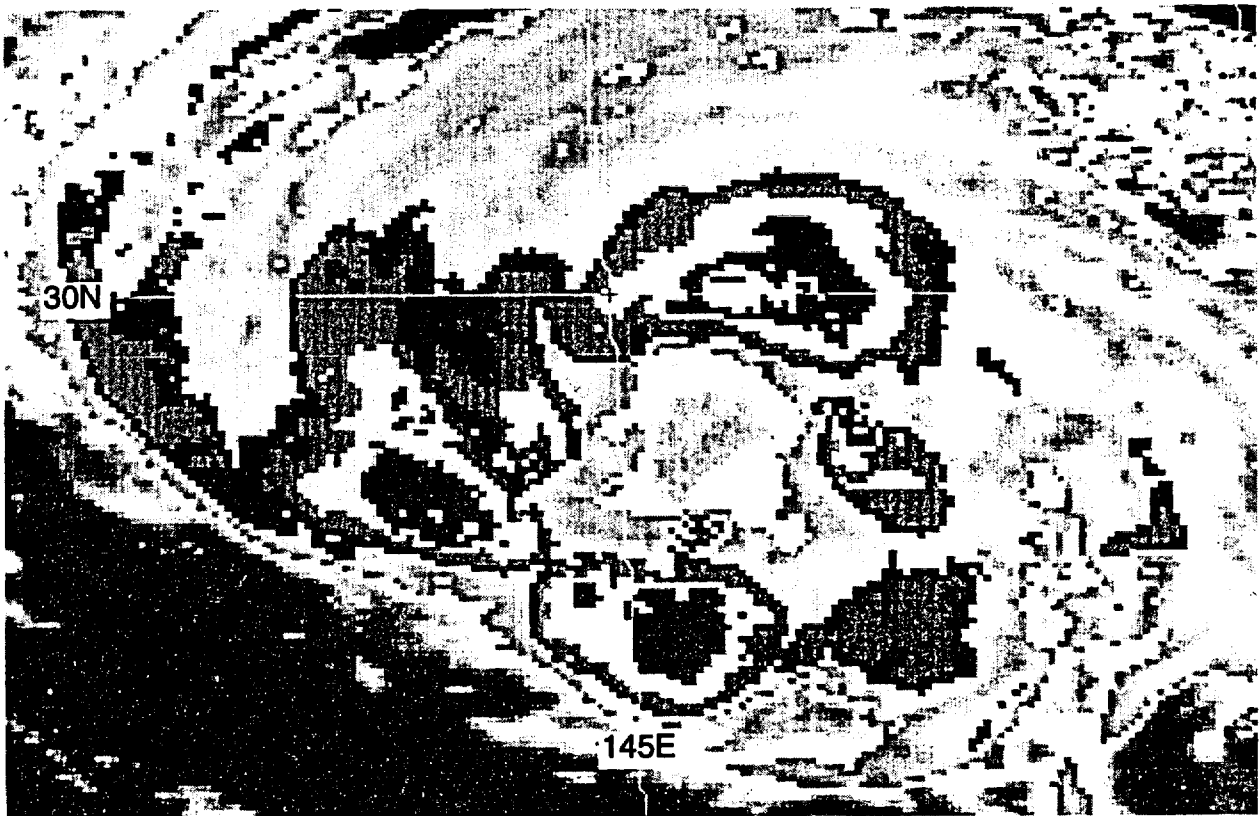


Figure 3-19-6 A ring of MCSs orbit a central clear region as a precursor to the formation of Orson's very large eye. (a) 302131Z August visible GMS imagery. (b) 302131Z August enhanced infrared GMS imagery.



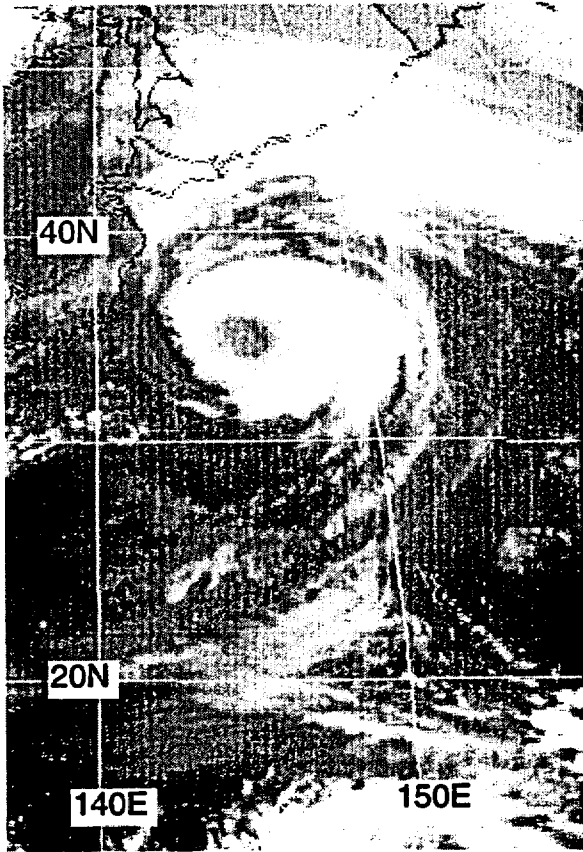
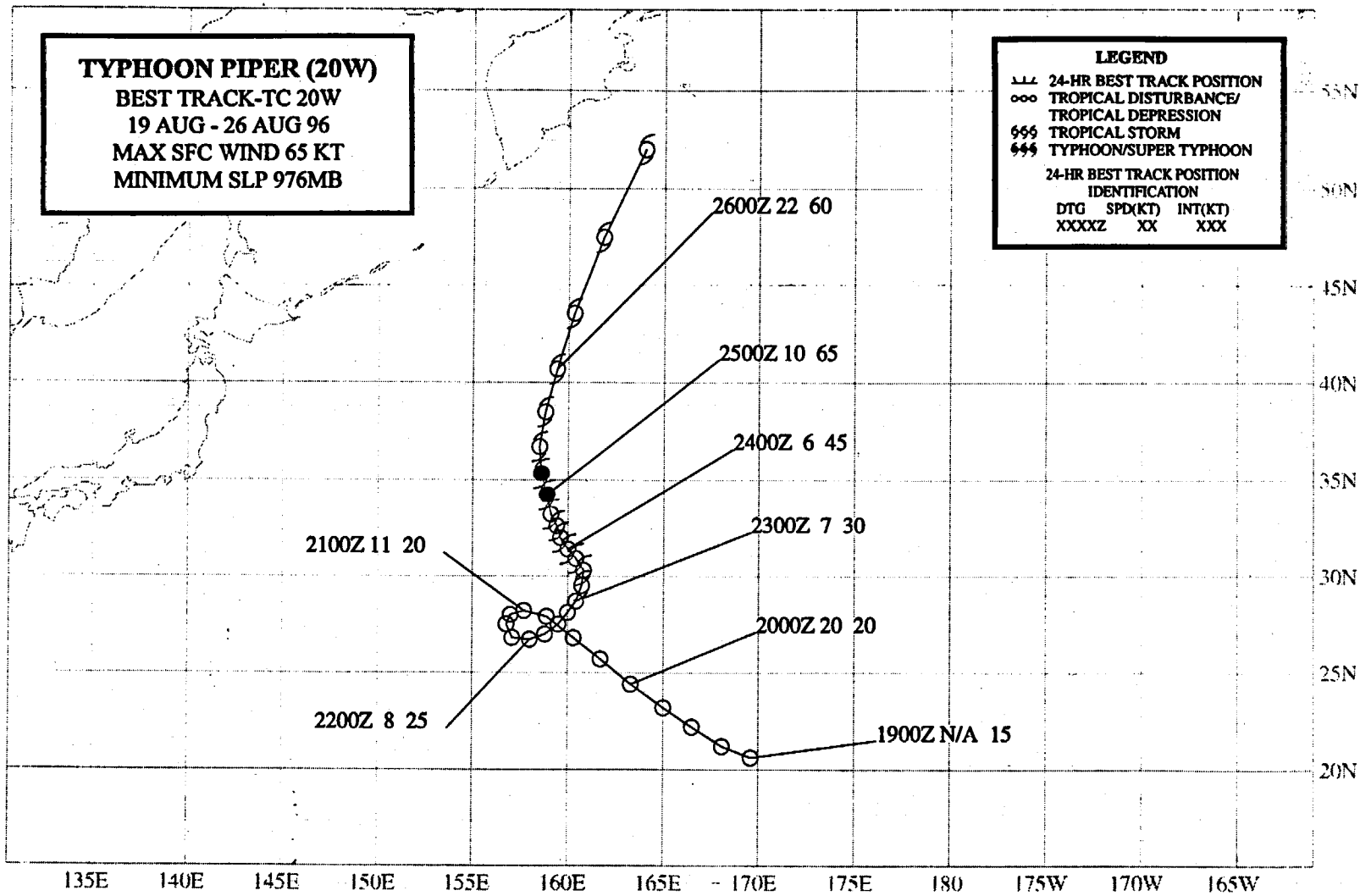


Figure 3-19-7 Orson's very large eye evokes the analogy of a "truck tire" rolling across the ocean (012231Z September infrared GMS imagery).



TYPHOON PIPER (20W)

I. HIGHLIGHTS

Piper was another of the TCs of 1996 which originated directly from a TUTT cell. It was a very small TC — the smallest in the WNP during 1996. Developing at a relatively high latitude to the east of Orson (19W), Piper was located at the eastern end of a reverse-oriented monsoon trough (RMT). Typical of TCs associated with a RMT, Piper's motion was north oriented.

II. TRACK AND INTENSITY

During 19 August, a well-defined TUTT cell was moving westward along 25°N and had crossed 165°E. Mesoscale convective systems populated the eastern through northern segment of a curved moisture band that wrapped into this TUTT cell (Figure 3-20-1a). Synoptic data at 190000Z indicated that a weak low-level cyclonic circulation was located west of this cloud band and close to the estimated center of the TUTT cell, prompting its inclusion on the 190600Z August Significant Tropical Weather Advisory. During the next two days, the low-level cyclonic circulation became associated with an area of deep convection. On 22 August, the deep convection consolidated under the anticyclonically curved flow on the eastern side of the TUTT cell, and scatterometry indicated the wind speeds had increased to 20 kt (10 m/sec) on the north side of the accompanying low-level circulation center (LLCC). This prompted JTWC to issue a Tropical Cyclone Formation Alert valid at 221500Z.

On 23 August, persistent deep convection in the eastern quadrant of the TUTT cell became coupled with well-defined anticyclonic flow aloft. The persistence of deep convection and its increased organization prompted the first warning on Tropical Depression (TD) 20W valid at

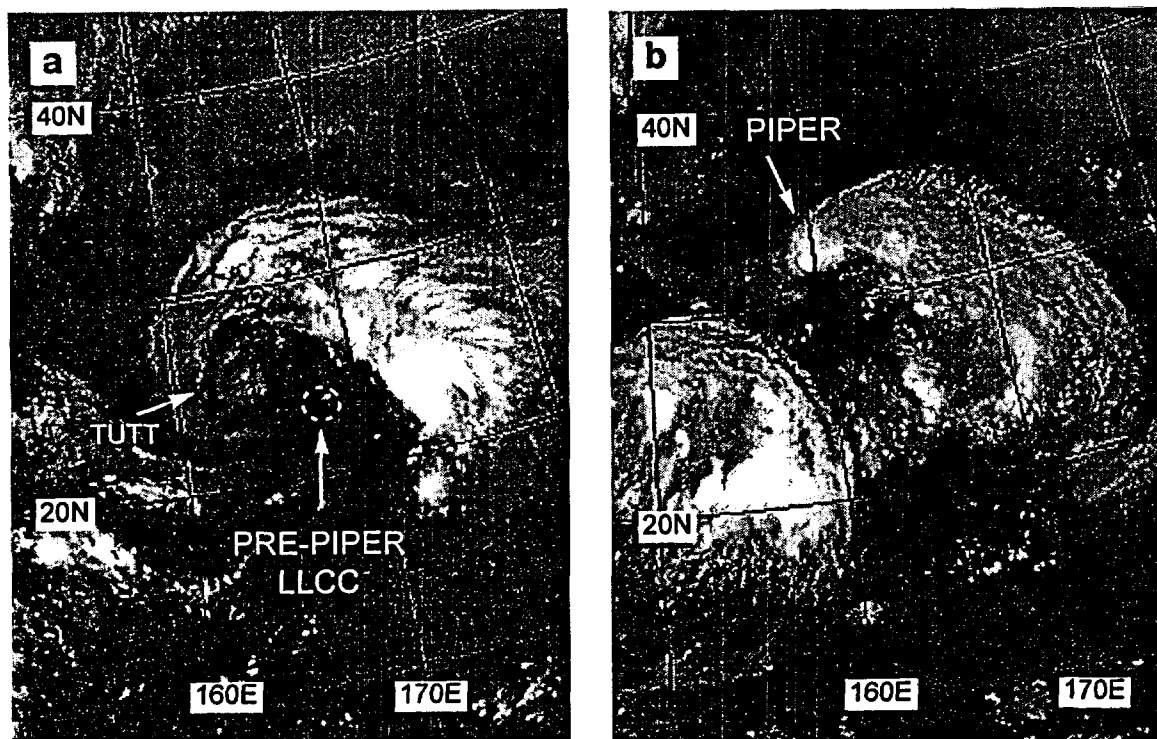


Figure 3-20-1 A westward moving TUTT cell (a) induces the formation of Piper (b). (192131Z August water-vapor GMS imagery and 240031Z August water-vapor GMS imagery respectively).

230000Z. Synoptic data at this time showed the monsoon westerlies had extended to the LLCC of TD 20W, creating a reverse-oriented monsoon trough which included the larger Orson (19W) to the west. Based on a satellite intensity estimate of 35 kt (18 m/sec), TD 20W was upgraded to Tropical Storm Piper on the warning valid at 230600Z. With a ridge located to its southeast, and a blocking high to its northeast, Piper moved on a north-oriented track.

Late on 24 August, Piper's small CDO moved north, became detached from the monsoon cloud band, and intensified. At 250000Z, Piper acquired a visible eye, and reached its peak intensity of 65 kt (33 m/sec) (Figure 3-20-2). Piper retained its small 7-nm (13-km) eye for about 12 hours (Figure 3-20-3a, b). During 26 August, Piper's central convection became a small well-defined CDO (Figure 3-20-4), as it accelerated to the north-northeast and slowly weakened. Late on 26 August, Piper's forward motion increased to more than 40 kt (75 km/hr) as it merged with a frontal cloud band which stretched southward from a low over the Kamchatka peninsula. The final warning was issued valid at 260600Z when Piper's CDO became associated with the frontal cloud band. Post analysis indicated Piper's CDO could be followed for an additional 12 hours as it sped northward within the frontal cloud band, and therefore, the final best track continues until 261800Z.

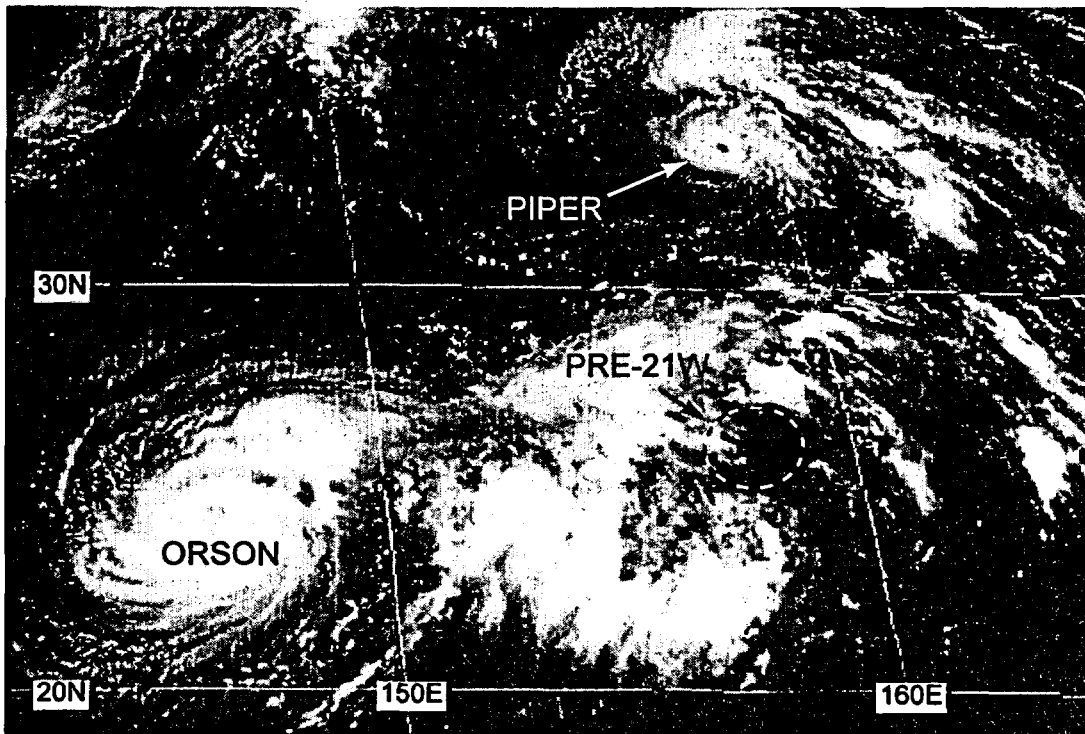


Figure 3-20-2
Piper at its peak intensity of 65 kt (33 m/sec) (242331Z August visible GMS imagery).

III. DISCUSSION

a. Tropical cyclogenesis induced by a TUTT cell

Piper originated directly from a TUTT cell (see Joy's (12W) summary for a more complete description of tropical cyclogenesis induced directly by a TUTT cell). This is well illustrated by water-vapor imagery (Figure 3-20-1a, b). Water-vapor imagery has only been available since the GMS-5 satellite became operational during June of 1995. It has allowed a greatly improved presentation of TUTT cells, and their movement and evolution can now be studied as never before. Water-vapor imagery should open new opportunities for research on the effects of the TUTT and its associated TUTT cells on TC genesis and TC development.

b. *Small size*

Like most TCs that form at high latitude in association with TUTT cells, Piper was a very small TC — the smallest of 1996. The diameter of its dense cirrus cloud shield was less than 100 nm (185 km) (Figure 3-20-3a, b), and it encompassed a very small eye whose diameter was 7 nm (13 km) on satellite imagery. As with many very small TCs, the intensity forecasts erred on the low side: on the first eight warnings (issued at six-hour intervals from 230000Z August to 241800Z August), the 24-hour intensity was under-forecast by anywhere from 5 to 25 kt; the 48-hour intensity was under-forecast by as much as 30 kt (15 m/sec).

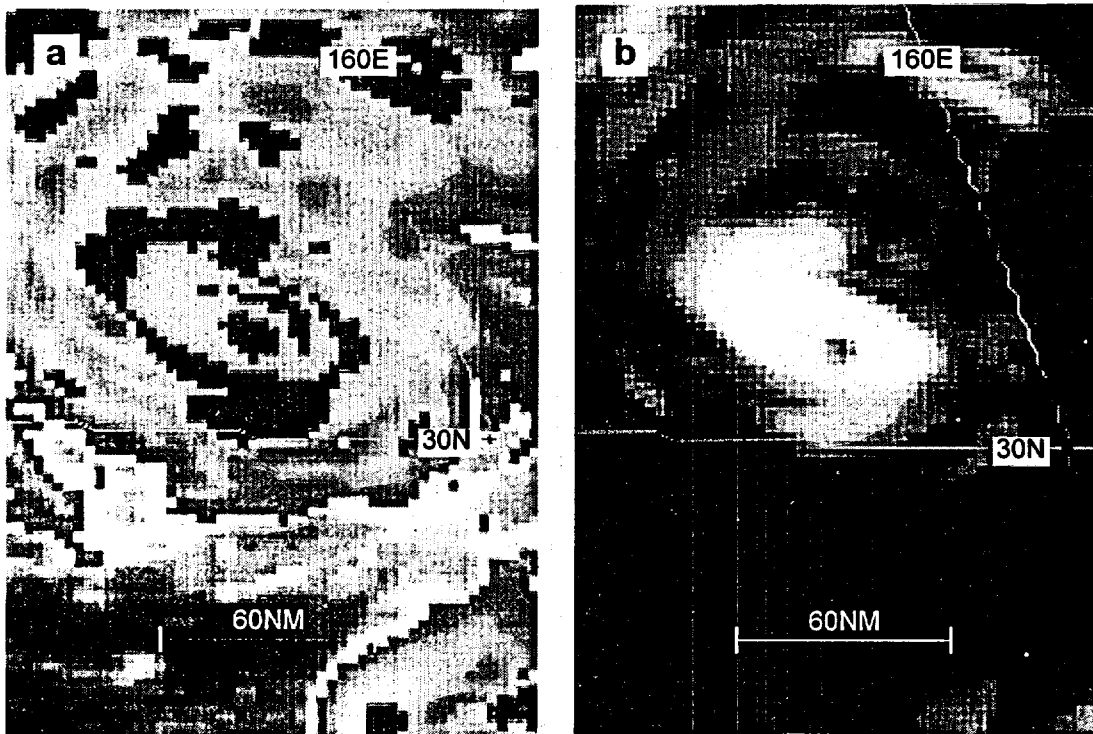


Figure 3-20-3a, b Piper was a very small TC — the smallest of 1996. Its eye was only 7 nm (13 km) in diameter, and its dense cold cirrus shield had a diameter of less than 100 nm (185 km). (a) 250931Z August enhanced infrared GMS imagery, and (b) 250931Z August high-contrast infrared GMS imagery.

c. *Development over cool SST*

Relatively few TCs in the WNP first attain typhoon intensity poleward of 30°N — during the 25-year period 1970 to 1994 only thirty-one of 729 TCs (4%) which formed in the WNP first attained 65-kt (33-m/sec) intensity at, or north, of 25°N; only twelve at, or north, of 30°N; and only one north of 35° N. Piper first attained 65-kt (33-m/sec) intensity at 34°N. It remained a typhoon for approximately nine hours, and fell below typhoon intensity after crossing 35°N. The sea-surface temperature (SST) at the point where Piper's intensity peaked was approximately 25°C (Figure 3-14-5). Piper remained a well-defined TC with an intensity of 60 kt (31 m/sec) near 40°N, (Figure 3-20-4), even though SSTs were only 20°C.

IV. IMPACT

No reports of damage or injury were received at the JTWC.

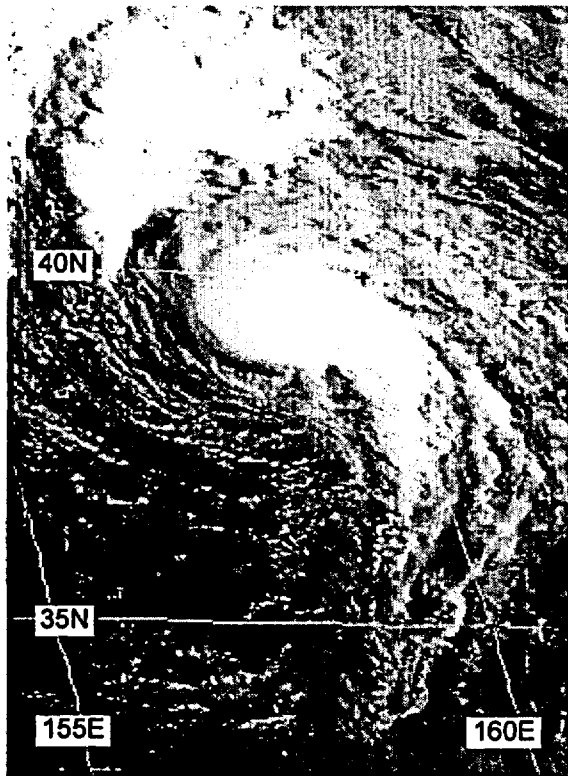


Figure 3-20-4 Piper's small well-defined CDO begins its northward acceleration over cooler SST and toward a frontal cloud band (252131Z August visible GMS imagery).

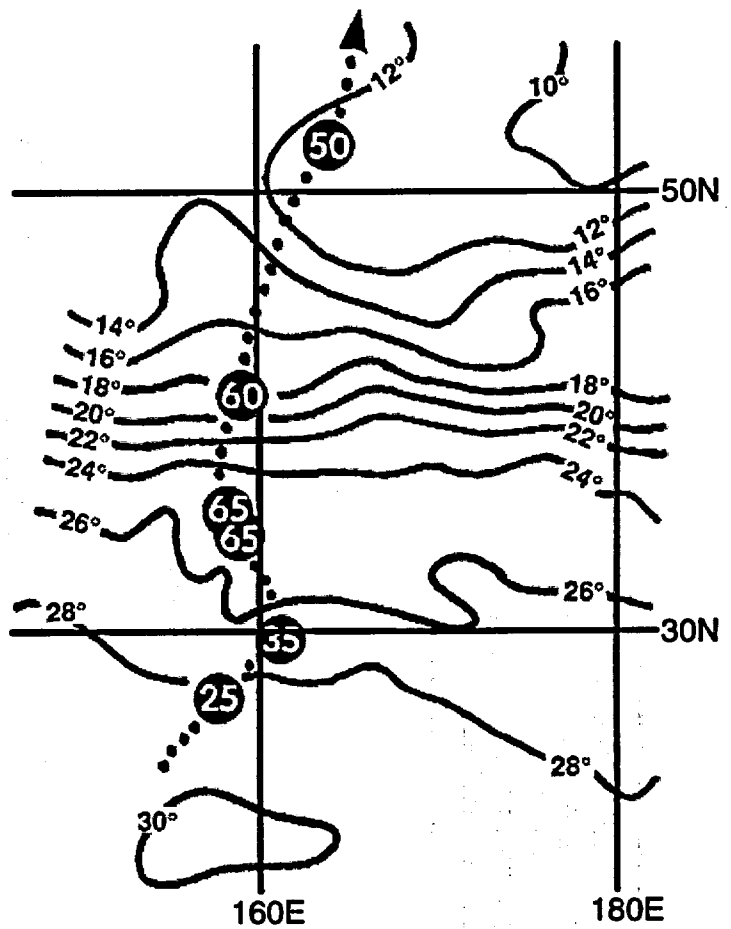
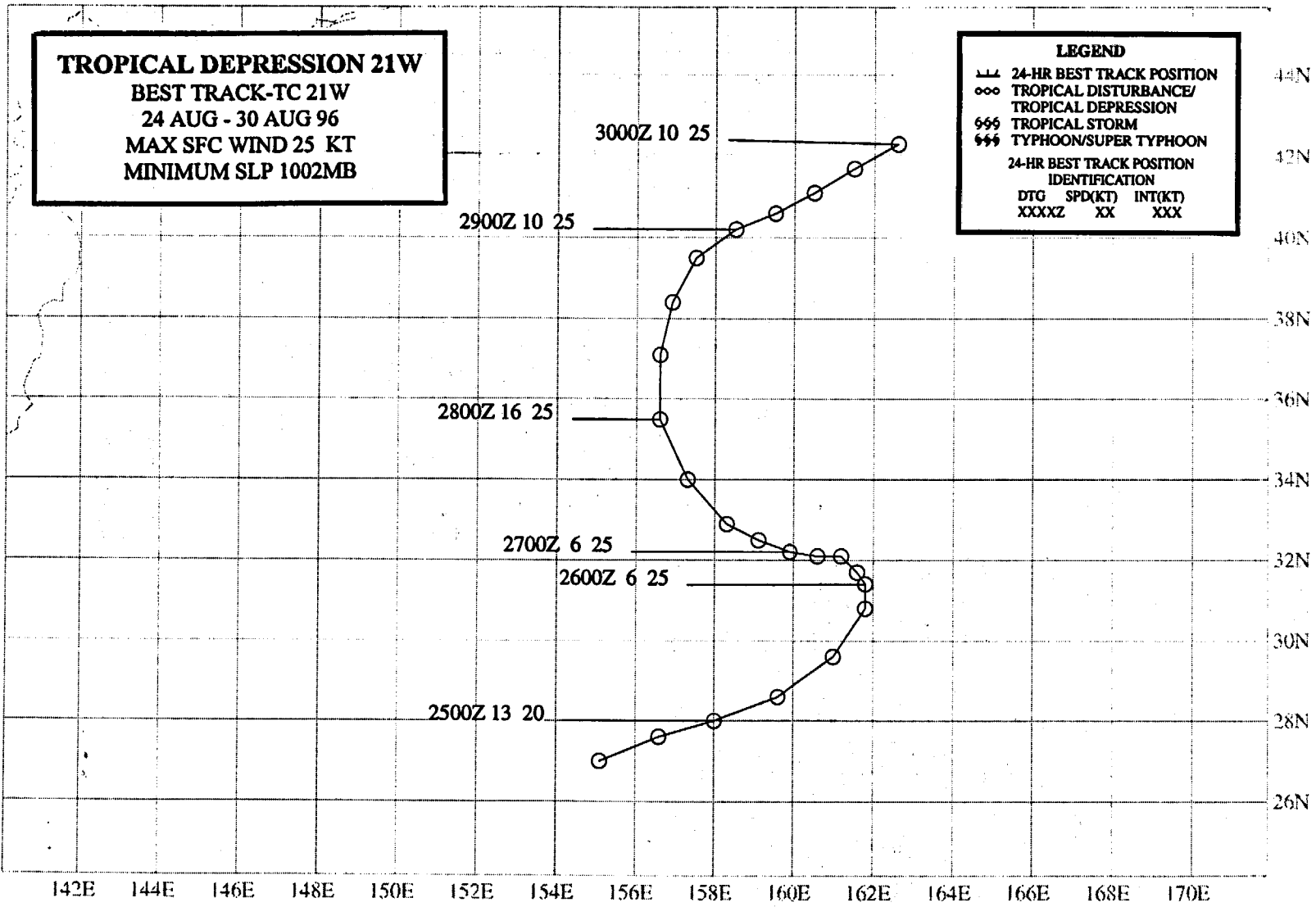


Figure 3-20-5 Piper reaches typhoon intensity at an unusually high latitude, and over relatively cool SST. (SST contours are based upon 220000Z August FNMOC analysis).



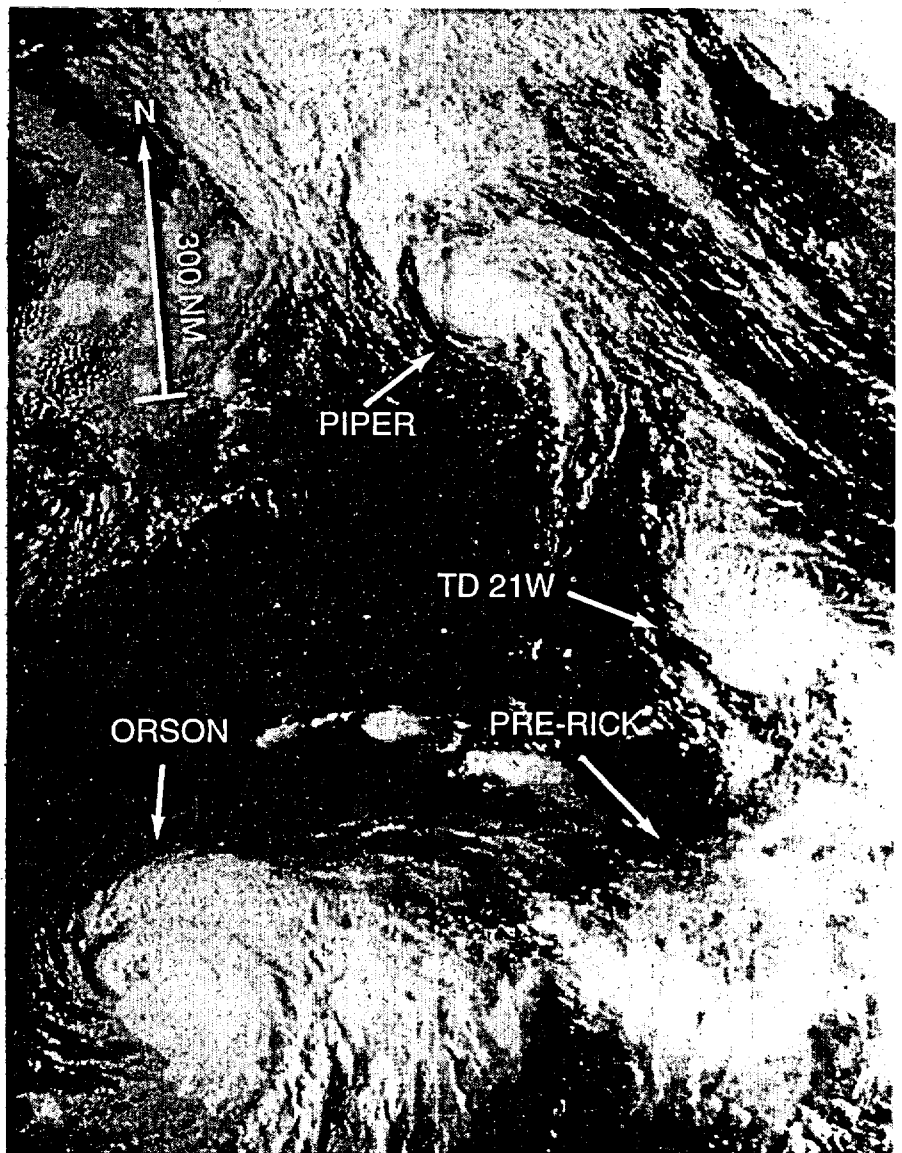
TROPICAL DEPRESSION 21W

Forming at the end of a northward-displaced monsoon trough, Tropical Depression 21W followed an "S"-shaped poleward-oriented track close on the heels of Typhoon Piper (20W) (Figure 3-21-1). Emerging rather quickly from the end of the monsoon trough, the tropical disturbance that became TD 21W was never mentioned on the Significant Tropical Weather Advisory, but rather, a Tropical Cyclone Formation Alert (TCFA) was issued at 252330Z August followed immediately by a warning valid at 260000Z. Remarks on the TCFA included:

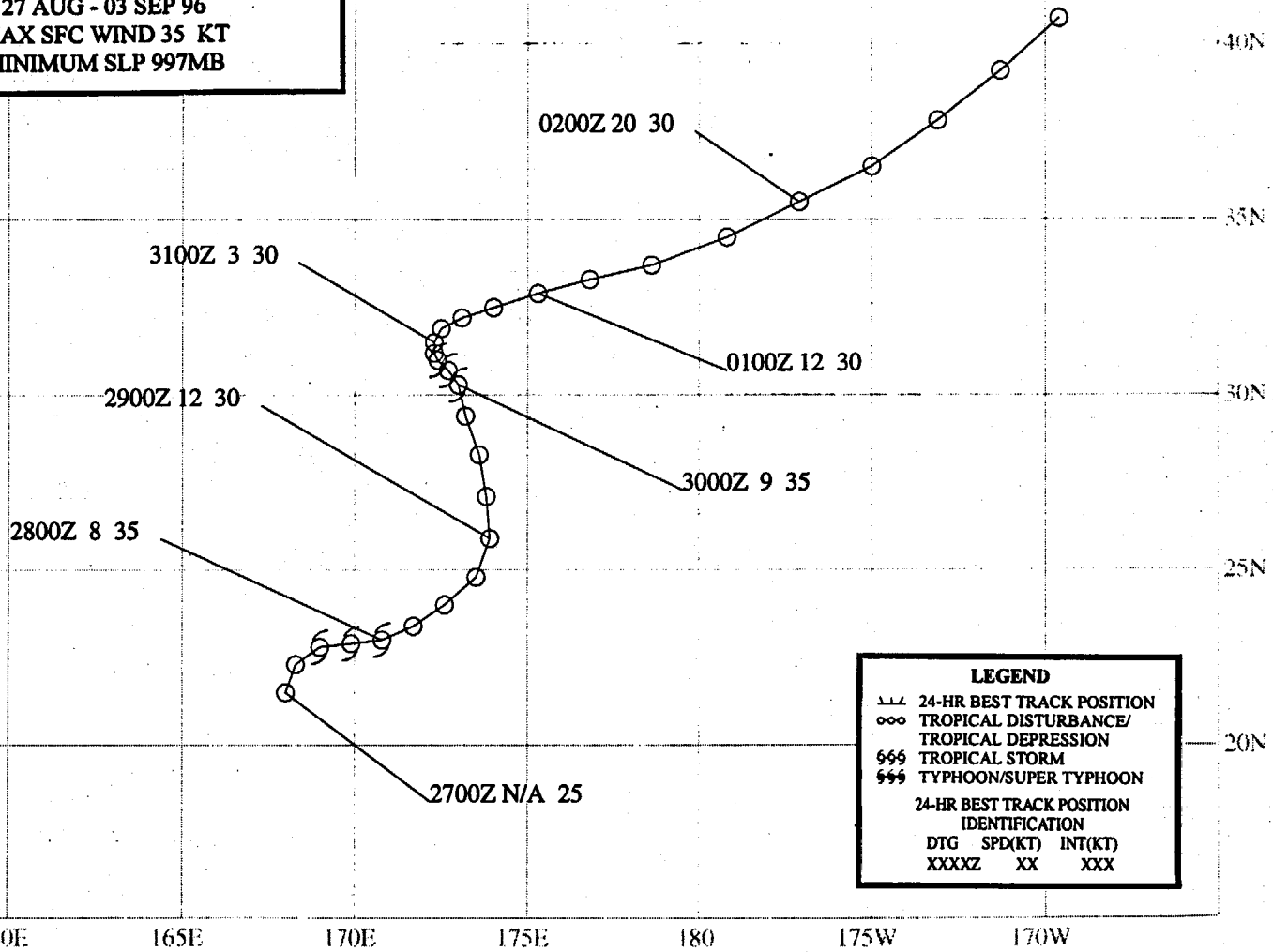
"A tropical disturbance has developed within the monsoon trough, between Tropical Storm Piper (20W) and Typhoon Orson (19W). Upper-level data favors continued development. At this time, the system is expected to follow Piper (20W) up the midlatitude trough axis. A warning message is forthcoming."

Soon after the first warning, TD 21W lost most of its central deep convection and it failed to mature (although a well-defined LLCC persisted). The final warning was issued valid at 271200Z, when it was thought that the LLCC of TD 21W was going to dissipate over water. The LLCC did not dissipate, however, and in post analysis it was carried as a 25 kt (13 m/sec) tropical depression for another 60 hours as it recurved on the final leg of its "S"-shaped track.

Figure 3-21-1 Tropical Depression 21W is forming at the end of the monsoon trough. With Piper (20W) to its north, and Orson (19W) to its southwest, TD 21W is set to move north and leave a vacancy at the end of the trough to be filled by yet another TC, Rick (22W) (252224Z August visible GMS imagery).



TROPICAL STORM RICK (22W)
BEST TRACK-TC 22W
27 AUG - 03 SEP 96
MAX SFC WIND 35 KT
MINIMUM SLP 997MB



LEGEND

- 24-HR BEST TRACK POSITION
- ooo TROPICAL DISTURBANCE/
TROPICAL DEPRESSION
- \$\$\$ TROPICAL STORM
- \$\$\$ TYPHOON/SUPER TYPHOON

24-HR BEST TRACK POSITION
IDENTIFICATION
DTG SPD(KT) INT(KT)
XXXXZ XX XXX

TROPICAL STORM RICK (22W)

I. HIGHLIGHTS

Rick formed at a high latitude at the end of a northward-displaced monsoon trough. The first warning was issued without a prior Tropical Cyclone Formation Alert when scatterometer data indicated the well-defined low-level circulation possessed winds of at least 30 kt (15 m/sec).

II. TRACK AND INTENSITY

During the last week of August, the axis of the monsoon trough was displaced well to the north of its normal location. Anchored at 25°N by the slow-moving Orson (19W), the axis of the monsoon trough extended east-northeastward toward the international date line. Prior to Rick's formation, two other TCs — Typhoon Piper (20W) and Tropical Depression 21W — formed at the end of this monsoon trough and moved on poleward-oriented "S"-shaped tracks.

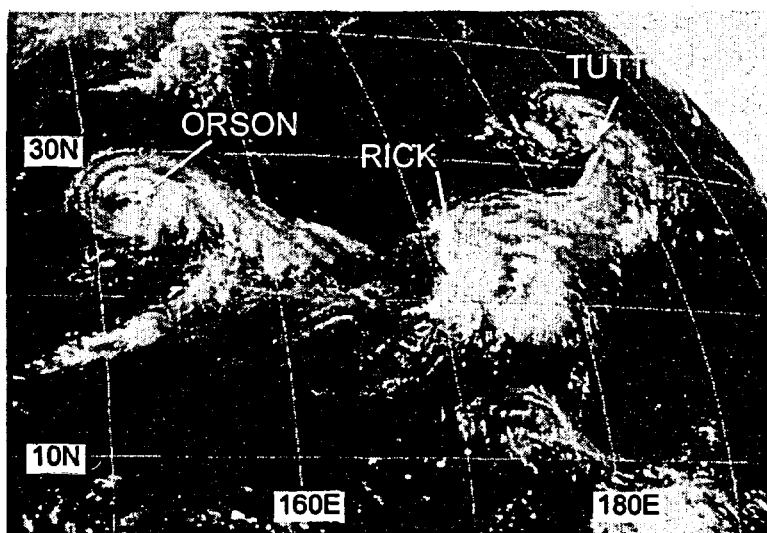


Figure 3-22-1 The tropical disturbance that became Rick is located between Orson (19W) and a TUTT cell. Scatterometer data at this time showed that it was already at tropical-storm intensity, and the final best track was adjusted accordingly (272130Z August infrared GMS imagery).

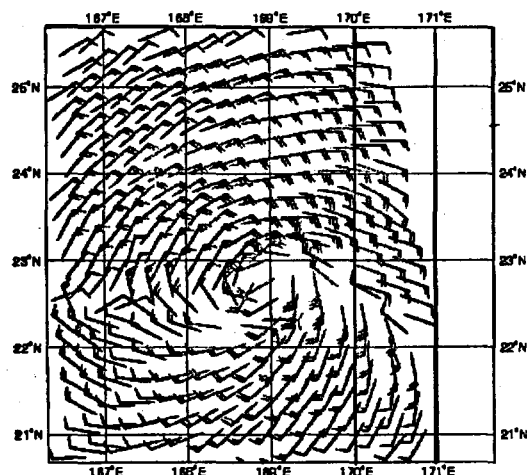


Figure 3-22-2 A well-defined LLCC with maximum winds of 30 kt accompanies "Rick's" cloud system at the time of the image in figure 3-22-1 (272110Z August ERS-2 scatterometer-derived winds).

The tropical disturbance which became Rick was located between Orson (19W) and a well-defined TUTT cell (Figure 3-22-1). This disturbance was first mentioned on the 260600Z August Significant Tropical Weather Advisory when synoptic data indicated that it was accompanied by a weak LLCC. When a scatterometer pass at 271121Z (Figure 3-22-2) revealed that a well-defined LLCC (with maximum winds of 30 kt) accompanied the poorly-organized cloud system shown in Figure 3-22-1, the JTWC issued the first warning (valid at 280000Z) on Tropical Depression (TD) 22W. In post analysis, the scatterometer pass was used to upgrade TD 22W to tropical-storm intensity at an earlier time than upgraded while in warning status.

Initially moving northeastward along the axis of the monsoon trough, TD 22W turned to the north when it approached a blocking high. After crossing 30°N, TD 22W slowed and its cloud pattern became better defined (Figure 3-22-3, see also Figure 3-21-1 in the summary of TD 21W). Better cloud organization and satellite-based microwave data (SSM/I) indicating 35 kt (18 m/sec)

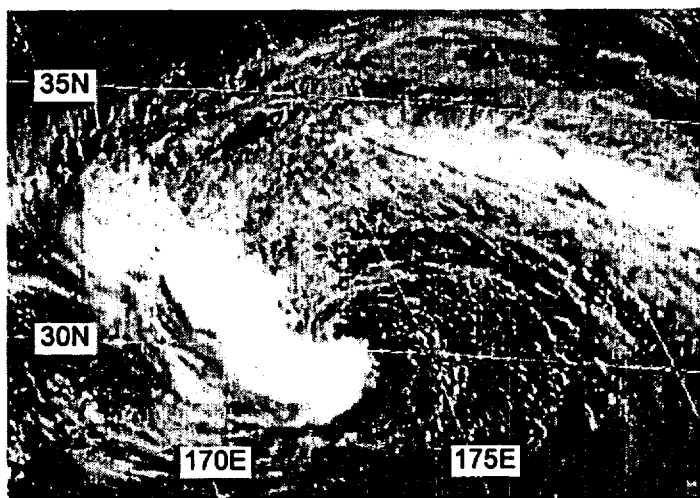


Figure 3-22-3 The primary band of deep convection coils around the western side of Rick's partially exposed LLCC (292131Z August visible GMS imagery).

prompted the JTWC to upgrade TD 22W to Tropical Storm Rick on the warning valid at 300000Z. On the warning valid at 301200Z, the system was downgraded to a tropical depression when the amount of its central deep convection decreased.

On 31 August, the system entered the accelerating westerlies regime north of the subtropical ridge. While Rick was moving east-northeastward at the base of an advancing frontal cloud band, its final warning was issued valid at 311200Z. The remnants of Rick continued to sweep northeastward within the frontal cloud band. The final best track carries the system across the international date line and north of 40°N.

III. DISCUSSION

a. High latitude of formation

Tropical cyclogenesis (TC genesis) is relatively rare east of 160°E and north of 20°N in the WNP. There are two synoptic conditions that lead to most of the TC genesis there: (1) TUTT-induced TC genesis, and (2) TC genesis that occurs when the monsoon trough has penetrated unusually far to the north and east. In Rick's case, the monsoon trough had migrated to an unusually high latitude, and the disturbance that became Rick formed at the eastern end of this trough. There was also a large well-defined TUTT cell northeast of this disturbance (Figure 3-22-1), but its role (if any) in Rick's development is not clear.

b. Scatterometer data

The first warning on Rick was based upon scatterometer data from the European Remote Sensing Satellite-2 (ERS-2) (Figure 3-22-2). The JTWC has access to scatterometer wind data, and has used it to help determine the position, intensity and wind distribution of TCs for nearly one and a half years. Some drawbacks of the scatterometer data are its small swath width, 180° directional ambiguity, relatively coarse resolution, limitations on the wind speeds it can accurately detect, and a low-speed bias.

The scatterometer pass which prompted the first warning on TD 22W (Figure 3-22-2) contains many 25-kt (13-m/sec) wind reports, with a maximum report of 30 kt (15 m/sec) just east of the system center. In real time, this was used to support a warning intensity of 30 kt, but, in post analysis was used to upgrade TD 22W to tropical-storm intensity at an earlier time. When compared with buoys and ship reports, the scatterometer winds generally have a low-speed bias (Quilfen, 1992; Laing, 1994; and Laing and Brenstrum, 1996). Laing and Brenstrum (1996) showed that the ERS-1 winds had a mean low-speed bias of about 4 kt (2 m/sec) when compared with the winds recorded on a New Zealand research ship (Figure 3-22-4). The magnitude of this bias increases with increasing wind speed. The low-speed bias increases to near 6 kt (3 m/sec) at wind speeds of 30 kt (15 m/sec). In operational practice, the JTWC treats a 30-kt scatterometer wind as representative of a 35-kt one-minute average 10-m wind. Hence, the 30-kt maximum scatterometer wind in Figure 3-22-2 was used in post analysis as grounds for upgrading the intensity of TD 22W from 30 kt to 35 kt (i.e., from a tropical depression to a tropical storm).

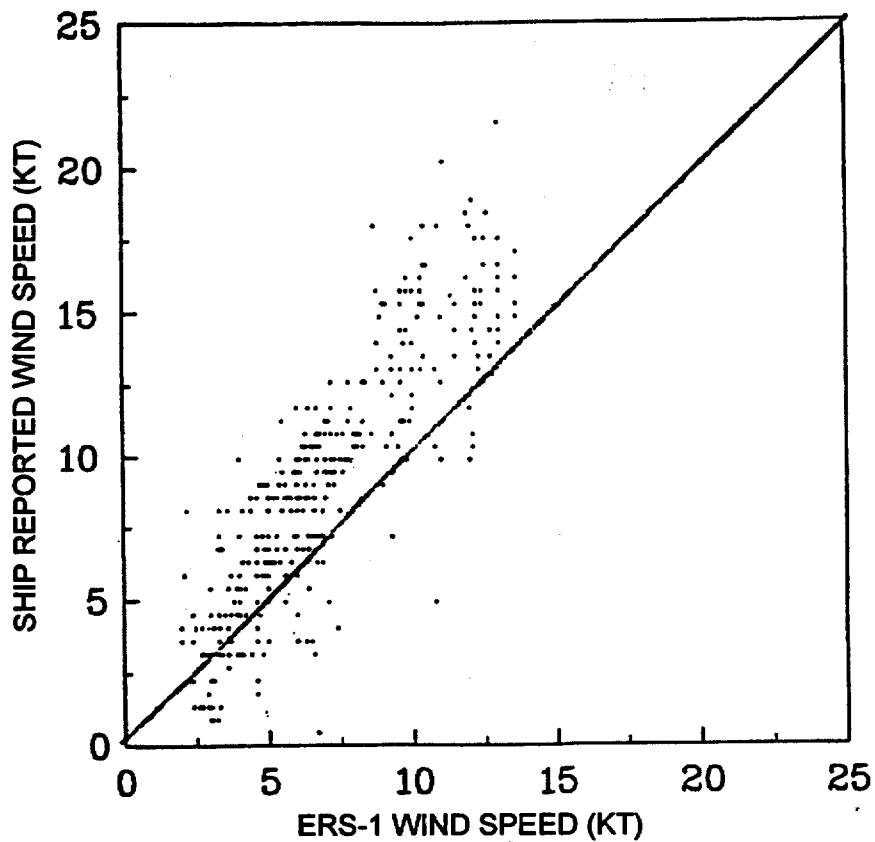
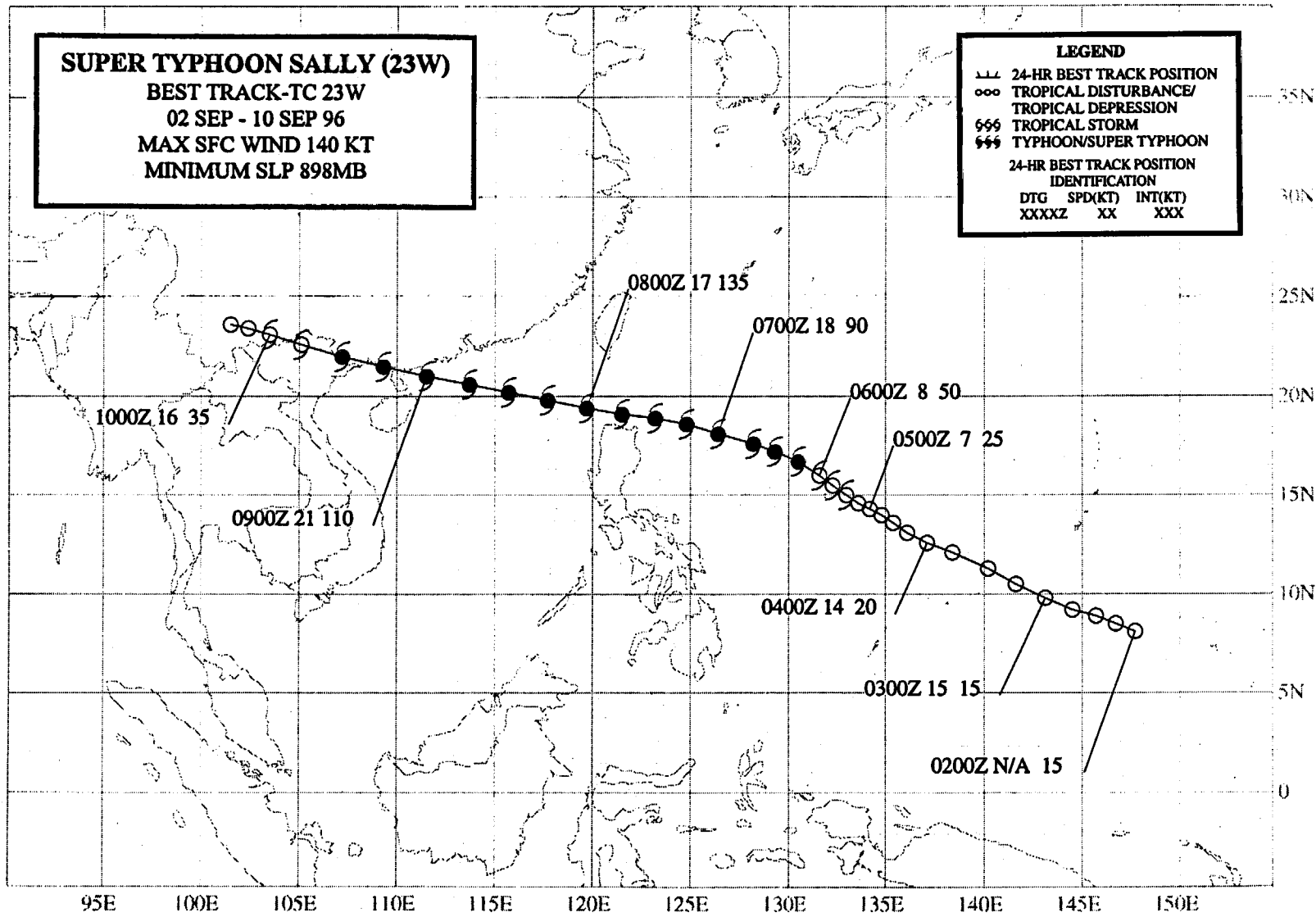


Figure 3-22-4 A comparison of the wind speeds recorded by the New Zealand research ship Tangaroa with wind speeds obtained from the ERS-1 scatterometer. That most of the points are above the 45° line indicate that the ship wind speeds are generally higher than those estimated by the scatterometer. (Figure adapted from Figure 2 of Laing and Brenstrum (1996).)

IV. IMPACT

No reports of damage or injury were received at the JTWC.



SUPER TYPHOON SALLY (23W)

I. HIGHLIGHTS

As the long-lived Orson (19W) recurved at the beginning of September, the unusual monsoon flow pattern of August (See figure 3-13-4 in Kirk's summary) gave way to a pattern more in line with climatology: the maximum cloud zone and the axis of the monsoon trough became established from the Philippines east-southeastward into Micronesia. Sally was the first of five significant TCs to develop in this new monsoon flow pattern. Forming to the southwest of Guam, Sally moved on a relatively steady west-northwest straight-moving track. It became a super typhoon while moving through the Luzon Strait, and later, though weaker, it made landfall in southwestern China where it caused extensive damage and considerable loss of life.

II. TRACK AND INTENSITY

On the first day of September, Typhoon Orson (19W) was recurving to the east of Japan, and the deep tropics of the WNP were abnormally free of deep convection. Over the next two days, as Orson (19W) recurved into the midlatitudes, amounts of deep convection in the low latitudes of the WNP began to rapidly increase as a new monsoon trough was becoming established there. On 02 September, when amounts of deep convection in the low latitudes of the WNP began to increase, a tropical disturbance quickly consolidated near the island of Guam. It was first mentioned on the 020600Z Significant Tropical Weather Advisory, which described it as follows:

"An area of convection is located near 11N 145E. Satellite imagery and synoptic data indicate a broad area of convection surrounding an inverted trough in the trade wind flow. . . ."

Early on 04 September, synoptic data showed that a low-level cyclonic circulation had formed in the monsoon trough in association with this disturbance. Cirrus outflow was well organized into an anticyclonic pattern with a center of symmetry over the LLCC. This prompted the JTWC to issue a Tropical Cyclone Formation Alert (TCFA) at 032300Z September. The MCSs comprising this disturbance were growing and collapsing at the typical 06- to 12-hour MCS time scale, creating some difficulty for the satellite analysts to accurately locate the LLCC. The uncertain knowledge of the location of the LLCC led to a second TCFA at 042300Z in order to carry the alert beyond the expiration of the first, and to give JTWC forecasters some time to gather information for the first warning (which was in preparation when the first TCFA was about to expire). As expected, the second TCFA was quickly followed by the first warning on Tropical Depression (TD) 23W, valid at 050000Z, when morning visible satellite imagery allowed for a more accurate determination of the position of the LLCC and indicated an intensity of 25 kt (13 m/sec). From this time onward (until peak), intensification proceeded at a faster than normal rate (i.e., 1.5 T numbers per day versus the normal 1 T number per day). TD 23W was upgraded to Tropical Storm Sally on the warning valid at 051800Z. The system became a typhoon at 060600Z, and a super typhoon at approximately 071600Z. The peak intensity of 140 kt (72 m/sec) occurred at 071800Z (Figure 3-23-1) as the cyclone moved through the Luzon Strait. Moving west-northwestward at nearly 20 kt (37 km/hr), the typhoon crossed the northern reaches of the South China Sea (SCS) under the steering influence of a dominant subtropical ridge. The system weakened as it moved across the SCS, but it was still potent with an intensity of approximately 100 kt (51 m/sec) when it made landfall on the Luichow peninsula in southwestern China. The typhoon crossed the Luichow peninsula and then moved along the Chinese Gulf-of-Tonkin coastline. The system went inland for good just north of China's border with Vietnam. The final warning was issued, valid at 091200Z, as the weakening TC continued its trek inland across the far north of Vietnam and southwestern China.

III. DISCUSSION

Sally's digital Dvorak (DD) numbers: a pattern begins to emerge

During 1996, the hourly time series of the DD numbers was computed and archived for all typhoons (during 1995, hourly DD numbers were computed for some selected TCs, Ward, for example). The hourly time series of Sally's DD numbers (Figure 3-23-2) shows a characteristic pattern that appears to be typical of some of the other very intense typhoons of 1996 and 1995:

1) the DD time series rises more rapidly than the best-track intensity (which is based primarily upon the manual application of Dvorak's techniques);

2) the DD time series peaks earlier than the best-track intensity;

3) the peak of the DD time series is approximately one-half of a T number higher than the best-track peak; and,

4) within 24 hours of the DD peak, there is a dramatic drop of the DD values of 2 or more T numbers, and then a recovery. Some or all of these behaviors are seen in the DD time series of Eve (07W), Dale (36W) and to a lesser extent Herb (10W) and Violet (26W).

These specific characteristic behaviors of the DD time series are closely tied to the evolution of the character of the eye. As TCs approach their peak intensity, their eyes are usually small and well defined. Why the DD numbers rise more quickly and peak earlier and higher than the best track has not been determined. The dramatic fall of the DD time series following the peak can usually be linked to the formation of concentric wall clouds. The DD numbers recover from the dramatic fall after the inner wall cloud collapses and a new larger eye is established.

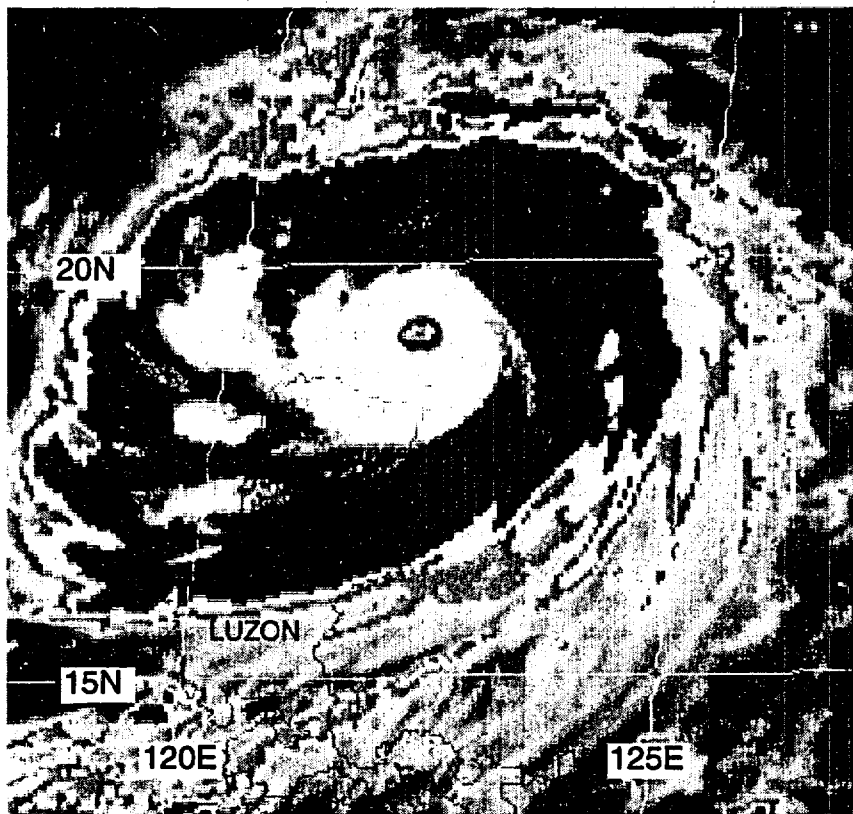


Figure 3-23-1 Sally shortly before reaching its peak intensity of 140 kt (72 m/sec) (071631Z September enhanced infrared GMS imagery). Enhancement curve is "MB".

IV. IMPACT

Sally was catastrophic in southern China. At least 114 people were reported killed with another 110 missing. The city of Zhanjiang on the east coast of the Luichow peninsula was one of the hardest hit. Here, 79 people were reported killed. Almost all trees in this city and its suburbs were reported to have been uprooted by high winds. Economic losses were described as the worst since 1954. Combined losses in the cities of Zhanjiang and Maoming were estimated at US \$1.5 billion.

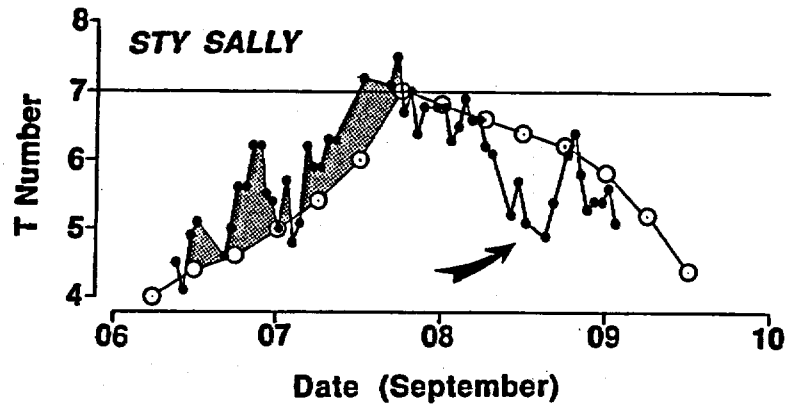


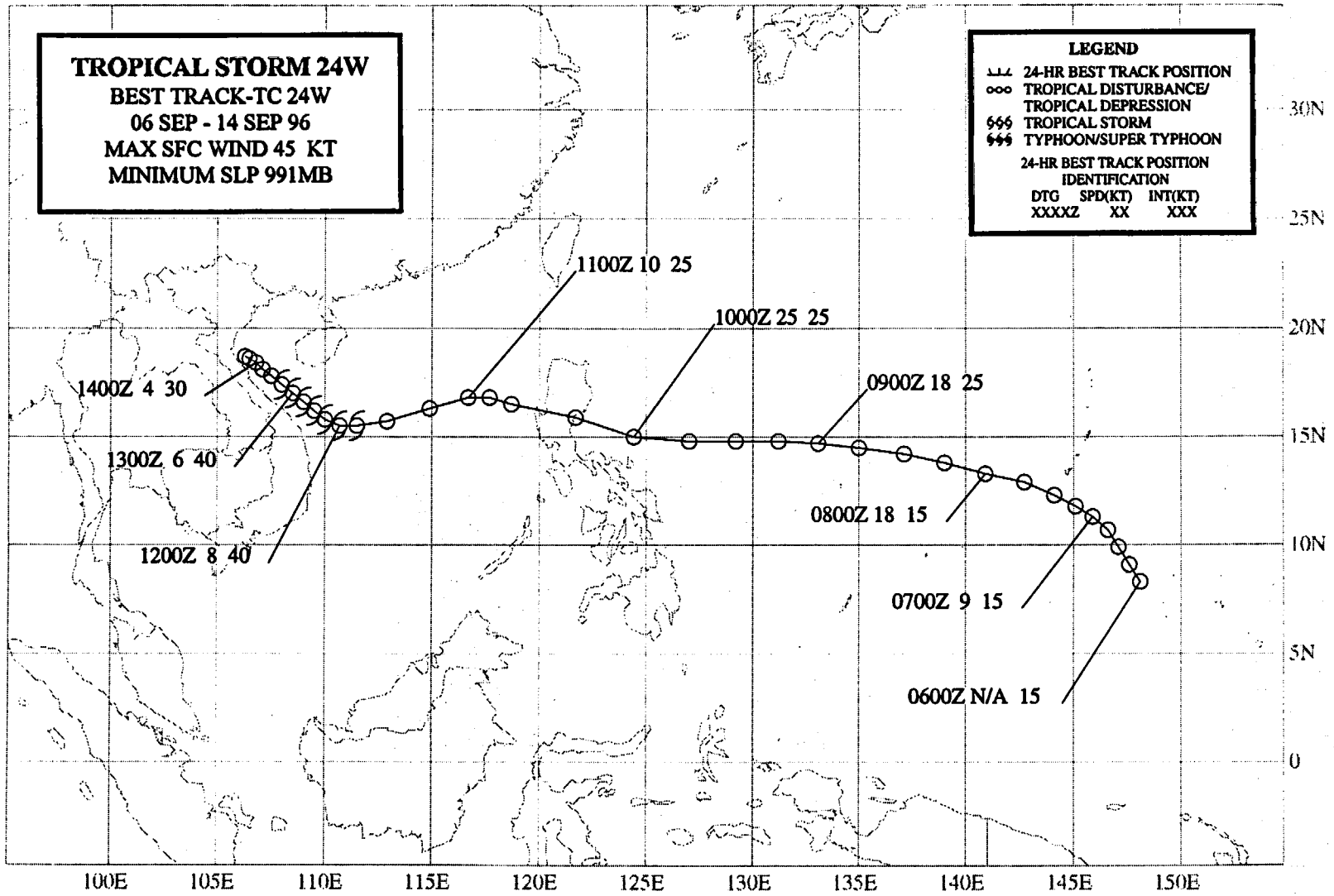
Figure 3-23-2 The time series of Sally's hourly DD numbers (small black dots connected by thin solid line). For comparison, the final best track intensity at six-hour intervals (converted to a T number) is superimposed (open circles connected by thin solid line). Shaded regions indicate that the DD number is higher than the best-track intensity. The arrow points to the relative minimum in the DD time series which occurred approximately 24 hours after the peak in the DD numbers.

TROPICAL STORM 24W
BEST TRACK-TC 24W
06 SEP - 14 SEP 96
MAX SFC WIND 45 KT
MINIMUM SLP 991MB

LEGEND

- 24-HR BEST TRACK POSITION
- ooo TROPICAL DISTURBANCE/
TROPICAL DEPRESSION
- 666 TROPICAL STORM
- 666 TYPHOON/SUPER TYPHOON

24-HR BEST TRACK POSITION
IDENTIFICATION
DTG SPD(KT) INT(KT)
XXXXZ XX XXX



142

TROPICAL STORM 24W

As the long-lived Orson (19W) recurved at the beginning of September, the unusual monsoon flow pattern of August (see figure 3-13-4 in Kirk's summary) gave way to a pattern more in line with climatology: the maximum cloud zone and the axis of the monsoon trough extended from the Philippines east-southeastward into Micronesia. Tropical Storm 24W was the second of five significant TCs to form in this trough.

On 07 September, an area of deep convection began to consolidate into a discrete tropical disturbance located near Guam. First mentioned on the 071600Z September Significant Tropical Weather Advisory, this disturbance became a large monsoon depression in the Philippine Sea by the morning of 09 September (Figure 3-24-1). Although the definition of a monsoon depression includes large size, the disturbance which became Tropical Storm 24W was exceptionally large with its loosely organized ensemble of MCSs stretching nearly 25° (1500 nm; 2800 km) from the Philippines to Guam. Based upon consolidation of deep convection into a smaller area, the JTWC issued a Tropical Cyclone Formation Alert valid at 090500Z. Remarks on this alert included:

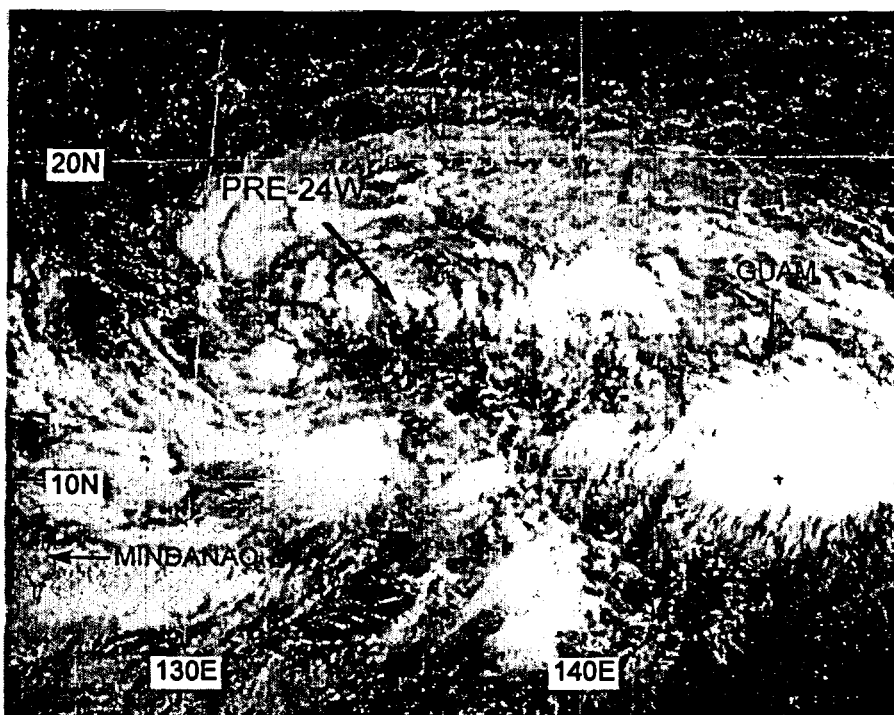


Figure 3-24-1 The cyclonic circulation center which became Tropical Storm 24W consolidated within a large monsoon depression. Another area of deep convection near Guam later detached from the monsoon depression and became Violet (26W) (082224Z September visible GMS imagery).

"Synoptic data and visible satellite imagery reveal the presence of a broad monsoon depression with the dominant circulation center [located near 15°N ; 133°E]. Convection associated with this disturbance is limited to a broad ring approximately 600 nm in diameter. Maximum sustained winds are limited to the convective regions on the periphery of this system. . . ."

The first warning on Tropical Depression (TD) 24W was issued valid an hour later at 090600Z based upon ship reports of 20 to 25 kt (10-13 m/sec) in the convective regions approximately 120 nm (220 km) to the north and southwest of the LLCC.

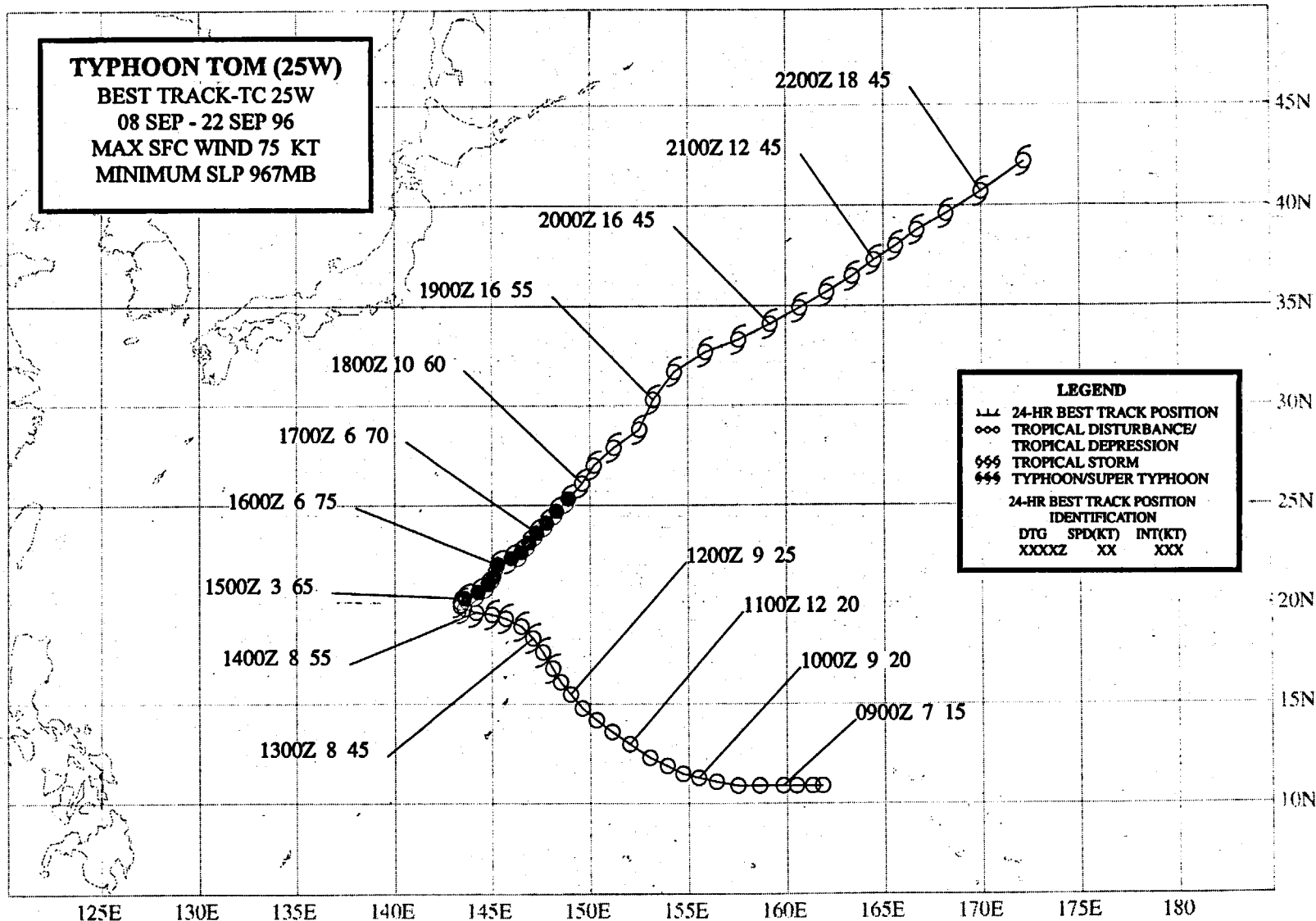
The monsoon depression which became TD 24W had a complex evolution. Not only

did it lead to the formation of TD 24W, but another cyclonic circulation associated with it became Violet (26W). This complexity is described in remarks on the 100600Z Significant Tropical Weather Advisory:

"An area of convection [pre-Violet] is located near 13N 140E. Satellite imagery and synoptic data indicate this is a convective region formerly associated with Tropical Depression 24W that has separated from TD 24W and remained quasi-stationary as TD 24W moves west. . . ."

On 10 September, TD 24W crossed Luzon and entered the South China Sea. During the following three days it traversed the SCS, moved into the Gulf of Tonkin on 14 September, and weakened. The final warning, valid at 141200Z, was issued when the system dissipated near the coast of northern Vietnam.

TD 24W was upgraded to a tropical storm in postanalysis based on synoptic data which indicated sustained winds in the system reached a peak of 45 kt (23 m/sec) at 120600Z.



TYPHOON TOM (25W)

I. HIGHLIGHTS

Tom was the third of five significant TCs to form in the monsoon trough. At one point, Tom, Violet (26W), Willie (27W) and a subtropical (ST) low existed simultaneously along the trough axis (Figure 3-25-1a, b). Due to the relative motions of these TCs (and the ST low), the trough axis became reverse oriented. Both Tom and Violet (26W) were large TCs. Tom also had an unusual structure featuring a "pin-hole" eye in a small central cloud mass surrounded by extensive peripheral rain bands within a large outer wind field. Tom is a good case for the argument that the core of a TC is largely independent of its outer structure.

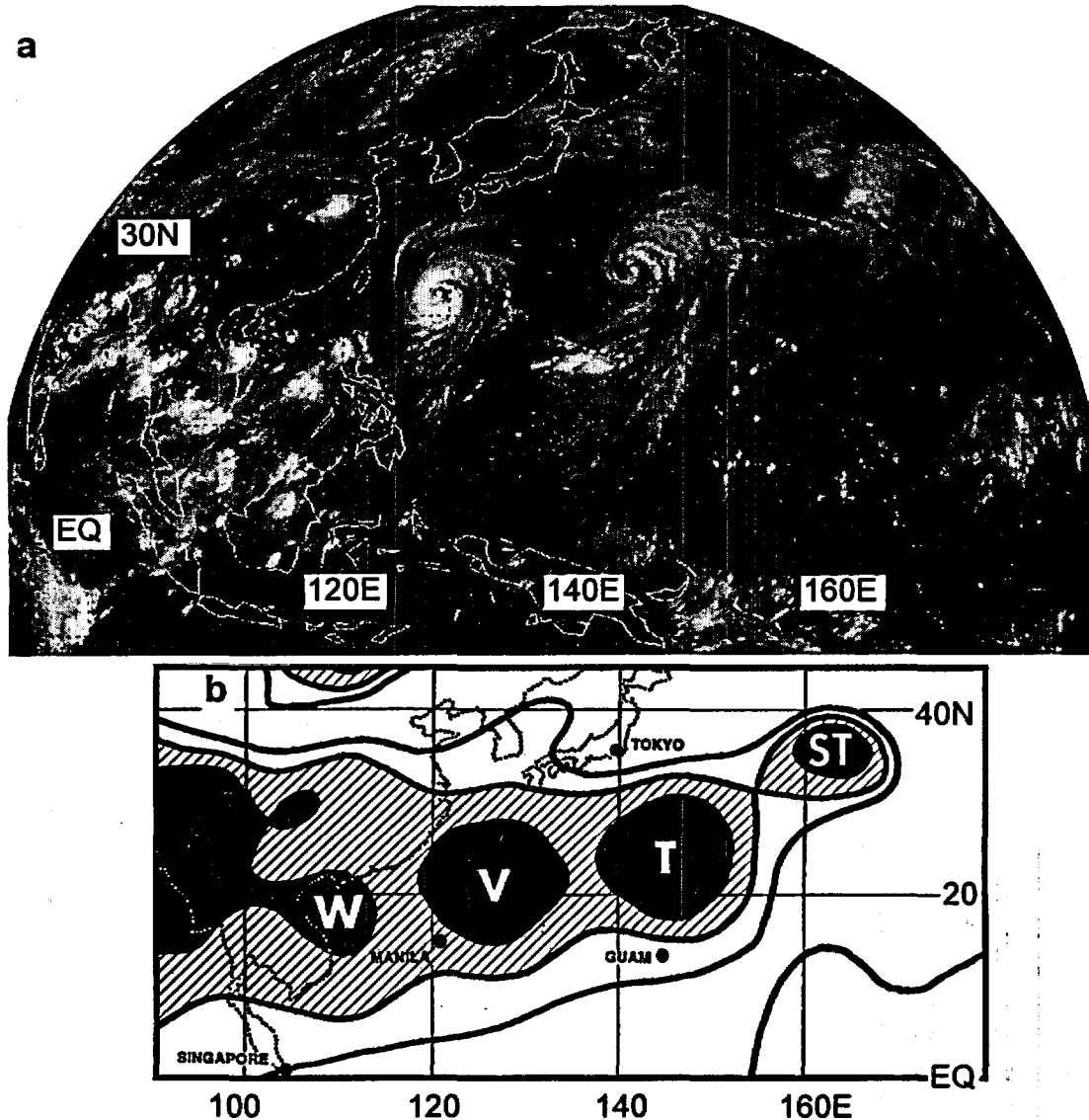


Figure 3-25-1 From west-to-east, TCs Willie (27W), Violet (26W), Tom (25W), and a subtropical low lie along the axis of a reverse-oriented monsoon trough. (a) 171231Z September infrared GMS imagery. (b) Sea-level pressure analysis (outer contour is 1010 mb, cross-hatched areas are between 1004 and 1008 mb, and black regions are less than 1004 mb) (Illustration based upon NOGAPS 170000Z September SLP analysis).

II. TRACK AND INTENSITY

During the second week of September, the cloudiness associated with the monsoon trough began to consolidate into discrete areas of persistent convection. A low-level cyclonic circulation located to the southwest of the easternmost of these areas became Tom, and was first mentioned on the 080600Z September Significant Tropical Weather Advisory. Embedded in an ensemble of poorly organized MCSs, the weak surface low drifted westward for two days with little development. Then, early on 11 September, the convection associated with the surface circulation became better organized, prompting the JTWC to issue a Tropical Cyclone Formation Alert valid at 102030Z. Moving toward the northwest, the deep convection associated with the system began to consolidate. Based on satellite intensity estimates of 25 kt (13 m/sec) and synoptic conditions deemed favorable for further development (e.g., good outflow in all quadrants as revealed by water-vapor derived

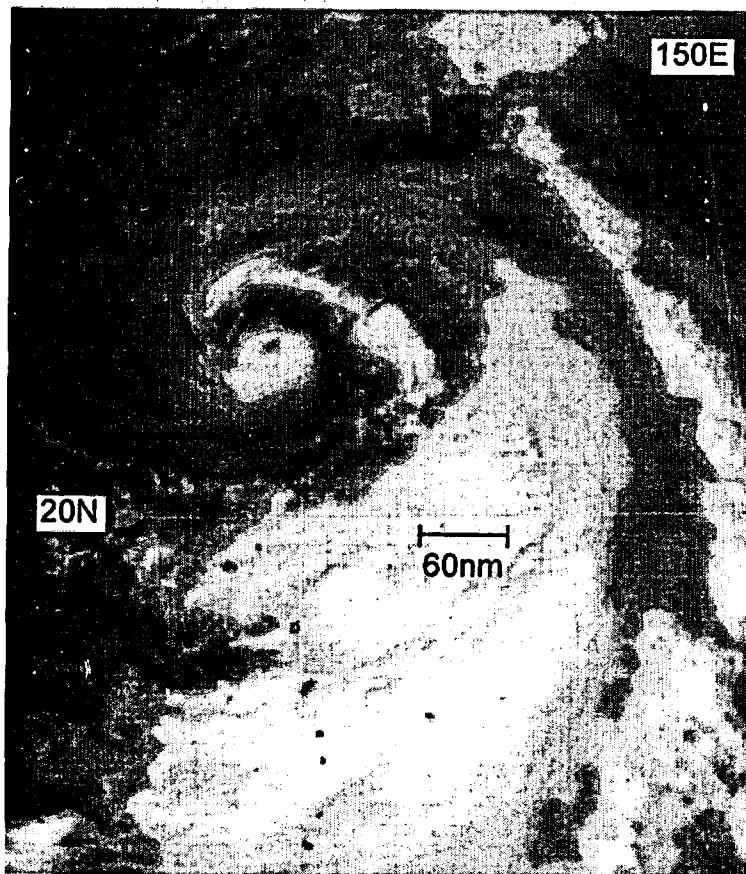


Figure 3-25-2 Tom reaches its peak intensity of 75 kt (39 m/sec). Note the small size of the eye and core cloud features with respect to the peripheral cloud features (160131Z September visible GMS imagery).

winds), the first warning on Tropical Depression (TD) 25W was issued valid at 111800Z. Moving slowly toward the northwest, TD 25W became Tropical Storm Tom on the warning valid at 121200Z. Tom became a typhoon at 150000Z. Also at 150000Z, Tom began to move slowly toward the northeast, almost at the same time as Typhoon Violet (26W) (located approximately 1100 nm (2050 km) to Tom's west-southwest) did likewise. The turn to the northeast of Tom and Violet (26W) was associated with the monsoon trough acquiring a reverse orientation (as mentioned in the 150000Z Prognostic Reasoning for Typhoon Tom).

A common behavior of typhoons moving northeastward in a reverse-oriented monsoon trough, Tom continued to intensify while moving northeastward at 6 kt (11 km/hr), reached its peak of 75 kt (39 m/sec) at 151800Z (Figure 3-25-2), and maintained that intensity until after 161800Z. Slowly gaining forward speed, Tom gradually weakened as it moved toward the northeast. It eventually became a large extratropical low, but not before undergoing a lengthy period of

extratropical transition for which the JTWC satellite forecasters instituted a new intensity estimation technique developed by Miller and Lander (1996) (see the discussion). Deemed to have nearly completed its extratropical transition, the final warning was issued valid at 200600Z.

III. DISCUSSION

a. *Tom's behavior in a reverse-oriented monsoon trough*

When the monsoon trough acquires a reverse orientation, a ridge of high pressure often builds to its south creating steering flow which causes TCs associated with the reverse-oriented monsoon trough (RMT) to move on north-oriented tracks. Premature eastward motion at low latitude is a common behavior of TCs located along the axis of an RMT. Such eastward turns at low latitude are not considered "classic recurvature" because the TC is being steered by dominating monsoonal flow rather than by entry into the midlatitude westerlies. Often, the subtropical ridge is still in-place to the north of the RMT, and the TC is seen to undergo "S" motion (i.e., making a turn back to the northwest while moving through the subtropical ridge and entering the midlatitude westerlies). Another characteristic behavior of TCs while embedded in an RMT is intensification of the TC while moving on a track with an eastward component of motion (such was the case with Tom). The monsoon trough within which Tom was embedded, became reverse oriented by virtue of the relative motion of Tom and Violet (26W) (Figure 3-25-3). Both of these TCs moved on similarly shaped tracks, however, there was a gradual cyclonic rotation of the two about their centroid so that Tom, once east-southeast of Violet, moved to the east-northeast of Violet. For further information regarding the behavior of TCs associated with an RMT see Lander (1996) and the discussion of reverse-trough formation and poleward-oriented motion in Carr and Elsberry (1994).

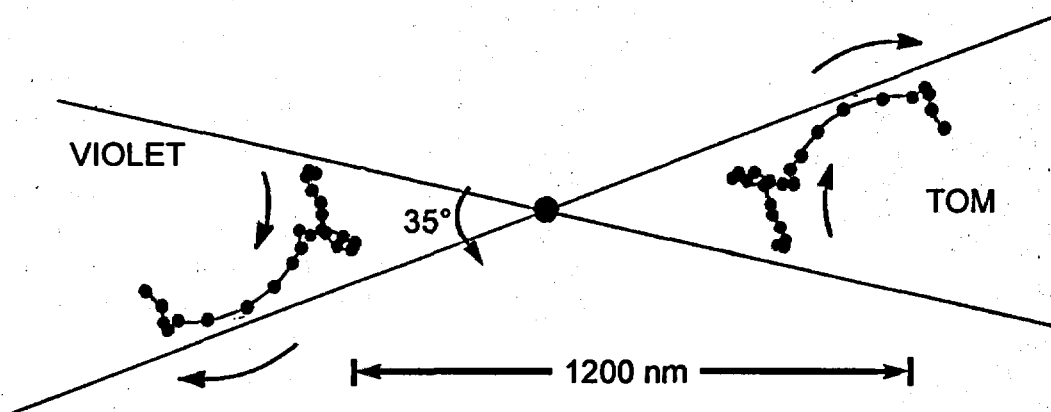


Figure 3-25-3 Centroid relative motion of Tom and Violet (26W). Dots are at 12-hour intervals beginning at 100000Z and ending at 220000Z.

b. *Unusual cloud signature*

When Tom reached its peak intensity of 75 kt (39 m/sec), it had an unusual structure featuring a "pin-hole" eye in a small central cloud mass surrounded by extensive peripheral rain bands within a large outer wind field (Figure 3-25-2). Tom is a good case for the argument that the core of a TC is largely independent of its outer structure. Take away the peripheral rain bands and the deep convection extending southwestward within the monsoon flow and Tom's small core is indistinguishable from a small TC with a small eye. By contrast, Typhoon Violet (26W) (located to the west of Tom) had a size similar to Tom, and yet the structure of its core was quite different: Violet's eye began small, but then expanded to a diameter on the order of 75 nm (140 km). The distinction between the TC core and its outer structure also has relevance to the evolution of monsoon depressions to conventional TCs (i.e., one of Dvorak's four data types). It is not clear by what pathway monsoon depressions become conventional TCs.

c. On the use of scatterometry to assess the wind distribution of large TCs

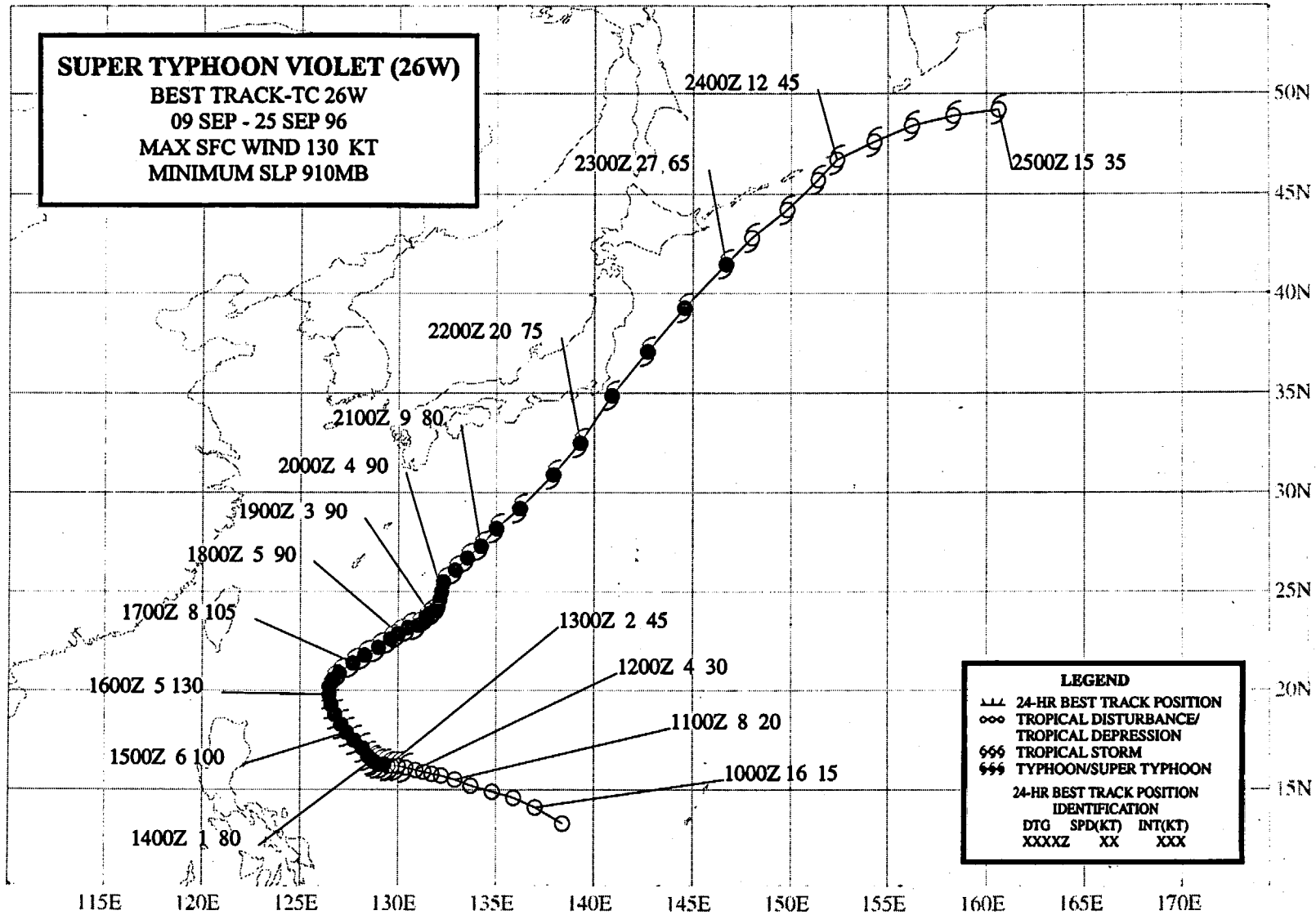
One of the limitations of the ERS-2 scatterometer data is its narrow swath width (approximately 7 degrees of great circle arc). When available, JTWC uses scatterometer data to evaluate the outer wind distribution of TCs (i.e., the radial extent of gales). For small TCs, the scatterometer often misses the TC for several passes, and even misses the peripheral gale area. For larger TCs like Tom, almost every scatterometer pass in the region of the TC samples a portion of its gale area, and thus, by piecing together the several hits on portions of the gale area, a picture of the wind distribution emerges—the problem of narrow swath width has less impact.

d. First use of the "XT" technique

A review of the 1994 and 1995 WNP TC data revealed the intensity estimates of a significant number of TCs that recurved and moved out of the tropics were underestimated by the TC satellite reconnaissance network which used Dvorak's techniques to determine intensity. Intensity estimates for Dan (06W) as it was recurving illustrate the problem (see Dan's (06W) summary). In order to address the problem of underestimating the intensity of TCs undergoing extratropical transition, satellite forecasters at the JTWC in conjunction with ONR-supported researchers at the University of Guam devised a technique (Miller and Lander, 1996) for estimating the intensity of TCs undergoing extratropical transition (see Dan's summary for more details on the technique). This technique yields XT (for extratropical transition) numbers that equate to wind speeds identical to Dvorak's T numbers of the same magnitude. The first application of the technique was on Tom as it was becoming extratropical. The JTWC satellite fix at 192330Z represented the first assignment ever of an XT number to a TC. The XT number determined for Tom at this time was XT 3.0. Other agencies using Dvorak's T numbers, or Hebert and Poteat's ST numbers were up to two T numbers lower than the JTWC intensity estimate. Scatterometer data and other synoptic data at the time supported the JTWC intensity estimate of XT 3.0 (i.e., 45 kt (23 m/sec)).

IV. IMPACT

No reports of damage or injury were received at the JTWC.



SUPER TYPHOON VIOLET (26W)

I. HIGHLIGHTS

As the long-lived Orson (19W) recurved at the beginning of September, the unusual monsoon flow pattern of August (See Figure 3-13-4 in Kirk's summary) gave way to a pattern more in line with climatology: the maximum cloud zone and the axis of the monsoon trough extended from the Philippines east-southeastward into Micronesia. Violet was the fourth of five significant TCs to form in this trough. At one point, Tom (25W), Violet, Willie (27W) and a subtropical (ST) low existed simultaneously along the trough axis (see Figure 3-25-1a, b in Tom's (25W) summary). Due to the relative motions of these TCs (and the ST low), the trough axis became reverse oriented. Violet was one of three TCs during 1996 which acquired a very large eye — the other two were Kirk (13W) and Orson (19W). Passing just off the southeastern tip of the Japanese main island of Honshu, Violet was responsible for extensive damage and loss of life.

II. TRACK AND INTENSITY

On 10 September, an area of deep convection began to consolidate into a discrete tropical disturbance located between the Philippines and Guam. The early stages of this tropical disturbance were somewhat complicated as noted in the remarks on the 100600Z Significant Tropical Weather Advisory: "An area of convection is located near 13N 140E. Satellite imagery and synoptic data indicate this is a convective region formerly associated with Tropical Depression 24W that has separated from TD 24W and remained quasi-stationary as TD 24W moves west. . . ." On 11 September, the disturbance became better organized, and remarks on the 110600Z Significant Tropical Weather Advisory included:

"The area of convection previously located near 13N 140E [has moved west]. . . . Synoptic data indicate this convective region lies near a broad cyclonic circulation along the monsoon trough. . . ."

Further consolidation of the deep convection and rapid improvements in the organization of the convection and of its outflow cirrus prompted JTWC to issue a Tropical Cyclone Formation Alert at 111100Z September, followed by the first warning on Tropical Depression (TD) 26W, valid at 111800Z. This is the same valid time for the first warning on the tropical depression that became Tom (25W) — a TC located approximately 1000 nm (1900 km) to the east-southeast of TD 26W. At the time of the first warning on TD 26W, NOGAPS was indicating TD 25W (Tom) would become the dominant system and engulf the smaller circulation of TD 26W. The official forecast reflected the dynamic guidance and dissipated TD 26W as a significant tropical cyclone in 36 hours. The dynamic guidance was in error, and TD 26W intensified and eventually became a large intense TC with a size comparable to that of Tom (25W) (see Figure 3-25-1b in Tom's summary). TD 26W was upgraded to Tropical Storm Violet on the warning valid at 121800Z. The system became a typhoon at 130600Z and reached its peak intensity of 130 kt (67 m/sec) at 160000Z (Figure 3-26-1).

After becoming a typhoon, Violet turned and began to move very slowly toward the northwest. When the typhoon reached its peak intensity at 160000Z, it began to track slowly toward the northeast in tandem with Tom (25W) (located approximately 1100 nm (2050 km) to Violet's east-northeast). The turn to the northeast of Violet and of Tom (25W) was associated with the monsoon trough acquiring a reverse orientation. Whereas Tom continued to intensify while moving northeastward, Violet began to weaken. As it weakened, its eye became very large (Figure 3-26-2) (see the discussion). Slowly gaining forward speed, Violet continued to weaken as it moved toward the

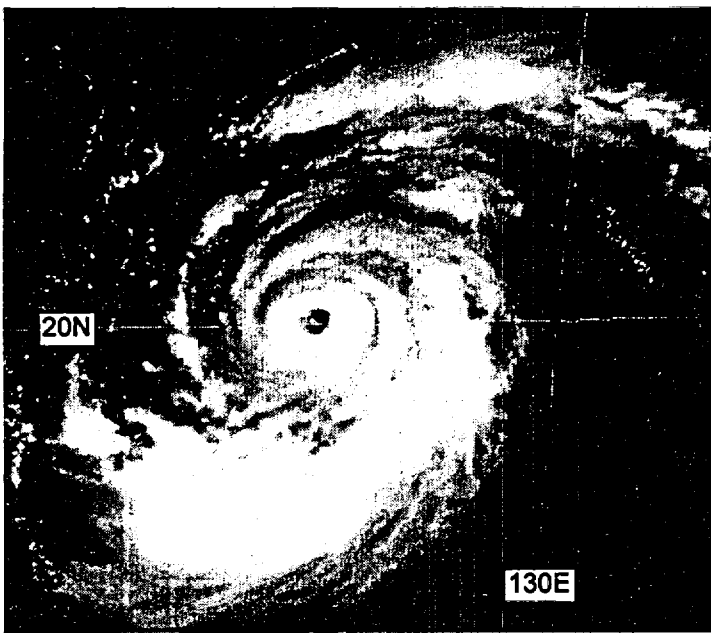


Figure 3-26-1 Violet at its peak intensity of 130 kt (67 m/sec) (160131Z September visible GMS imagery).

northeast. Its large eye passed just offshore to the east of the Tokyo area. High winds and heavy rains caused damage and loss of life in southeastern Japan (see the Impact section). The final warning was issued valid at 230000Z as the typhoon continued on a northeastward track toward the eastern end of the Kuril Island chain where it became an extratropical low.

III. DISCUSSION

a. *Violet's behavior in a reverse-oriented monsoon trough*

The monsoon trough within which Violet was embedded, became reverse oriented by virtue of the relative motion of Tom (25W) and Violet (see Figure 3-25-3 in Tom's summary). Both of these TCs moved on similarly shaped tracks, however,

there was a gradual cyclonic rotation of the two about their centroid so that Tom, once east-south-east of Violet, moved so as to be located to the east-northeast of Violet. For more details on the characteristics of TC motion in a reverse-oriented monsoon trough see Tom's (25W) summary.

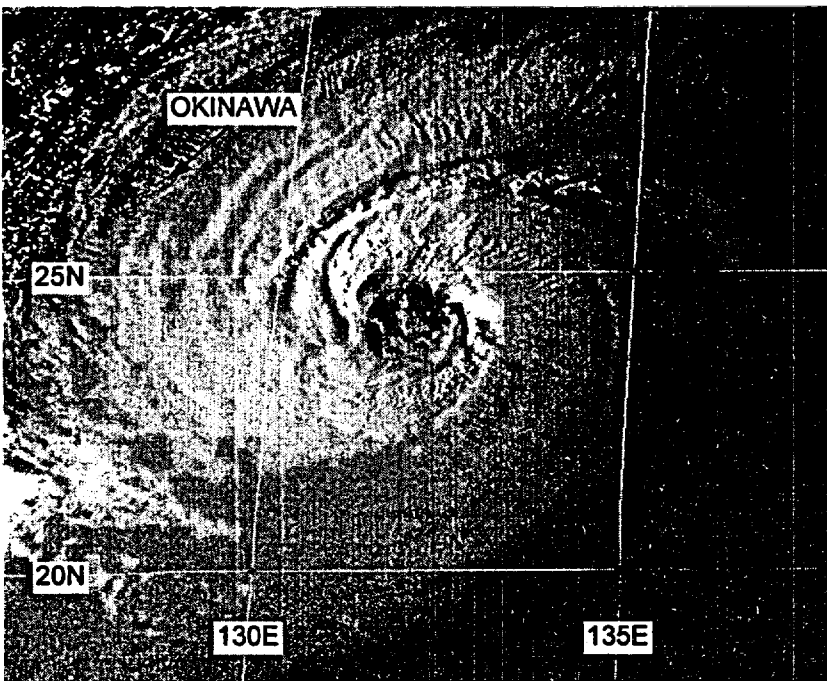


Figure 3-26-2 Violet was one of three WNP TCs during 1996 which acquired a very large eye with a maximum satellite-observed diameter greater than 75 nm (140 km) (190831Z September visible GMS imagery).

b. *Very large eye*

Violet was one of three TCs during 1996 — the other two were Kirk (13W) and Orson (19W) — that acquired very large eyes. Violet's eye evolved greatly during its life: it was at times a banding eye, a large ragged eye, an eye with concentric wall clouds, a small well-defined eye, and a very large eye. The changes in the character of Violet's eye were reflected in fluctuations of Violet's digital Dvorak (DD) numbers (Figure 3-26-3). From 172330Z to 201130Z Violet's satellite-observed eye diameter exceeded 45 nm (85 km) (Figure 3-26-4). From 190450Z to 192030Z the eye diameter ranged from 62 to 79 nm (115 to 145 km) (Table 3-26-1).

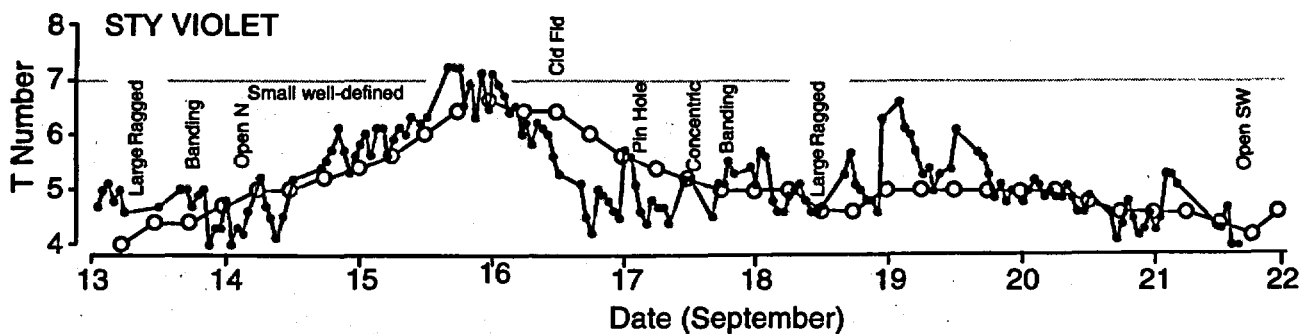


Figure 3-26-3 Violet's DD time series for the period 130130Z September through 211830Z September. Small black dots are the hourly DD values, open circles are the best track intensity (converted to a T number). Comments on the structure of the eye are included.

Table 3-26-1 Eye diameter of Violet from satellite during its period of very large eye size.

DTG (Z)	T Number	Satellite-derived eye diameter (nm)
172330	4.0	52
180230	---	45
180330	---	65
180430	---	42
180501*	4.0	58
180511*	4.0	64
182030	---	46
182111	4.5	55
182330	5.0	63
190230	---	59
190450	4.5	76
190530	5.0	62
190828	4.5	72
190830	---	78
191130	5.0	75
191630	---	79
191730	5.0	78
192030	---	71
192330	4.5	59
200230	---	49
200430	4.5	51
200830	---	64
201130	4.0	72

* These fixes are from different agencies using the same NOAA-14 pass.

c. Gravity waves

When Violet passed through the eastern part of the Kuril Island chain on 24 September, the rugged high islands produced a spectacular display of gravity waves in the low and middle cloud field (Figure 3-26-5). Such displays of terrain-induced gravity waves are commonly observed in the flow of typhoons which are becoming extratropical. Stabilization of the lower atmosphere by ocean chilling sets up conditions favorable for these gravity waves. In the deep tropics (e.g., over the islands of the Philippines), terrain-induced gravity waves in the circulation of a TC are far less common.

IV. IMPACT

Violet was responsible for killing seven people and injuring 44 others in southeastern Japan. Based on radar and satellite data, the center of Violet's large ragged eye passed approximately 80 nm (150 km) to the east-southeast of the Tokyo metropolitan area, and about 30 nm (55 km) east of the coastal cities of Tateyama and Choshi in Chiba prefecture. The western wall cloud passed over Tokyo and nearby areas, dumping 10.4 inches (265 mm) of rain in 24 hours on Tokyo's main business district (the third-largest 24-hour rainfall recorded there since 1876), and producing wind gusts to near 100 kt (51 m/sec) in exposed coastal areas. Tateyama (on the

southern tip of Chiba prefecture) recorded a peak gust to 106 kt (55 m/sec) and a minimum SLP of 969 mb. No significant damage occurred at Fleet Activities Yokosuka, although numerous trees were uprooted or blown down and fencing along a sea wall was torn down due to wave action.

Figure 3-26-4 A close-up view of Violet's very large eye. The relatively clear region in the eye has a diameter of approximately 60 nm in this image (190038Z September visible DMSP imagery).

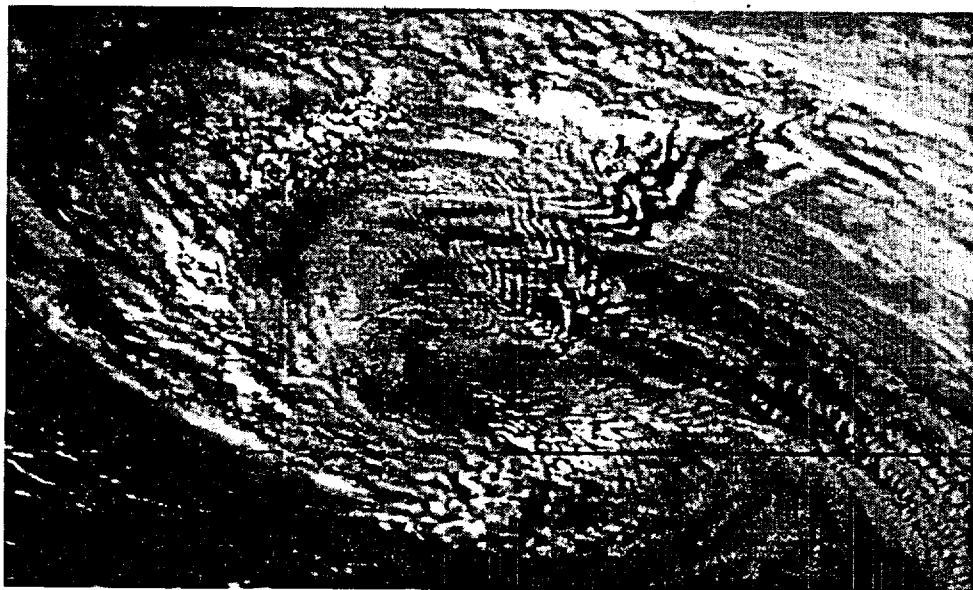
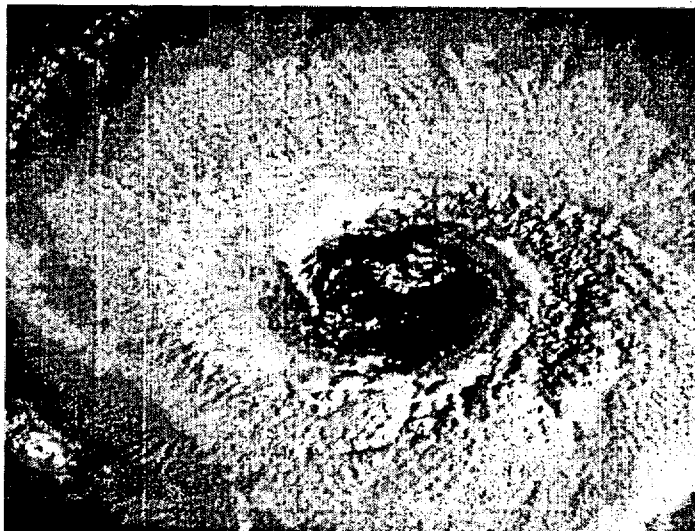
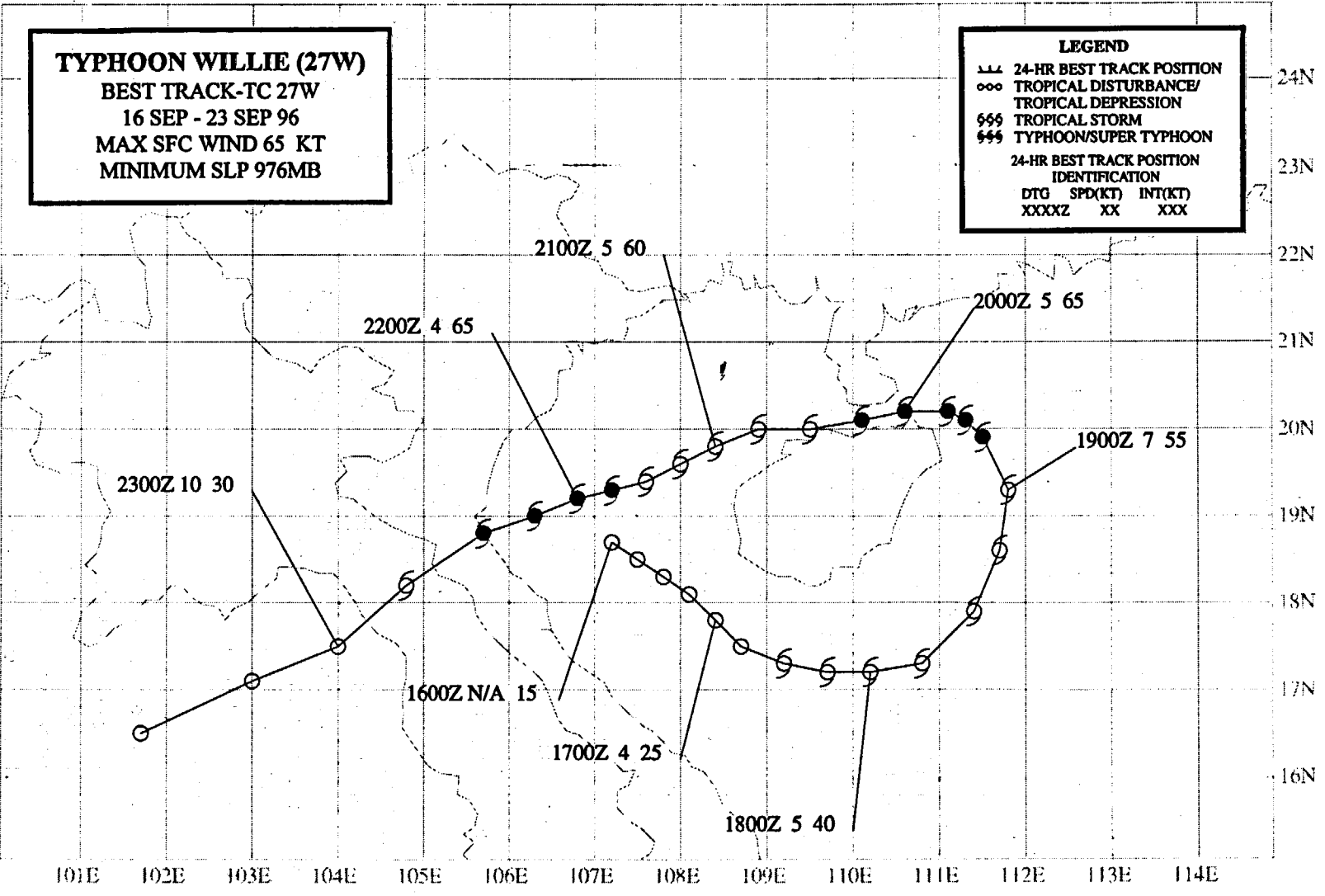


Figure 3-26-5 A multitude of gravity waves is apparent in the low and middle clouds of Violet as the system moves northeastward over the Kuril Islands (240332Z September visible GMS imagery).



TYPHOON WILLIE (27W)

I. HIGHLIGHTS

Never more than 90 nm (170 km) from shore, Willie circumnavigated Hainan Island while undergoing a counter-clockwise loop. Willie was a small TC, and was part of a three-TC outbreak along the monsoon trough, with the larger TCs Tom (25W) and Violet (26W) to its northeast.

II. TRACK AND INTENSITY

On 17 August, the axis of the monsoon trough stretched from Bangladesh to the Gulf of Tonkin, and from there into the WNP where the large typhoons Tom (25W) and Violet (26W) and a subtropical low had formed along it (see Figure 3-25-1a, b in Tom's (25W) summary). The small area of deep convection that became Willie was first mentioned on the 170600Z September Significant Tropical Weather Advisory based on its persistence near a low-level cyclonic circulation located to the southwest of Hainan Island. The area of deep convection moved to the east-southeast and became better organized, prompting the JTWC to issue a TCFA at 171130Z followed by the first warning, valid at 171800Z, on Tropical Depression (TD) 27W. Six hours later, TD 27W was upgraded to Tropical Storm Willie based on several data sources:

- 1) a 171000Z report (received later at the JTWC) of 35 kt (18m/sec) sustained wind from the M/V GECO Emerald (a ship servicing the oil rigs south of Hainan);

- 2) a scatterometer pass at 171521Z supporting 35 kt one-minute sustained wind near the LLCC; and,

- 3) a significant improvement in convective organization.

During the afternoon of 19 August Willie acquired a ragged eye and became a typhoon (Figure 3-27-1). Willie maintained a peak intensity of 65 kt (33 m/sec) for 24 hours as it rounded the northeastern end of

Hainan. The system weakened slightly after passing through the narrow Hainan Strait, but became a minimal typhoon once again as it crossed the Gulf of Tonkin on a west-southwest track. As a minimal typhoon, Willie made landfall at approximately 221200Z in northern Vietnam near Vinh. Continuing on a southwestward track it crossed Laos into Thailand. The final warning, valid at 230000Z, was issued as the weakening system moved into northeastern Thailand and dissipated.

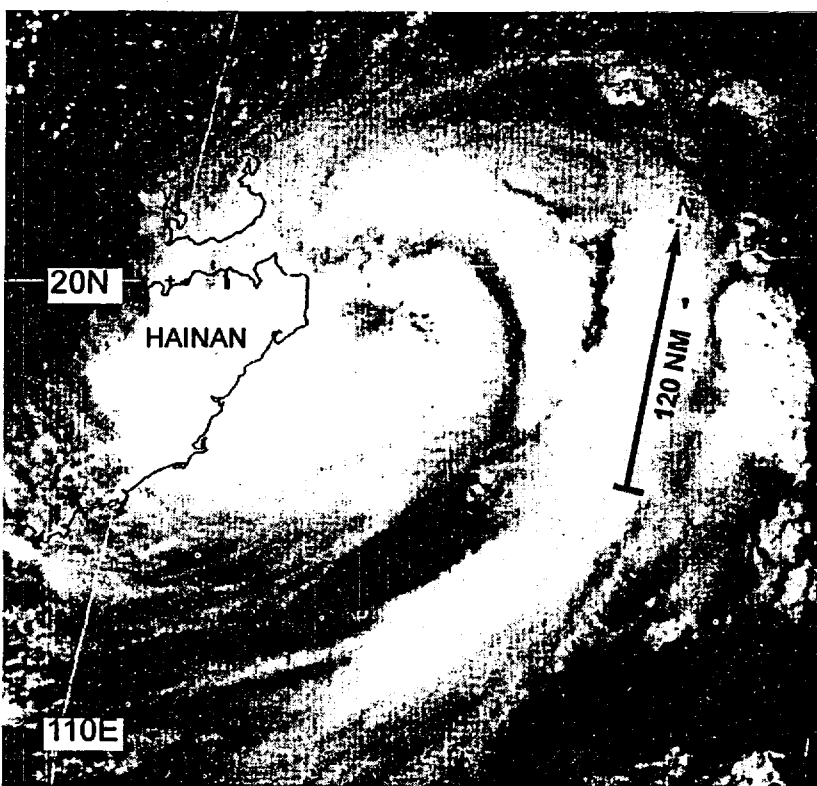


Figure 3-27-1 Willie becomes a typhoon (190531Z September visible GMS imagery).

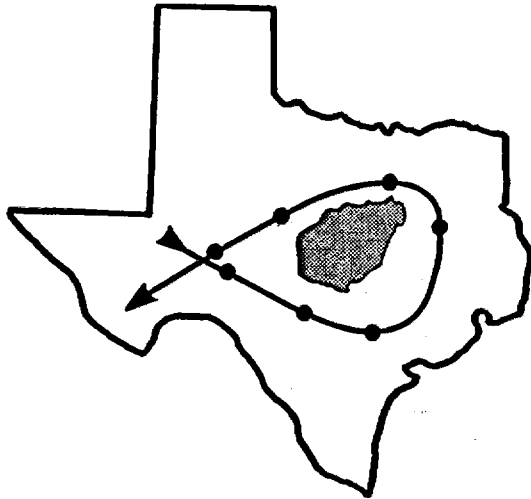


Figure 3-27-2 Willie's counter-clockwise loop fits comfortably within the boundaries of the State of Texas. Hainan Island (shaded) is superimposed. Dots show Willie's position at 24-hour intervals.

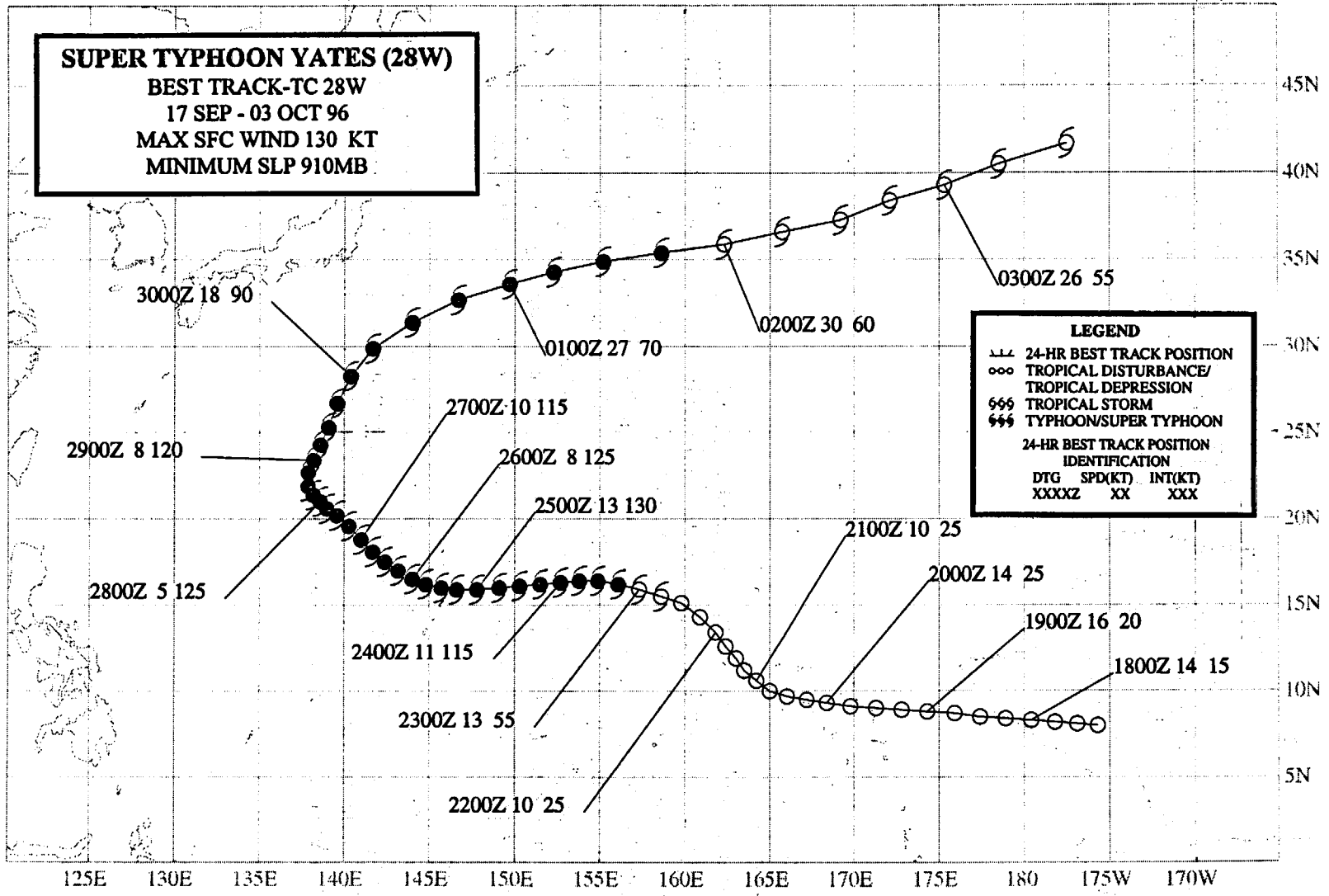
III. DISCUSSION

Unusual motion

Willie circumnavigated Hainan Island while undergoing a counter-clockwise loop. The dimensions of the oval-shaped loop were 300 nm by 180 nm (550 km by 330 km) which would fit comfortably within the boundaries of the State of Texas (Figure 3-27-2). The eastward motion of Willie during the first portion of its track is consistent with its position at the southwestern end of a reverse-oriented monsoon trough with typhoons Tom (25W) and Violet (26W) located further to the east-northeast along the trough axis. Initially steered eastward by deep monsoon flow along the trough axis, Willie turned toward the north and then toward the west, as Tom (25W) and Violet (26W) exited the tropics and a ridge gradually built to the north and east of Willie.

IV. IMPACT

At least 38 people were reported killed, dozens injured and 96 missing on Hainan Island. Willie smashed homes, washed away fishing boats and dumped up to 16 inches (400 mm) of rain on areas of this island province. Most of the deaths were attributed to flooding. No reports of damage or injuries in Vietnam were received at the JTWC.



SUPER TYPHOON YATES (28W)

I. HIGHLIGHTS

While passing between Saipan and Anatahan (two islands in the Northern Marianas), Yates was observed with Guam's NEXRAD. Although Yates became a super typhoon, its surface wind field was relatively compact, and it possessed a very small satellite-observed eye for much of its life. Yates and Zane (29W) developed in the same monsoon trough, at approximately the same time, and recurved simultaneously along similarly shaped and spatially-proximate tracks.

II. TRACK AND INTENSITY

During early September, five TCs — Sally (23W), TS 24W, Tom (25W), Violet (26W), and Willie (27W) — formed in the monsoon trough. This very active monsoon trough moved northward, became reverse oriented, and by the final week of September had migrated to a relatively high latitude. As this monsoon trough exited the tropics, a new monsoon trough formed at low latitudes, and was the site of development for the next two TCs in the WNP: Yates and Zane (29W).

The tropical disturbance which became Yates was mentioned on the Significant Tropical Weather Advisory as early as 170600Z September, when a persistent area of deep convection was observed at low latitude just east of the international date line. At this time the WNP was still dominated by the reverse-oriented monsoon trough which contained Tom (25W), Violet (26W) and Willie (27W). The low latitudes of the WNP were dominated by high pressure and low-level easterly flow, and the pre-Yates tropical disturbance was the only significant area of deep convection which was deemed to have any chance of becoming a TC. During the next three days, this disturbance traveled westward into the Marshall Islands. Amounts of deep convection associated with this disturbance began to increase, along with a gradual increase in the amount and extent of deep convection throughout the rest of Micronesia. On 21 September, a small area of persistent deep convection consolidated northwest of Kwajalein. Visible and water-vapor satellite imagery indicated good upper-level anticyclonic outflow over this disturbance, prompting the JTWC to issue a TCFA at 210100Z. Over the next 24 hours, the small system showed no signs of development, but maintained its organization. Thus, a second TCFA was issued at 220100Z. During the night of 22 September, the pre-Yates tropical disturbance rapidly acquired well-organized cyclonically-curved convective cloud bands surrounding a small area of persistent deep convection over the LLCC. Based upon this improvement in convective organization, the first warning on Tropical Depression (TD) 28W was issued valid at 221800Z. Within three hours after its issuance, the first warning was amended to indicate that TD 28W was a tropical storm. The amended warning stated:

"Tropical Storm Yates (28W) is moving west-northwestward at 14 knots. Justification [for amendment]: this warning has been amended based on intensity. Satellite analysis indicates that this system is [of] tropical storm intensity. Due to its small size and diffluent [divergent] winds aloft, rapid intensification is expected. . . ."

Yates did indeed intensify rapidly. During the period 221800Z to 231200Z it increased from a minimal tropical storm to a typhoon with an intensity of 115 kt (59 m/sec). The equivalent pressure fall of 57 mb during this 18-hour time period (or 3.2 mb/hr) met the criterion for explosive deepening (i.e., a decrease in the minimum sea-level pressure of a TC of 2.5 mb/hr for at least 12 hours) as defined by Dunnavan (1981). At 250000Z, Yates reached its peak intensity of 130 kt (67 m/sec) (Figure 3-28-1). Yates was a minimal super typhoon for only six hours, and then its intensity fell slightly to 125 kt (64 m/sec) as it passed between the islands of Saipan and Anatahan. During

the four-day period 250000Z to 290000Z, Yates remained a powerful typhoon as its intensity fluctuated slightly between 115 and 125 kt (59 to 64 m/sec) and maintained a very small eye which was, at times, cloud filled.

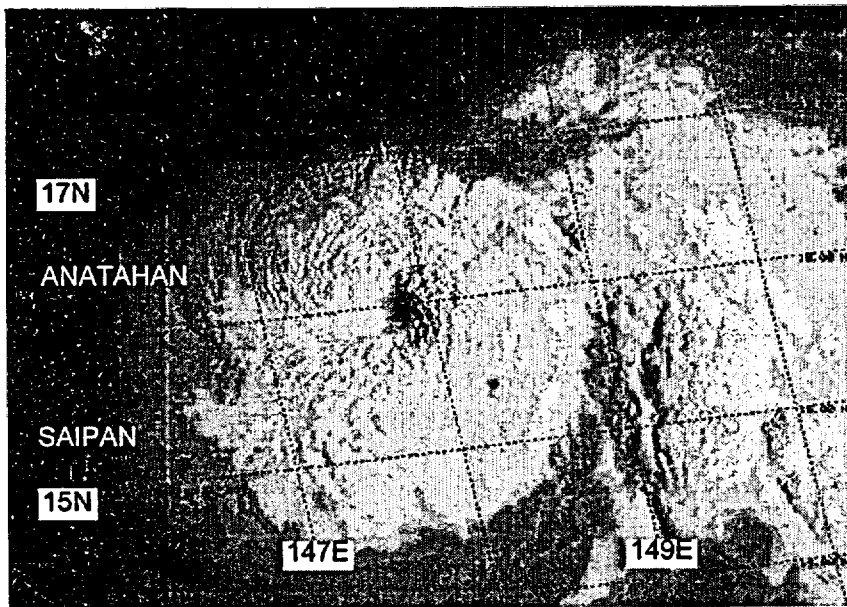


Figure 3-28-1 Yates at peak intensity of 130 kt (67 m/sec) (242319Z September visible DMSP imagery).

Late on 28 September, Yates began to recurve. It moved slowly toward the north-northeast on 29 September, and then on 30 September, it entered the deep-layer westerly air flow of the midlatitudes, turned more toward the east and accelerated. The final warning was issued valid at 011800Z October as the system neared the completion of its extratropical transition. Yates became a powerful extratropical low in the North Pacific after it crossed the international date line (Figure 3-28-2).

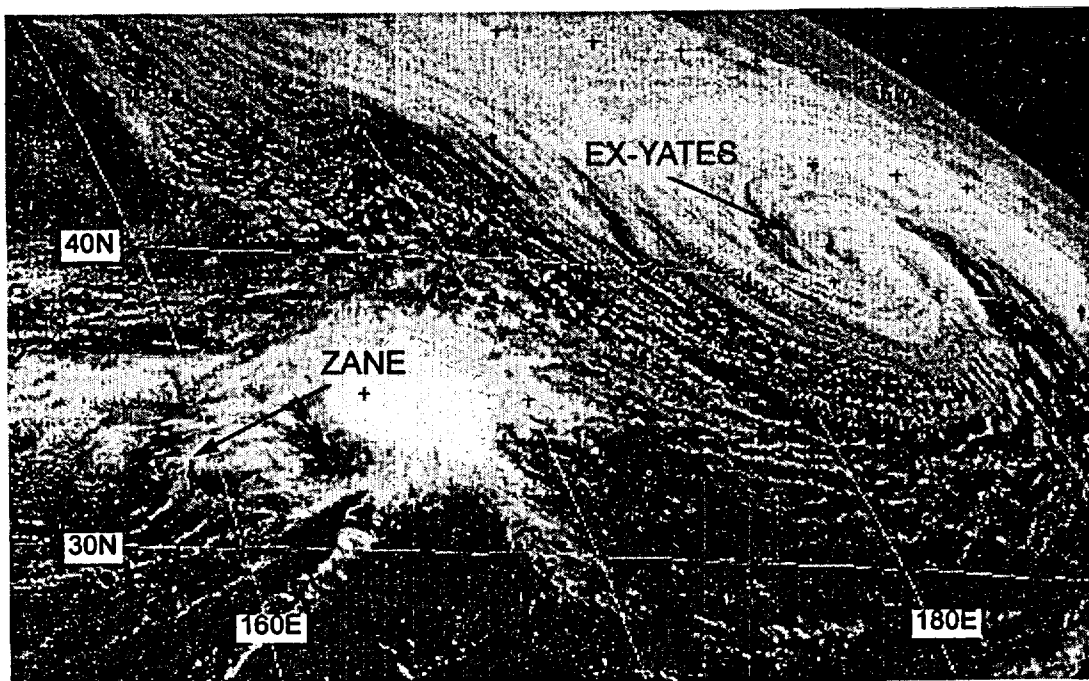


Figure 3-28-2 After recurvature, Yates became an intense extratropical low in the central North Pacific, while Zane (29W) slowed and dissipated (032331Z October visible GMS imagery).

III. DISCUSSION

a. *Persistent pin-hole eye*

Visible and infrared satellite imagery indicated that Yates possessed a very small, or "pin-hole", eye (i.e., a diameter of 10 nm or less) throughout most of its life. Many typhoons which acquire a pin-hole eye usually evolve to possess a larger eye (see the summaries of Super Typhoon Dale (36W) and Super Typhoon Ward (1995)). The evolution from pin-hole eye to larger eye typically begins with the formation of concentric wall clouds. Having formed concentric wall clouds, the outer wall cloud contracts as the small eye and inner wall cloud collapse. Eye wall replacement processes are described more fully by Willoughby (1982, 1990). Yates was somewhat unusual in that it retained a pin-hole eye for four days.

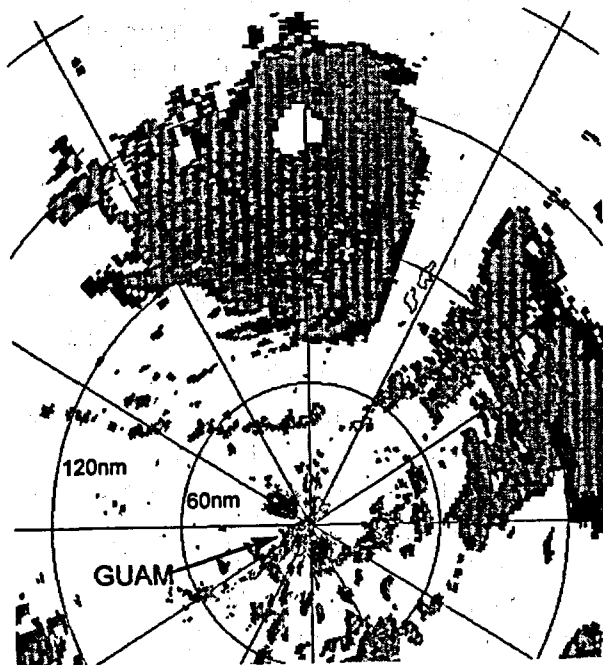


Figure 3-28-3 Yates maintained a well-defined 18 nm (33 km) diameter eye on NEXRAD as it passed to the north of Guam (251844Z September base reflectivity NEXRAD product).

b. *Passage though Guam's NEXRAD coverage*

On 25 September, Yates passed between the islands of Saipan and Anatahan. Its small eye passed approximately 50 nm (100 km) to the north of Saipan, 20 nm (40 km) to the south of Anatahan, and 155 nm (290 km) to the north of Guam. Yates was close enough to Guam to be scanned with Guam's NEXRAD (Figure 3-28-3). The following comments were received in an after-action report by the Andersen AFB NEXRAD operators:

"Yates' well-defined circular eye became visible on radar [at] 25/0131Z shortly after being upgraded to STY intensity and continued to track west at 14 kt average. [Its] symmetrical eye, with an average diameter of 18 nm [33 km], was well surrounded with up to ninety percent high reflectivity wall cloud. . . . [it] went out of range on 26/0834Z. . . Yates never came within [the] 124 nm (230 km) velocity range. . . Reflectivity products were sufficient to fix its eye and movement with a high degree of accuracy. . . ."

It is interesting to note that in Yates' case, the radar-observed eye was larger than the satellite-observed eye. On satellite, the eye diameter was approximately 10 nm (18 km) when not cloud filled. That the pin-hole eye of Figure 3-28-1 had a larger diameter on radar than that which was seen on the satellite imagery implies that cirrus of the wall cloud was obscuring the eye somewhat.

c. *Segregation of TCs into families based upon monsoon trough evolution*

The tendency of the monsoon trough of the WNP to form and then migrate northward lends itself to a natural segregation of TCs into "families" with the commonality among the TCs within each "family" being that they were associated with the same monsoon trough. The five-TC sequence of early September — Sally (23W), TS 24W, Tom (25W), Violet (26W), and Willie (27W) — all had in common an origin within the same monsoon trough. By late September, this monsoon trough moved northward, became reverse oriented, and migrated to higher latitude as TCs Tom (25W) and Violet (26W) carried it with them out of the tropics. As this trough exited the tropics, a new monsoon trough formed at low latitudes, and was the site of development for the next two

TCs in the WNP: Yates and Zane (29W). Yates and Zane therefore comprise another "family" by virtue of their development within the same monsoon trough.

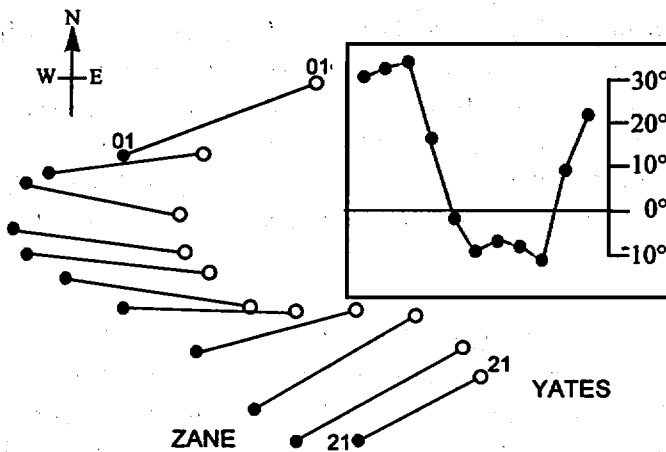


Figure 3-28-4 A schematic illustration of the similarly shaped and spatially proximate recurving tracks of both Yates and Zane (29W). Thin lines connect the TCs at 24 hour intervals beginning at 210000Z September and ending at 010000Z October. The inset shows the bearing of Yates from Zane at 24-hour intervals during the same time period. Positive values indicate Yates north of Zane.

d. *Direct, semi-direct, and indirect TC interaction*

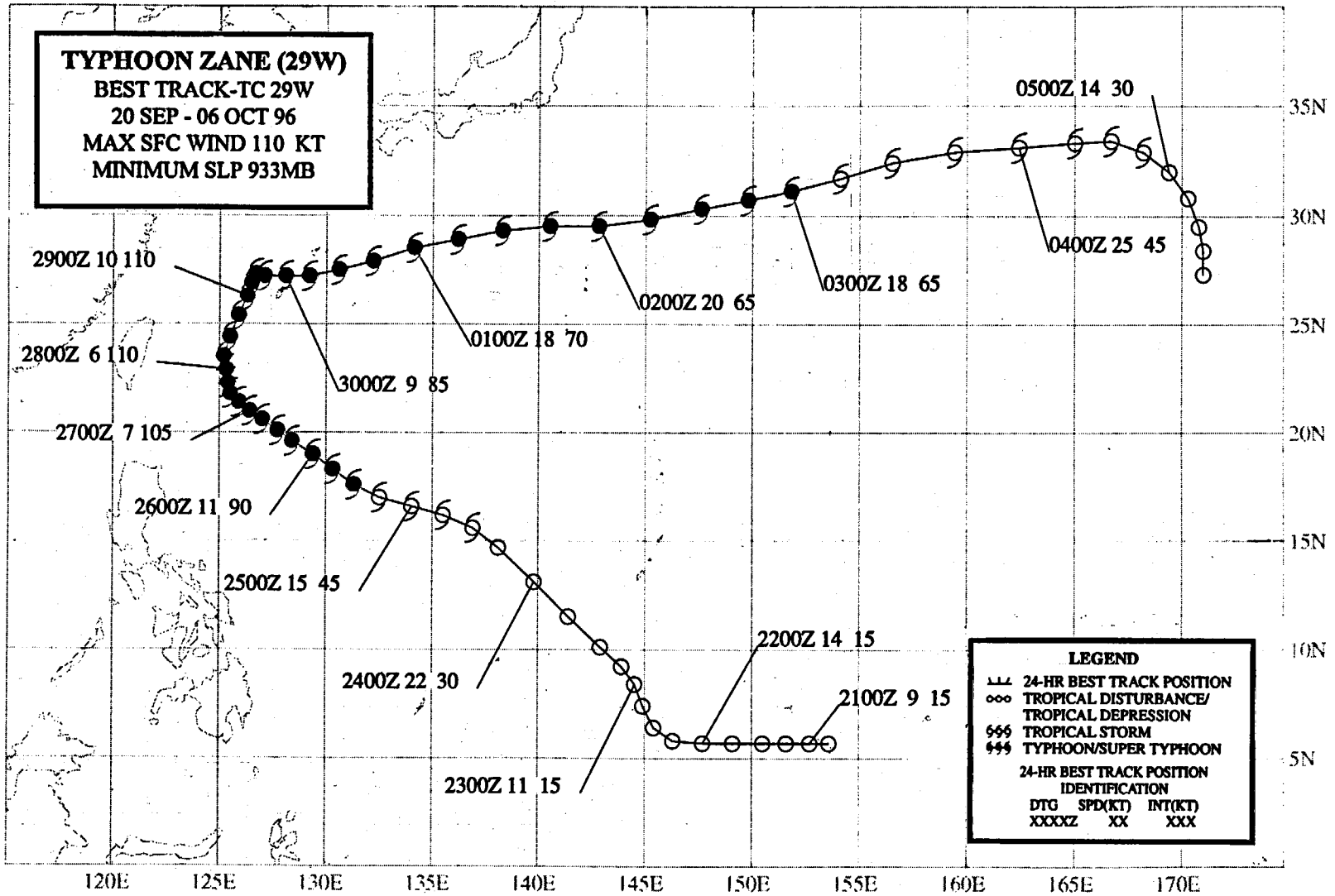
Like Tom (25W) and Violet (26W) before them, Yates and Zane moved on nearly identical spatially-proximate recurving tracks (Figure 3-28-4). The inset of Figure 3-28-4 shows the bearing of Yates from Zane. Note the initial cyclonic change of bearing, followed by a period of anticyclonic change of bearing, then as Yates recurved, the change of bearing was once again cyclonic. Although these two TCs approached to within 780 nm (1450 km), there is little evidence that the TCs were mutually advecting each other (i.e., the Fujiwhara effect) during any of the periods of relative cyclonic orbit. In the Systematic and Integrated Approach, there are three basic kinds of TC interactions: direct (a

mutual cyclonic orbit resulting from the TCs being advected by each other's outer winds), semi-direct (a mutual cyclonic orbit resulting from the alteration by one TC of the steering flow between the other TC and the subtropical ridge), and indirect (i.e., a mutual anticyclonic orbit resulting from the establishment of a ridge between the two TCs). Yates and Zane (29W) had motion characteristics suggestive of semi-direct and indirect TC interaction. The mutual anticyclonic orbit of Yates and Zane during the period 23 to 26 September (manifested in a south-of-west track for Yates) are typical of indirect TC interaction. The periods of mutual cyclonic orbit at the beginning and at the end of the tracks is consistent with semi-direct TC interaction. It is often difficult to differentiate between semi-direct and direct TC interaction, but one clue is often the separation distance. True direct interaction of two TCs usually occurs when the TCs are within 780 nm (1450 km) of each other. Yates and Zane were at this threshold, and it is possible that they may have interacted directly, especially at the end of their tracks when the cyclonic orbit increased rapidly.

TC interaction often results in complicated forecast scenarios. When Yates and Zane came abreast of one another at the same latitude, it was unclear which of the two would recurve first. Zane (29W) had been gaining latitude faster than Yates, and once south of Yates, it moved so as to be at a higher latitude. When Zane slowed near Okinawa, Yates turned to the north, accelerated, and moved to a higher latitude relative to Zane. Yates then recurved ahead of Zane.

IV. IMPACT

Because of Yates' small size, there was only minor damage on Saipan and Anatahan. On Saipan, Yates felled several trees and caused minor flooding. On Anatahan, where estimated winds of 80 kt (41 m/sec) were reported, tin roofs were blown off houses and the entire taro crop was destroyed. Only a handful of people live on the island and they were reported safe and in possession of plenty of food after the cyclone's passage.



TYPHOON ZANE (29W)

I. HIGHLIGHTS

Zane and Yates (28W) developed in the same monsoon trough, at approximately the same time, and recurved simultaneously along similarly-shaped and spatially-proximate tracks. The typhoon affected both Taiwan and Okinawa. Passing Okinawa, Zane came within range of Kadena's NEXRAD. After recurvature, Zane maintained its central deep convection despite being embedded in deep-layer westerly flow to the north of the subtropical ridge.

II. TRACK AND INTENSITY

During early September, five TCs — Sally (23W), TS 24W, Tom (25W), Violet (26W), and Willie (27W) — formed in the monsoon trough. This very active monsoon trough moved northward, and became reverse oriented. By the final week of September, it had migrated to a relatively high latitude as TCs Tom (25W) and Violet (26W) carried the trough with them out of the tropics. As this monsoon trough exited the tropics, a new monsoon trough formed at low latitudes, and was the site of development for the next two TCs in the WNP — Yates (28W) and Zane.

While the WNP was still dominated by the reverse-oriented monsoon trough which contained Tom (25W), Violet (26W) and Willie (27W), the low latitudes of the WNP were dominated by high pressure and low-level easterly flow. As Tom (25W) and Violet (26W) recurved, a new monsoon trough formed in Micronesia. Deep convection associated with this monsoon trough consolidated within two areas. The eastern area became Yates (28W) and the western area became Zane. The large area of deep convection which became Zane was larger than the one which became Yates (28W) and is a good example of a monsoon depression (Figure 3-29-1). It was first mentioned on the 201900Z Significant Tropical Weather Advisory. This monsoon depression moved westward and, typical of monsoon depressions, it was several days before deep convection persisted near the low-level circulation center. When the deep convection persisted near the LLCC, a TCFA was issued at 230600Z. A second TCFA was issued at 232030Z in order to reposition the alert box. Based on satellite intensity estimates of 25 kt (13 m/sec), the first warning on Tropical Depression (TD) 29W was issued, valid at 240000Z September. Remarks on this warning included:

"... Tropical Depression 29W is located in the monsoon trough equatorward of the subtropical ridge. TD 29W is located approximately 800 nm west of Typhoon Yates (28W). Satellite imagery indicates the presence of weak ridging to the southeast of 29W. The rapid north-northwestward movement of TD 29W is associated with the enhanced southerly steering component associated with the weak ridging between TD 29W and Typhoon Yates (28W). . . ."

The rationale for the motion of TD 29W in this remark is a good description of what is known as "indirect TC interaction" in the "Systematic and Integrated Approach". Yates' (28W) summary contains a more complete description of the interaction between Zane and Yates.

During the night of 24 September, deep convection rapidly consolidated over the LLCC of TD 29W and, on the warning valid at 241200Z, TD 29W was upgraded to Tropical Storm Zane. Soon after the formation of Zane's CDO, the peripheral cloudiness in the monsoon depression was suppressed and the areal extent and amount of deep convection became smaller. Moving northwestward, Zane intensified and became a typhoon at 251200Z. The peak intensity of 110 kt (57 m/sec) was reached at 280000Z, which was maintained until 291200Z. During this time, the typhoon moved on a slow northward track and passed approximately 90 nm (170 km) to the west of Okinawa. On 29 September, Zane slowed and made a sharp turn to the east, passing approximately

20 nm (40 km) to the north of the northern end of Okinawa (Figure 3-29-2) and, despite being embedded in westerly flow north of the subtropical ridge maintained typhoon intensity. On 02 October, Zane (still a typhoon) possessed a very unusual cirrus outflow pattern: cirrus debris streamed eastward on both the north and south sides of the system, evoking the analogy of debris being stripped from a comet by the solar wind (Figure 3-29-3a) (see the discussion). On 03 October, westerly shear finally began to have an effect, and the LLCC of Zane became partially exposed on the west side of the deep convection. At 031200Z, the final warning was issued, as Zane began its extratropical transition. After the final warning, the system moved east and then south as it encountered the vigorous outer circulation of the large intense extratropical low which was once Yates (28W) (see Figure 3-28-2 in Yates' (28W) summary).

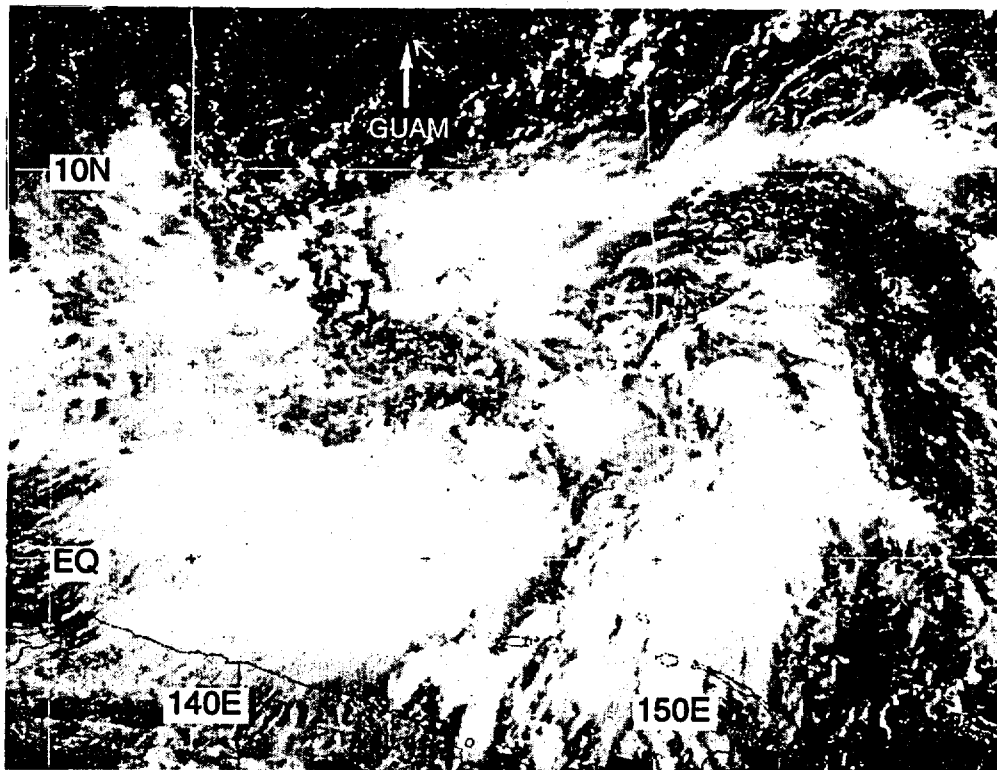


Figure 3-29-1 Zane originated from this monsoon depression located to the south of Guam (212224Z September visible GMS imagery).

III. DISCUSSION

a. *Origin as a monsoon depression south of Guam*

Zane began as a monsoon depression near Guam. Initially it was a large ensemble of mesoscale convective systems embedded within a region of lowered sea-level pressure. It lacked persistent central deep convection, and the maximum winds in the system were displaced outward from the low-level circulation center. Eventually as the system moved toward the northwest, the circulation intensified, and persistent central deep convection became established marking its transition to a conventional TC. Cam's (05W) summary contains a detailed discussion of the structure and evolution of monsoon depressions in the WNP.

b. Passage within range of Guam's and Kadena's NEXRADs

When forming near Guam, some of the rainbands (that were part of the monsoon depression which became Zane) came within the range of Guam's NEXRAD. One of the most interesting features of these rainbands was the presence of mesoscale vortices associated with convective cells in these rainbands. These mesovortices were detected by the meso-alert algorithm of the NEXRAD. Mesoscale vortices are often associated with tornadic activity over land, however, tornadic activity (e.g., tornadic waterspouts) have yet to be associated with NEXRAD-observed mesoscale vortices near Guam. They frequently are seen when tornadic activity is occurring in TC rainbands over land in the US mainland.

When Zane passed close to Okinawa, it came within range of the NEXRAD's velocity detection capability. Nothing unusual was noted as the well-defined radar eye of Zane passed. The base velocity product showed maximum inbound and outbound velocities on the order of 115 kt (59 m/sec) at altitudes of approximately 5,000 ft.

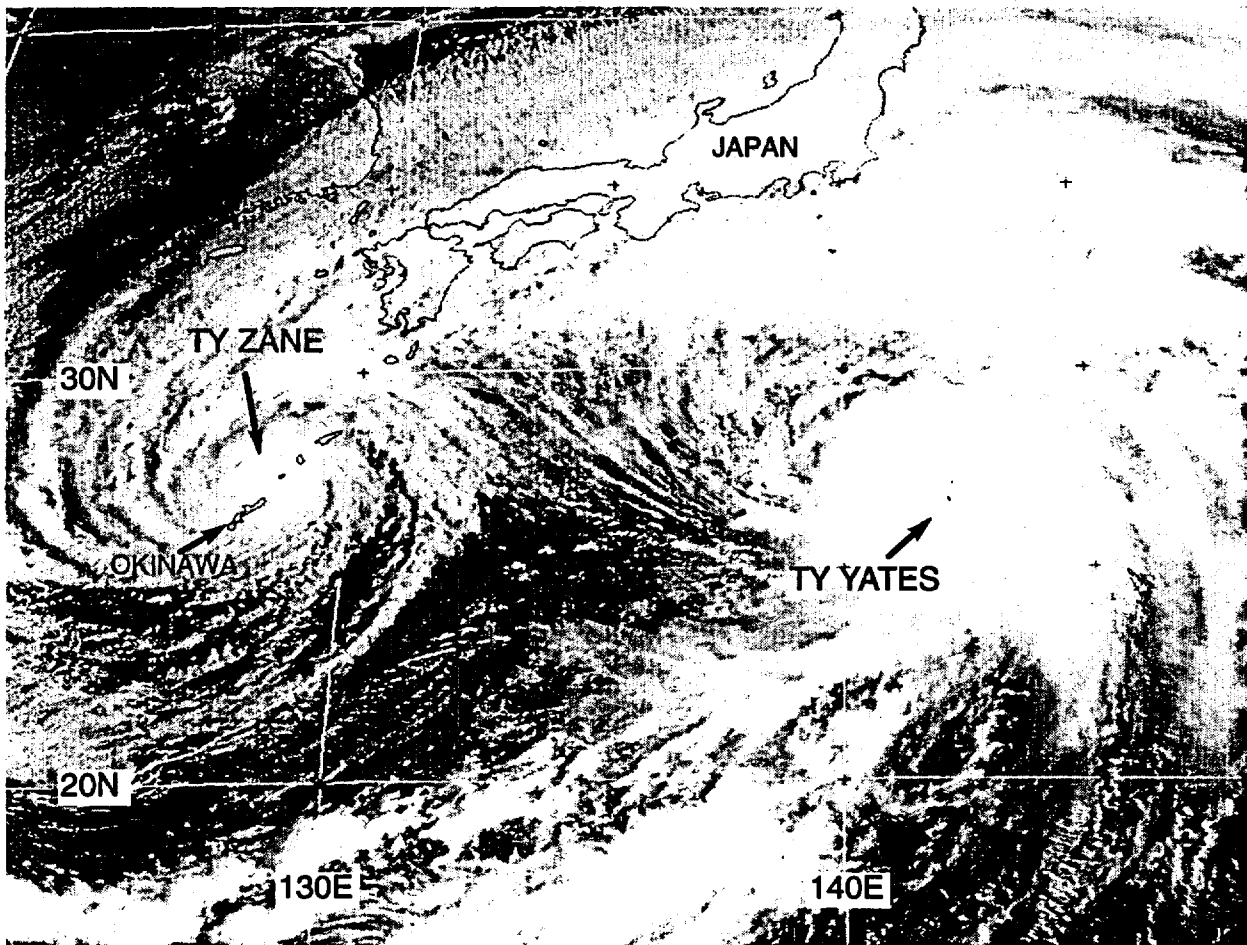


Figure 3-29-2 The rainbands of Zane sweep across Okinawa while at its closest point of approach to that island. Typhoon Yates (28W) is seen approximately 900 nm (1700 km) to the east of Zane (292224Z September visible GMS imagery).

c. Unusual persistence as a tropical cyclone while embedded in midlatitude westerlies

On 02 October, Zane (still a typhoon) possessed a very unusual cirrus outflow pattern: cirrus debris streamed eastward on both the north and south sides of the system, evoking the analogy of debris being stripped from a comet by the solar wind (Figure 3-29-3a). Water-vapor derived winds clearly show the upper-level winds to the north and south of Zane were from the west (Figure 3-29-3b). Zane was moving approximately 20 kt (37 km/hr) to the east-northeast at this time, while the azimuthally averaged 200-mb wind (at a radius of 300 nm) around the TC was from the west at approximately 50 kt. One might expect that a TC in such an environment would shear apart. This did not happen to Zane. The maintenance of Zane's CDO under apparent shearing conditions, and the near symmetry of the cirrus outflow within strong westerly winds aloft are unusual phenomena that raise questions about the relationship between the structure of a TC and the vertical shear of the horizontal wind.

IV. IMPACT

No reports of serious damage or injuries in Okinawa were received at the JTWC. About US \$50 thousand in damage was reported by US military installations on Okinawa —mostly downed trees and power lines. Another US \$118 thousand in damage was reported on the island, mostly to crops. Highest wind gusts reported on Okinawa were 79 kt (41 m/sec) at Kadena AB and 64 kt (33 m/sec) at Naha. Up to 12 inches (307 mm) of rain soaked the island. In Taiwan, heavy rains from Zane triggered mudslides that killed two people.

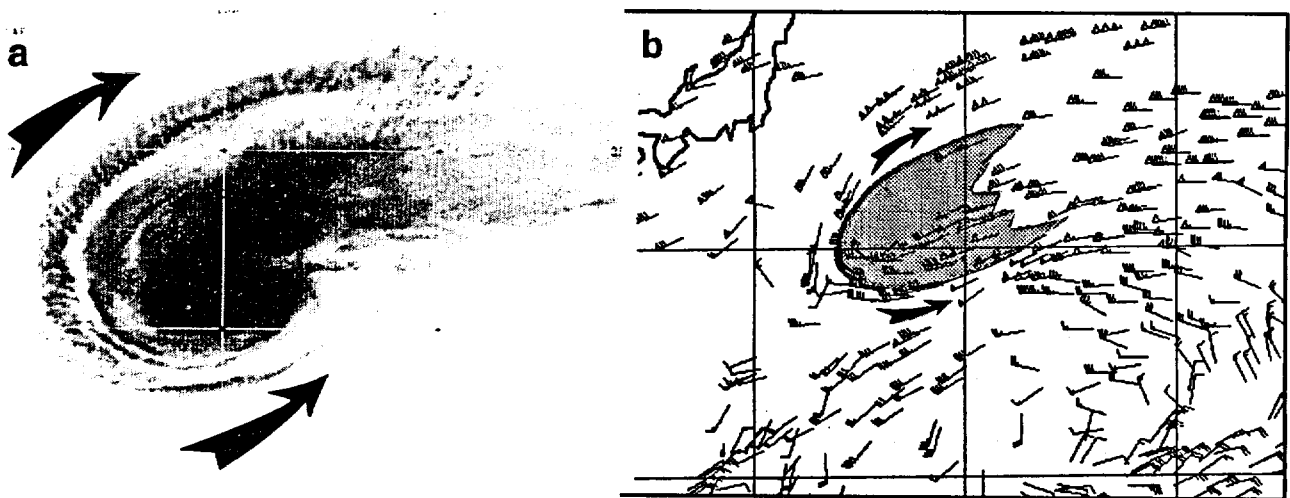
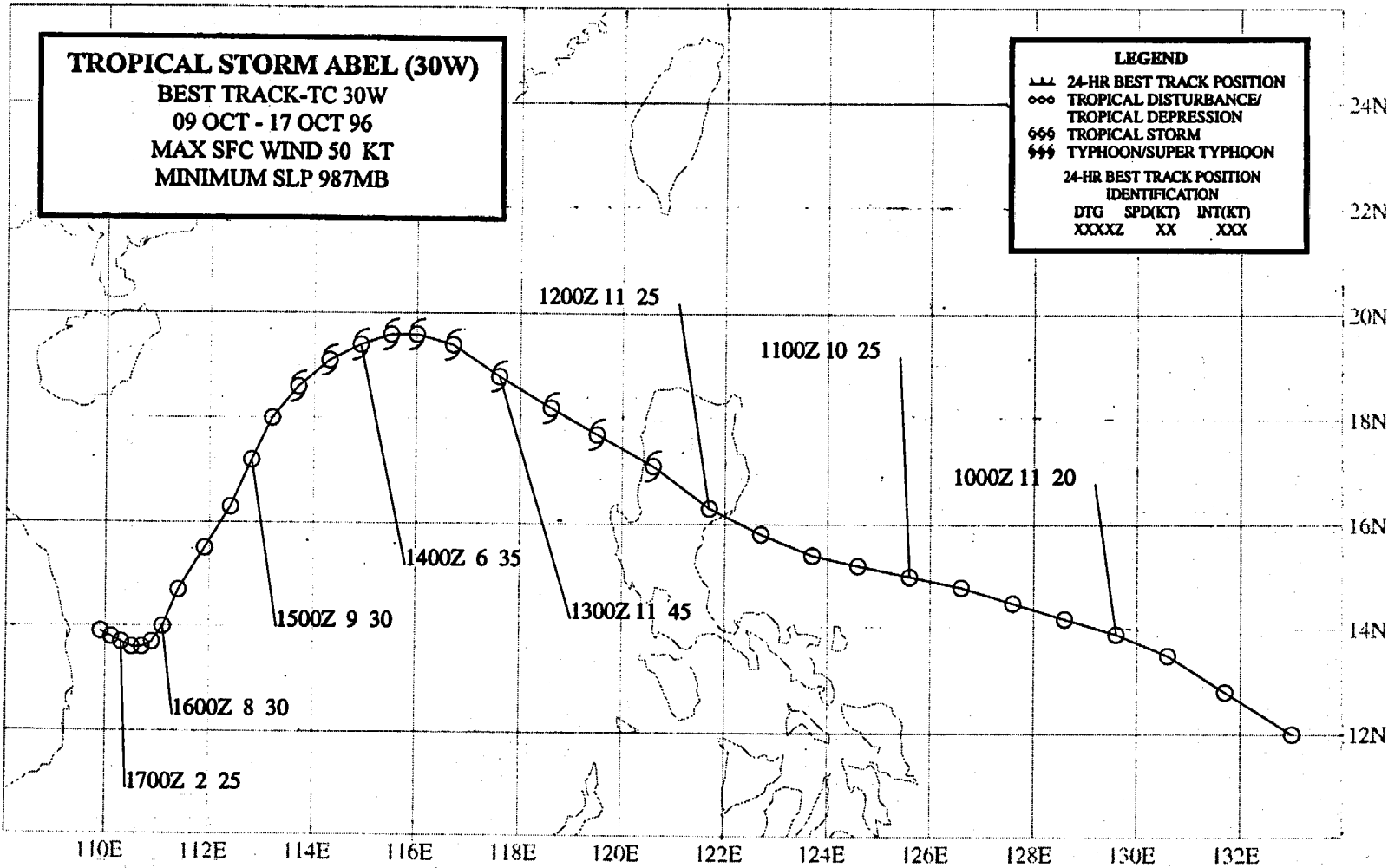


Figure 3-29-3 (a) Cirrus outflow is carried off to the east by strong upper-level westerly winds on both the north and south sides of Zane (021624Z October infrared GMS imagery, inverted-IR enhancement). (b) Water-vapor derived upper-tropospheric winds show Zane (the shaded region) was completely embedded in a westerly airstream. The divergence from the typhoon's convection caused the winds to split and go around the TC (021200Z October water-vapor derived upper-tropospheric winds).



TROPICAL STORM ABEL (30W)

I. HIGHLIGHTS

Abel originated from a monsoon depression in the Philippine Sea, crossed Luzon, and became a tropical storm in the South China Sea. Forced to move southwestward by the northeast monsoon, it dissipated over water while approaching the coast of southern Vietnam.

II. TRACK AND INTENSITY

At the beginning of October, Yates (28W) and Zane (29W) recurved and moved into the midlatitudes. After this, for about one week, the low latitudes of the WNP became relatively free of deep convection, and there was a break in TC activity. By the end of the first week of October, amounts of deep convection began to increase in the low latitudes of the WNP, and became concentrated within two large areas: one near Guam and the other north of the Marshall Islands. The area of deep convection located near Guam moved westward and became a monsoon depression in the Philippine Sea. With the help of animated high-resolution visible satellite imagery, a LLCC was detected south of a band of persistent deep convection, embedded in the large cyclonic circulation of the monsoon depression. This LLCC was mentioned on the 100600Z October Significant Tropical Weather Advisory. Shortly thereafter, at 100730Z, the JTWC issued a TCFA when conditions appeared to favor the formation of a TC. Remarks on the TCFA included:

". . . Latest animated visual satellite imagery indicates a well defined low-level circulation has developed [east of the Philippines]. Newly developed convection is primarily to the north of the circulation center but is showing signs of improved organization. . . ."

The first warning on Tropical Depression (TD) 30W was issued valid at 110000Z. Remarks on the first warning included:

"A tropical depression has formed in the Philippine Sea approximately 80 nm east-northeast of Catanduanas Island in the Philippines. Animated visual satellite imagery . . . and data from several ships . . . indicates that a partially exposed 1003 mb low-level circulation exists within a larger monsoonal circulation that stretches almost 400 nm to the northeast of the [LLCC]. . . ."

On 12 October, the system crossed the island of Luzon and entered the South China Sea. Perhaps as a result of lee-side effects, northerly gale-force winds were reported over water as soon as the low-pressure center reached the northwestern tip of Luzon. In real time, satellite intensity estimates below 35 kt (18 m/sec) were favored over the gale-force ship reports, and TD 30W was upgraded to Tropical Storm Abel on the warning valid at 131200Z. In post analysis, however, the satellite imagery was reevaluated, the ship reports of gale force winds were given a higher weight, and TD 30W became a tropical storm at 120600Z. Abel reached its peak intensity of 50 kt (26 m/sec) at 121200Z.

On 14 October, Abel began to move toward the southwest under the influence of high pressure over southern China, which contributed to strong low-level northeasterly flow to Abel's west and north. While moving toward the southwest, Abel began to weaken. The deep convection accompanying the well defined LLCC on 16 October (Figure 3-30-1) decayed, and the final warning was issued, valid at 170600Z, as the system dissipated over water while approaching the coast of southern Vietnam.

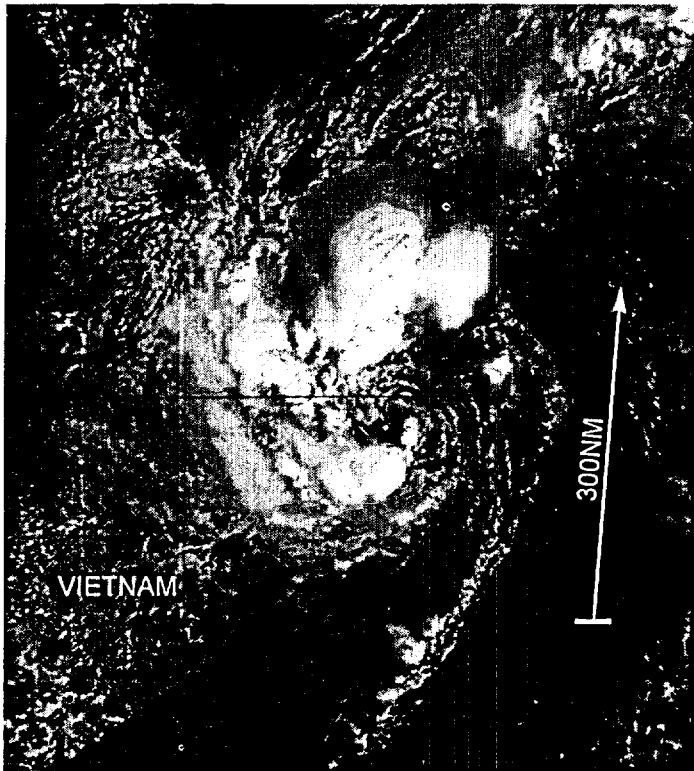


Figure 3-30-1 Abel moves slowly toward the coast of southern Vietnam, its well-defined LLCC is surrounded by cells of deep convection (160331Z October visible GMS

III. DISCUSSION

Unusual structure revealed by animated visible satellite imagery

When Abel was forming east of the Philippines, animation of visible satellite imagery indicated that the LLCC was displaced well to the south of the deep convection and also well to the south of the center of symmetry of the cirrus outflow (Figure 3-30-2). It is common for satellite fixes to be too far north in the monsoon depression stage of TC development, but in the case of Abel, the LLCC was unusually distant from the deep convection and the center of symmetry of the upper-level anticyclonic pattern of the cirrus. Synoptic data, and scatterometer data also supported this large displacement.

IV. IMPACT

As the weakening Abel approached Vietnam, rough seas overturned 146 boats and two fishermen were lost. At least 11 other people were reported missing.

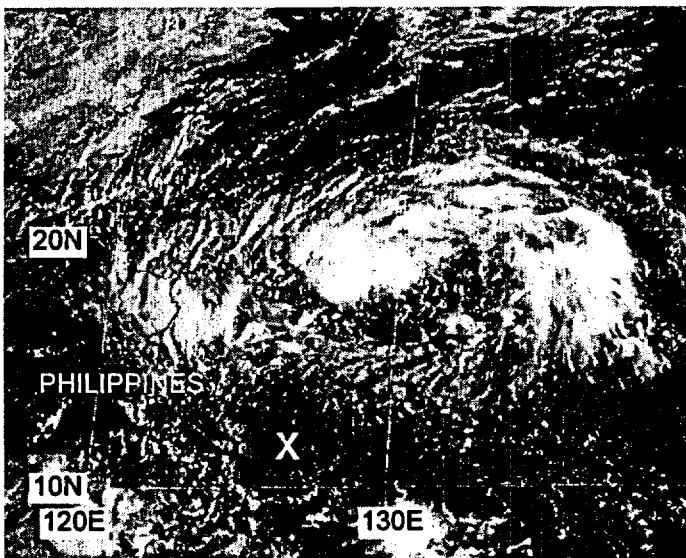


Figure 3-30-2 Animation showed that the LLCC (labeled, X) of the pre-Abel monsoon depression was displaced unusually far from its deep convection and from the center of symmetry of its upper-level cirrus outflow (102331Z October visible GMS imagery).

TROPICAL DEPRESSION 31W

BEST TRACK-TC 31W

10 OCT - 18 OCT 96

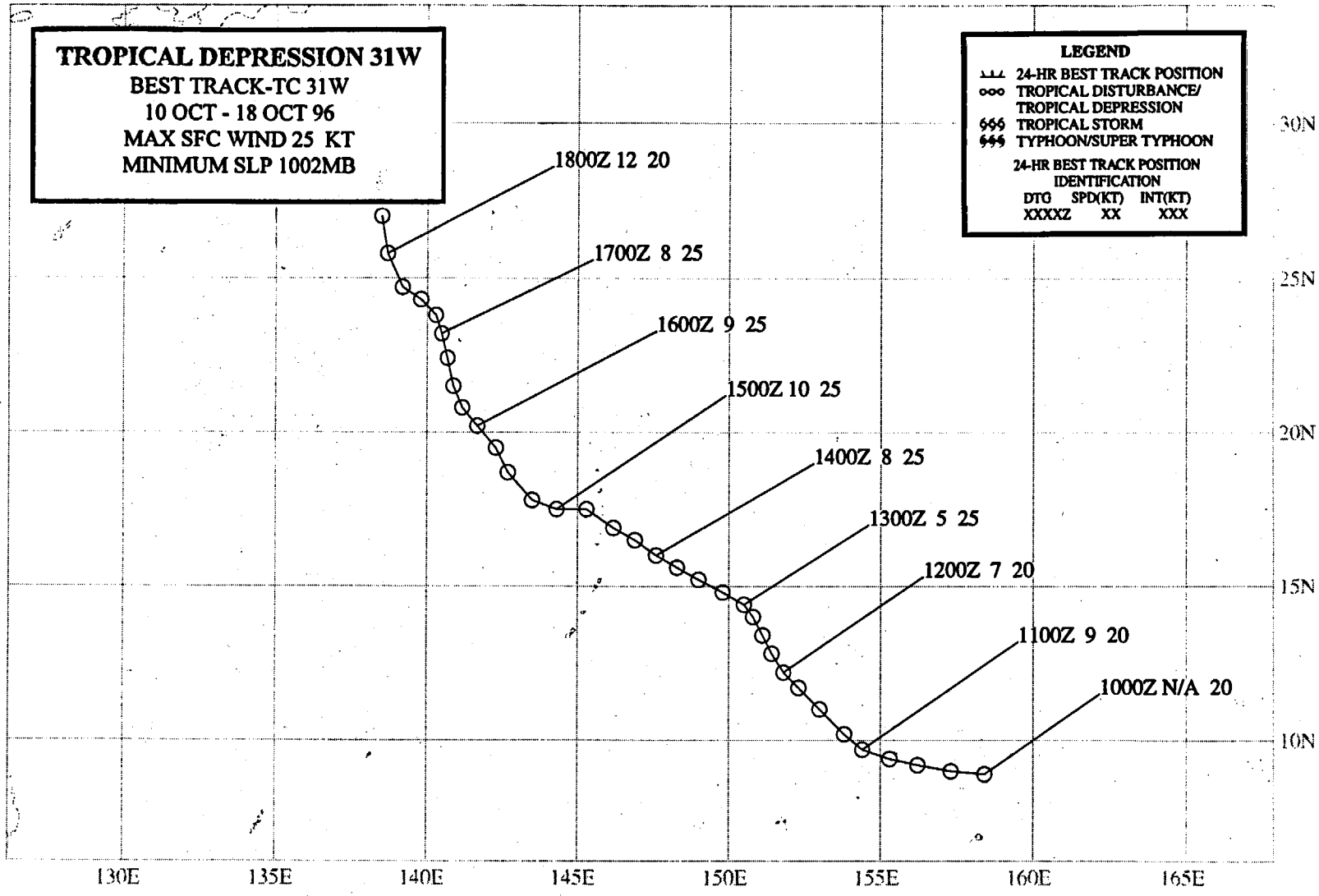
MAX SFC WIND 25 KT

MINIMUM SLP 1002MB

LEGEND

- 24-HR BEST TRACK POSITION
- ooo TROPICAL DISTURBANCE/
TROPICAL DEPRESSION
- 666 TROPICAL STORM
- 666 TYPHOON/SUPER TYPHOON

24-HR BEST TRACK POSITION
IDENTIFICATION
DTG SPD(KT) INT(KT)
XXXXZ XX XXX



TROPICAL DEPRESSION 31W

For much of October, winds throughout most of Micronesia were light and variable in association with a weak monsoon trough. Deep convection (loosely organized into discrete ensembles of MCSs) was located in an east-west zone across the low latitudes of the WNP. Several of the tropical disturbances in this maximum cloud zone became significant TCs. The first TC of October, Abel (30W), originated from a monsoon depression in this cloud band. The next two TCs following Abel — Tropical Depression (TD) 31W and Typhoon Beth (32W) — developed simultaneously during the middle of the month (Figure 3-31-1). The tropical disturbance which became TD 31W originated southeast of Guam, and was located approximately 600 nm (1100 km) southeast of the tropical disturbance which became Beth (32W). This tropical disturbance was first mentioned on the 100600Z October Significant Tropical Weather Advisory. On 13 October, the pre-TD 31W disturbance acquired a clearly defined LLCC on satellite imagery, prompting the JTWC to issue a Tropical Cyclone Formation Alert at 130330Z October. The first warning on TD 31W, valid at 130600Z, soon followed when satellite intensity estimates indicated 25 kt (13 m/sec).

Moving toward the northwest, TD 31W exhibited a shear-type cloud pattern (Figure 3-31-2) for all of its life. Satellite intensity estimates and the best-track intensities remained at 25 kt (13 m/sec) for several days. During the night of 17 October, the deep convection associated with TD 31W decreased in amount and became sheared well to the east of the LLCC. The final warning on TD 31W was issued, valid at 171200Z, as the system dissipated over water.

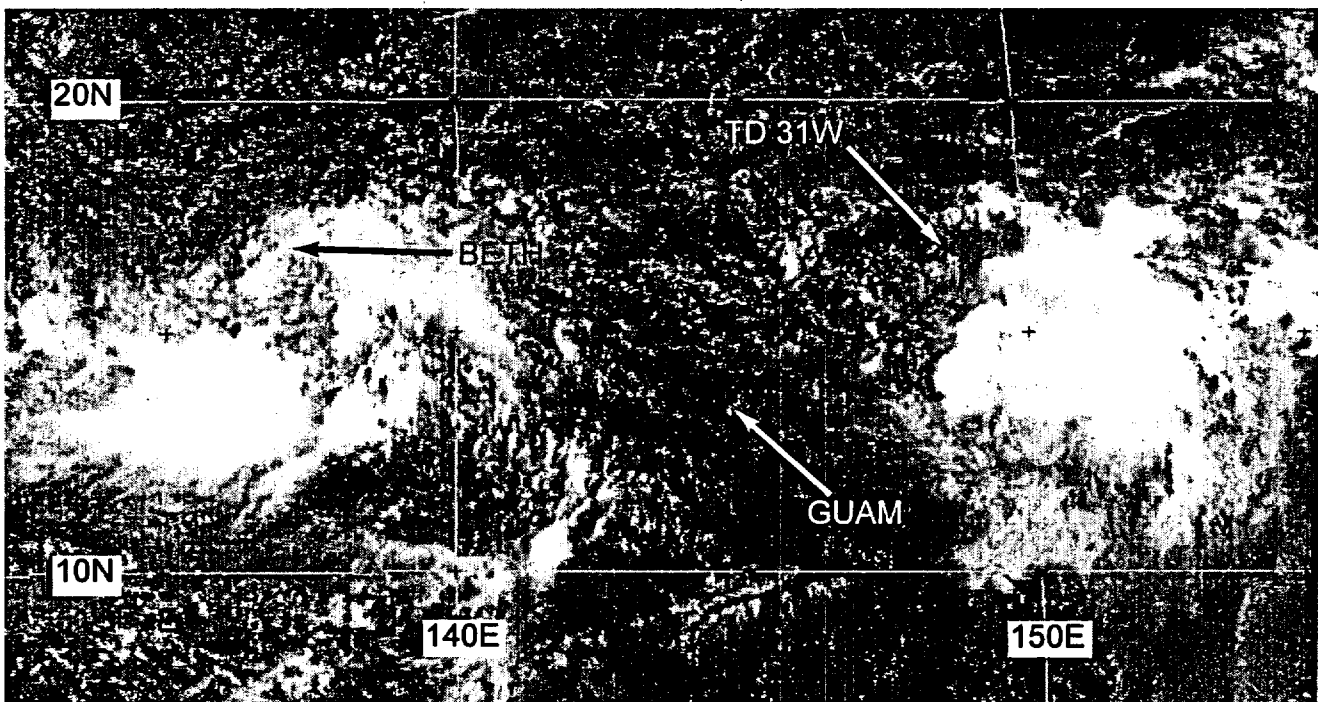


Figure 3-31-1 Typhoon Beth (32W) and TD 31W developed simultaneously. Beth became a typhoon, but TD 31W failed to become a mature TC (122331Z October visible GMS imagery).

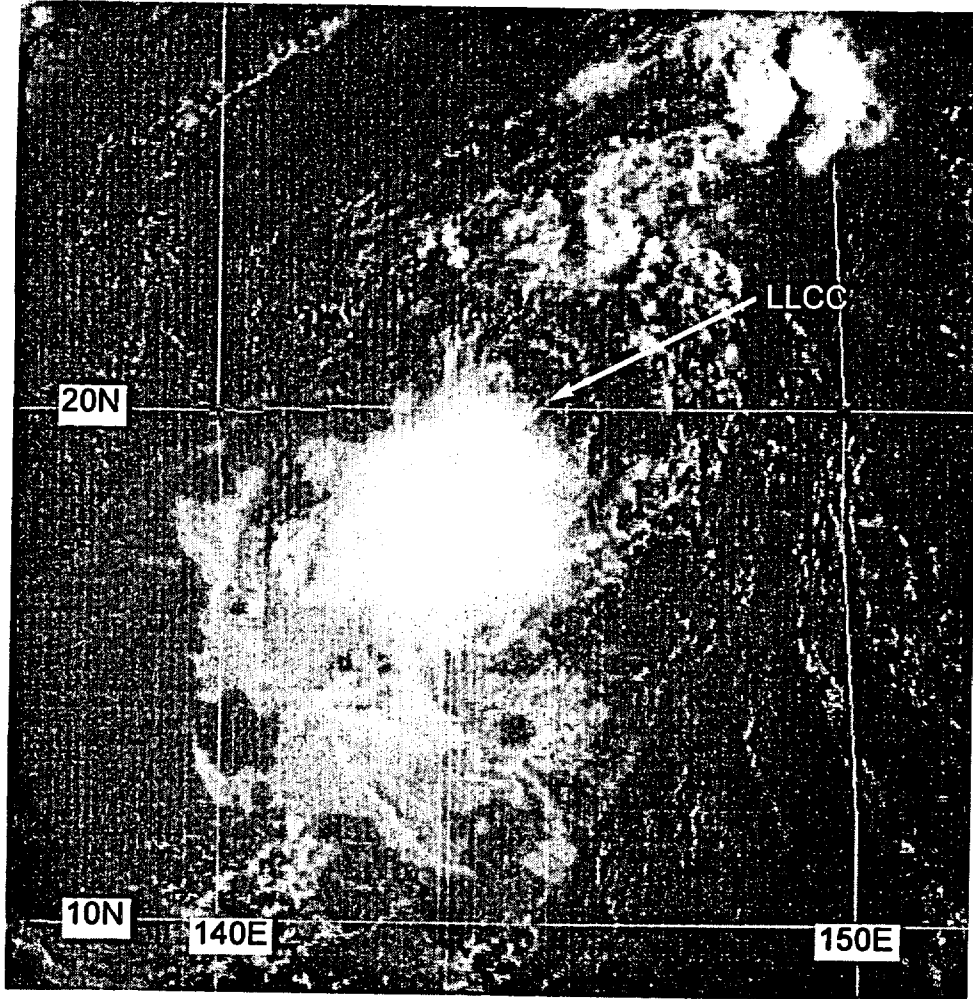


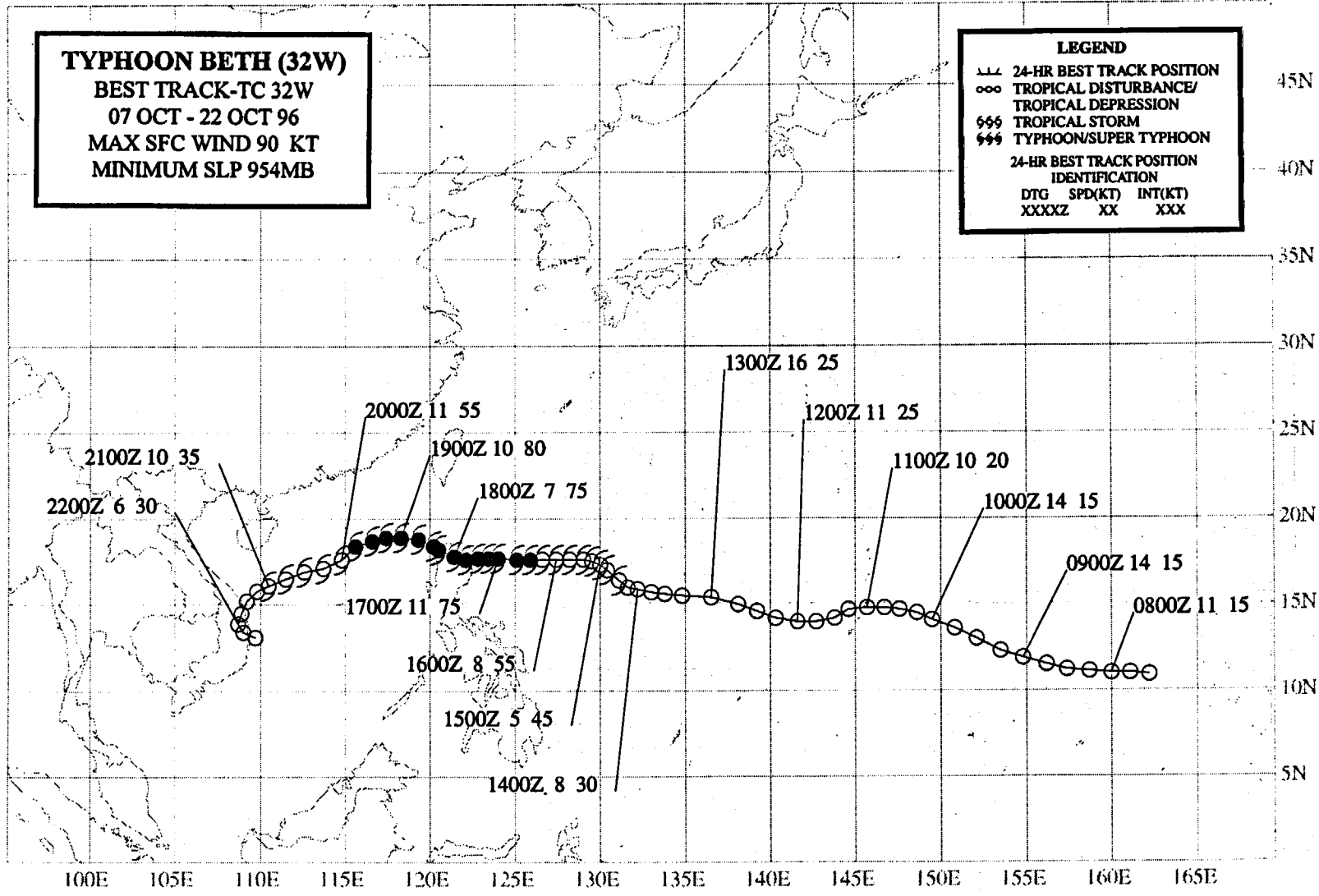
Figure 3-31-2 For all its life, TD 31W exhibited a shear-type cloud pattern. The LLCC is located to the north of the deep convection in this image (152224Z October visible GMS imagery).

TYPHOON BETH (32W)
BEST TRACK-TC 32W
07 OCT - 22 OCT 96
MAX SFC WIND 90 KT
MINIMUM SLP 954MB

LEGEND

- 24-HR BEST TRACK POSITION
- ooo TROPICAL DISTURBANCE/
TROPICAL DEPRESSION
- 666 TROPICAL STORM
- 999 TYPHOON/SUPER TYPHOON

24-HR BEST TRACK POSITION
IDENTIFICATION
DTG SPD(KT) INT(KT)
XXXXZ XX XXX



TYPHOON BETH (32W)

I. HIGHLIGHTS

The tropical disturbance which became Beth was first detected in the eastern Caroline Islands. It developed very slowly, and four Tropical Cyclone Formation Alerts were issued on the system prior to the first warning. Passing over Guam, it produced a thunderstorm with a spectacular display of cloud-to-ground lightning (unusual in the maritime tropics). Beth became a typhoon in the Philippine Sea and passed over Luzon where loss of life was reported. Encountering the north-east monsoon in the South China Sea, it turned to the southwest, weakened, and made landfall in central Vietnam.

II. TRACK AND INTENSITY

For much of October, winds throughout most of Micronesia were light and variable in association with a weak monsoon trough. Deep convection (loosely organized into discrete ensembles of MCSs) was located in an east-west zone across the low latitudes of the WNP. Several of the tropical disturbances in this maximum cloud zone became significant TCs. The first TC of October, Abel (30W), originated from a monsoon depression in this cloud band. The next two TCs — Tropical Depression (TD) 31W and Beth (32W) — developed simultaneously during the middle of

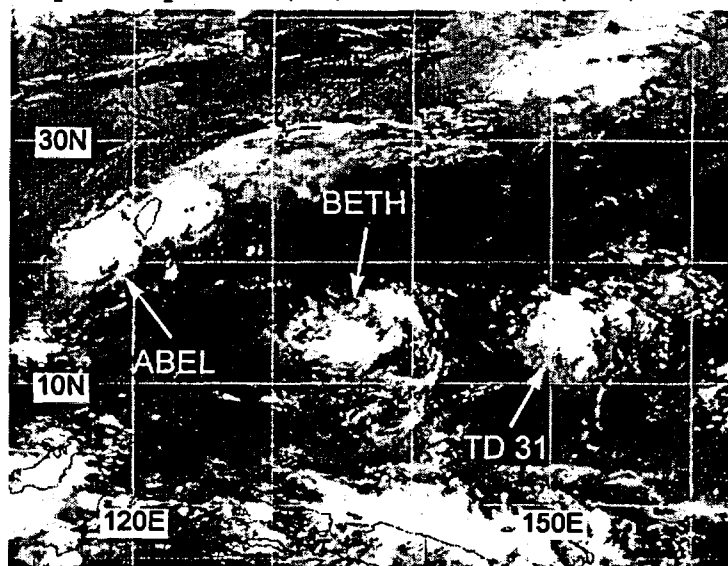


Figure 3-32-1 The tropical disturbances which became Beth and TD 31W developed simultaneously while Abel (30W) moved across the South China Sea (122331Z October infrared GMS imagery).

the month (Figure 3-32-1). The tropical disturbance which became Beth originated in the eastern Caroline Islands. It was first mentioned on the 071800Z Significant Tropical Weather Advisory. The system moved westward, and in the late afternoon of 11 October, synoptic data from Guam and Saipan, visible satellite imagery, and NEXRAD products indicated that a weak LLCC was associated with an area of increasing deep convection near Guam and Saipan. This prompted the JTWC to issue the first TCFA at 110730Z. At 111200Z, a second TCFA was issued in order to reposition the alert box to account for indications on NEXRAD data that a second LLCC had formed to the east of Guam. At 120130Z October, a third TCFA was issued to move the alert box further to the

west to incorporate indications on visible satellite imagery that the primary LLCC had moved to a position 260 nm (480 km) west of Guam. The pre-Beth tropical disturbance moved west and did not intensify, although conditions still appeared favorable for further development, and a fourth TCFA was issued at 130000Z. During the night of 13 October, the deep convection in the pre-Beth tropical disturbance consolidated near the LLCC and became organized into a well-defined curved band. The first warning, valid at 131200Z, was issued on Tropical Depression (TD) 32W. The cloud pattern of TD 32W evolved into a sheared pattern type with the LLCC exposed on the eastern side (Figure 3-32-2). When satellite imagery indicated an intensity of 35 kt (18 m/sec), TD 32W was

upgraded to Tropical Storm Beth on the warning valid at 150000Z. Beth became a typhoon at 161200Z and reached its peak intensity of 90 kt (46 m/sec) at 171200Z just prior to landfall on the

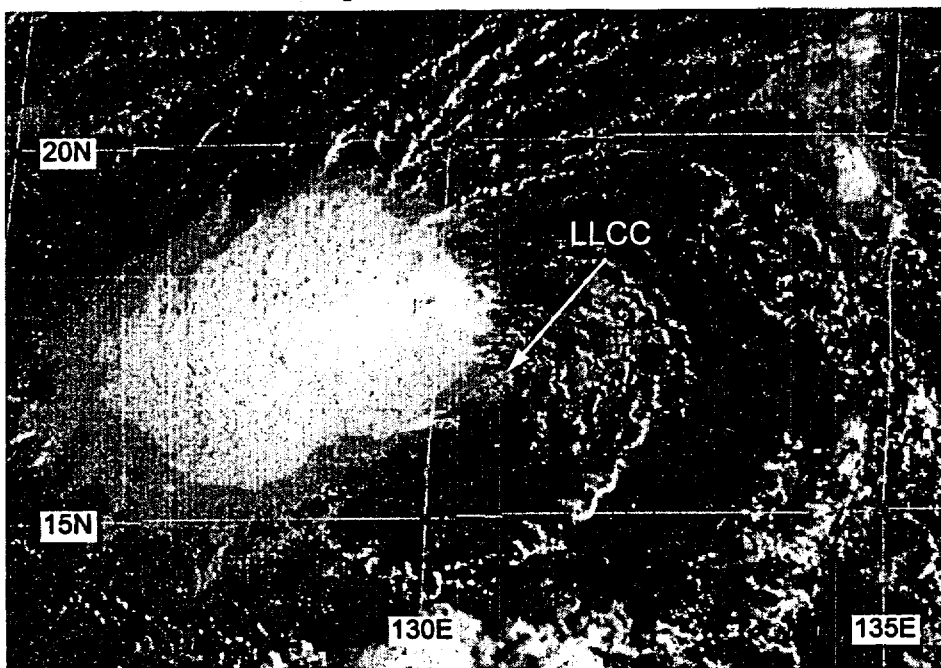


Figure 3-32-2 Beth's LLCC is partially exposed to the east of the deep convection, indicating the presence of easterly vertical wind shear (142224Z October visible GMS imagery).

east coast of northern Luzon (Figure 3-32-3). While crossing northern Luzon, Beth weakened only slightly to 75 kt (39 m/sec), and then reintensified to 80 kt (41 m/sec) at 181200Z when it entered the South China Sea. The period of reintensification was short-lived and by the morning of 20 October, the deep convection became sheared to the east of Beth's LLCC as the system weakened steadily over water. As Beth began to weaken, it began to move toward the west-southwest in response to high pressure over southern

China and a strengthening of low-level northeasterly flow to its west and north. The final warning was issued, valid at 211800Z, as the poorly defined LLCC reached the coast of central Vietnam and dissipated.

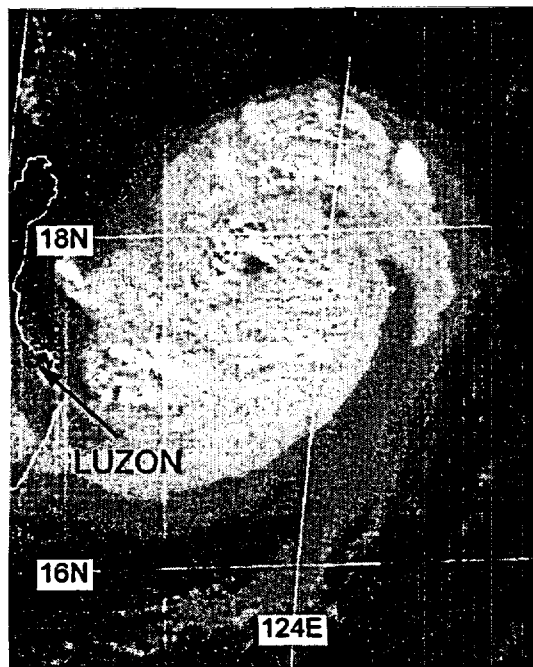


Figure 3-32-3 Beth acquires a small visible eye shortly before reaching peak intensity (170424Z October visible GMS imagery).

III. DISCUSSION

a. *Lightning in the maritime tropics*

On the night of 11 October, a thunderstorm associated with the pre-Beth tropical disturbance produced a spectacular display of cloud-to-ground (CG) lightning on Guam. Frequent CG lightning is rare on Guam, even in large cumulonimbus clouds with tops exceeding 50,000 ft. Indeed, lightning frequencies are low in general over the maritime regions when compared with lightning frequencies within thunderstorms over large land areas (Orville and Henderson 1986). The cause of reduced lightning frequencies in maritime cumulonimbus clouds has been narrowed to two primary mechanisms:

1) reduced vertical velocities in maritime thunderstorms; and,

2) differences between the continental versus maritime aerosols which comprise the cloud condensation nuclei.

A more detailed discussion of the mechanisms of cloud electrification are beyond the scope of this summary.

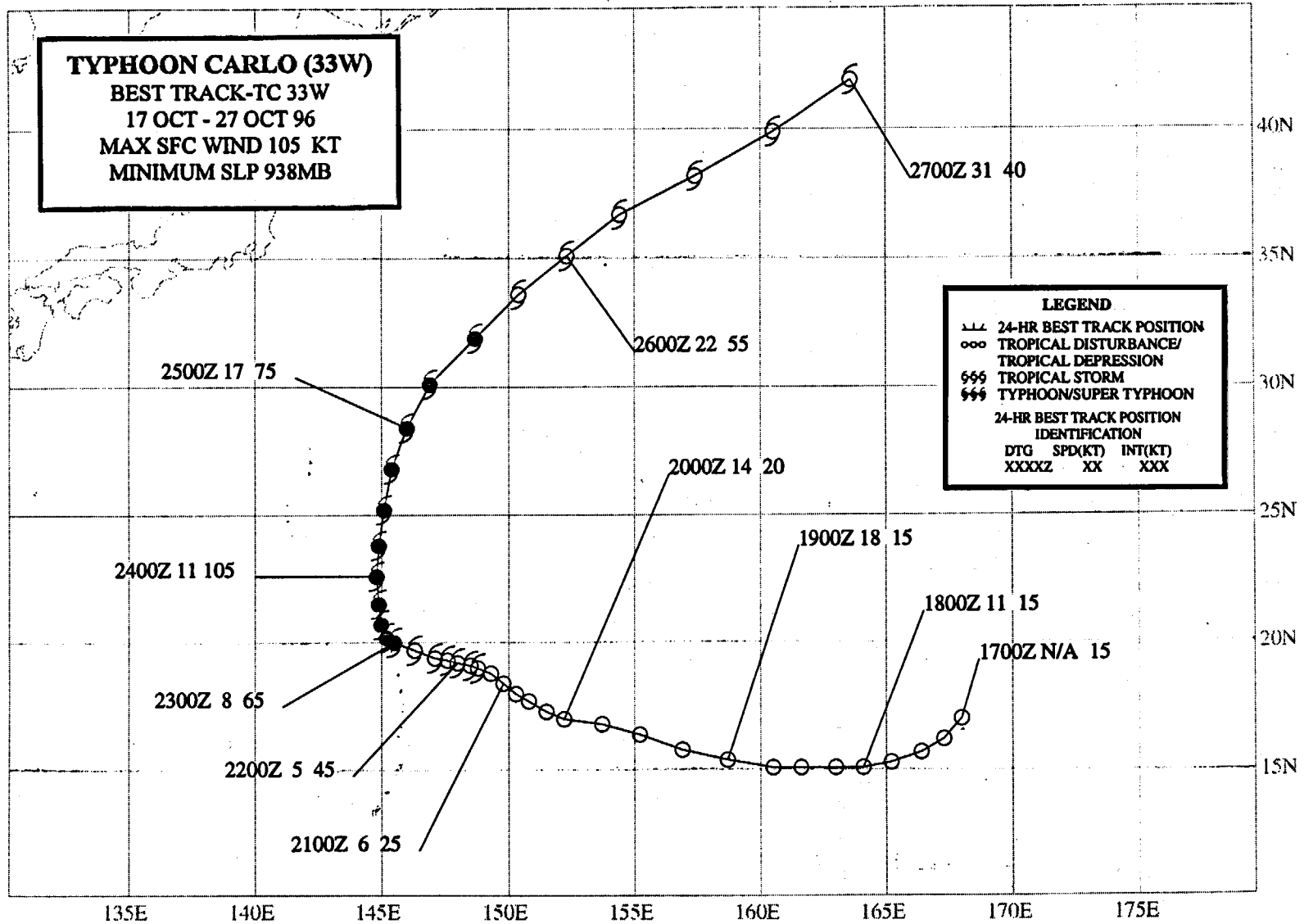
In the case of the relatively frequent CG lightning discharges in the 11 October Guam thunderstorm, only one other unusual factor was noted: reflectivity values as high as 60 dBZ on the NEXRAD composite reflectivity product persisted in the core of the thunderstorm as it moved southwestward across Guam.

b. Intensification of a sheared TC

One of the factors known to influence genesis and development of a TC is vertical shear of the horizontal wind: too much shear, and the TC is torn apart. Zehr (1992) found that an 850-200 mb wind shear of 15 kt (8 m/sec) or greater was unfavorable for TC genesis and development. On the morning of 15 October, Beth possessed a shear-type cloud pattern (Figure 3-32-2), and the LLCC was partially exposed on the east side of the deep convection. Shear is often detrimental to the further development of a TC. In Beth's case, however, the system intensified despite the shear and by 17 October, Beth was a typhoon with a visible eye and a symmetrical pattern of cirrus outflow (Figure 3-32-3). It is a difficult forecast problem to determine whether vertical shear is going to inhibit development, or whether the TC will continue to develop despite a shearing environment. Fundamental questions remain in the case of intensification in a sheared environment: does the TC outflow manage to overcome the shear? Does the shear decrease? Do changes occur in its vertical profile?

IV. IMPACT

At least three people were reported dead after Beth moved across the northern Philippines. The TC tore away roofs, smashed windows, and triggered floods. In the hardest-hit province of Cagayan, Beth damaged municipal buildings and crops, and eroded roads.



TYPHOON CARLO (33W)

I. HIGHLIGHTS

Carlo's TUTT-cell-induced formation is one of the best examples of this process witnessed during 1996. Water-vapor imagery provided detailed information on the evolution of upper-level winds, clouds, and moisture for this event. Carlo reached its peak intensity after its apparent "point of recurvature" — unusual behavior of TCs which recurve. Accelerating to a speed of 30 kt (55 km/hr), Carlo was absorbed into the frontal cloud band of an intense extratropical low.

II. TRACK AND INTENSITY

On 17 October, three TCs were active in the western part of the WNP: Abel (30W) (in the South China Sea), TD 31W (halfway between Guam and Japan), and Beth (32W) (near the coast of Luzon). Elsewhere in the tropics of the WNP, amounts of deep convection were below normal and the low-level winds were predominantly from the east. The only area of deep convection considered to have potential for TC formation was associated with a TUTT cell, and was centered near 17°N 168°E. It was first mentioned on the 170600Z October Significant Tropical Weather Advisory. Moving westward on the northern side of the TUTT cell (Figure 3-33-1), this tropical disturbance (which became Carlo) gradually became more organized. At 200230Z October, the JTWC issued a TCFA when persistent deep convection (located in a region of divergent upper-level flow) consolidated near the LLCC. Based on satellite intensity estimates of 25 kt (13 m/sec), the first warning on Tropical Depression (TD) 33W was issued valid at 210000Z.

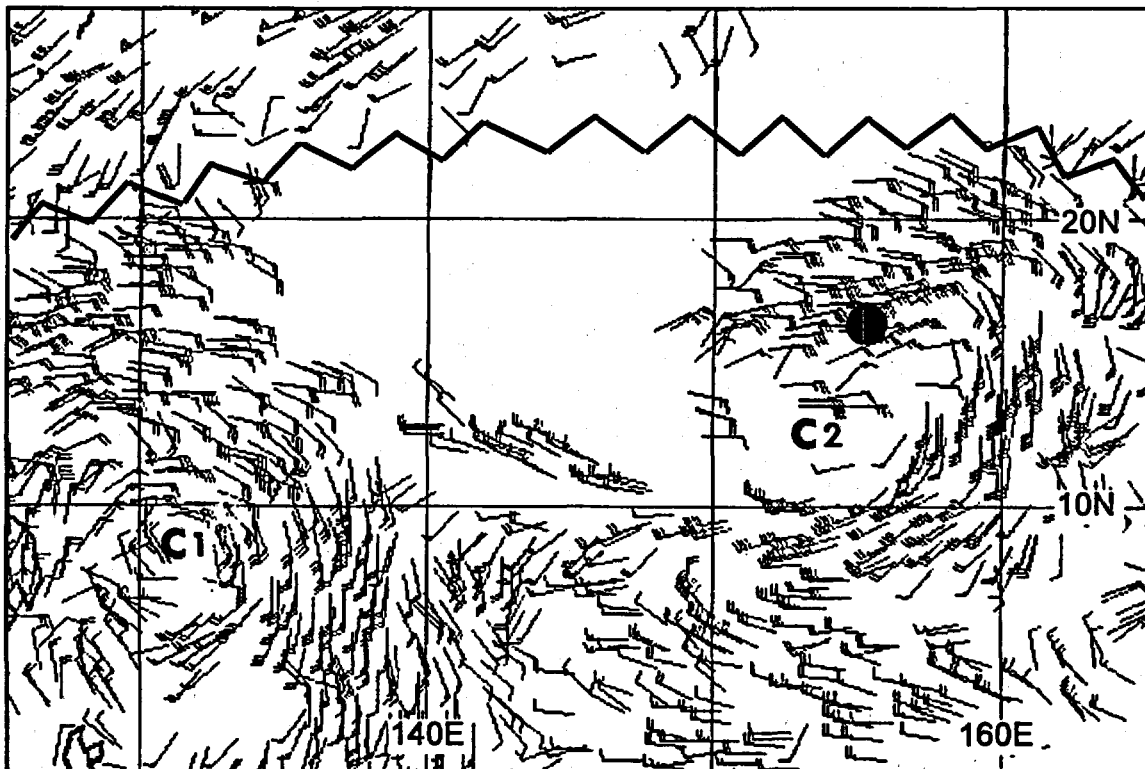


Figure 3-33-1 The location of the LLCC of the pre-Carlo tropical disturbance (shown by the black dot) is under the easterly upper-level flow to the north of a TUTT cell (labeled, C2). Another TUTT cell (labeled, C1) is located further to the west. The zig-zag line indicates the upper-level subtropical ridge axis (191025Z October GMS water-vapor winds).

Developing a CDO, TD 33W was upgraded to Tropical Storm Carlo on the warning valid at 211200Z. Carlo became a typhoon at 230000Z as a small ragged eye formed within its CDO (Figure 3-33-2). After becoming a typhoon, Carlo turned northward and further intensified, reaching a peak intensity of 105 kt (54 m/sec) at 240000Z. Late on 24 October, Carlo began a gradual turn toward the northeast accompanied by an increase in its speed of translation. Westerly shear began to affect Carlo and by 250000Z the typhoon weakened to 80 kt (41 m/sec); at 251800Z the intensity dropped to 60 kt (31 m/sec). The system continued to weaken as it accelerated to the northeast. The final warning was issued, valid at 261800Z, as the system moved northeastward at

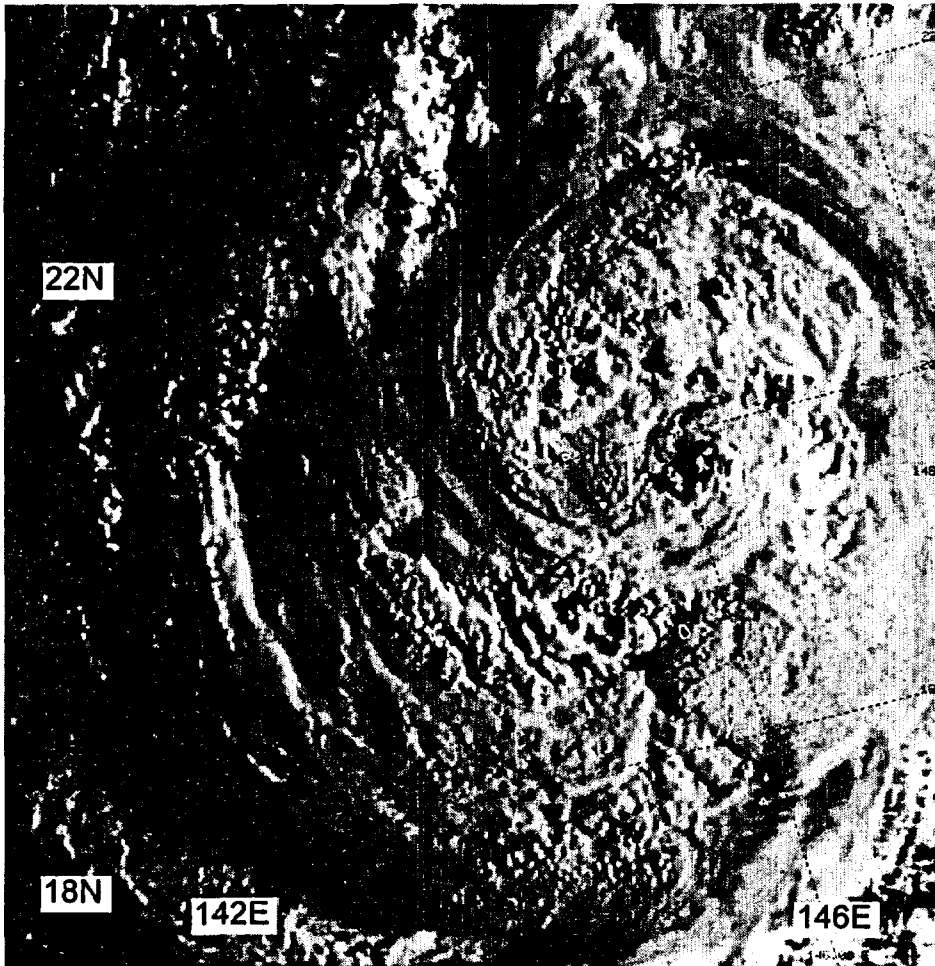


Figure 3-33-2 An overshooting cloud top casts a shadow over Carlo's incipient eye (222101Z October visible DMSP imagery).

29 kt (54 km/hr), lost its deep convection, and began to merge with a frontal cloud band.

III. DISCUSSION

a. Tropical cyclogenesis induced by a TUTT cell

Water vapor imagery (Figure 3-33-3) showed that Carlo formed in an area of upper-level moisture (with embedded deep convection) on the north side of a TUTT cell. Typical of TCs which form in association with TUTT cells, Carlo formed north of 15°N latitude, was embedded in low-level easterly flow, and was isolated in a cloud-minimum region south of the subtropical ridge. See Joy (12W) for a more detailed discussion of TUTT-related TC genesis.

b. Peak intensity after making a sharp turn toward the north

Most typhoons that undergo classic recurvature (i.e., a roughly "<"-shaped track which features initial steady west-northwestward motion, then a northward turn while slowing, followed by an acceleration toward the northeast) reach peak intensity at, or before, the point of recurvature; where the point of recurvature is identified as that point where the typhoon reaches its westernmost longitude (JTWC, 1994). Many TCs do not undergo classic recurvature. Some never recur, while others move on a track type designated by the Japan Meteorological Agency (JMA) (1976) as north-

oriented. North-oriented TC tracks have been renamed poleward-oriented tracks in Carr and Elsberry (1996) to make the concept applicable to both the Northern and Southern Hemispheres. TCs that move on north-oriented tracks move generally on long, northward paths from their genesis location and may feature large meanders and abrupt turns to the left or right (Lander 1996). North-oriented tracks occur predominantly during July through October. Carr and Elsberry found that a TC may undergo north-oriented motion for only a portion of its track — even if some, or most, of the track was of some other type (e.g., straight moving). A characteristic behavior of some TCs undergoing north-oriented motion is reaching peak intensity after acquiring a persistent eastward component of motion, but before the TC begins to significantly increase its speed of translation within the "accelerating westerlies" regime north of the subtropical ridge. Synoptic regimes associated with specific TC behavior, such as "poleward oriented" and "accelerating westerlies", are described in Carr and Elsberry (1996), and briefly at the beginning of this chapter.

Carlo reached peak intensity while moving north-northeastward on the north-oriented leg of its track. It weakened as it entered the "accelerating-westerly" regime north of the subtropical ridge.

IV. IMPACT

No reports of damage or injuries were received at JTWC.

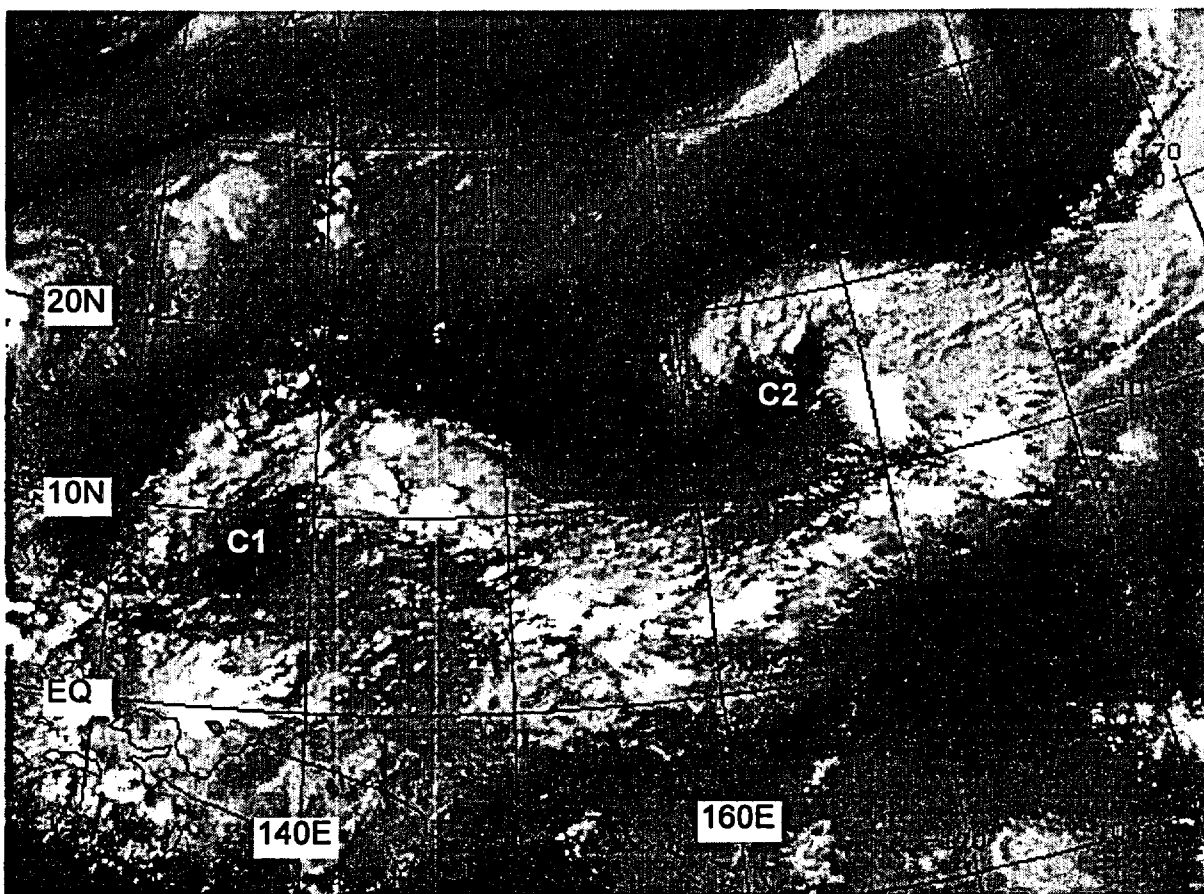


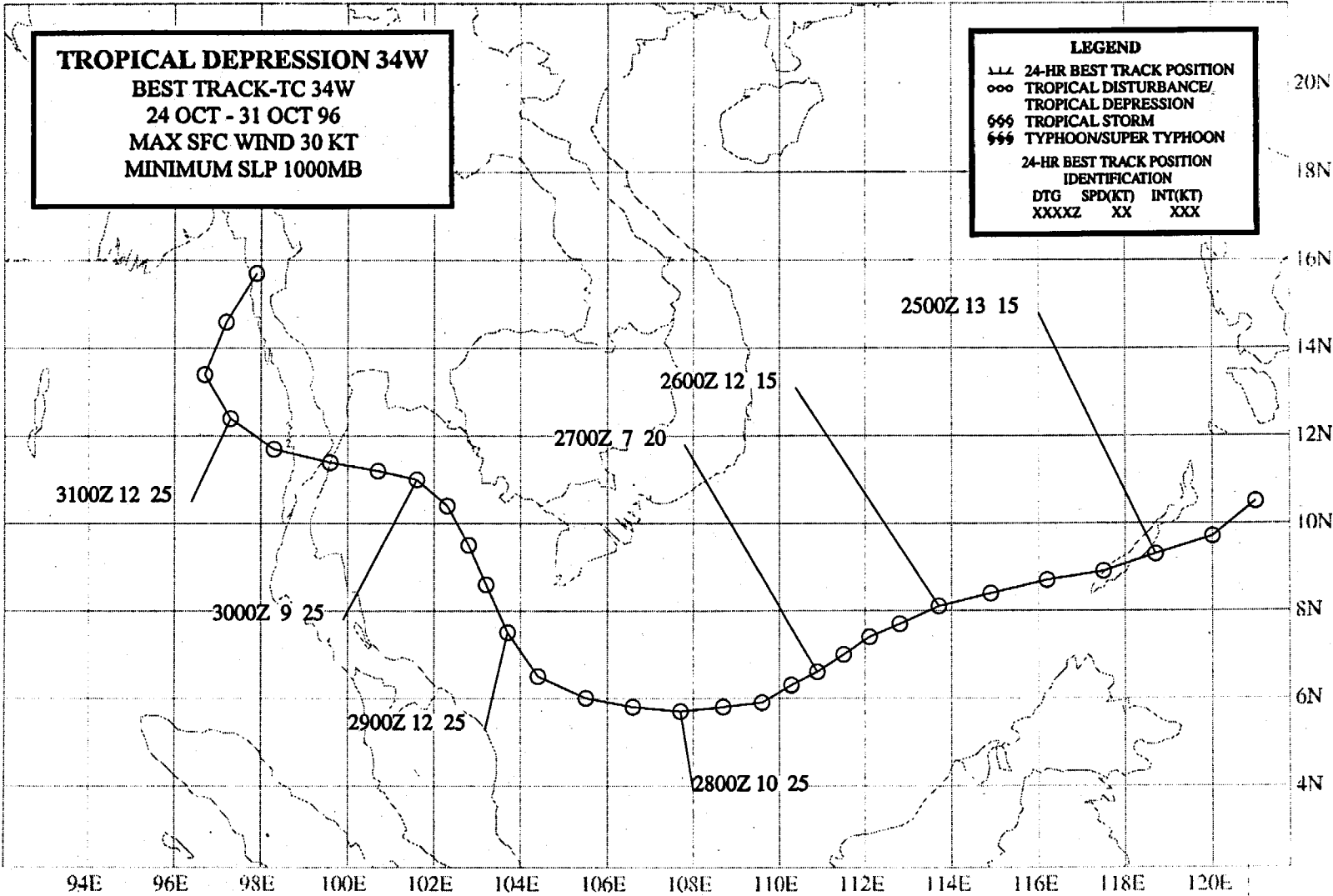
Figure 3-33-3 Two TUTT cells (C1 and C2) show prominently in water vapor imagery. Carlo formed under the moist tongue on the north side of TUTT cell C2 (180033Z October water vapor GMS imagery).

TROPICAL DEPRESSION 34W
BEST TRACK-TC 34W
24 OCT - 31 OCT 96
MAX SFC WIND 30 KT
MINIMUM SLP 1000MB

LEGEND

- 24-HR BEST TRACK POSITION
- ooo TROPICAL DISTURBANCE/
TROPICAL DEPRESSION
- 666 TROPICAL STORM
- 888 TYphoon/SUPER TYphoon

24-HR BEST TRACK POSITION
 IDENTIFICATION
 DTG SPD(KT) INT(KT)
 XXXXZ XX XXX



TROPICAL DEPRESSION 34W

The tropical disturbance which became Tropical Depression (TD) 34W originated from an area of persistent deep convection over the central Philippines. As the deep convection drifted west-southwestward across the South China Sea, a weak LLCC persisted to the eastern edge of the convection. The tropical disturbance was first mentioned on the 270600Z October Significant Tropical Weather Advisory when water vapor satellite imagery indicated that an upper-level anticyclone was forming over the deep convection. Although the cloud system remained poorly organized (Figure 3-34-1), JTWC anticipated further development and issued the first TCFA at 272030Z. A scatterometer pass over the system at 280251Z indicated a well-defined LLCC with wind speeds of 15 to 25 kt (8 to 13 m/sec) on its north side and equatorial westerlies to the south. A second TCFA followed at 282030Z. Based upon ship reports and satellite intensity estimates of 25 kt (13 m/sec), JTWC issued the first warning on TD 34W valid at 290600Z. TD 34W tracked northwestward across the Gulf of Thailand, crossed the Isthmus of Kra and became completely disorganized after moving into the Bay of Bengal. The final warning was issued valid at 301800Z. On 31 October, the remnants of TD 34W turned northward and dissipated over southern Myanmar. In postanalysis, a ship report near the LLCC of 30-kt winds and 1004 mb pressure at 271200Z was used to upgrade the maximum intensity of the best track to 30 kt.

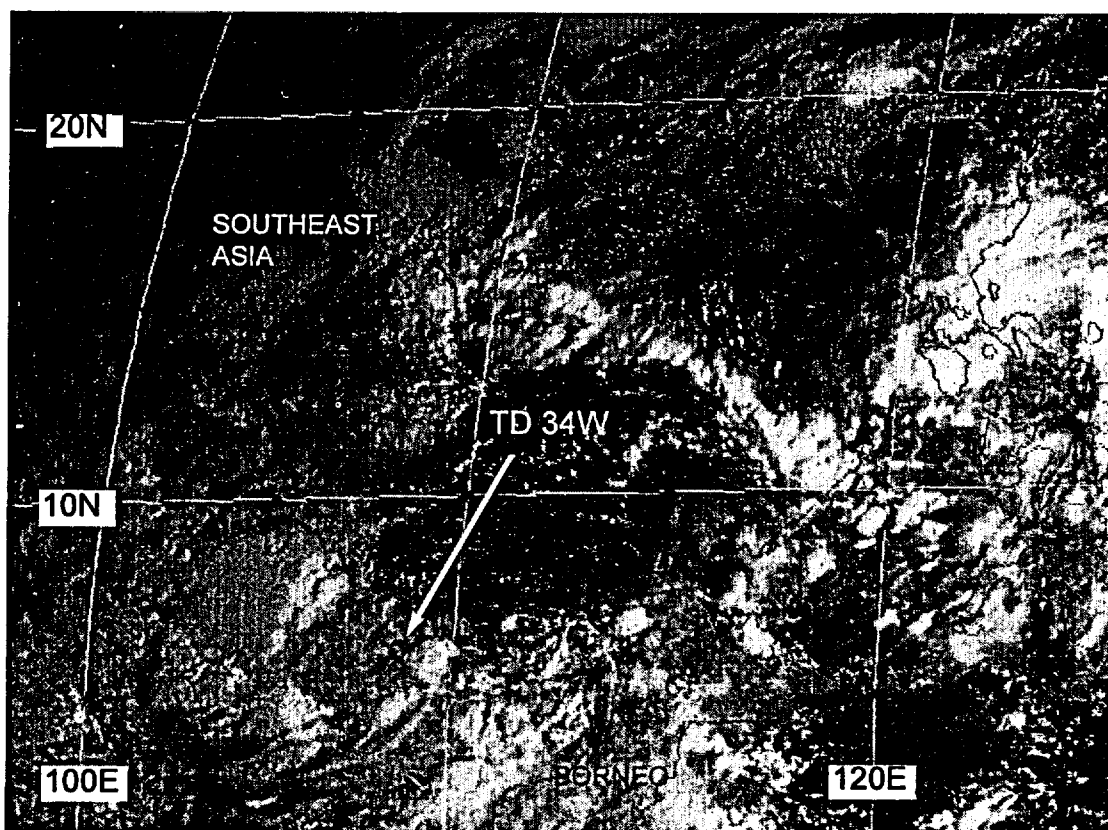


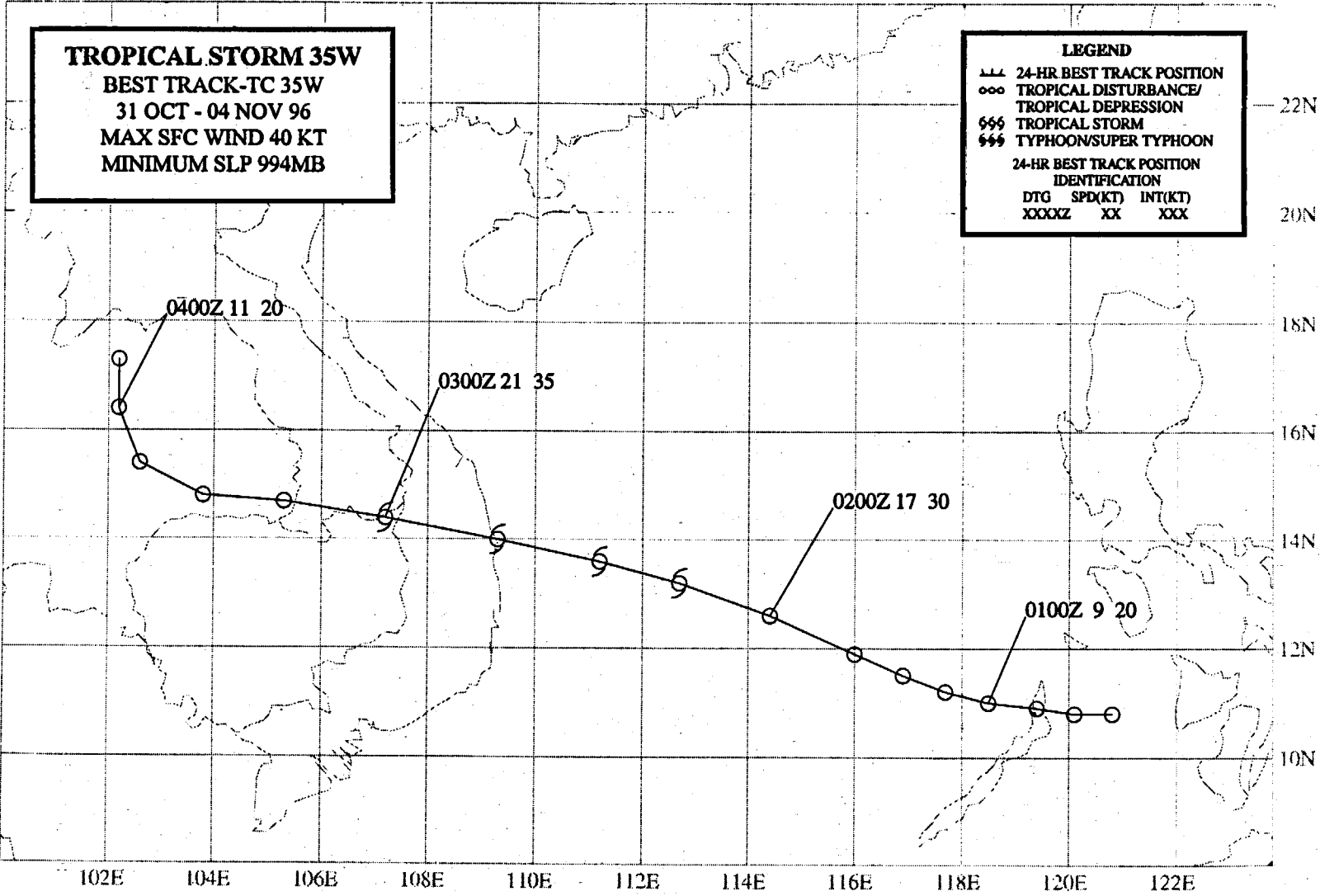
Figure 3-34-1 TD 34W moves west-southwestward in the South China Sea. Most of the deep convection lies to the west of the LLCC (272331Z October visible GMS imagery).

TROPICAL STORM 35W
BEST TRACK-TC 35W
31 OCT - 04 NOV 96
MAX SFC WIND 40 KT
MINIMUM SLP 994MB

LEGEND

--- 24-HR BEST TRACK POSITION
 ○○ TROPICAL DISTURBANCE/
 TROPICAL DEPRESSION
 ☺☺ TROPICAL STORM
 ☼☼ TYPHOON/SUPER TYPHOON

24-HR BEST TRACK POSITION
 IDENTIFICATION
 DTG SPD(KT) INT(KT)
 XXXXZ XX XXX



TROPICAL STORM 35W

On the last day of October, the tropical disturbance that became Tropical Storm (TS) 35W formed over the Philippines at nearly the same location as Tropical Depression (TD) 34W had formed a week earlier. The tropical disturbance was first mentioned on the 010600Z November Significant Tropical Weather Advisory when a persistent area of deep convection was observed over the South China Sea to the west of a weak LLCC in the Sulu Sea. The convection persisted and JTWC issued a TCFA at 011430Z. Falling pressures (3 mb in 24 hours), 25-kt synoptic reports and satellite intensity estimates led to the issuance of the first warning valid at 020000Z. The TC moved westward and acquired the structure of a monsoon depression (Figure 3-35-1) as it approached Vietnam. A final warning was issued, valid at 030600Z, as the remnants of the cyclone dissipated over Southeast Asia.

In postanalysis, synoptic reports and satellite imagery indicate that this TC most probably reached tropical storm intensity at 020600Z, and peaked at 40 kt six hours later. Thus, TD 35W was redesignated as TS 35W.

It is interesting to note that TS 35W was accompanied in the Southern Hemisphere by TC Melanie/Bellamine (05S)(Figure 3-35-2), as the TC activity in the Southern Hemisphere got off to a prolific start during the latter half of 1996.

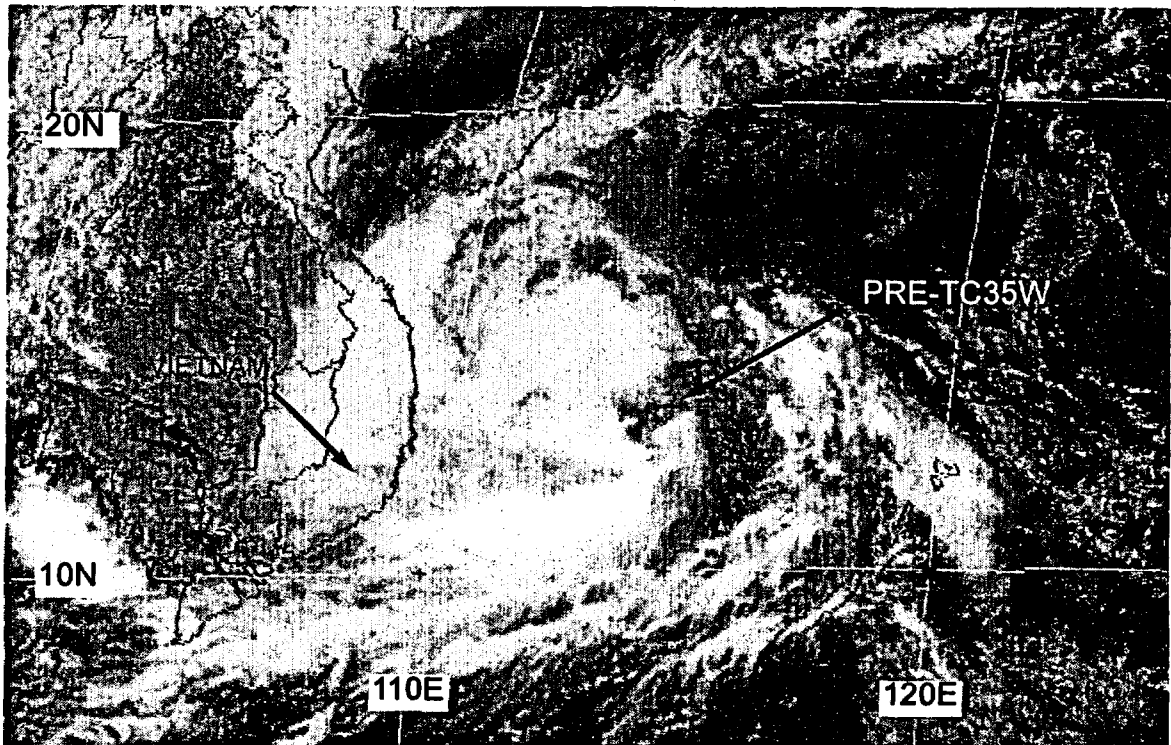


Figure 3-35-1 The monsoon depression just to the east of central Vietnam is approaching tropical storm intensity (020424Z November visible GMS imagery).

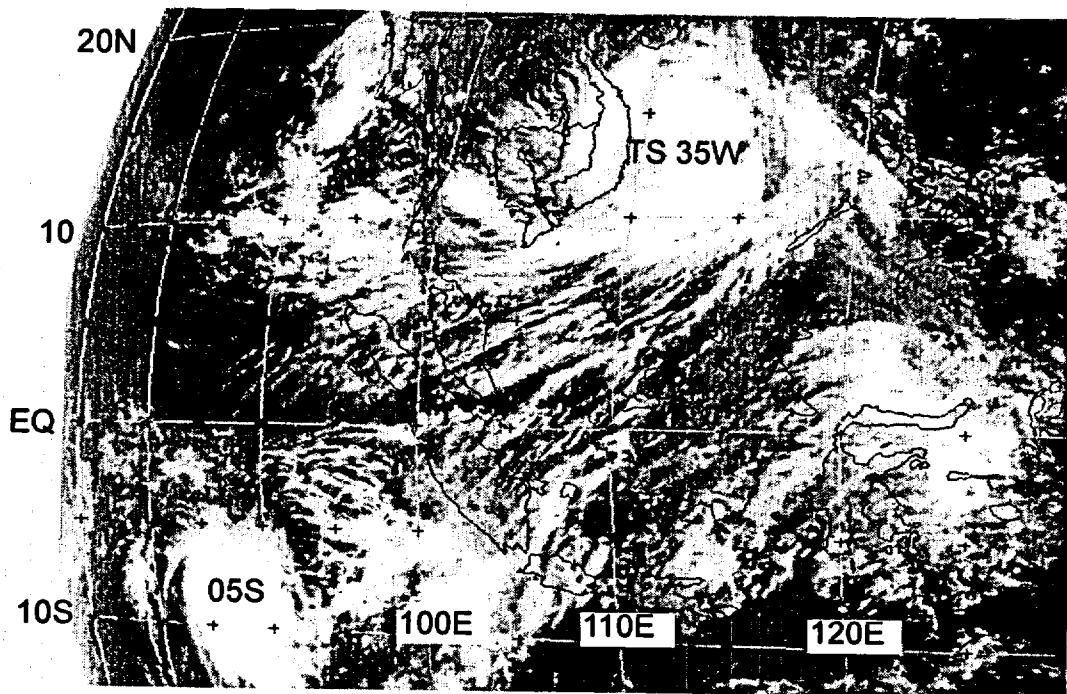
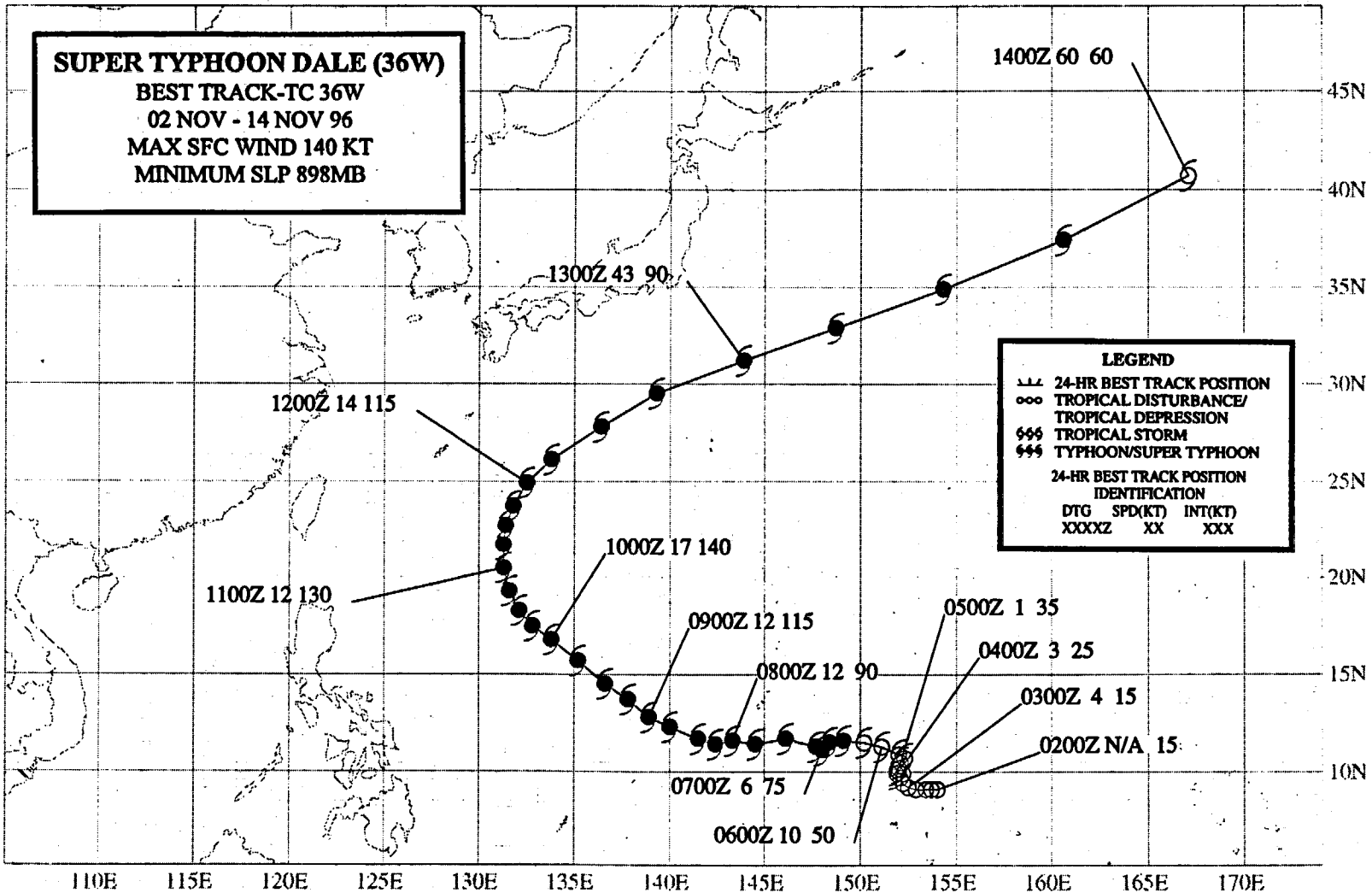


Figure 3-35-2 TS 35W is accompanied by TC Melanie/Bellamine (05S) in the Southern Hemisphere (020424Z November infrared GMS imagery).



SUPER TYPHOON DALE (36W)

I. HIGHLIGHTS

Dale was a large and very intense typhoon that formed at the eastern end of the near-equatorial trough. Its passage resulted in phenomenal seas and surf on Guam's western shore. The equatorial westerly wind burst that preceded Dale's formation was accompanied by very low sea-level pressure reports along the equator. Passing 110 nm to the south of Guam, Dale was observed by Guam's NEXRAD. Dale caused an estimated \$3.5 million worth of damage on Guam.

II. TRACK AND INTENSITY

From late October through the first day of November, the tropics of the WNP were dominated by easterly low-level wind and upper-level westerly wind; and, with the exception of the South China Sea, deep convection was disorganized and widely scattered. Beginning on 02 November, the amount of deep convection in the low latitudes of the WNP began to increase in association with lowering pressure throughout Micronesia accompanied by the onset of a near-equatorial trough along 5°N. On 03 November, the deep convection consolidated into two distinct clusters: one centered near 7°N 138°E (which became Ernie (37W)), and the other centered near 8°N 150°E (which became Dale). The pre-Dale cluster of deep convection was first mentioned on the 030600Z November Significant Tropical Weather Advisory when satellite imagery and synoptic data indicated the presence of a cyclonic circulation accompanied by a relatively low central pressure (1002 mb) and extensive divergence aloft (as indicated by animated water-vapor GMS imagery). With a continued fall of the central pressure, and improvements to the satellite cloud signature, a Tropical Cyclone Formation Alert was issued at 031800Z, followed by the first warning on Tropical Depression (TD) 36W, valid at 040600Z.

With an extensive surge in the southwesterly flow to its south and equally strong easterly winds to its north, TD 36W remained nearly stationary for approximately 24 hours while it slowly gained intensity. On the warning valid at 151200Z, TD 36W was upgraded to Tropical Storm Dale based upon satellite intensity estimates of 35 kt (18 m/sec) and a buoy report indicating that the central pressure had fallen below 996 mb (indicative of winds of at least 37 kt on the Atkinson and Holliday (1977) wind-pressure relationship). After becoming a tropical storm, Dale began to move westward, intensified, and became a typhoon at 061800Z. At approximately 071400Z Dale (moving west along 11.5°N) passed 110 nm (205 km) to the south of Guam where peak gusts reached 74 kt (38 m/sec) and high waves inundated some coastal roads and overtopped 100-ft (30-m) sea cliffs (see the Discussion and the Impact sections). Dale came within range of Guam's NEXRAD, which detected winds in excess of 100 kt (51 m/sec) in the lower troposphere (see the Discussion section).

On 09 November, while to the west of Guam in the Philippine Sea, Dale became a super typhoon with a peak intensity of 140 kt (72 m/sec) (Figure 3-36-1). On 10 November, Dale slowed and began a turn toward the north, and on 11 November reached its point of recurvature (i.e., the westernmost longitude). After recurvature, Dale accelerated rapidly to the east-northeast reaching translation speeds in excess of 60 kt (110 km/hr) after 140000Z. The final warning was issued, valid at 131800Z, when completion of extratropical transition was expected within six hours.

III. DISCUSSION

a. *Extremely low equatorial sea-level pressure associated with Dale's formation*

The sea-level pressure (SLP) along the equator has spatial and temporal variations of small

magnitude when compared with the magnitude of the SLP variations at higher latitudes. In the mean, the global equatorial SLP ranges from a maximum of approximately 1015.5 mb in the eastern Atlantic to a minimum of approximately 1008.5 mb in the WNP (Sadler et al. 1987). Lacking the Coriolis effect, and large inertial forces (e.g., centrifugal forces in atmospheric vortices such as typhoons), the pressure gradients on the equator must only be sufficient to drive the wind against friction. As such, a pressure gradient of 1 mb per 1000 km can support a sustained 10-m marine surface wind of 20 kt (10 m/sec). Even the vast easterly wind flow across the tropical Pacific is accompanied by an east-west pressure drop (along the equator) of only 4 mb from the eastern equatorial Pacific to the WNP. Given this background, it is now clear that the very low SLP readings of 1002 mb, and SLP changes of 10 mb along the equator in the WNP during the life of Dale are extraordinary.

While Dale and Ernie (37W) were forming at low-latitude in the WNP, the SLP throughout Micronesia was steadily falling. Even along the equator, to the south of the developing Dale, the SLP steadily fell to extraordinarily low values (Figures 3-36-2 and 3-36-3). On 04 November, several ships near the equator reported a SLP of 1002 mb or less. Values of SLP this low are rarely

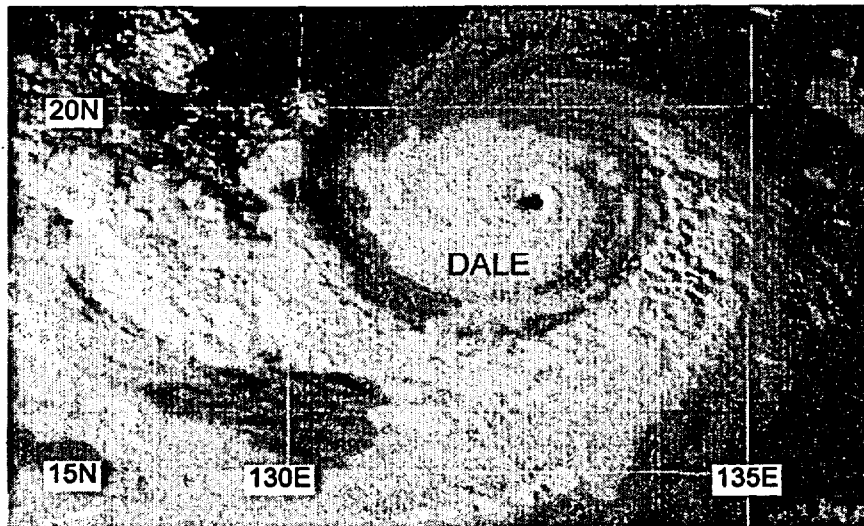


Figure 3-36-1 Dale nears its peak intensity of 140 kt (72 m/sec) (090530Z November visible GMS imagery).

seen along the equator. Morrissey (1988) examined the SLP reports of ships within two degrees of the equator along a principal north-south shipping lane between 148°E to 152°E. The ship reports used by Morrissey were extracted from the Comprehensive Ocean-Atmosphere Data Set (COADS) for an 80-year (1900-1979) period. From his analysis (Figure 3-36-4), few, if any, SLP reports below 1004 mb are found along the equator in this region. Ironically,

approximately 10 days after the very low SLP readings (and after Dale had exited the tropics), the equatorial SLP and the SLP throughout Micronesia rose to exceedingly high values. The SLP of 1013.5 mb on the equator on 14 November was, according to Figure 3-36-4, about as high as the SLP ever gets there.

b. Dale as seen by Guam's NEXRAD

On the night of 07 November, Dale passed 110 nm (205 km) to the south of Guam. Guam experienced the peripheral rain bands of Dale, but never entered the eye wall cloud (Figure 3-36-5). For much of the time during Dale's closest point of approach (CPA), Guam remained within a dry wedge between the outer rain bands and the eye wall cloud. The air was laden with salt spray, and some light rain which allowed the NEXRAD to obtain a deep vertical profile of the wind velocity (Figure 3-36-6). The highest winds of approximately 100 kt (51 m/sec), persisted in a layer between about 6,000 and 13,000 ft. At the gradient level (3,000 ft), the NEXRAD detected 75-kt (39-m/sec)

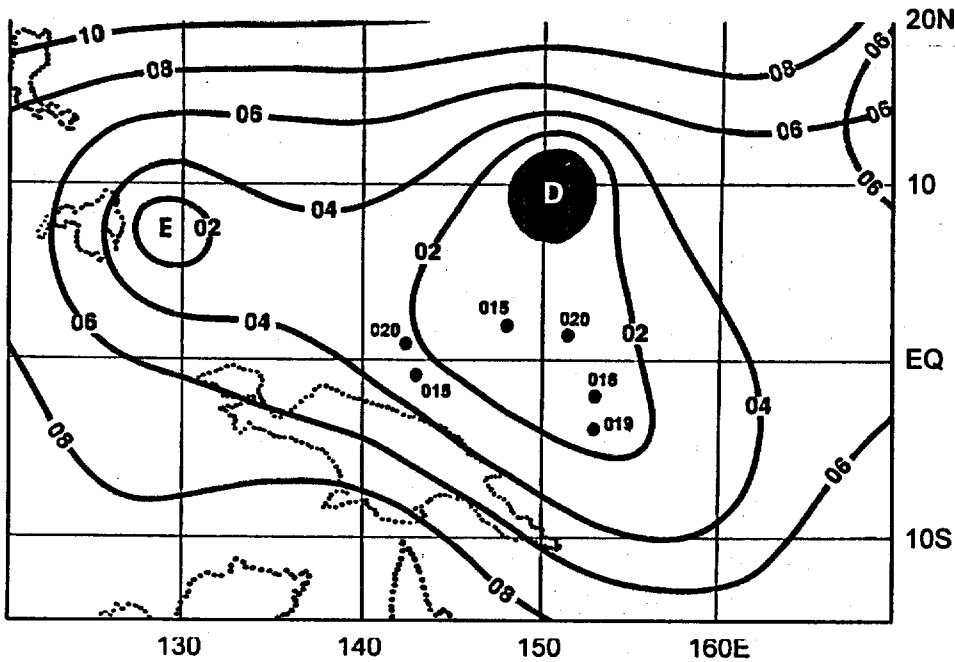


Figure 3-36-2 Sea-level pressure analysis based upon a composite of ship observations at 040600Z and 041800Z November. Individual ships near the equator with reports of 1002 mb or lower are indicated. D = Dale, E = Ernie, and SLP contours are drawn at 2 mb intervals.

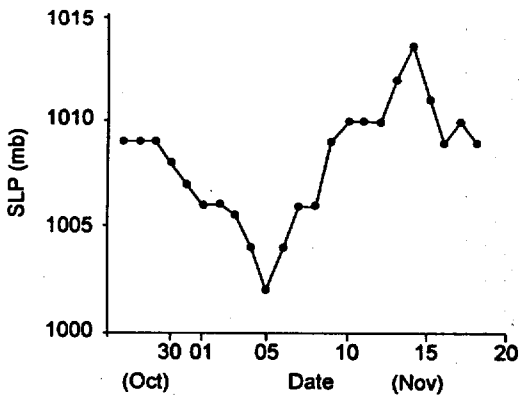


Figure 3-36-3 Time series of the equatorial SLP near 150°E based upon ship observations.

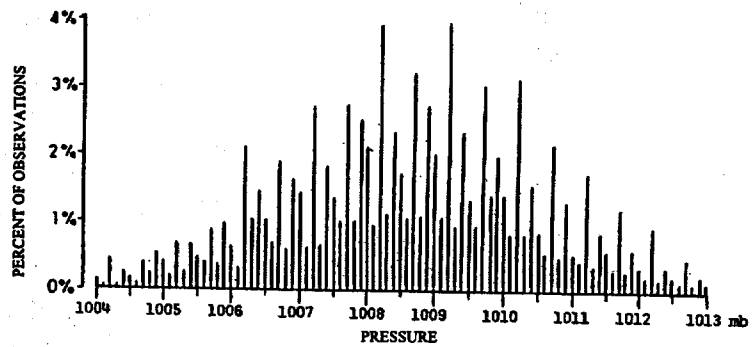
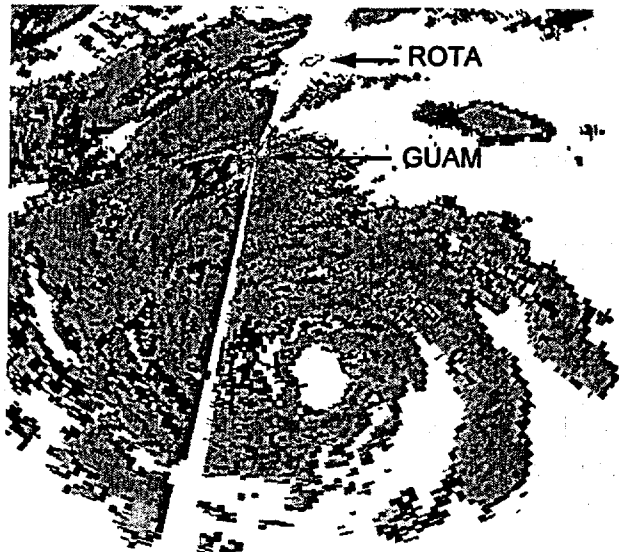


Figure 3-36-4 Histogram of ship SLP reports extracted from the COADS data set in the box bounded by 2°N and 2°S from 148°E to 152°E (adapted from Morrissey, 1988).

Figure 3-36-5 NEXRAD base reflectivity showing the eye, wall cloud and peripheral rain bands of Dale as it nears its CPA to Guam. Guam remained in the dry wedge between the outer rain bands and the eye-wall cloud for an extended period (071458Z NEXRAD base reflectivity product).



winds (not shown in Figure 3-36-6) which correlated well with the peak gusts observed on Guam (Figure 3-36-7). Although the maximum winds in a typical TC are expected to be at the gradient level, NEXRAD coverage of Dale showed they were considerably higher in altitude. Perhaps the lack of deep convection and associated torrential rain were factors in the relatively elevated level of the wind maximum during Dale's passage by Guam.

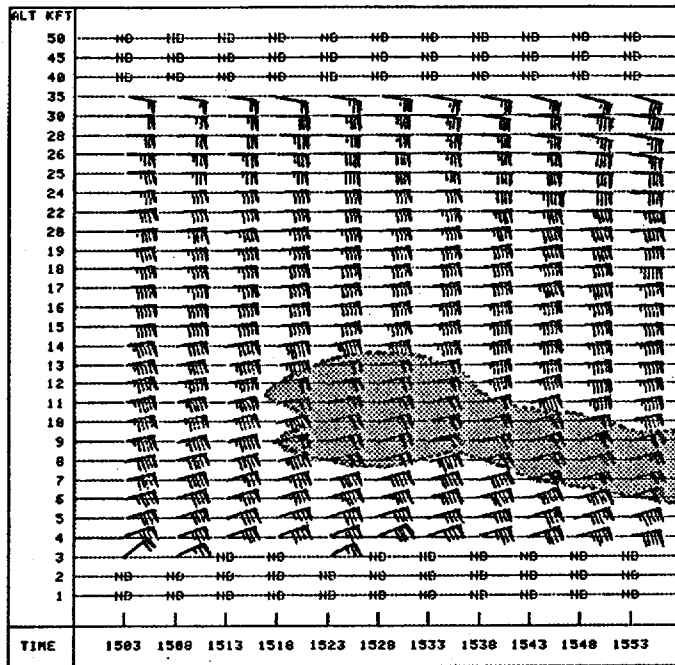


Figure 3-36-6 The NEXRAD velocity azimuth display (VAD) wind profile near the time of Dale's CPA to Guam showing winds of 100 kt (51 m/sec) or more between 6,000 and 12,000 ft (shaded region) (071553Z NEXRAD VAD wind profile product).

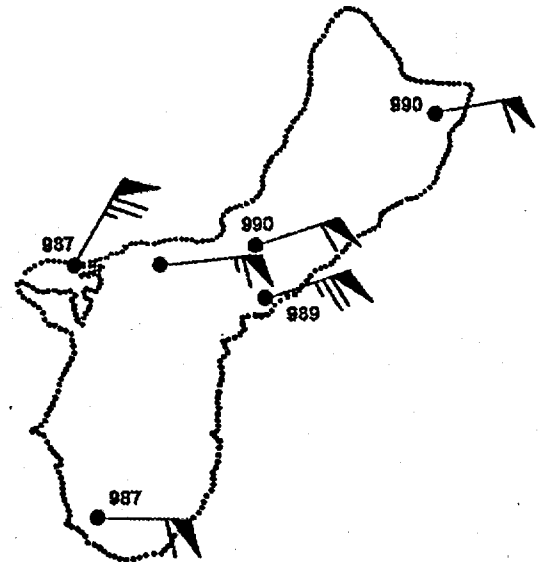


Figure 3-36-7 Peak gusts and minimum SLP recorded at several selected sites on Guam during Dale's passage.

c. Dale's digital Dvorak (DD) numbers

The time series of Dale's DD numbers (Figure 3-36-8) peaked at approximately 090600Z with values of approximately T 7.5. After this peak, the DD numbers fell sharply to below T 5.0 by 100000Z. The warning and best-track intensity lag the peak DD numbers by about six hours, and do not reflect the sharp drop in the DD numbers after the peak. As the DD numbers are considered experimental, and are not used operationally, it is not expected that the warning intensity would be strongly tied to them. The DD numbers do, however, often reflect prominent observable changes in the characteristics of the TC. In Dale's case, the rapid drop of the DD numbers after the peak occurred because concentric eye walls formed. At peak intensity, Dale had a well-defined small eye (Figure 3-36-1). When the DD numbers fell, it was because concentric eye walls formed (Figure 3-36-9a, b). The default radius used to define the eye-wall cloud-top temperature in the DD algorithm is 30 nm. This radius fell between the inner and outer eye walls, and resulted in the period of low DD values after the peak. The radius used to define the eye-wall cloud-top temperature is an adjustable parameter on the MIDDAS system, and when set to 10 nm, it was able to measure the inner eye wall. This resulted in DD numbers of about one T number higher than those computed

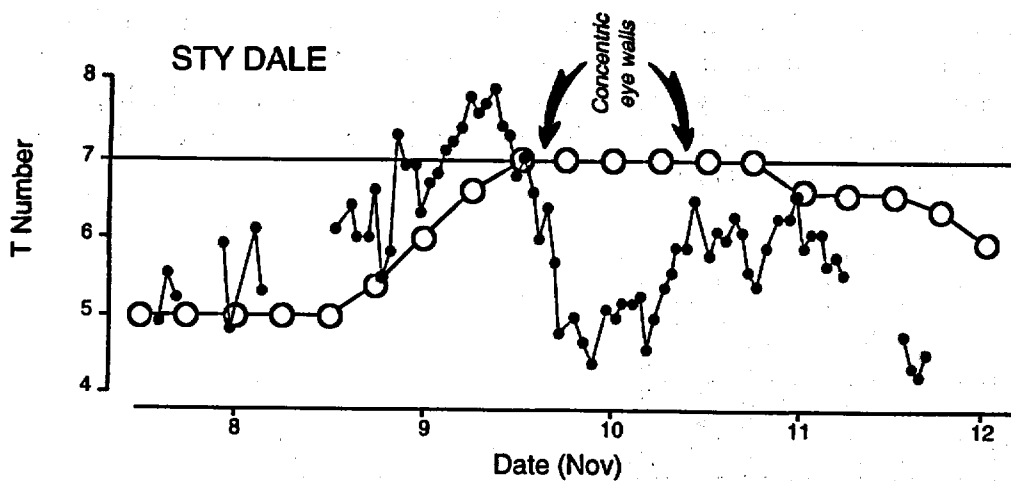


Figure 3-36-8 A time series of Dale's hourly DD numbers (small black dots) compared with the warning intensity converted to a T number (larger open circles at six-hour intervals). The large drop in the DD numbers after the peak was the result of the formation of concentric eye walls.

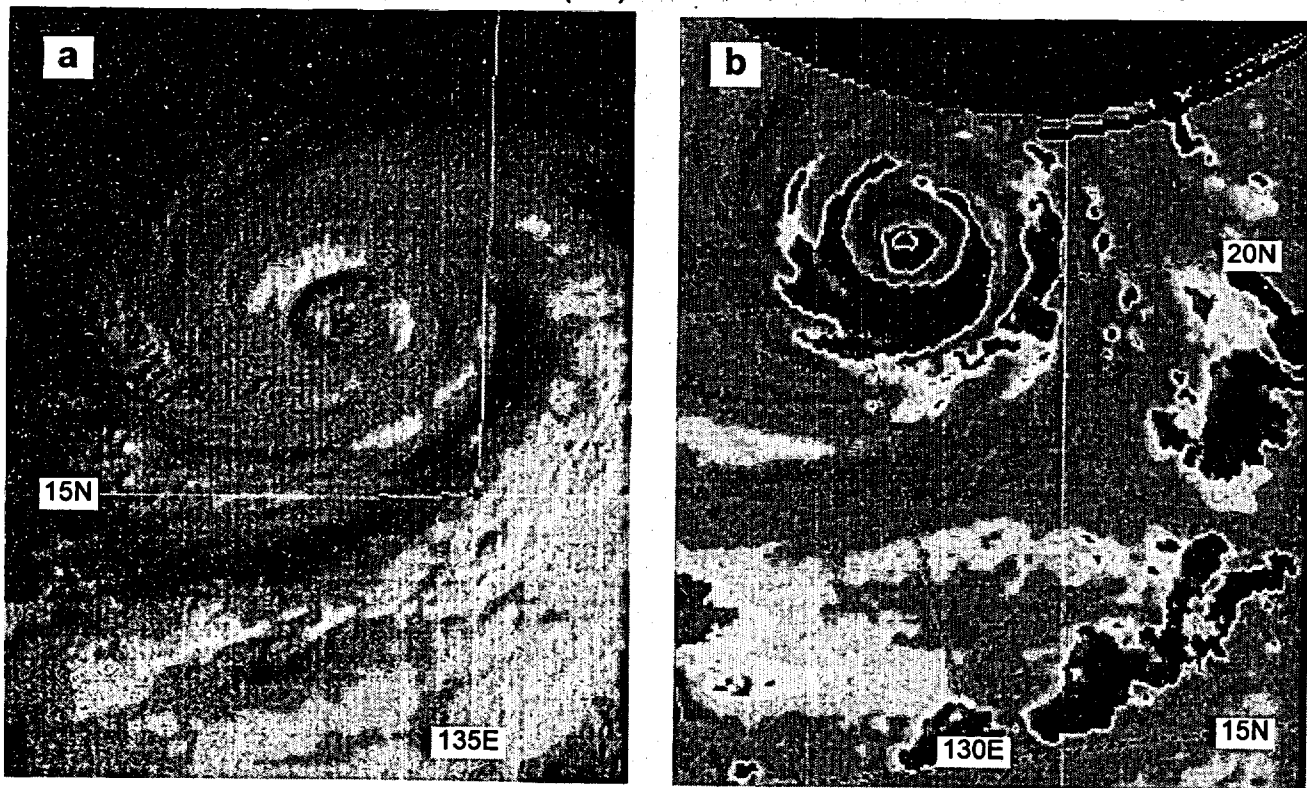


Figure 3-36-9 Dale's concentric eye walls as indicated by (a) visible satellite imagery (092331Z visible GMS imagery), and (b) microwave imagery (110117Z November 85 GHz SSM/I DMSP imagery).

using the default radius during the time when Dale possessed concentric eye walls. The structural changes of Dale show that, though automated, the DD algorithm still requires a satellite analyst to adjust its adaptable parameters and determine the quality of its output.

d. The generation of phenomenal seas in the periphery of a typhoon

While phenomenal surf is common on the eastern shores of Guam when typhoons pass to the south, it is rare that a typhoon produces phenomenal surf on the west side of Guam. Generally, on the north side of a westward moving typhoon, the seas are increased due to the increased wind on that side, but more importantly, due to the artificial fetch that is created as the moving typhoon

keeps up with its own wave train and allows the sea state to rise to its full potential. On the south side of westward-moving typhoons, there is a severe fetch restriction, and the seas can't reach their fully arisen state.

After Dale passed Guam, a very large swell of 20 to 30 feet pounded the western shores of Guam for two days. The wave run-up overtopped 100 ft (30 m) sea cliffs on Orote Point on the west side of Guam (Figure 3-36-10). Such extreme swell from the west is not common on Guam. Even the passage of the large Super Typhoon Yuri only 80-nm south of Guam during November 1991 and the direct eye passage over Guam of the 105-kt (54-m/sec) Omar (1992) did not result in very large westerly swell on Guam. Clearly, some special conditions are required for a typhoon to generate these conditions. Such swell is clearly not directly related to the intensity of the typhoon or even to its size (Yuri was both very intense and very large). It appears that in order for a typhoon to generate phenomenal westerly swell on Guam it must be accompanied by a large region of monsoonal gales extending to its south and west. This was true of Dale and also of the only other typhoon in recent history (Andy, 1989) that was known to have produced phenomenal surf on the west side of Guam. Another phenomenal surf event on the west side of Guam was not produced by a typhoon at all, but by a persistent monsoonal gale area that was associated with a monsoon gyre in the Philippine Sea in 1974.

IV. IMPACT

Dale affected the island of Guam and caused problems for ships at sea. Damage on Guam was mainly caused by high surf, first from the east and later from the west. High surf from the east washed out sections of the coastal road on the southeastern side of the island. Later, surf run-up from the west overtopped 100 ft sea cliffs and damaged Navy housing on Orote Point Naval Activities. Currents and surges inside the reef generated by the west swell also eroded and flooded the beach fronts. Damage estimates for Guam were approximately \$3.5 million. Dale also caused damage in the Pulep Atoll, the Hall Islands and several islands of the Chuuk Atoll. The U.S. Coast Guard provided relief supplies to people on these islands. High seas contributed to the loss of the cattle ship, M/V Guernsey Express, enroute for Japan from Australia. Navy helicopters from Guam, USNS Zeus and Kilauea and U.S. Coast Guard search and rescue worked together to rescue the crew of 18 as the ship was sinking.



Figure 3-36-10 Sea water explodes 100 ft into the air as a wave reflecting off the Orote Point cliff line meets an oncoming breaker (Photo courtesy of Major R. Edson).

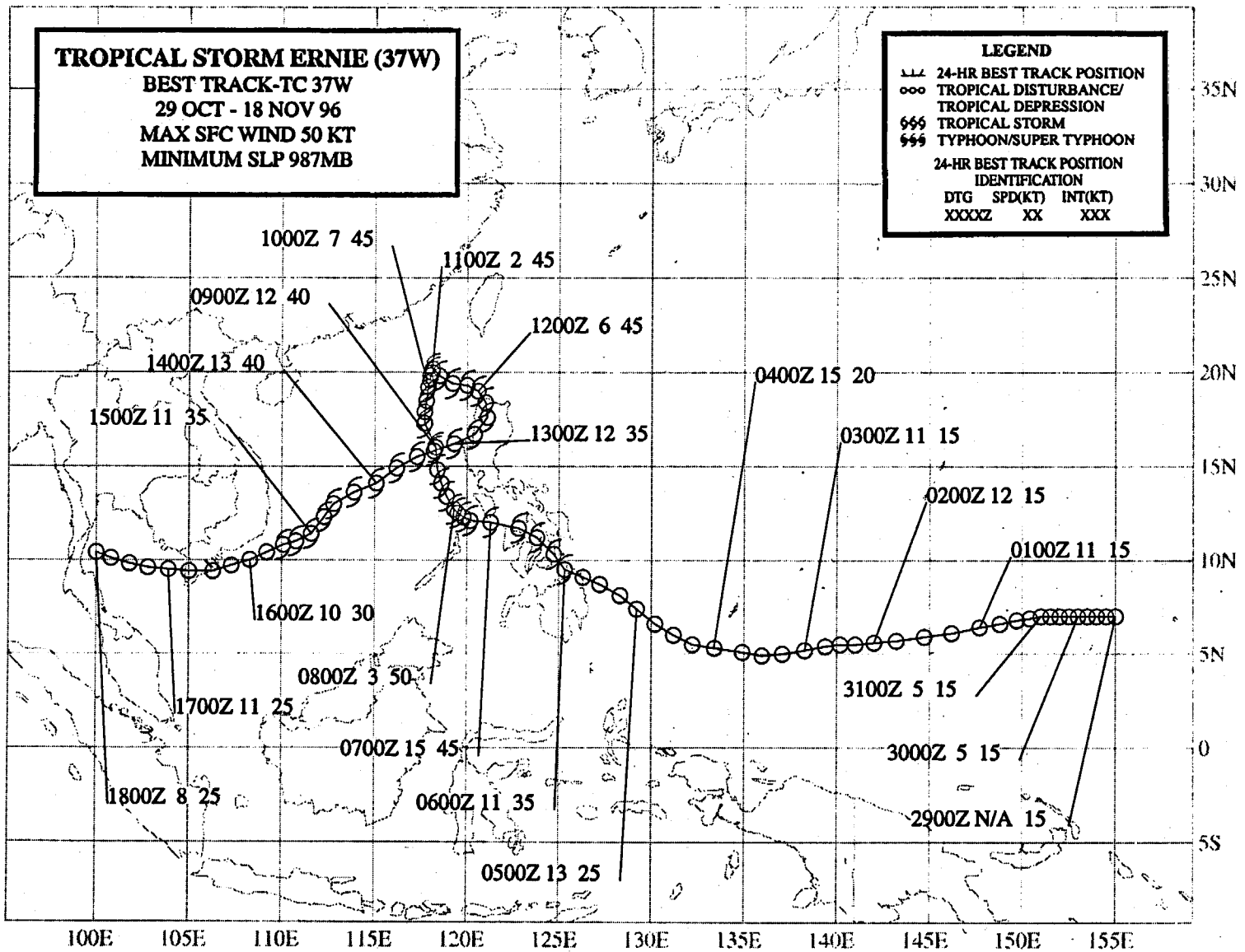
TROPICAL STORM ERNIE (37W)

BEST TRACK-TC 37W
29 OCT - 18 NOV 96
MAX SFC WIND 50 KT
MINIMUM SLP 987MB

LEGEND

- 24-HR BEST TRACK POSITION
- TROPICAL DISTURBANCE/
TROPICAL DEPRESSION
- ⊖ TROPICAL STORM
- ⊕ TYPHOON/SUPER TYPHOON

24-HR BEST TRACK POSITION
IDENTIFICATION
DTG SPD(KT) INT(KT)
XXXXZ XX XXX



TROPICAL STORM ERNIE (37W)

I. HIGHLIGHTS

At the start of the second week of November, four TCs existed simultaneously in the WNP — Ernie, Dale (36W), Tropical Storm (TS) 38W, and Tropical Depression (TD) 39W. Ernie, Dale (36W) and TD 39W formed in the monsoon trough, while TS 38W developed in association with a TUTT cell. After entering the South China Sea, Ernie executed a clockwise loop as it merged with TD 39W. Earlier, while crossing the Philippines, Ernie was responsible for loss of life and extensive property damage.

II. TRACK AND INTENSITY

During the first week of November, a near-equatorial trough formed along approximately 5°N latitude in the WNP. Deep convection associated with this trough consolidated into two distinct systems: the easternmost became Dale (36W) and the westernmost became Ernie. The pre-Ernie tropical disturbance was first mentioned on the 290600Z October Significant Tropical Weather Advisory when satellite imagery and synoptic data indicated that a weak LLCC was associated with an area of persistent deep convection. Development of this disturbance was slow, perhaps hindered by persistent vertical wind shear from the east-northeast, and its transformation into a monsoon depression. Late on 03 November, a small area of deep convection near the core of the monsoon depression persisted; leading to the issuance, valid at 031800Z November, of a TCFA. The first warning on TD 37W followed, valid at 041200Z. Based on satellite intensity estimates, TD 37W was upgraded to Tropical Storm Ernie at 060600Z as the system moved into the central islands of the Philippine archipelago.

On 07 November, Ernie moved into the South China Sea, slowed, and intensified. Satellite imagery indicates that Ernie reached peak intensity of 50 kt (26 m/sec) at 070600Z. As the system reached peak intensity, it made an abrupt turn to the north, perhaps in response to strengthening southwesterly monsoonal flow into Dale (36W) (located to Ernie's east), and also the effects of a binary interaction with TD 39W (which had formed to Ernie's northeast). On 10 November, Ernie subsumed the weakening circulation of TD 39W (Figure 3-37-1) in a merger representing the final stage of a binary interaction (see the Discussion section). After the merger, Ernie executed a clockwise loop which saw the system make landfall in northwestern Luzon before moving back into the South China Sea. As Dale (36W) recurved, Ernie began to move toward the southwest in response to steering influences of a well-entrenched northeast monsoon over the northwestern portion of the South China Sea. In the time span of three and one-half days, Ernie traversed the South China Sea, slowly weakened, and made landfall on the southern tip of Vietnam. The final warning was issued, valid at 170000Z, as the weakened TC moved westward into the Gulf of Thailand and dissipated.

III. DISCUSSION

Merger of Ernie with TD 39W

Ernie and TD 39W underwent a binary interaction that ended in the merger of the two systems. The separation distance between the two systems was always within the 400 nm (740 km) separation threshold noted by Lander and Holland (1993) for TC merger. Though the centroid-relative motion of the two systems shows a clear cyclonic orbit (Figure 3-37-2), only the actual track of TD 39W shows clear signs of orbit. The merger of Ernie with TD 39W was asymmetric in that the smaller TD 39W was sheared and subsumed into the larger circulation of Ernie. Note that even in such cases, the centroid-relative motion of each TC will always be a mirror image of the other's.

IV. IMPACT

In the central Philippines, Ernie was reported to have killed 16 people and caused \$US 4.1 million damage to property.

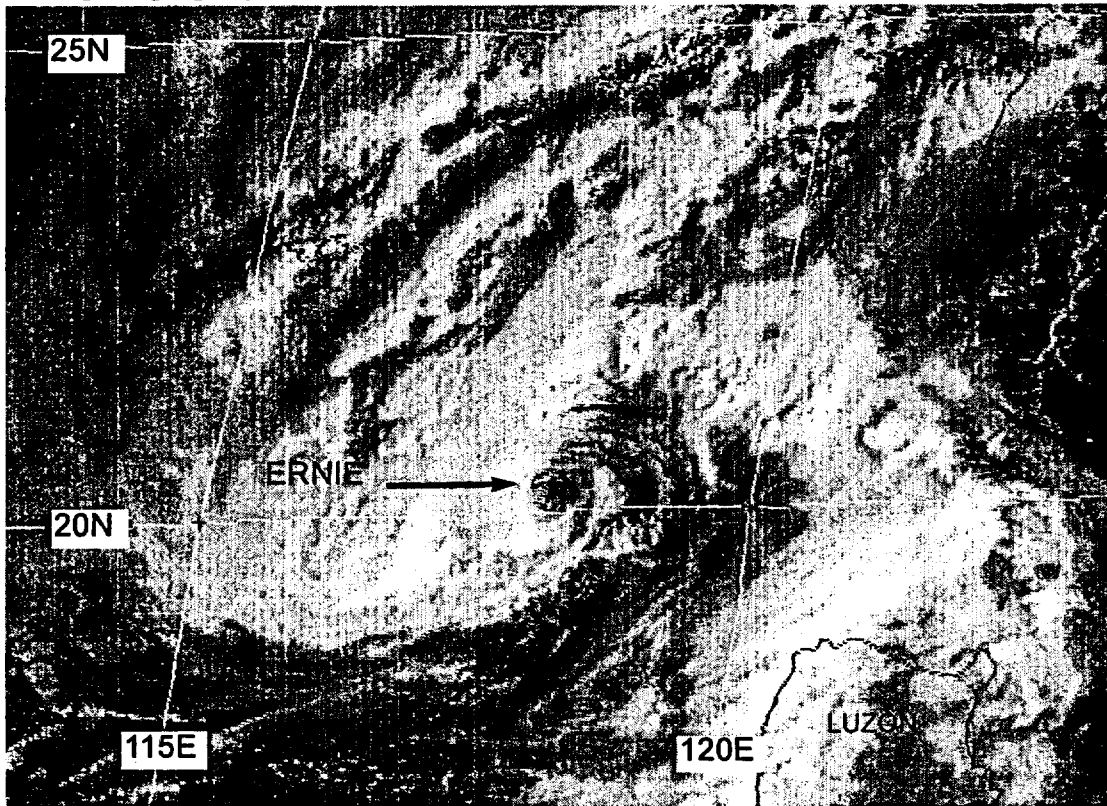


Figure 3-37-1 Tropical Storm Ernie (37W) shortly after its merger with TD 39W. An exposed low-level circulation center is visible (102331Z November visible GMS imagery).

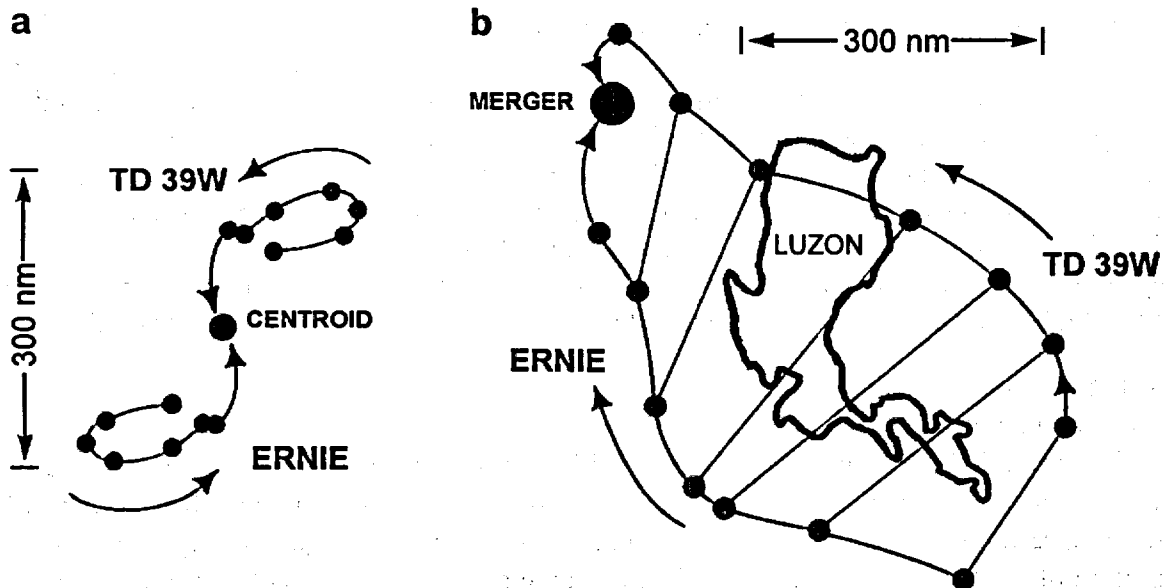
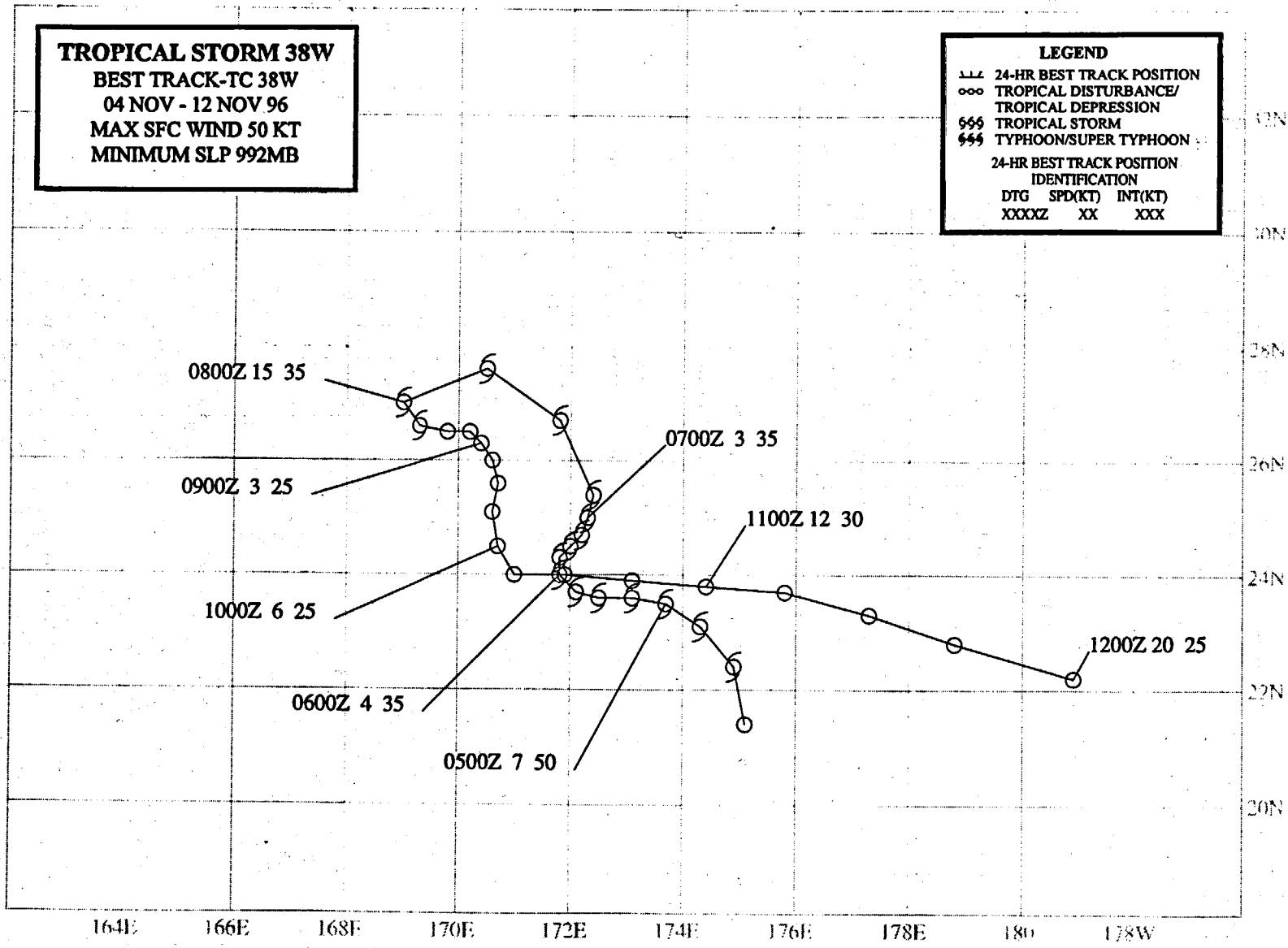


Figure 3-37-2 (a) The complex binary interaction of Ernie with TD 39W is revealed by a diagram of its centroid-relative motion which features a period of anticyclonic relative orbit prior to the period of cyclonic orbit leading to merger. (b) The tracks of these TCs do not as clearly exhibit the properties of the mutual interaction. Dots are at 12-hour intervals beginning at 061200Z November. Merger occurs at 100000Z.

TROPICAL STORM 38W
BEST TRACK-TC 38W
04 NOV - 12 NOV 96
MAX SFC WIND 50 KT
MINIMUM SLP 992MB

LEGEND
 --- 24-HR BEST TRACK POSITION
 ooo TROPICAL DISTURBANCE/
 TROPICAL DEPRESSION
 666 TROPICAL STORM
 666 TYPHOON/SUPER TYPHOON
 24-HR BEST TRACK POSITION
 IDENTIFICATION
 DTG SPD(KT) INT(KT)
 XXXXZ XX XXX



TROPICAL STORM 38W

I. HIGHLIGHTS

Tropical Storm (TS) 38W was the third unnamed WNP TC of 1996 which was considered in real time to have only been a tropical depression, but was determined in postanalysis to have reached tropical storm intensity. TS 38W was unusual in that it developed in association with a very late-in-the-year TUTT cell. During its 8-day life, TS 38W traced a highly erratic 1500 nm (2800 km) track, but it ultimately dissipated only 180 nm (335 km) from where it was first detected.

II. TRACK AND INTENSITY

While Dale (36W) and Ernie (37W) were developing east of the Philippines on 04 November, the tropical disturbance which became TS 38W was first detected as a circulation which formed in direct association with an unusually late-in-the-year TUTT cell. This disturbance was first mentioned on the 040600Z November Significant Tropical Weather Advisory. As cloud organization continued to improve, a TCFA was issued valid at 050600Z. The first warning on Tropical Depression 38W, valid at 060600Z, was prompted by the detection on the ERS-2 scatterometry data of 30-kt (15-m/sec) winds in association with a well-defined LLCC (Figure 3-38-1). In postanalysis, a reassessment of ship, microwave, scatterometer, and conventional visible and infrared satellite data revealed the need to upgrade the peak intensity of the tropical depression to an unnamed tropical storm (see the Discussion). The final warning was issued, valid at 080600Z, when all the deep convection sheared away to the northeast leaving the LLCC completely exposed.

Tropical Storm 38W exhibited a highly erratic track during its life over open water at relatively high latitude near the international date line. The erratic motion featured initial northwestward motion, followed by a counterclockwise loop, and finally (as the system dissipated) a two day period of eastward motion. The end result of the erratic motion was 1500 nm (2800 km) of total distance covered, but an end point only 180 nm (335 km) removed from the place of origin.

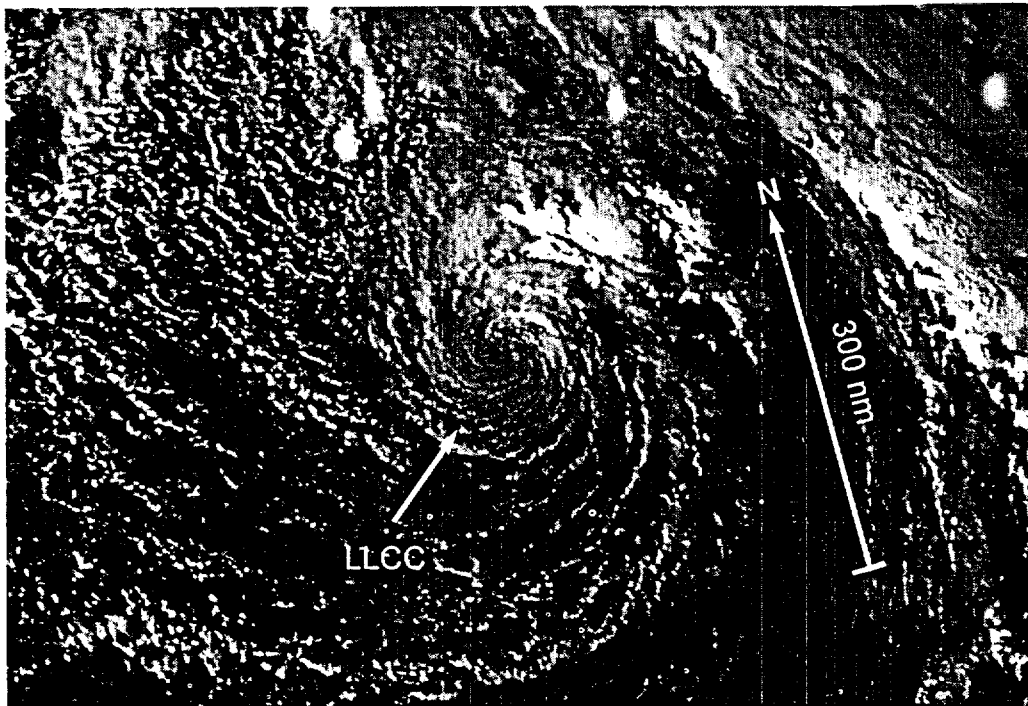


Figure 3-38-1
Tightly wound low-level cloud lines describe the well defined LLCC of TS 38W (060426Z November visible GMS imagery).

III. DISCUSSION

Postanalysis upgrade from tropical depression to tropical storm

Because of an unconventional structure for a TC (a large well-defined LLCC with most of the deep convection displaced a few hundred kilometers to the northeast — a structure common to many TUTT cell-related TCs, and also to subtropical cyclones) (Figure 3-38-1), the real-time satellite intensity estimates for TS 38W were only 25-30 kt (12-15 m/sec). A ship report at 050000Z with a pressure of 997 mb and a 50-kt (26-m/sec) north-northwesterly wind was considered suspect in real time. In postanalysis however, scatterometer data, microwave and visible satellite imagery were reassessed and judged to be supportive of an upgrade of TD 38W to a tropical storm. At 041200Z and 081200Z, ERS-2 scatterometer data showed a maximum wind speed of 35 kt (18 m/sec) near the LLCC of the system. The SSM/I at 050700Z (Figure 3-38-2) and visible satellite data at 060426Z (Figure 3-38-1) both confirmed that the TC possessed a very well organized and tightly wound LLCC that made plausible the 50-kt (26-m/sec) ship report. Additional features on the satellite imagery, including the "herringbone" pattern of the low-level cumulus extending outward from the LLCC on the northern semicircle indicated near-gale force winds in that area, also supported an increased intensity estimate. Hence TD 38W became TS 38W in postanalysis — the third such occurrence during 1996. Use of new satellite technologies (e.g., scatterometry and microwave imagery) and new understanding of TC structure have made such upgrades more common than in the past. The hope is to refine satellite applications to the point where more accurate assessments can be made in real time.

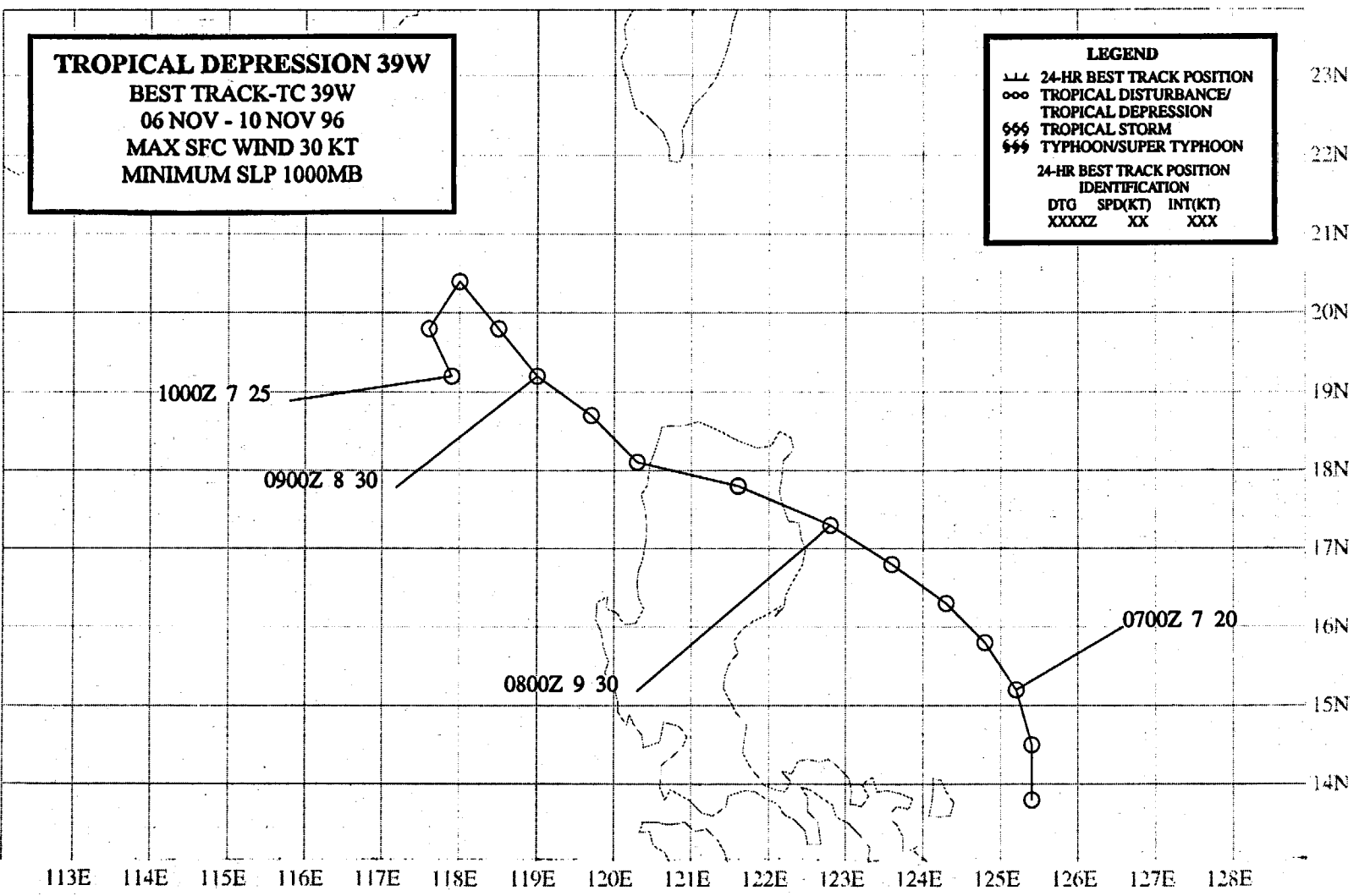
IV. IMPACT

No reports of damage or injuries were received at the JTWC.



Figure 3-38-2 A mosaic of successive passes of 85-GHz horizontally polarized microwave imager data showing the circulations of Dale (36W) and TS 38W. Note the tight wrap of the low and middle cloud associated with TS 38W (Mosaics of 85-GHz horizontally polarized microwave DMSP imagery - the easternmost pass over TS 38W was dated 050715Z November).

200



TROPICAL DEPRESSION 39W

Tropical Depression (TD) 39W formed in the monsoon trough which extended eastward from Ernie (37W) across the central Philippines and into the Philippine Sea. When satellite imagery indicated that deep convection was becoming better organized east of Luzon, and satellite and ship reports indicated the presence of a LLCC associated with this area of deep convection, the tropical disturbance which became TD 39W was first mentioned on the 070600Z November Significant Tropical Weather Advisory. As the system tracked northwestward toward Luzon, a TCFA was issued at 080630Z. The TCFA was quickly superseded by the first warning, valid at 080600Z, and was based on ship wind reports of 25 kt (12 m/sec) and sea-level pressure reports near 1000 mb from land stations on the northeast coast of Luzon. The system tracked over the northern tip of Luzon and entered the South China Sea off the northwest tip of Luzon while retaining its peak intensity of 30 kt (15 m/sec). The final warning on TD 39W was issued, valid at 090600Z, as the system began to weaken while undergoing a binary interaction with Ernie (37W) (Figure 3-39-1; also see Figure 3-37-2 in Ernie's summary for a graphical depiction of the binary interaction of TD 39W with Ernie (37W)). On 10 November, the remnants of TD 39W were absorbed by the circulation of Ernie. No reports of damage or injuries were received at the JTWC.

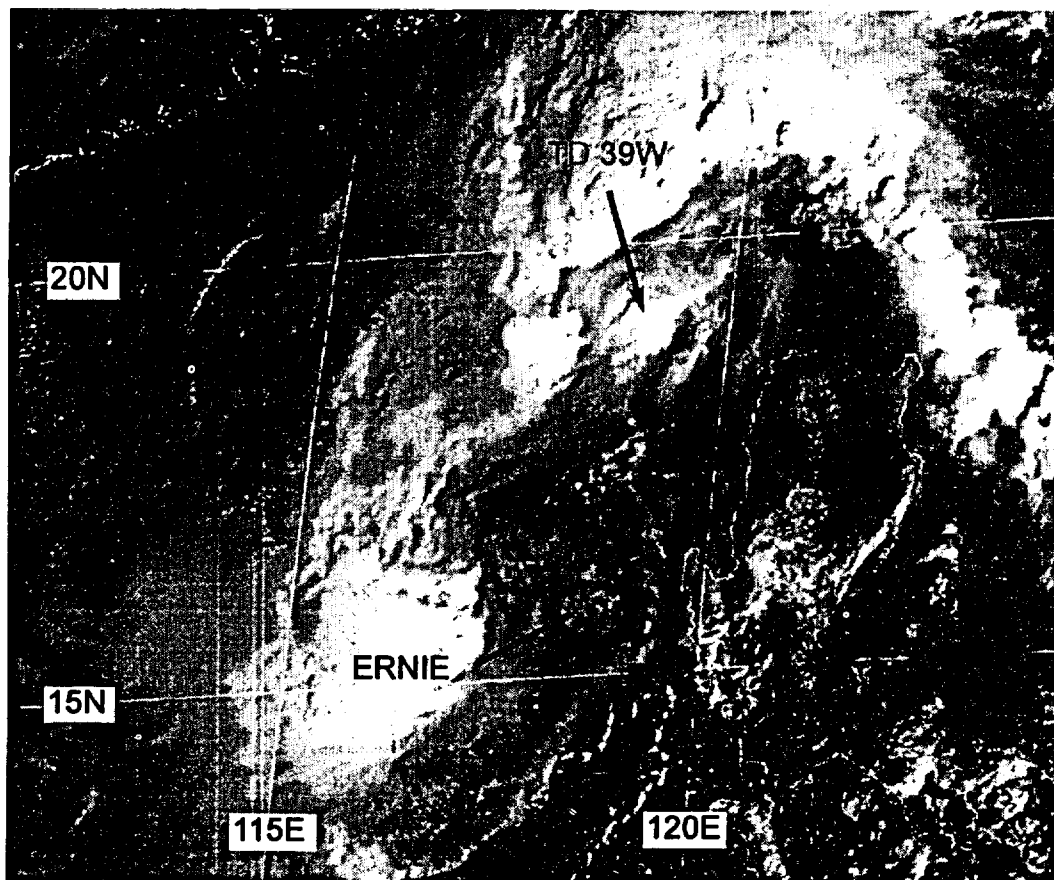
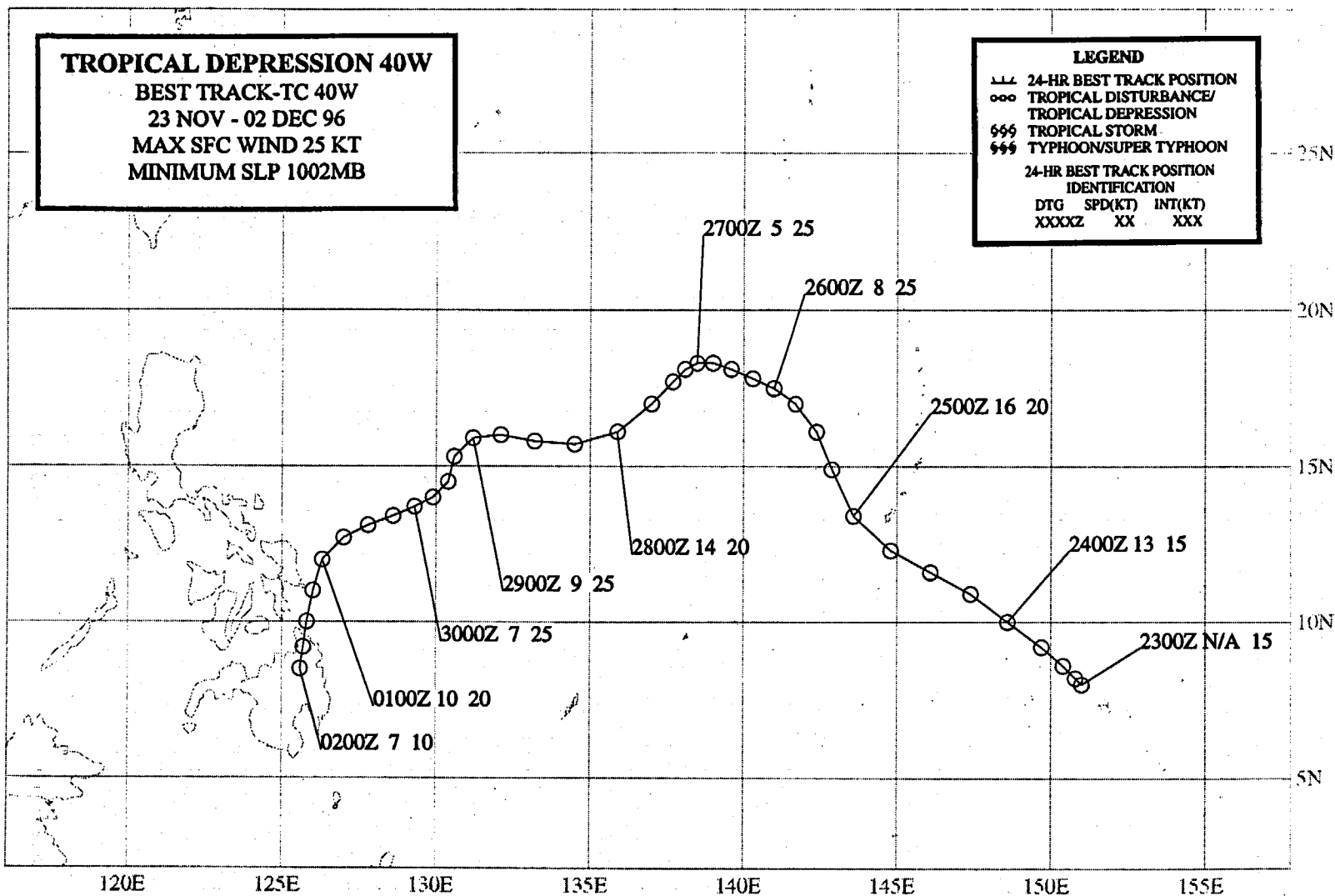


Figure 3-39-1 TD 39W and Ernie (37W) are approaching one another as they undergo a binary interaction (090033Z November visible GMS imagery).



TROPICAL DEPRESSION 40W

After Dale (36W) recurved, and Ernie (37W) moved into the South China Sea, the WNP experienced a break in TC activity. Overall sea-level pressures rose across the WNP tropics and light winds dominated the low latitudes. The break was short-lived, however, as increased convection soon spread across Micronesia and a large monsoon depression developed there. On 23 November, the monsoon depression was centered near Chuuk, and its growing size and increasing organization prompted its first mention on the 231800Z Significant Tropical Weather Advisory. The system drifted northwestward toward Guam, and continued consolidation and organization of the deep convection (Figure 3-40-1) prompted the JTWC to issue a TCFA at 241430Z. This was followed by the first warning on Tropical Depression (TD) 40W, valid at 250000Z. The northwestward motion of TD 40W continued until 27 November when the TC encountered a region of enhanced northeasterly low-level flow associated with an approaching shear line. Interaction with the shear line resulted in a track change to the southwest. As vertical wind shear increased, TD 40W weakened and a "final" warning was issued valid at 270000Z. Two days later, however, deep convection redeveloped within the LLCC and a "regenerated" warning followed, valid at 290000Z. The renewed deep convection did not last long — dissipation ensued and the final warning was issued valid at 010000Z December. On 02 December, the remnants of TD 40W dissipated over Mindanao, but not before unleashing torrential rains on Catanduenas province in the Philippines. Landslides resulting from this heavy precipitation were responsible for at least 14 deaths.

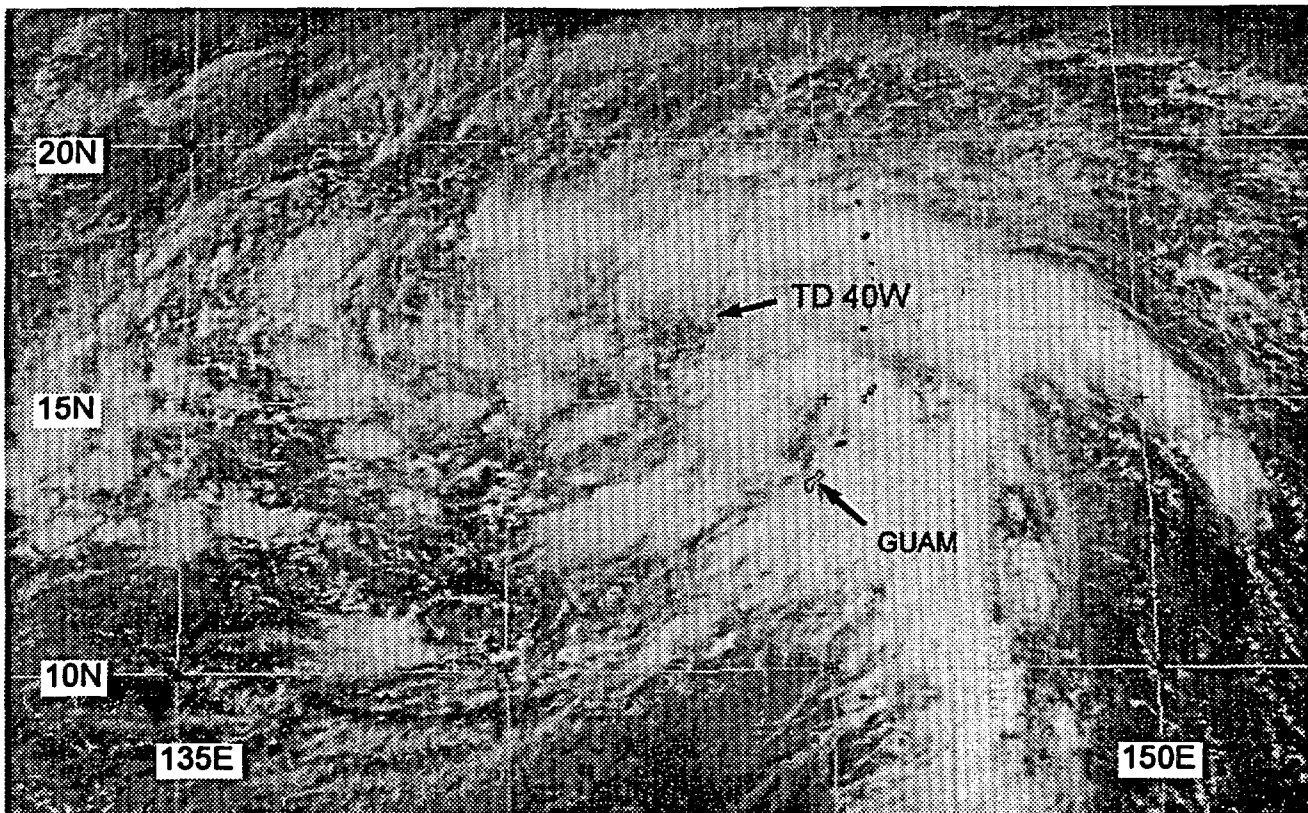
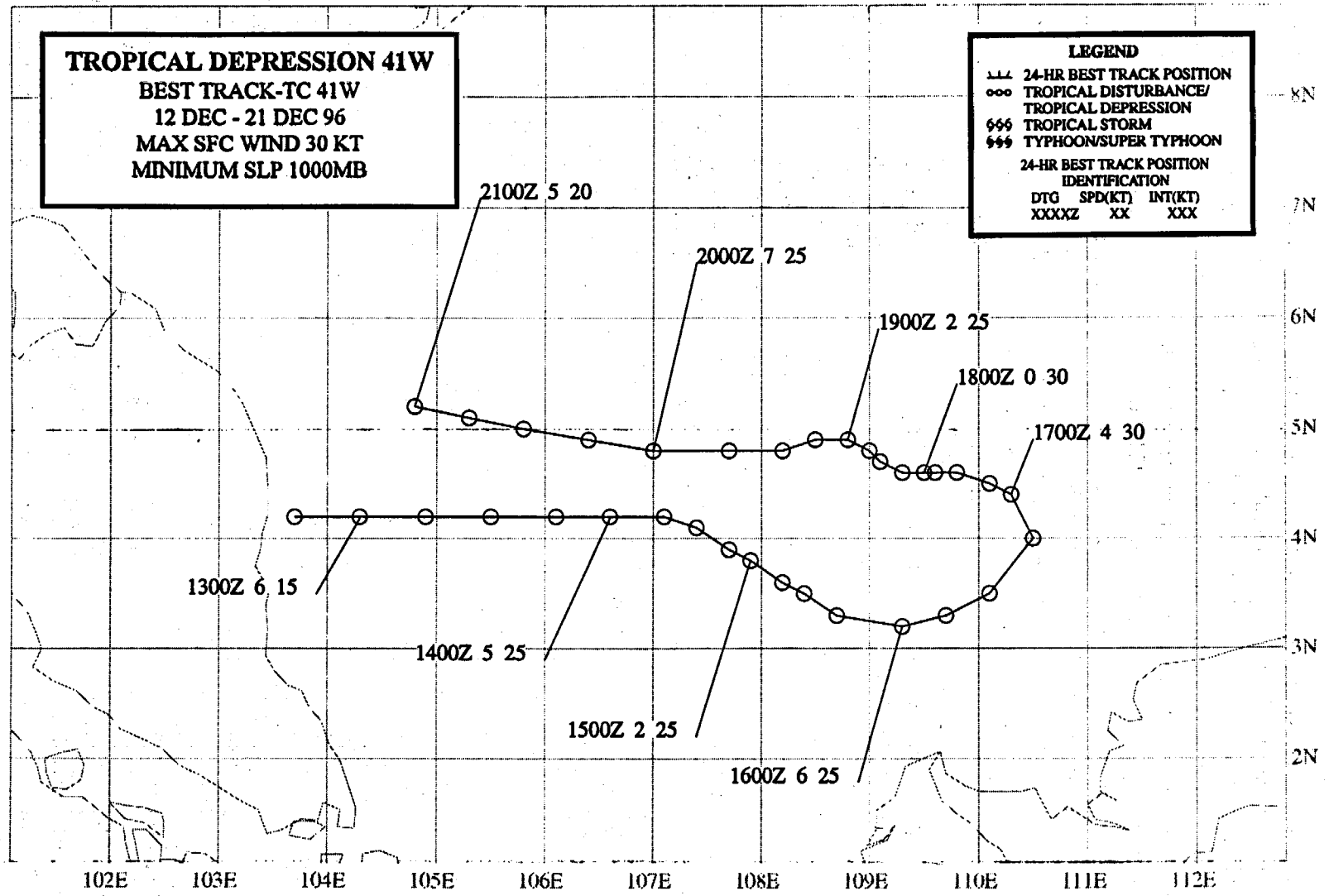


Figure 3-40-1 The monsoon depression which became TD 40W organizes its deep convection near Guam just prior to the first warning (242330Z November visible GMS imagery).

204



TROPICAL DEPRESSION 41W

After Tropical Depression 40W dissipated over the southern Philippines, there was a break in TC activity in the WNP until 10 December, when an area of deep convection became persistent in the South China Sea. On 13 December, synoptic data indicated a weak LLCC (located east of the Malay peninsula) was associated with this area of deep convection. The system moved eastward along the northern edge of a equatorial westerly wind burst (WWB) (Figure 3-41-1). Based upon synoptic data indicating a well-defined LLCC with maximum sustained wind speeds of 25 kt (13 m/sec), the first warning on Tropical Depression (TD) 41W was issued, valid at 140600Z December. Remarks on the first warning included:

" . . . The low-level circulation is in an area of convergence between the northeasterly monsoon and an equatorial westerly wind burst. Development is being aided by this strong WWB. . . " The strength and depth of the WWB to the south of TD 41W appeared to be the dominant steering mechanism, and TD 41W moved eastward until 16 December when the TC approached the northwest coast of Borneo. Here, the TC gradually turned northward and then westward as it came under the steering influence of the northeast monsoon. After doubling back toward the Malay peninsula, the TC continued westward and dissipated on 21 December when located near the location where it formed a week earlier. Strong upper-level easterlies persisted throughout the lifetime of TD 41W, and the resultant vertical wind shear likely limited the intensity of TD 41W to its peak of 30 kt (15 m/sec).

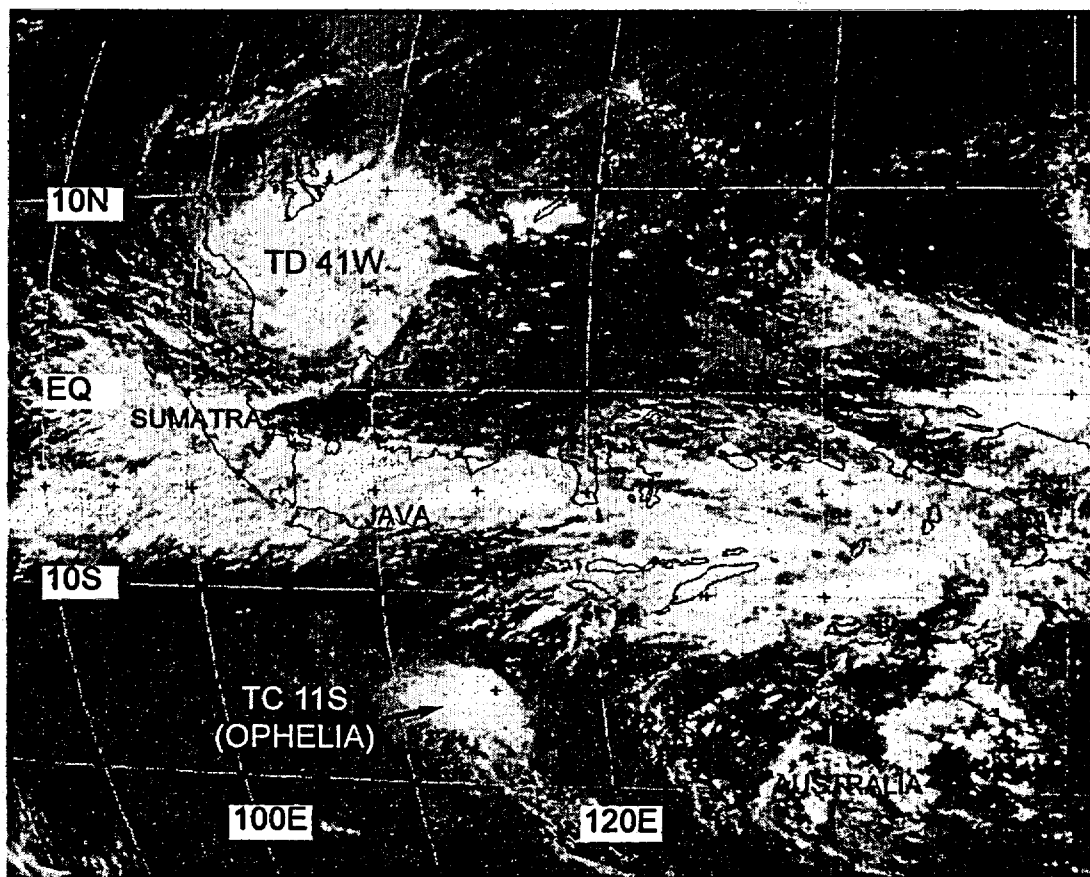
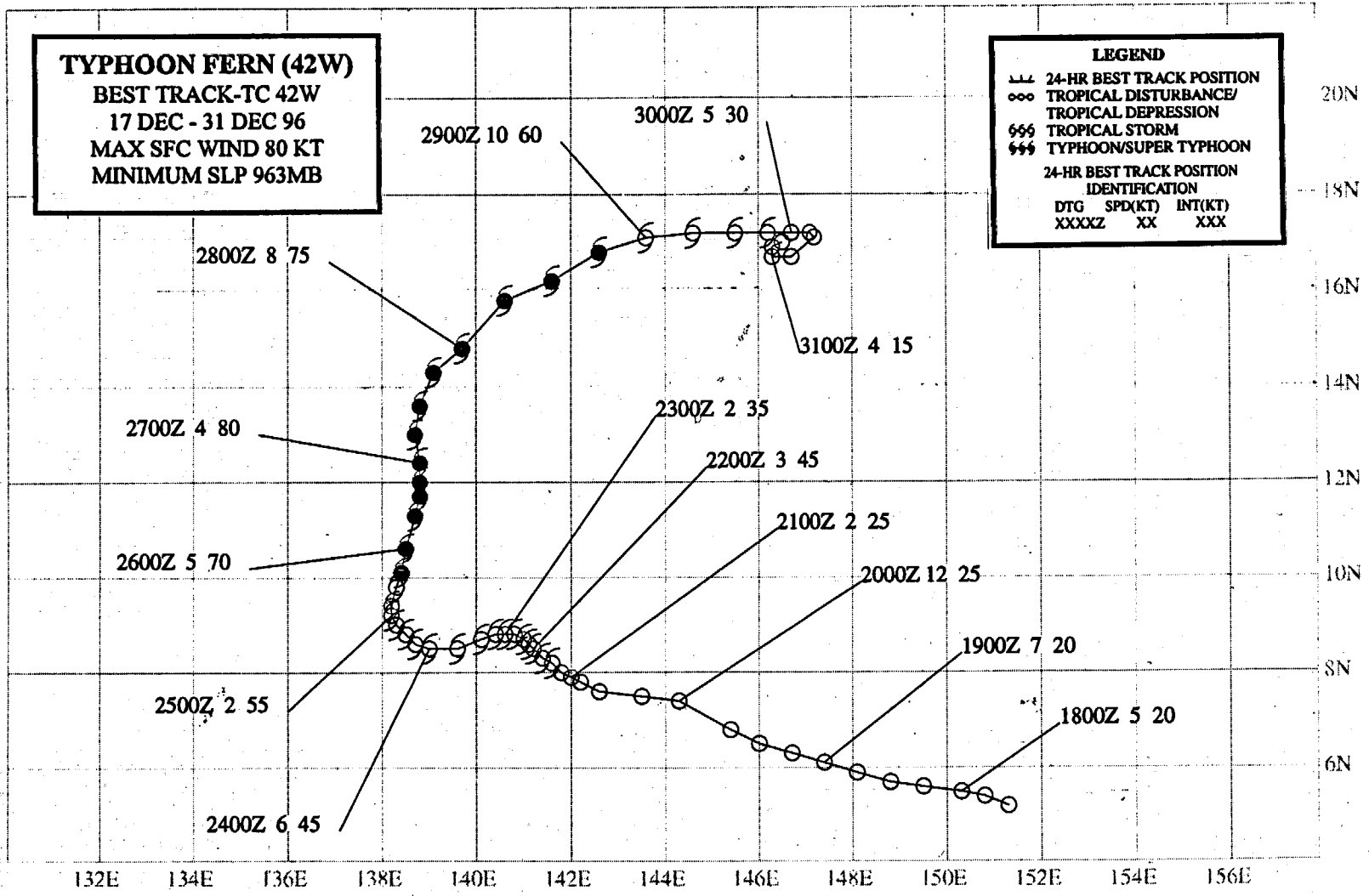


Figure 3-41-1 An extensive east-west cloud band associated with a equatorial WWB separates TD 41W (located in the South China Sea) and TC 11S (Ophelia) located in the Southern Hemisphere to the south of Java (170531Z December infrared GMS imagery).



TYPHOON FERN (42W)

I. HIGHLIGHTS

The last typhoon of 1996, Fern formed at low latitude in association with a strong equatorial westerly wind burst (WWB). While passing over Yap, strong winds and torrential rains caused property damage and personal injury. Eight people were rescued at sea when high seas and winds crippled the cargo vessel, "Mister Bill", while it was enroute from Guam to Yap.

II. TRACK AND INTENSITY

During the second half of December, twin low-latitude monsoon troughs became established between approximately 100°E and 170°E. A band of low-level westerly winds persisted between the two trough axes. A total of five TCs — two in the Northern Hemisphere (Fern and Greg (43W)), and three in the Southern Hemisphere (Ophelia (11S), Phil (12P), and Fergus (13P)) — formed along the respective monsoon trough axis (see Figure 3-43-1 in Greg's (43W) summary).

On 14 December, deep convection began to increase along the equator between approximately 140°E and 160°E in association with an intensifying WWB. A poorly defined LLCC located south-southeast of Guam was noted on the 190600Z December Significant Tropical Weather Advisory. Moving slowly westward, this disturbance remained poorly defined until 21 December when an area of deep convection began to consolidate near a LLCC. Low sea-level pressure (SLP) of 1001 mb and evidence of upper-level divergence over the LLCC (on animated water vapor imagery) prompted the JTWC to issue a TCFA at 211500Z December. The first warning on Tropical Depression (TD) 42W, valid at 211800Z, soon followed based on synoptic data indicating falling SLP in the developing TC (998 mb at 211800Z). Six hours later, on the warning valid at 220000Z, TD 42W was upgraded to Tropical Storm (TS) Fern based on satellite and synoptic data. For the next two days, TS Fern moved slowly westward and remained near minimal TS intensity. On 24 December, the tropical storm turned northward and slowly approached Yap. On Christmas day, Fern passed over Yap (Figure 3-42-1a,b), where SLP fell to 983 mb and a peak wind gust of 63 kt (32 m/sec) was recorded at the Weather Service Office (WMO 91415) (Figure 3-42-2a,b). For several hours peak wind gusts in excess of 50 kt (26 m/sec) on Yap occurred in the westerly flow as Fern moved away to the north. Fern became a typhoon at 251800Z approximately 12 hours after passing over Yap. Continuing to move slowly north for the next three days on the north-oriented portion of its track, Fern reached its peak intensity of 80 kt (41 m/sec) at 261200Z. Reaching peak intensity after turning northward is a common behavior of TCs in north-oriented patterns (see the Discussion). On 28 December, Fern encountered a strong shear line in the low levels and, located within deep-layer westerly steering flow to the north of the subtropical ridge, it began to move toward the east-northeast and weaken. Fern gradually dissipated as it moved eastward along the shear line, and the final warning was issued valid at 300600Z December.

III. DISCUSSION

Peak intensity after recurvature

Most typhoons that undergo classical recurvature (i.e., a roughly "<"-shaped track which features initial steady west-northwestward motion, then a northward turn while slowing, followed by an acceleration toward the northeast) reach peak intensity at, or before, the point of recurvature; where the point of recurvature is identified as that point where the typhoon reaches its westernmost longitude (JTWC 1994). Many TCs do not undergo classical recurvature. Some never recurve, while others move on a track type designated by the Japan Meteorological Agency (JMA) (1976) as north-

oriented. North-oriented tracks occur predominantly during July through October. Carr and Elsberry (1996) found that a TC may undergo north-oriented motion for only a portion of its track — even if some, or most, of the track was of some other type (e.g., straight-moving). A behavior commonly exhibited by TCs undergoing north-oriented motion — and Fern provides a good example — is reaching peak intensity after turning northward or northeastward, but before the speed of translation of the TC significantly increases.

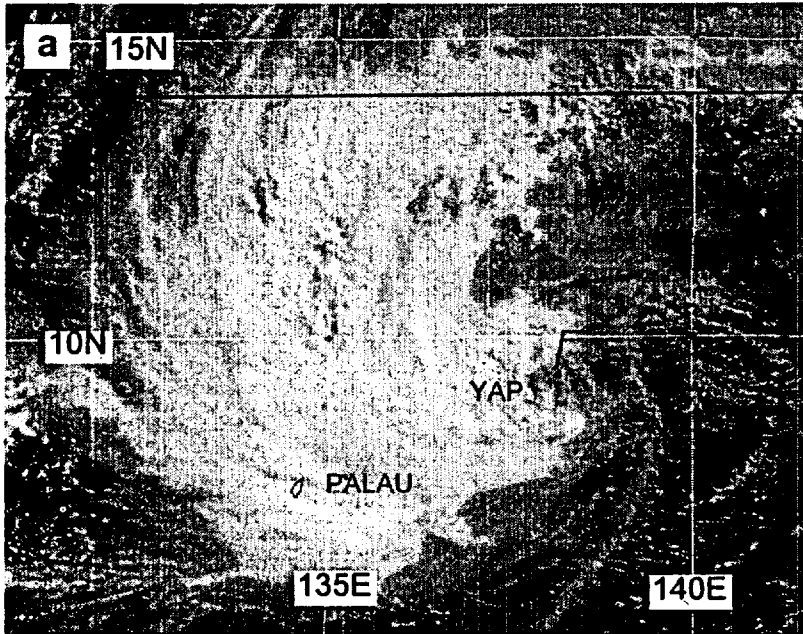
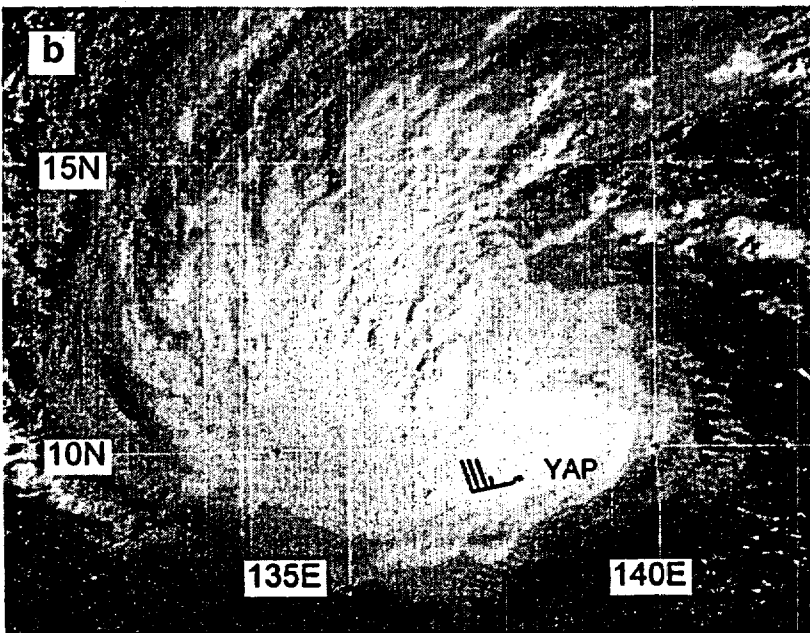


Figure 3-42-1a,b Fern intensifies as it moves directly over Yap: (a) 250531Z December visible GMS imagery, (b) 260631Z December visible GMS imagery.

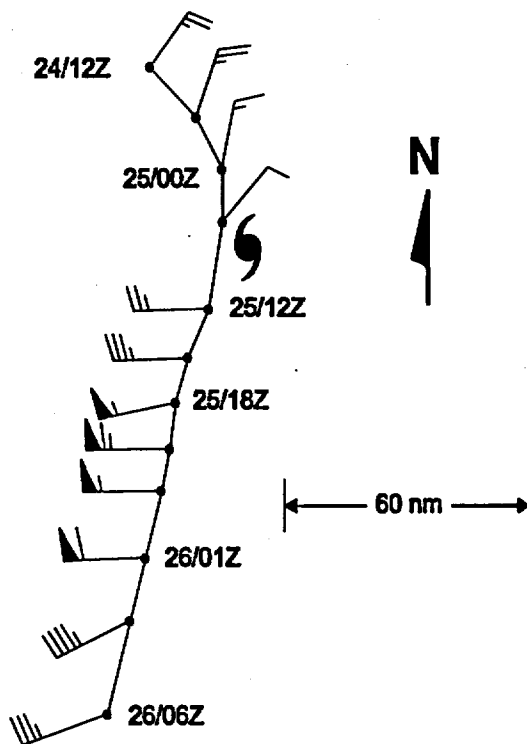


Fern reached peak intensity while moving northward on the north-oriented leg of its track. It weakened when its speed of translation began to climb as it entered the "accelerating westerlies" regime north of the subtropical ridge. Synoptic regimes, such as "poleward oriented" and "accelerating westerlies", associated with specific TC behavior are described in Carr and Elsberry (1996). (See Carlo's (33W) summary for a discussion of a typhoon that underwent similar intensity changes as it moved on a north-oriented track).

IV. IMPACT

Fern passed directly over the island of Yap. High wind and heavy rain there caused an estimate of nearly US\$ 3 million in damage and clean-up costs. Damage to roads and bridges of US \$1.5 million was the highest single-item total. One person was reported injured. At sea, a Maltese tanker rescued eight people who abandoned a cargo ship, the "Mister Bill", after it was crippled by high seas while enroute from Guam to Yap. All (including a five-year-old girl) were unharmed. The eight people had entered a life raft which was spotted by a Navy search-and-rescue aircraft.

a



b

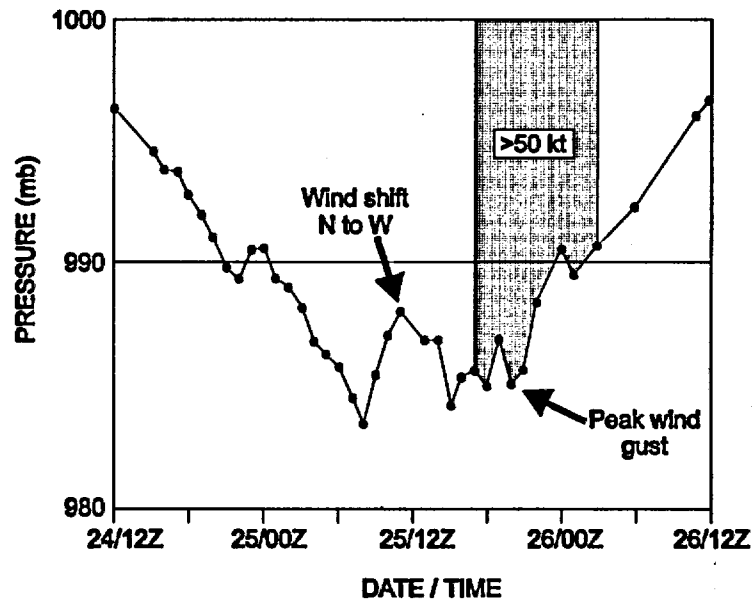
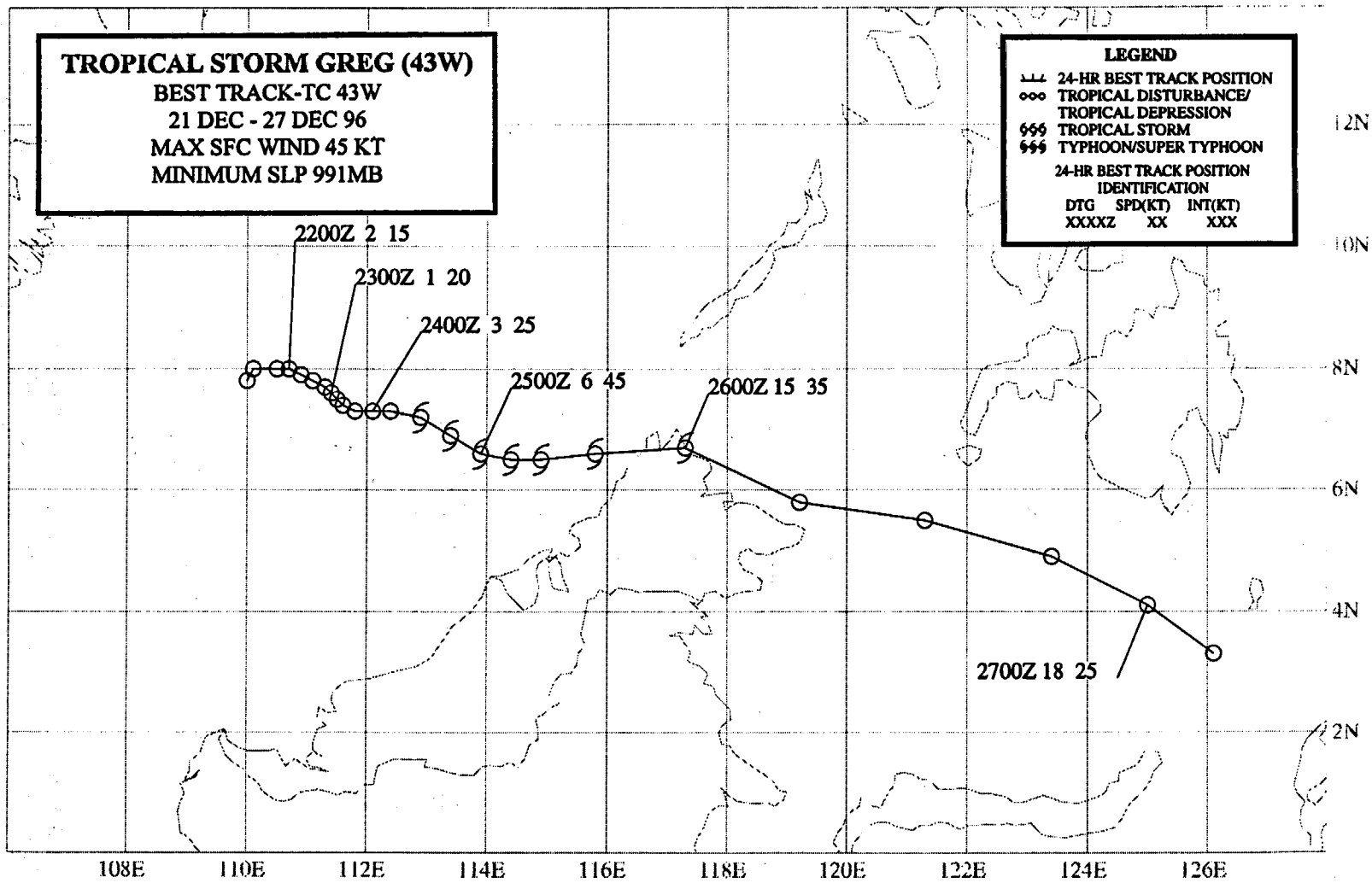


Figure 3-42-2a,b Schematic depiction of (a) peak gusts and (b) sea-level pressure (SLP) recorded at Yap (WMO 91415) during Fern's passage. The peak gust data are recorded with respect to Fern's center. The time series of SLP is based on hourly reports received at the JTWC. Shaded region on SLP diagram indicates wind speeds in excess of 50 kt.

TROPICAL STORM GREG (43W)
BEST TRACK-TC 43W
21 DEC - 27 DEC 96
MAX SFC WIND 45 KT
MINIMUM SLP 991MB

LEGEND
 --- 24-HR BEST TRACK POSITION
 ooo TROPICAL DISTURBANCE/
 TROPICAL DEPRESSION
 999 TROPICAL STORM
 999 TYPHOON/SUPER TYPHOON
 24-HR BEST TRACK POSITION
 IDENTIFICATION
 DTG SPD(KT) INT(KT)
 XXXXZ XX XXX



210

TROPICAL STORM GREG (43W)

I. HIGHLIGHTS

The last significant TC of 1996, Greg was one of the year's most unusual. It formed at low latitude in the South China Sea and moved toward the east-southeast. While passing over the northern tip of Borneo, Greg was responsible for the loss of many lives in the East Malaysian State of Sabah.

II. TRACK AND INTENSITY

During the second half of December, twin low-latitude monsoon troughs became established between approximately 100°E and 170°E. A band of strong low-level westerly winds persisted between the two trough axes. A total of five TCs — two in the Northern Hemisphere (Fern (42W) and Greg) and three in the Southern Hemisphere (Ophelia (11S), Phil (12P), and Fergus (13P)) — formed within these monsoon troughs (Figure 3-43-1).

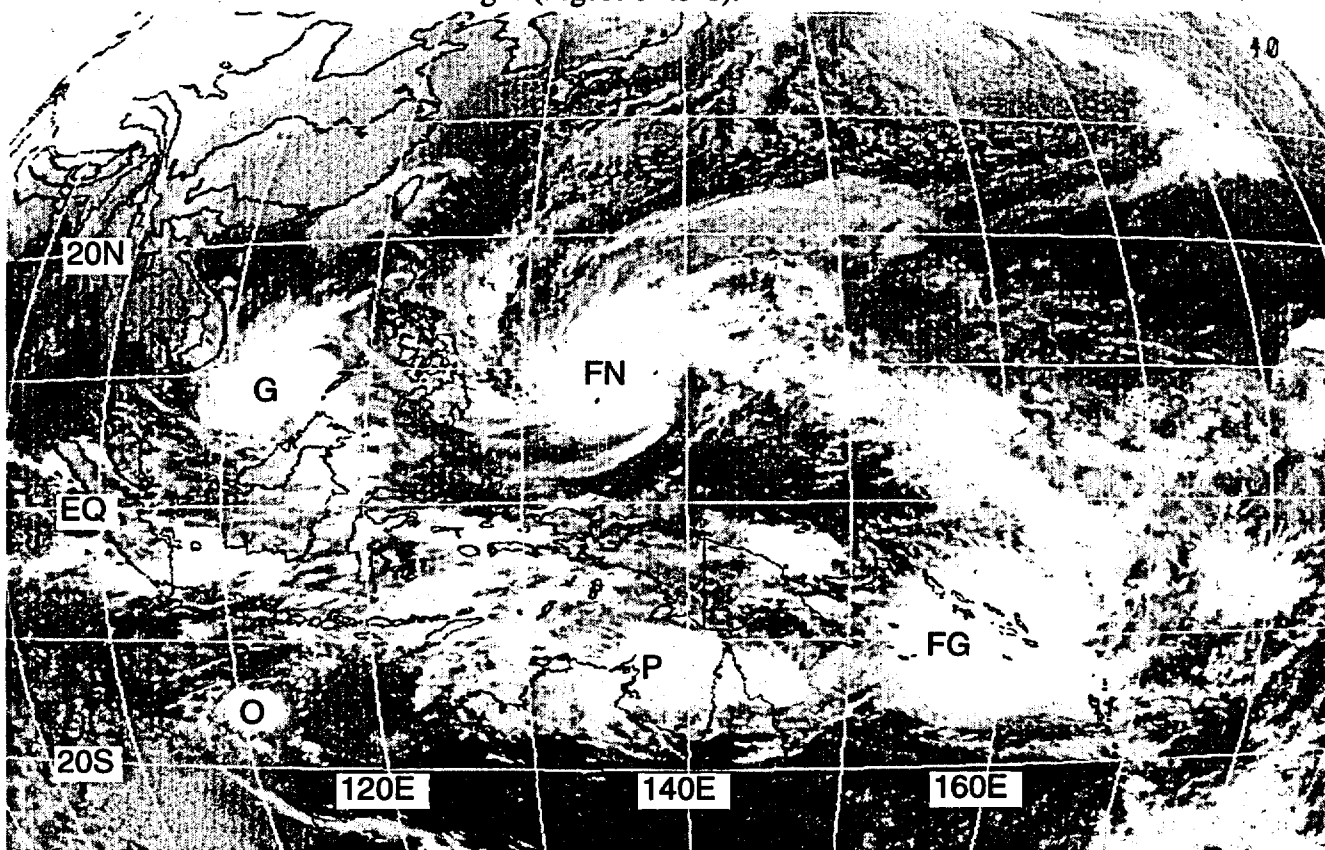


Figure 3-43-1 Five TCs — Greg (G), Fern (FN), Ophelia (O), Phil (P), and Fergus (FG) — lie within twin monsoon troughs (242330Z December infrared GMS imagery).

The tropical disturbance which became Greg was first mentioned on the 210600Z Significant Tropical Weather Advisory when an area of persistent deep convection was observed in the low latitudes of the South China Sea. On 23 December, this area of deep convection began to show signs of becoming better organized. Remarks on the 232100Z Significant Tropical Weather Advisory included:

"[An] area of convection . . . remains near 7N 112E. Animated infrared satellite imagery indicates that the convective organization associated with this system has improved over the past 12 hours in response to an equatorial westerly wind burst. Gradient-level [westerly and southwesterly] winds reported [by stations in East Malaysia are near 30 kt (15 m/sec).] . . ."

JTWC issued a TCFA at 240400Z as visible and microwave satellite imagery indicated that convective organization was improving, and water-vapor imagery supported upper-level divergence over the system. The first warning on Tropical Depression (TD) 43W soon followed, valid at 240600Z. TD 43W was upgraded to Tropical Storm Greg on the warning valid at 250000Z. In postanalysis, however, reanalysis of satellite data determined that Greg most probably became a tropical storm at 241200Z. Continuing to move on a very unusual east-southeastward track, Greg reached a peak intensity of 45 kt (23 m/sec) at 250000Z (Figure 3-43-2) and maintained this intensity until making landfall on the northern tip of Borneo. The final warning was issued, valid at 270600Z, when most of the deep convection associated with the system collapsed as Greg dissipated south of the Philippines.

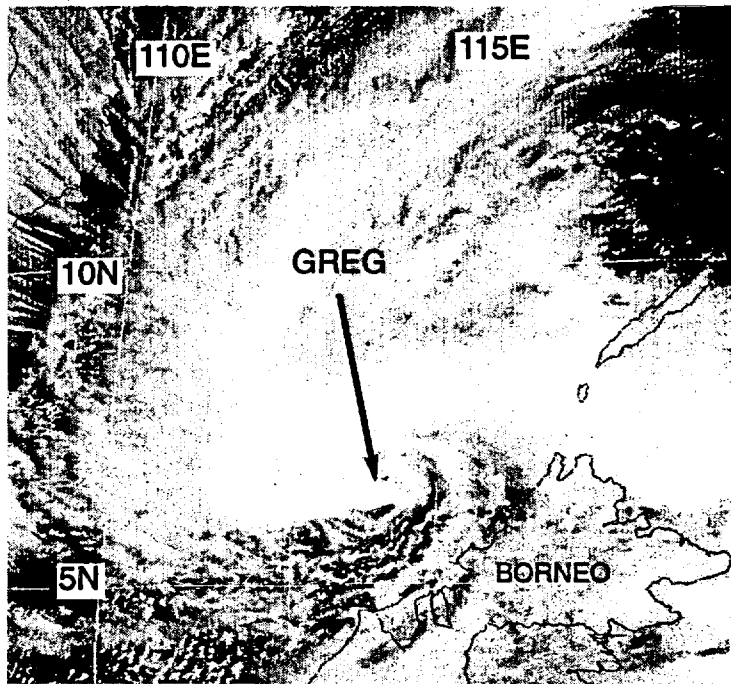


Figure 3-43-2 Greg at peak intensity of 45 kt (23 m/sec) bears down on the northwest coast of Borneo (250231Z December visible GMS imagery).

III. DISCUSSION

a. *On the importance of microwave imagery*

During the night of 24 December, as Greg (then TD 43W) was moving east-southeastward toward the northern tip of Borneo, a DMSP satellite passed over the system at 241452Z. Microwave imagery from this pass (Figure 3-43-3) indicated that a well-organized curved band of deep convection accompanied the LLCC. DMSP passes outside of the range of the Guam ground station are received several hours time-late at the JTWC via the MISTIC system. This imagery was used in postanalysis to upgrade Greg to a tropical storm earlier than indicated on the warnings. Though received late, the microwave imagery was nevertheless used to help support the real-time upgrade of Greg to a tropical storm at 250000Z.

b. Greg's unusual east-southeastward motion

Greg's east-southeastward motion from near 8°N 110°E to near 3°N 126°E was very unusual. TCs which form within (or move into) the South China Sea late in the year are often blocked from moving west by well-established northeasterly monsoon flow. Such TCs often remain quasi-stationary or move southwestward and dissipate. Greg formed in the SCS when an unusual large-scale wind pattern dominated the region: a belt of low-level westerly winds existed in equatorial latitudes between twin monsoon troughs (i.e., one north, the other south of the equator). With the Northeast Monsoon blocking its motion to the west, it is hypothesized that the strong westerly winds to the south of Greg provided the flow asymmetry responsible for its eastward motion. This factor, plus the existence of the large circulation of Fern (42W) to Greg's northeast were cited on prognostic reasoning messages as possible sources of the east-southeastward movement of Greg.

IV. IMPACT

Greg was responsible for loss of life and extensive damage to property in the East Malaysian State of Sabah (located on the northwest coast of Borneo). At least 124 lives were reported lost with another 100 reported missing primarily due to flooding from torrential rains. In Kota Kinabalu, the capital of the State of Sabah, high wind scattered billboards and other debris, and broke windows in the 30-story government building.

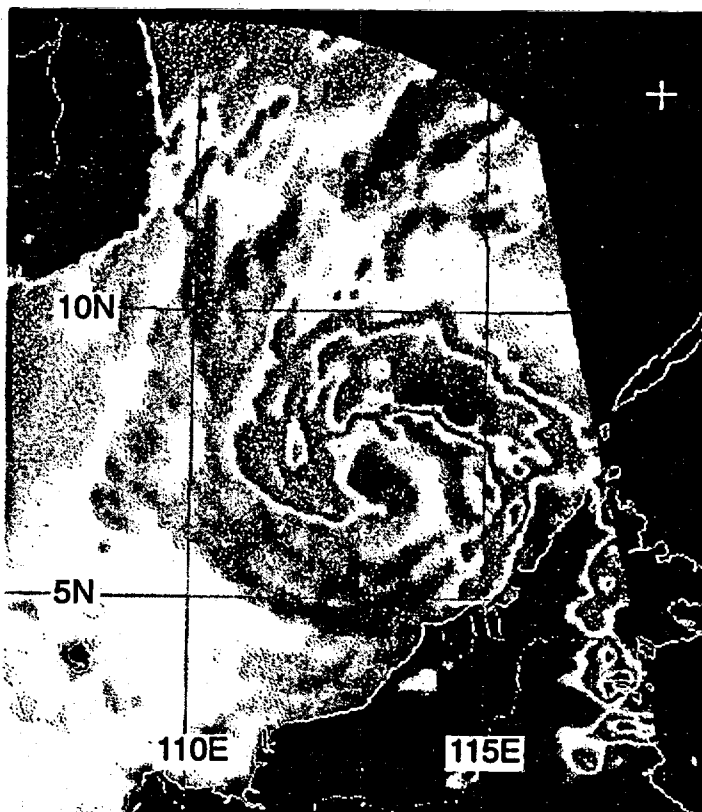


Figure 3-43-3 A well-defined spiral band of deep convection, wrapping almost one complete turn from tip to tail around Greg's LLCC, helped to support the postanalysis upgrade of the timing of tropical storm intensity (241452Z December horizontally polarized 85 GHz SSM/I DMSP imagery).

3.2 NORTH INDIAN OCEAN TROPICAL CYCLONES

In 1996, eight significant tropical cyclones occurred in the North Indian Ocean. Five of these were in the Bay of Bengal and three in the Arabian Sea (Table 3-5). Spring and fall in the North Indian Ocean are periods of transition between major climatic controls, and the most favorable seasons for tropical cyclone activity. This year was no exception

(Table 3-6). The total number, eight, was three over than the 22-year average of five. Eight also tied with the total in 1987, however 1992 still holds the record, 13.

The best track composite is shown in Figure 3-9. There are four cyclones of typhoon intensity (a record) — the most intense being TC 07B. The track of TC 08B is unusual due to its length and large clockwise loop in the Bay of Bengal.

Table 3-5 NORTH INDIAN OCEAN SIGNIFICANT TROPICAL CYCLONES FOR 1996

TROPICAL CYCLONE	PERIOD OF WARNING	NUMBER OF	MAXIMUM SURFACE		ESTIMATED
		WARNINGS ISSUED	WINDS-KT	(M/SEC)	MSLP (MB)
01B	07 MAY - 08 MAY	6	40	(21)	994
02A	11 JUN - 11 JUN	4	40	(21)	994
03B	02 JUN - 17 JUN	20	45	(23)	988*
04A	10 JUN - 19 JUN	8	65	(33)	972*
05A	22 OCT - 26 OCT	15	65	(33)	976
	28 OCT - 31 OCT	15			
06B	25 OCT - 29 OCT	16	45	(23)	991
07B	03 NOV - 07 NOV	16	115	(59)	927
08B	28 NOV - 06 DEC	35	75	(39)	967

TOTAL 135

*MSLP based on synoptic reports

The criteria used in Table 3-6 are as follows:

1. If a tropical cyclone was first warned on during the last two days of a particular month and continued into the next month for longer than two days, then that system was attributed to the second month.
2. If a tropical cyclone was warned on prior to the last two days of a month, it was attributed to the first month, regardless of how long the system lasted.
3. If a tropical cyclone began on the last day of the month and ended on the first day of the next month, that system was attributed to the first month. However, if a tropical cyclone began on the last day of the month and continued into the next month for only two days, then it was attributed to the second month.

Table 3-6 Legend

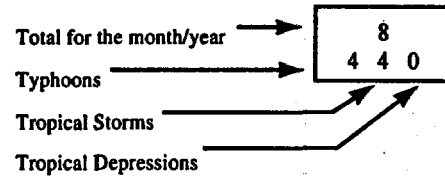


Table 3-6 DISTRIBUTION OF NORTH INDIAN OCEAN TROPICAL CYCLONES FOR 1975-1996

YEAR	JAN	FEB	MAR	APR	MAY	JUN	JUL	AUG	SEP	OCT	NOV	DEC	TOTALS
1975	1	0	0	0	2	0	0	0	0	1	2	0	6
	010	000	000	000	200	000	000	000	000	100	020	000	3 3 0
1976	0	0	0	1	0	1	0	0	1	1	0	1	5
	000	000	000	010	000	010	000	000	010	010	000	010	0 5 0
1977	0	0	0	0	1	1	0	0	0	1	0	2	5
	000	000	000	000	010	010	000	000	000	010	000	110	1 4 0
1978	0	0	0	0	1	0	0	0	0	1	2	0	4
	000	000	000	000	010	000	000	000	000	010	200	000	2 2 0
1979	0	0	0	0	1	1	0	0	2	1	2	0	7
	000	000	000	000	100	010	000	000	011	010	011	000	1 4 2
1980	0	0	0	0	0	0	0	0	0	0	1	1	2
	000	000	000	000	000	000	000	000	000	000	010	010	0 2 0
1981	0	0	0	0	0	0	0	0	1	0	1	1	3
	000	000	000	000	000	000	000	000	010	000	100	100	2 1 0
1982	0	0	0	0	1	1	0	0	0	2	1	0	5
	000	000	000	000	100	010	000	000	000	020	100	000	2 3 0
1983	0	0	0	0	0	0	0	1	0	1	1	0	3
	000	000	000	000	000	000	000	010	000	010	010	000	0 3 0
1984	0	0	0	0	1	0	0	0	0	1	2	0	4
	000	000	000	000	010	000	000	000	000	010	200	000	2 2 0
1985	0	0	0	0	2	0	0	0	0	2	1	1	6
	000	000	000	000	020	000	000	000	000	020	010	010	0 6 0
1986	1	0	0	0	0	0	0	0	0	0	2	0	3
	010	000	000	000	000	000	000	000	000	000	020	000	0 3 0
1987	0	1	0	0	0	2	0	0	0	2	1	2	8
	000	010	000	000	000	020	000	000	000	020	010	020	0 8 0
1988	0	0	0	0	0	1	0	0	0	1	2	1	5
	000	000	000	000	000	010	000	000	000	010	110	010	1 4 0
1989	0	0	0	0	1	1	0	0	0	0	1	0	3
	000	000	000	000	010	010	000	000	000	000	100	000	1 2 0
1990	0	0	0	1	1	0	0	0	0	0	1	1	4
	000	000	000	001	100	000	000	000	000	000	001	010	1 1 2
1991	1	0	0	1	0	1	0	0	0	0	1	0	4
	010	000	000	100	000	010	000	000	000	000	010	000	1 3 0
1992	0	0	0	0	1	2	1	0	1	3	3	2	13
	000	000	000	000	100	020	010	000	001	021	210	020	3 8 2
1993	0	0	0	0	0	0	0	0	0	0	2	0	2
	000	000	000	000	000	000	000	000	000	000	200	000	2 0 0
1994	0	0	1	1	0	1	0	0	0	1	1	0	5
	000	000	010	100	000	010	000	000	000	010	010	000	1 4 0
1995	0	0	0	0	0	0	0	0	1	1	2	0	4
	000	000	000	000	000	000	000	000	010	010	200	000	2 2 0
1996	0	0	0	0	1	3	0	0	0	2	2	0	8
	000	000	000	000	010	120	000	000	000	110	200	000	4 4 0
(1975-1995)													
MEAN	0.2	0.1	0.1	0.2	0.6	0.6	0.1	0.1	0.3	0.9	1.4	0.6	4.8
CASES	3	1	1	4	12	12	1	1	6	19	29	12	101

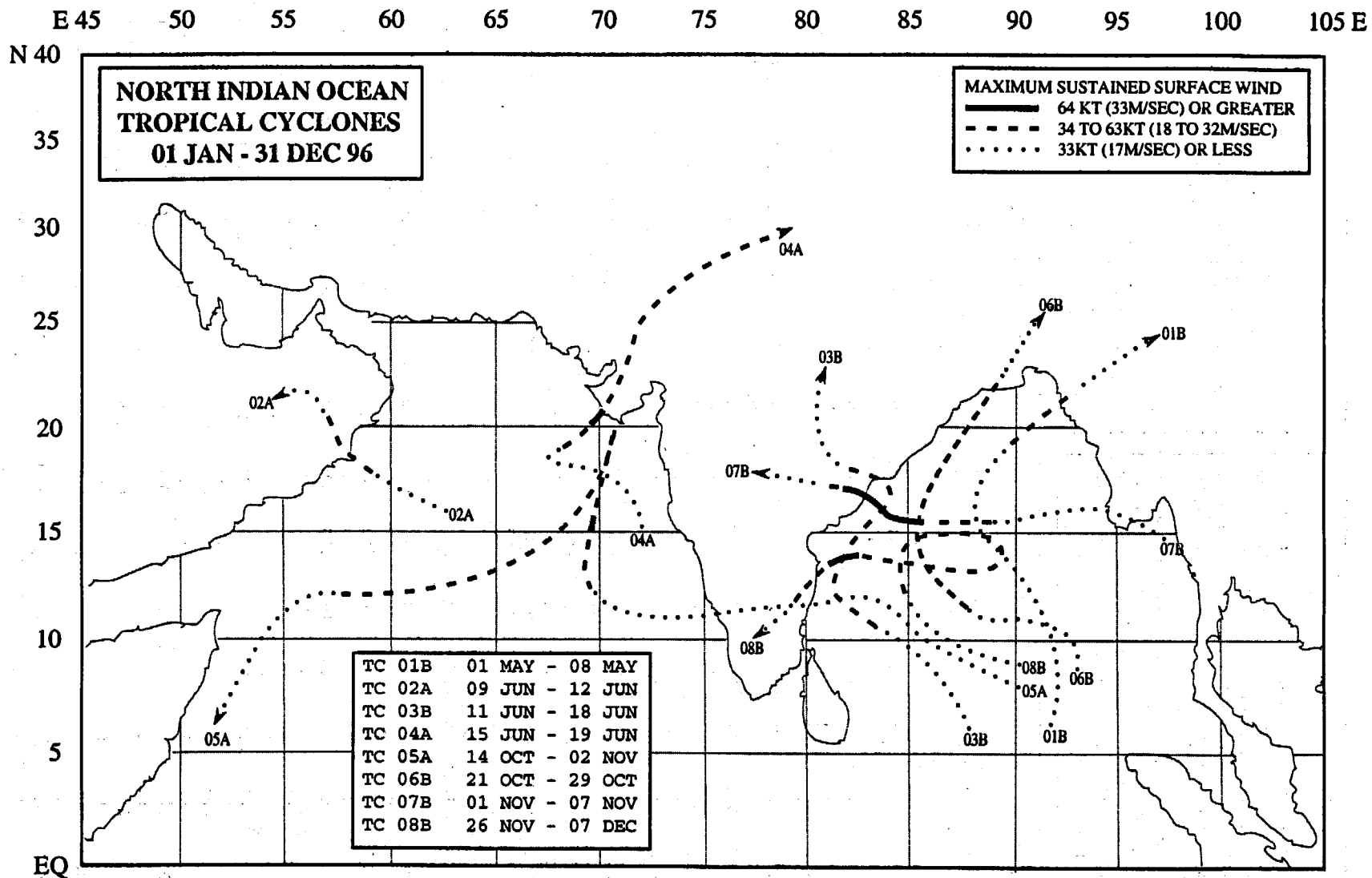
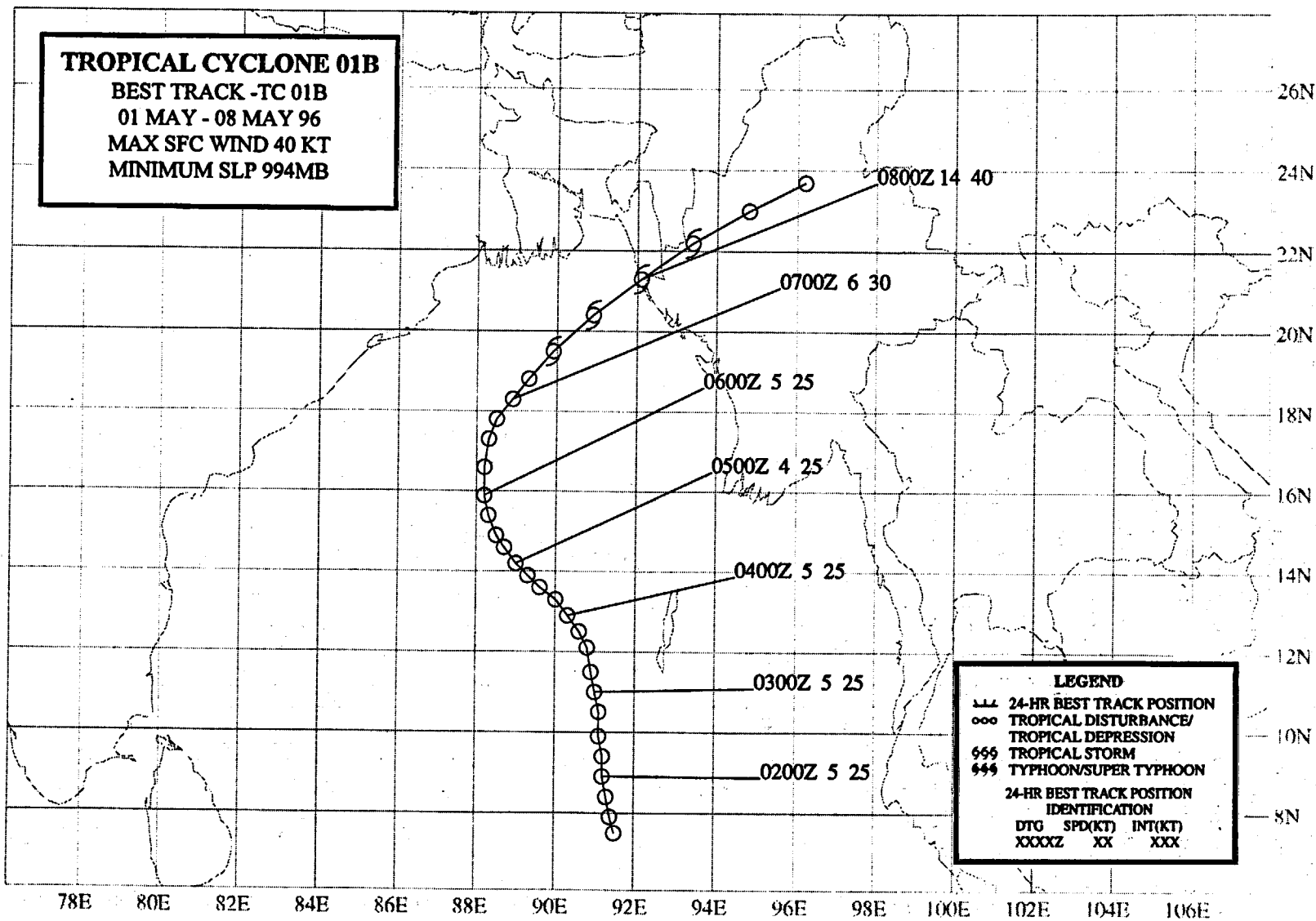


Figure 3-9 Composite of best tracks for North Indian Ocean tropical cyclones for 1996.



TROPICAL CYCLONE 01B

On the first day of May, the tropical disturbance that was to become TC 01B was first observed as a broad area of deep convection in the monsoon trough, 240 nm (440 km) northwest of Sumatra. In the Southern Hemisphere, a "twin" cyclone, which would become Jenna (28S), was also developing (Figure 3-01B-1) in conjunction with the same equatorial westerly wind burst. At 020230Z, the Significant Tropical Weather Advisory was reissued to include both the persistent deep convection associated with pre-TC 01B and the first warning for TC 28S. As the pre-TC 01B disturbance tracked slowly northward, its cloud system organization finally improved to a point where JTWC issued the first TCFA at 051230Z. A second TCFA followed at 061230Z which stated: "... [Although] the [cloud] system organization has changed little from the previous alert ... [it] should improve in the low-shear environment . . [near] the ridge [axis].." Based on DMSP SSM/I and ERS-2 scatterometer data, indicating 30-kt (15-m/sec) winds near the LLCC, JTWC issued the first warning, valid at 070000Z. Intensification continued until TC 01B reached a peak of 40 kt (21 m/sec) at 071800Z — six hours prior to making landfall near Cox's Bazar. Cox's Bazar (WMO 41992) experienced a maximum sustained wind of 40 kt (21 m/sec) and a minimum sea-level pressure of 993 mb. The cyclone dissipated over the mountainous terrain of Myanmar less than a day later. The JTWC received no reports of death or significant damage.

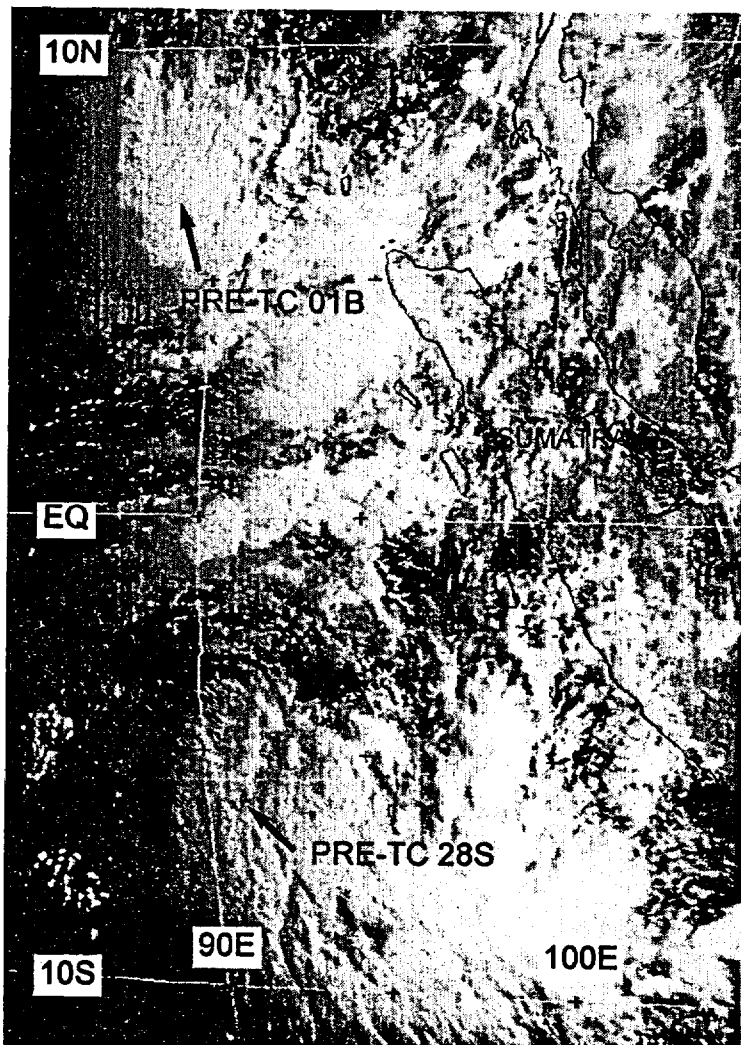
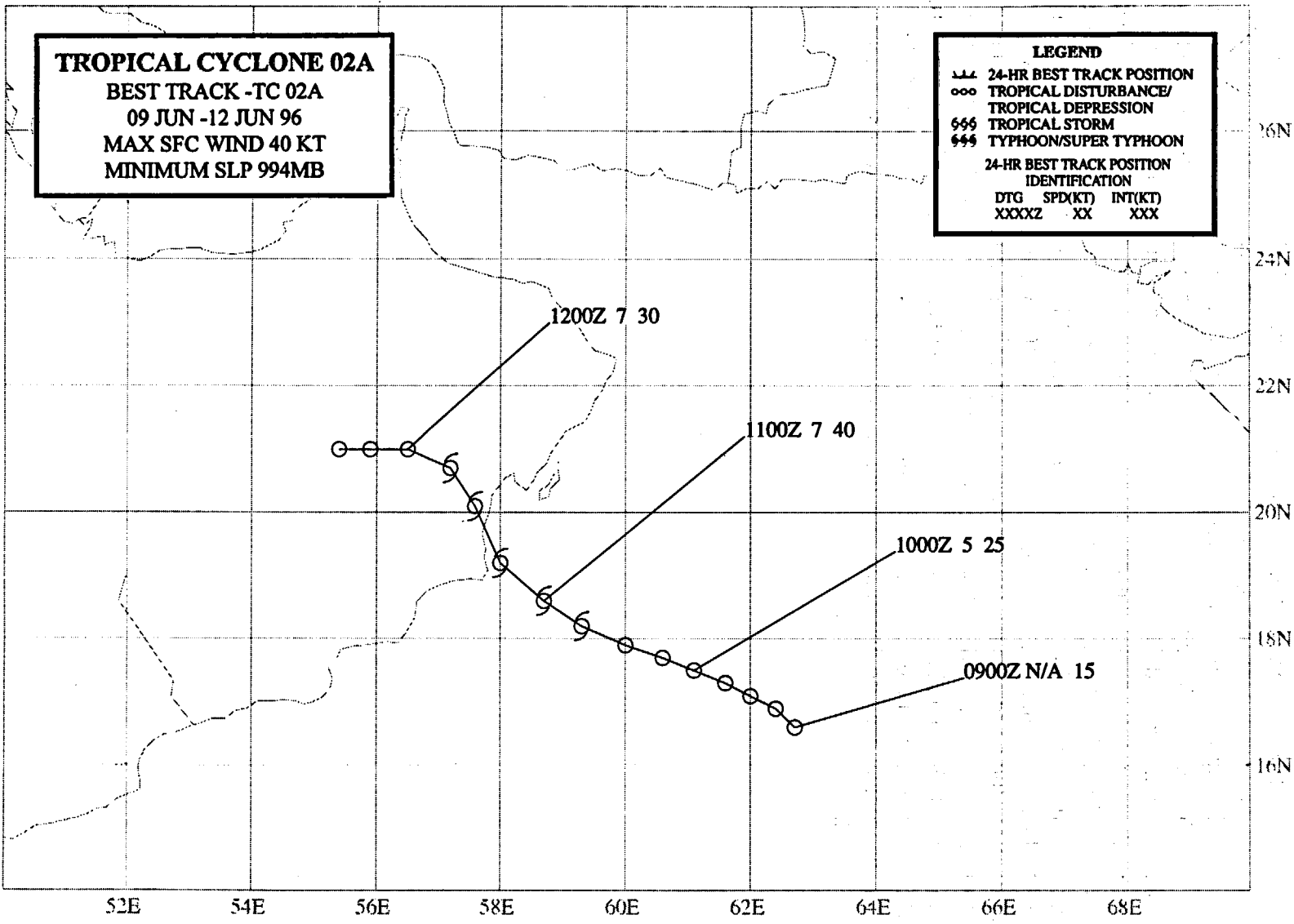


Figure 1-01B-1 The "twin" cyclones — pre-TC 01B and TC 28S — consolidate near the equator (020031Z May visible GMS imagery).



TROPICAL CYCLONE 02A

The second of eight 1996 North Indian Ocean cyclones, TC 02A was the first of three to occur in the Arabian Sea. The tropical disturbance which became TC 02A was initially observed as an area of poorly organized convection in the northwestern Arabian Sea 800 nm (1480 km) northeast of Somalia. Because the convection persisted, the Significant Tropical Weather Advisory was reissued at 092000Z June to include first mention of the disturbance. Based on a combination of infrared, microwave imager, and ERS-2 scatterometer data indicating sustained surface winds of 20-30 kt (10-15 m/sec), a TCFA was issued, valid at 102000Z. Moderate vertical wind shear was expected to slow intensification, however, intensification continued and the first warning was issued, valid at 110000Z. As TC 02A approached the coast, Fahad (WMO 41262), an inland air base on the Arabian Peninsula, recorded maximum sustained 10-minute mean northerly winds of 35 kt (17 m/sec) at 110300Z and Masirah (WMO 41268) recorded a minimum sea-level pressure of 994 mb at 110000Z. The system continued on a west-northwestward track at a peak of 40 kt (21 m/sec) until making landfall 70 nm (130 km) southwest of Al Masirah Island at 110900Z. Figure 3-02A-1 shows TC 02A a few hours before landfall. The final warning was issued, valid at 111800Z, as the remnants of the tropical cyclone dissipated over the desert. No reports of death or significant damage were received.

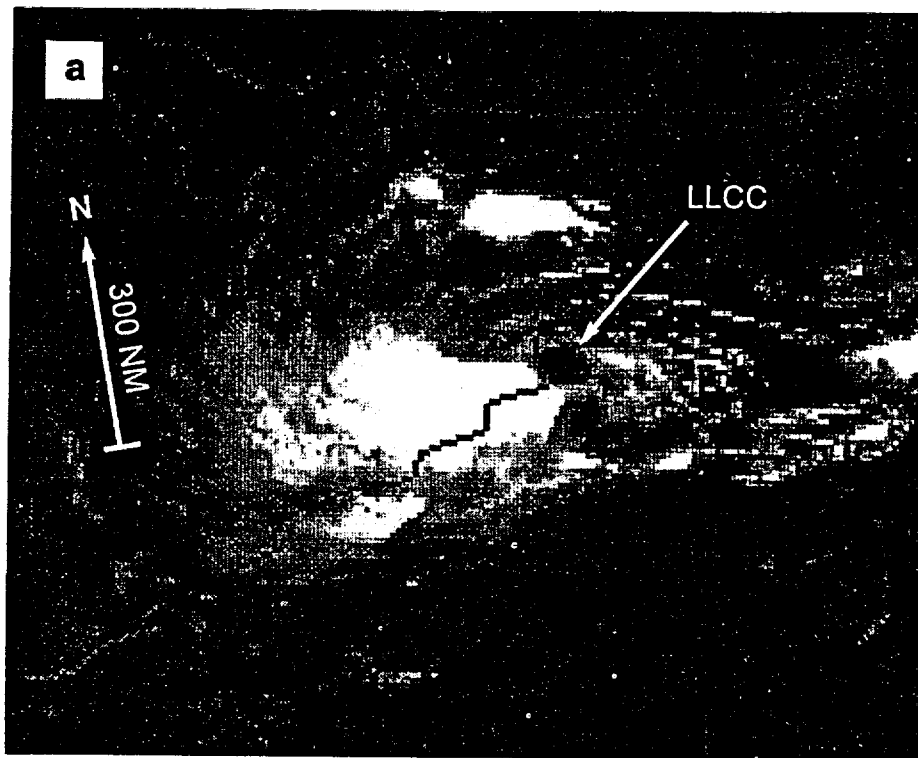
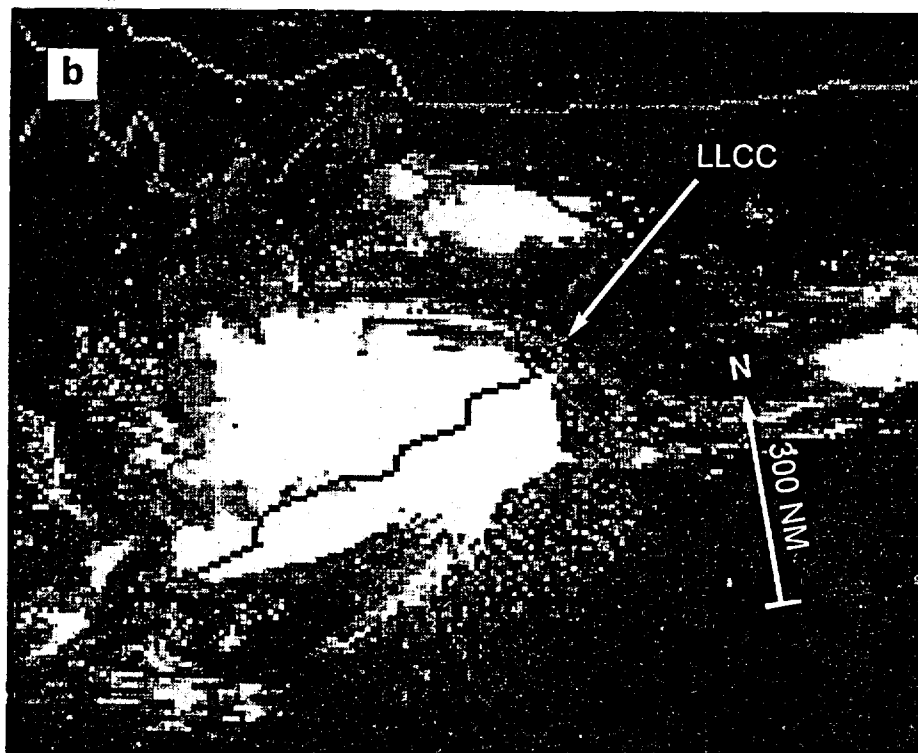


Figure 3-02A-1 TC 02A shortly before making landfall in Oman. Note the significant difference in the cloudiness as viewed in the visible (a) and infrared (b) images. The LLCC is apparent in the visible, but not in the infrared (DMSP imagery courtesy of the Space Physics Interactive Data Resource (SPIDR) Internet site maintained by the National Geophysical Data Center).

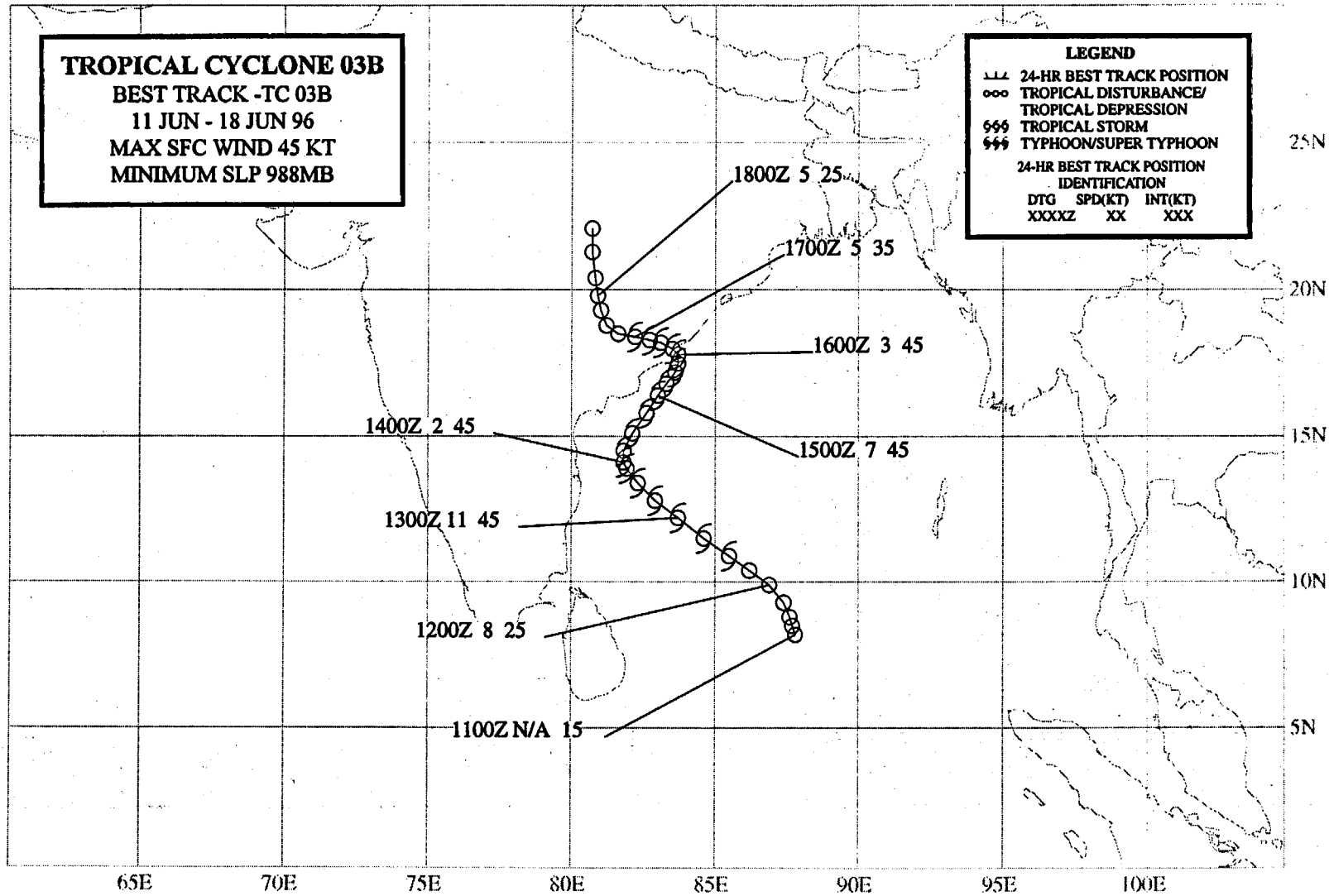


TROPICAL CYCLONE 03B
BEST TRACK - TC 03B
11 JUN - 18 JUN 96
MAX SFC WIND 45 KT
MINIMUM SLP 988MB

LEGEND

--- 24-HR BEST TRACK POSITION
 ooo TROPICAL DISTURBANCE/
 TROPICAL DEPRESSION
 \$\$\$ TROPICAL STORM
 \$\$\$ TYPHOON/SUPER TYPHOON

24-HR BEST TRACK POSITION
 IDENTIFICATION
 DTG SPD(KT) INT(KT)
 XXXXZ XX XXX



222

TROPICAL CYCLONE 03B

The convection associated with the tropical disturbance that became Tropical Cyclone 03B (TC 03B) consolidated rapidly in the monsoon trough, prompting JTWC to issue a TCFA at 111930Z June. Based on animated satellite imagery, indicating increased convective organization, the first warning was issued, valid at 120600Z. Eighteen hours later, TC 03B reached its maximum intensity of 45 kt (23 m/sec), which it maintained for nearly four days (Figure 3-03B-1). As the cyclone began to weaken, its track changed to a northeastward motion. The cyclone changed to a west-northwest track at 160000Z and made landfall five hours later about 25 nm (46 km) northeast of Vishakhapatnam (WMO 43149) on the Andhra Pradesh coast of India. Vishakhapatnam observed 30-kt (10-minute average) (15 m/sec) sustained winds and a minimal sea-level pressure of 987 mb at 160000Z. Waltair (43150) also reported 30 kt (15 m/sec) winds at that time. Once TC 03B was over land, JTWC issued a final warning valid at 170000Z.

Despite the relative weakness of the cyclone, torrential rains accompanied TC 03B inland (Figure 3-03B-2). Flooding from the heavy rains resulted in the loss of 175 lives, more than 3,000 families homeless, and extensive damage. News reports also indicated 270 people (mostly fishermen) were missing.

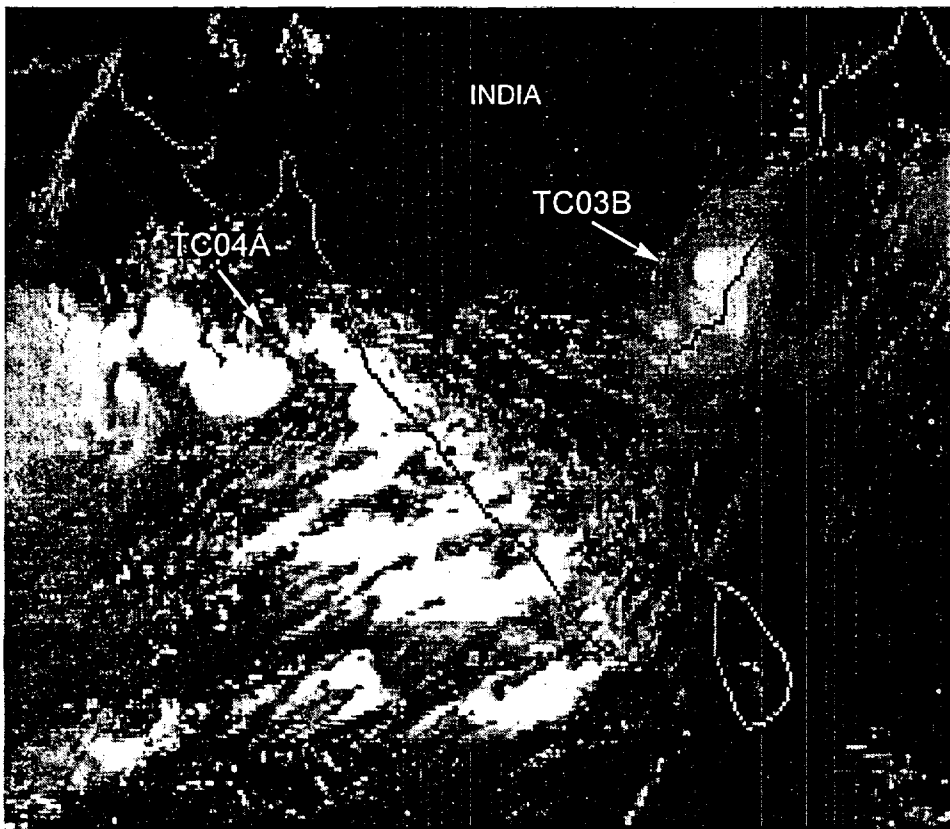


Figure 3-03B-1 As the LLCC of TC 03B nears the coast, deep convection builds inland (160350Z June visible DMSP imagery downloaded from the Space Physics Interactive Data Resource (SPIDR) Internet site maintained by National Geophysical Data Center (NGDC)).

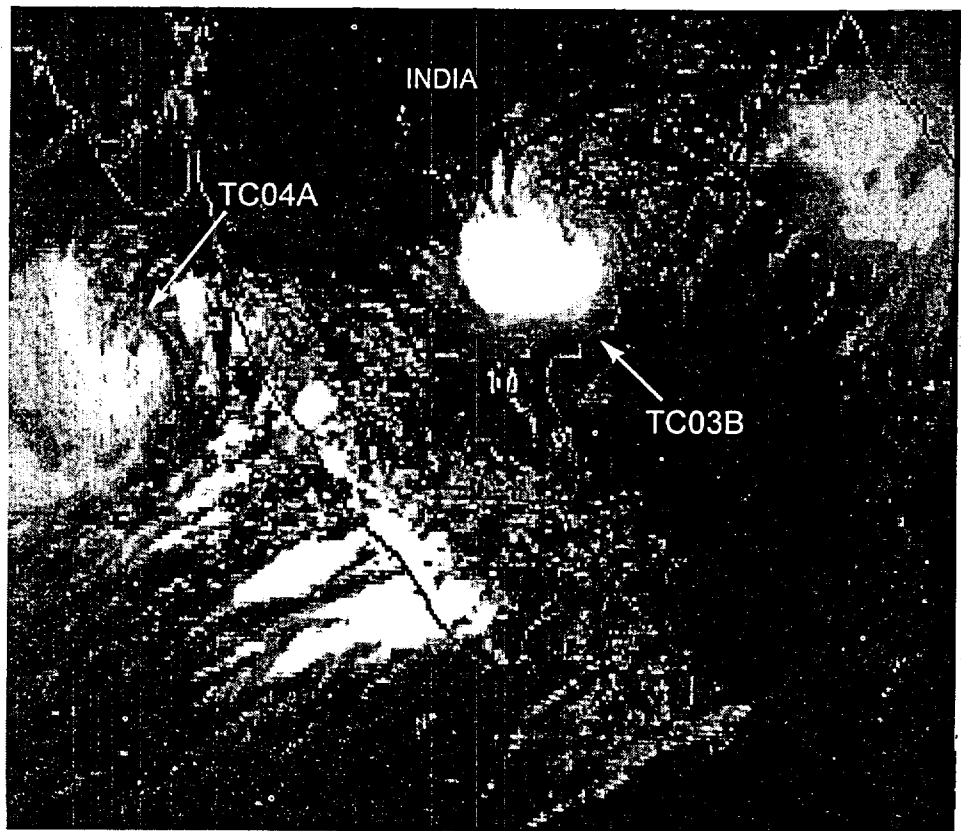
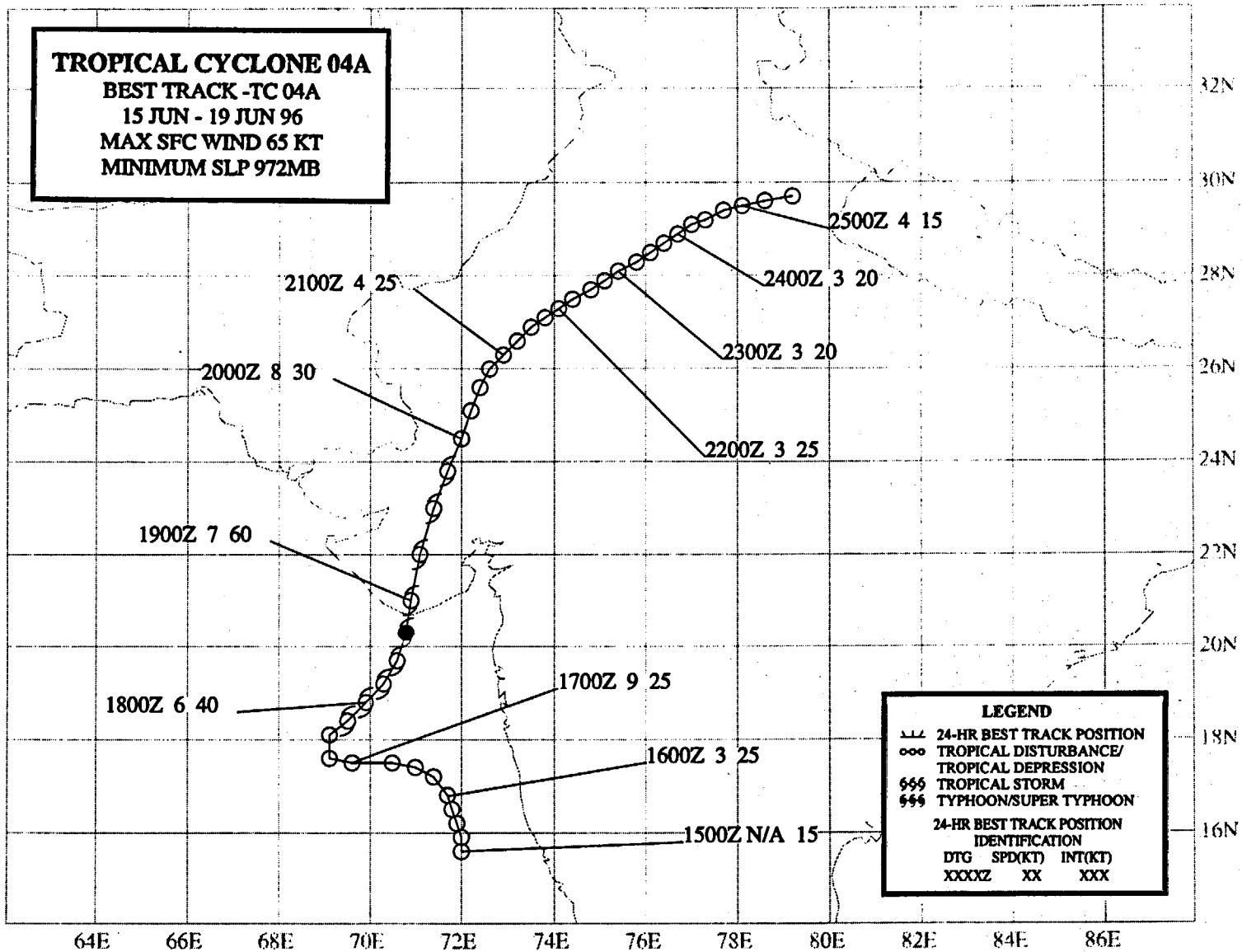


Figure 3-03B-2 In comparison with Figure 3-03B-1, approximately 24 hours later, the convection associated with TC 03B has increased dramatically and is producing widespread torrential rains (170337Z June visible DMSP imagery downloaded from SPIDR).



TROPICAL CYCLONE 04A

On 15 June, a day before TC 03B made landfall on the east coast of India, convection associated with the monsoon depression that became TC 04A was first detected on satellite imagery off the west coast of India 210 nm (390 km) south-southwest of Bombay. Although poorly organized, the convection persisted and was first mentioned on the Significant Tropical Weather Advisory at 170700Z. A TCFA was issued at 170730Z June after conventional and microwave satellite data indicated that the wind field had become better organized, and a first warning followed, valid at 171800Z. As TC 04A moved northward and intensified, available Dvorak intensity estimates peaked at 45 kt (23 m/sec). However, synoptic data supported a maximum of 65 kt (33 m/sec) as the cyclone approached the coast. TC 04A made landfall near Diu at 182300Z. Diu is located on the coast of India 330 nm (610 km) southeast of Karachi. Veraval (WMO 42909) reported a minimum sea-level pressure of 974 mb at 182300Z. Rajkot (WMO 42737), 75 nm (139 km) inland, reported a minimum sea-level pressure of 980 mb at 190600Z and 10-minute sustained wind of 46 kt (24 m/sec) at 191200Z. Figure 3-04A-1 shows the 3-hourly surface winds at Rajkot which reflect the passage of the cyclone. JTWC issued the final warning valid at 191200Z, as TC 04A dissipated inland. Figure 3-04A-2 shows convection associated with TC 04A as it moved northward into India.

The maximum storm surge on the southern coast was estimated to be 20 feet (6 meters). Indian government agencies reported 47 people were killed by the cyclone.

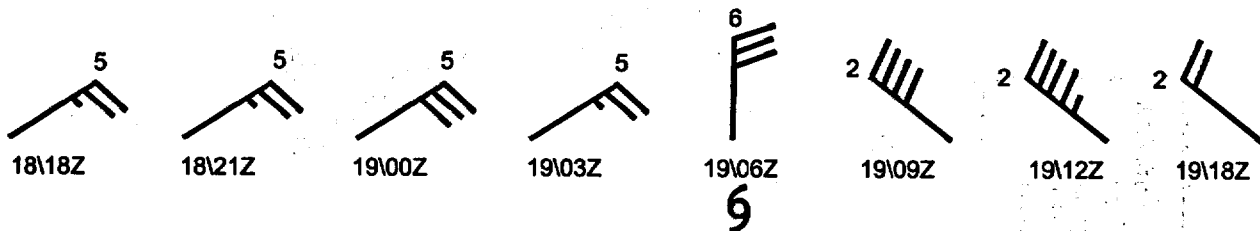


Figure 3-04A-1 Surface wind reports at Rajkot, India (WMO 42737) reflect the passage of TC 04A.

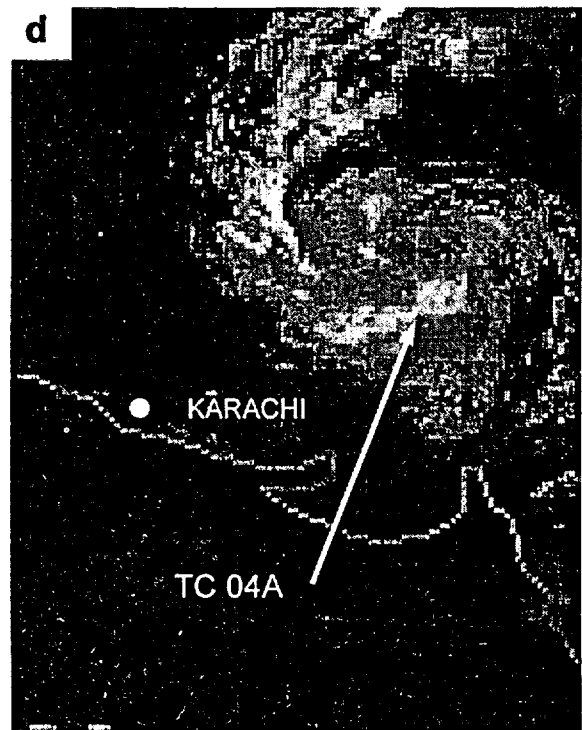
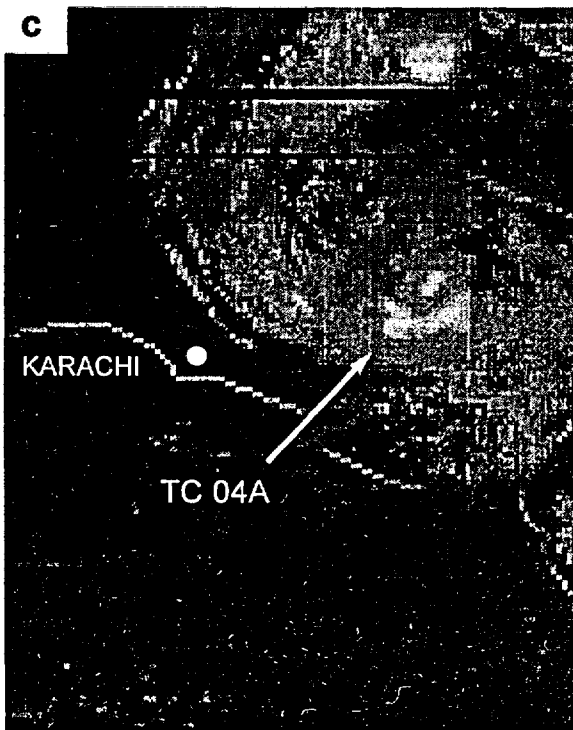
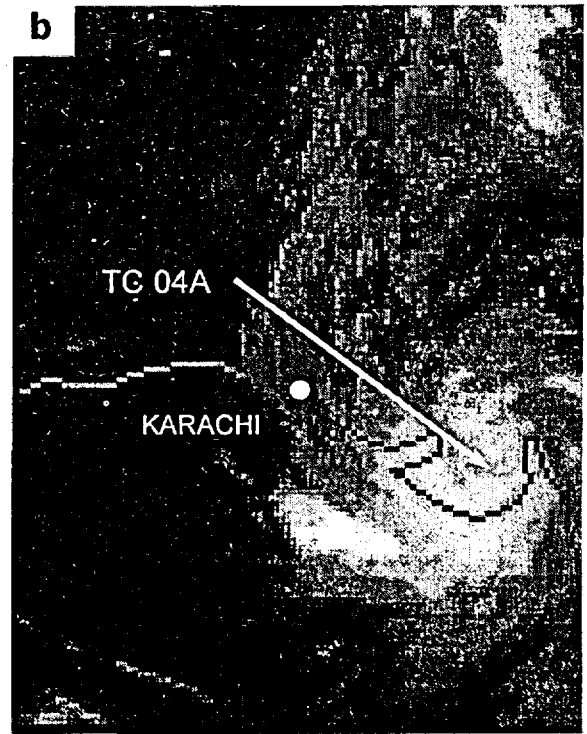
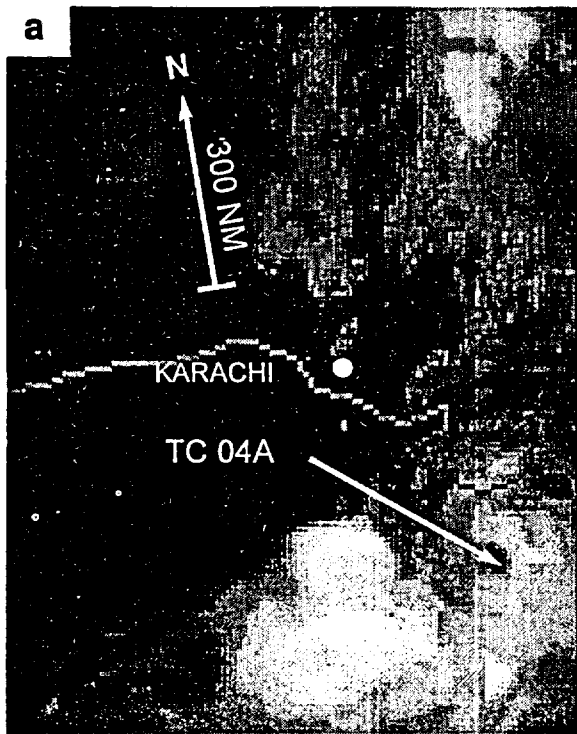


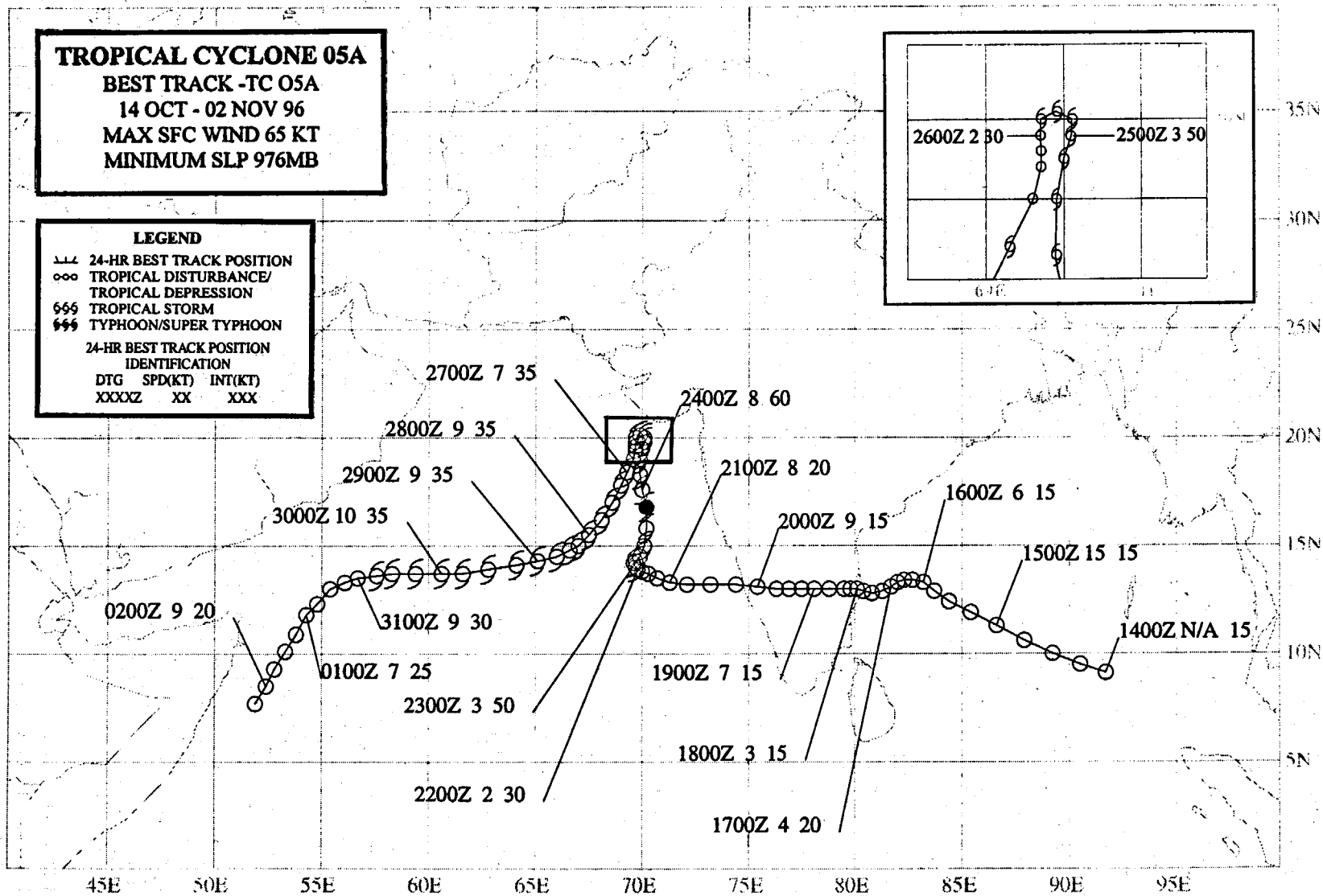
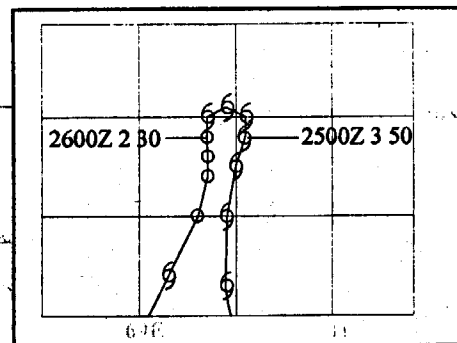
Figure 3-04A-2 Visible imagery — (a) 180507Z June; (b) 190455Z; (c) 200443Z; and (d) 210431Z — covering a 4-day period tracks TC 04A's passage from the Arabian Sea northward into India (Visible DMSP imagery downloaded from SPIDR).

TROPICAL CYCLONE 05A

BEST TRACK - TC 05A
14 OCT - 02 NOV 96
MAX SFC WIND 65 KT
MINIMUM SLP 976MB

LEGEND

- 24-HR BEST TRACK POSITION
 - ooo TROPICAL DISTURBANCE/
TROPICAL DEPRESSION
 - 666 TROPICAL STORM
 - 666 TYPHOON/SUPER TYPHOON
- 24-HR BEST TRACK POSITION
IDENTIFICATION
DTG SPD(KT) INT(KT)
XXXXZ XX XXX



TROPICAL CYCLONE 05A

I. HIGHLIGHTS

Tropical Cyclone 05A (TC 05A), the third Arabian Sea cyclone of 1996, initially started as a mid-October disturbance in the Bay of Bengal, and had one of the most unusual tracks in North Indian Ocean cyclone history. It moved across southern India into the Arabian Sea, stopped, turned north, and intensified. Near 20°N 70°E, the system turned to the southwest, and remained on that track for nine days before dissipating near the Somalia coast. TC-05A was one of the longest-lived cyclones ever in the North Indian Ocean. The Arabian Sea generally averages about one cyclone per year.

II. TRACK AND INTENSITY

TC 05A was first observed as a suspicious area of convection in the southwest Bay of Bengal, about 350 nm (648 km) east of Madras (WMO 43279) on 14 October. After crossing the southern part of the Indian Peninsula and entering the Arabian Sea at speeds ranging from 3-13 kt (5.5-24 km/hr), the disturbance began to organize, and a Tropical Cyclone Formation Alert was issued at 211600Z based on an observed increase in convective curvature and low-level cloud lines in satellite imagery. Shortly thereafter, the disturbance abruptly stopped, began to intensify, and turned to the north near 70°E. The first warning was valid at 221200Z based on a Dvorak T-number of T2.5 (35 kt; 18 m/sec) (Figure 3-05A-1). The system reached an intensity of 65 kt (34 m/sec) (Figure 3-05A-2) on its northward track, then suddenly stopped its northward movement about 50 nm (93 km) south of the southern coast of Gujarat State of northwestern India, after running into strong northeasterly shear. Six hours later, the system began to rapidly weaken from the shear, and took a south-southward track. The final warning was issued at 260000Z, but the system was monitored for regeneration. Figure 3-05A-3 shows the remnants of the cyclone on microwave imagery. These remnants of TC 05A drifted south, away from the region of strong vertical wind shear which had blown away the deep convection. A second Tropical Cyclone Formation Alert was generated at 271600Z when a ship indicated the remnants of TC 05A had a central pressure of 996 mb and 35-kt (18-m/sec) sustained winds. At 280000Z, warnings were resumed for the regenerated cyclone. The system remained, on a southwestward track at minimal tropical-storm intensity. TC 05A finally weakened about two days later, and the final warning was issued at 311200Z while the depression was 60 nm (111 km) northeast of Socotra Island (Figure 3-05A-4).

III. IMPACT

No reports of injuries or damage were received at the JTWC.

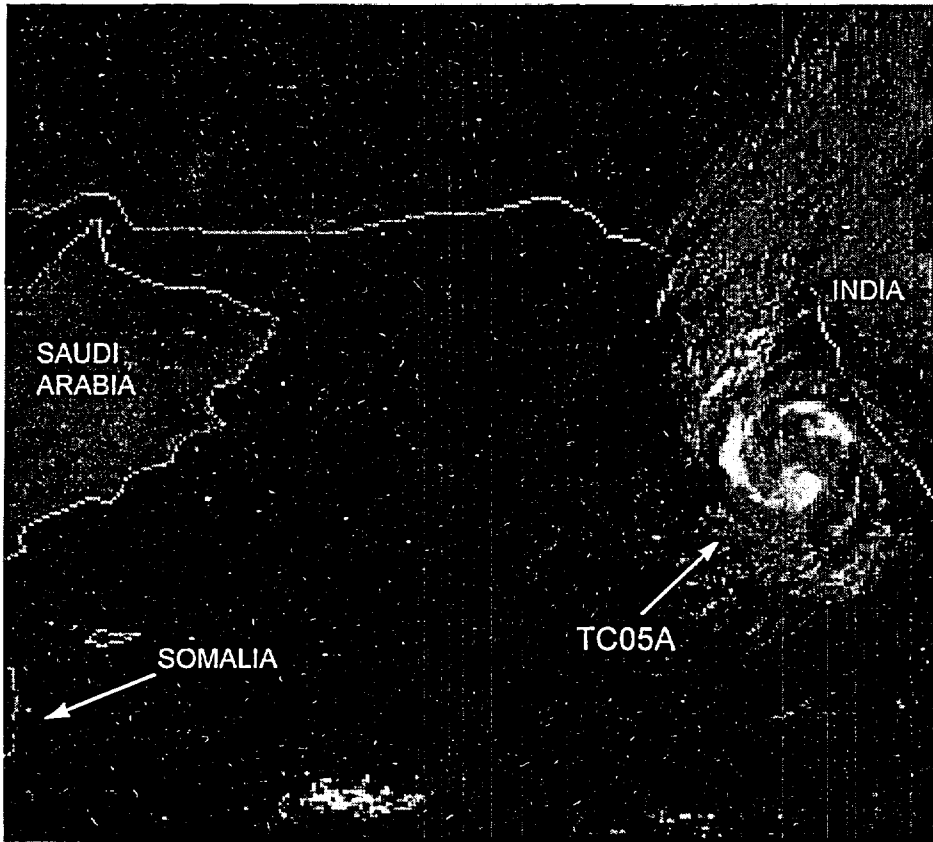


Figure 3-05A-1 TC-05A as deep convection begins to build over the LLCC. (230450Z October DMSP visible imagery). (Imagery downloaded from the Space Physics Interactive Data Resource (SPIDR) internet site maintained by NGDC).

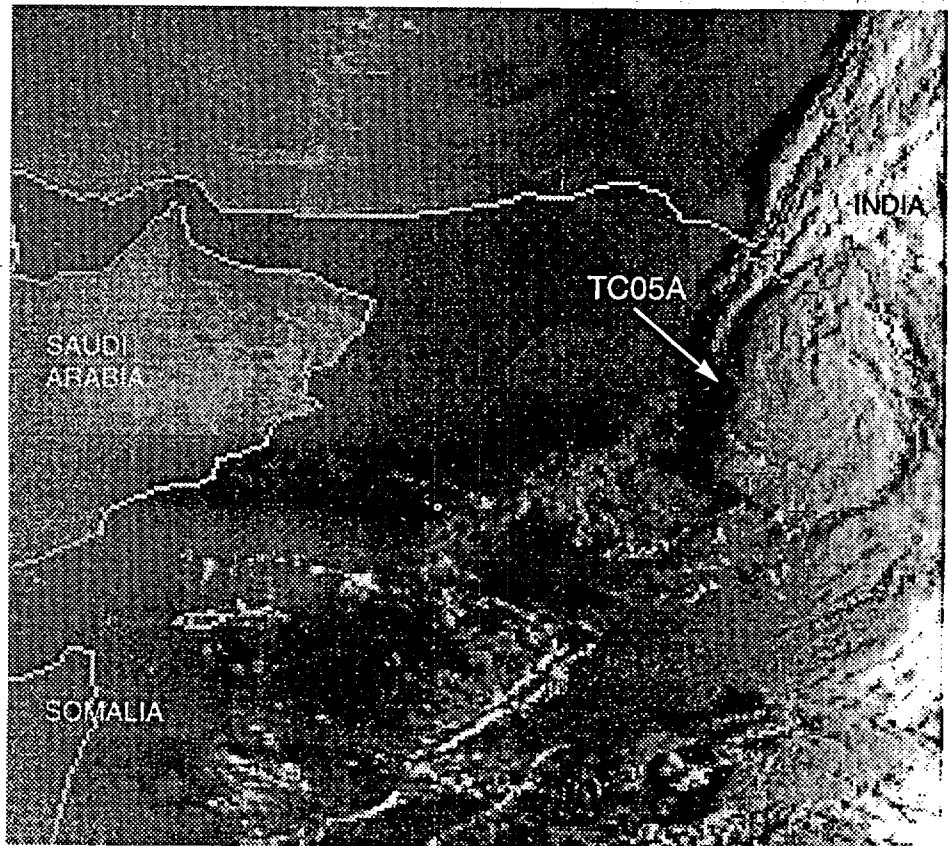


Figure 3-05A-2 TC-05A at a Dvorak T4.0 (240114Z October DMSP visible imagery). (Imagery downloaded from SPIDR).

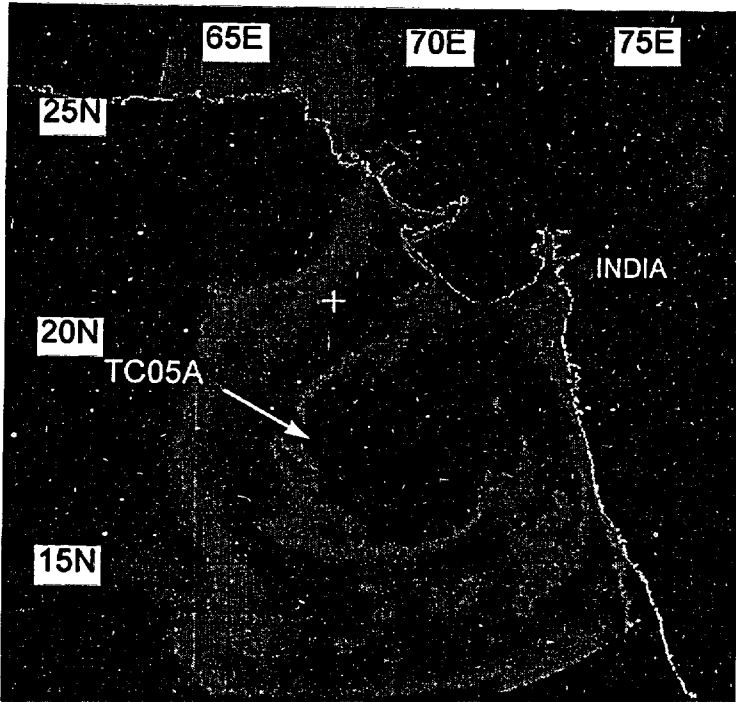
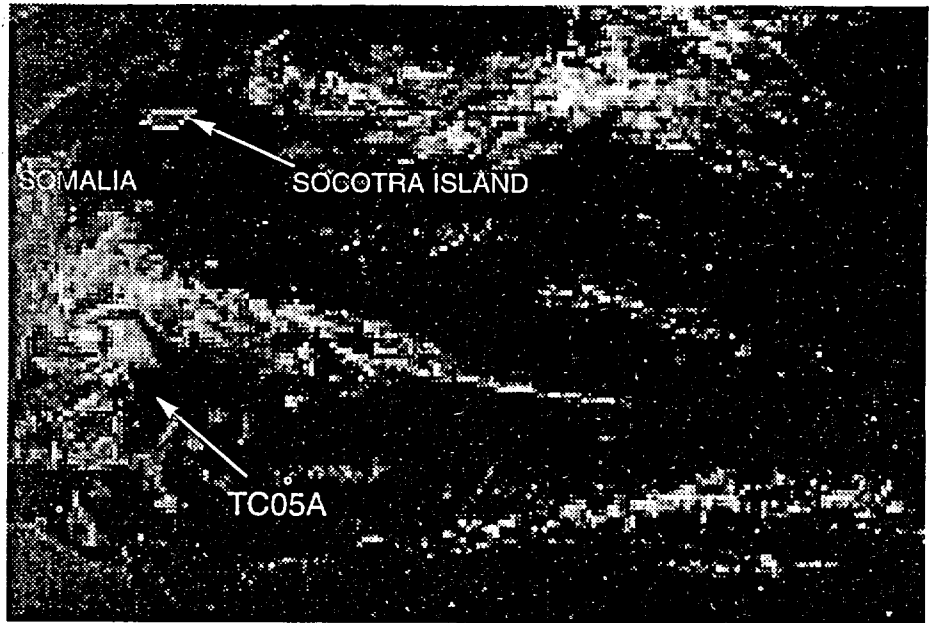


Figure 3-05A-3 The remnants of TC-05A after it had sheared from the convection. The dark circulation signifies low-and-middle-level clouds. (270127Z October DMSP microwave imagery).

Figure 3-05A-4 The remnant LLCC of TC-05A as it approached the Somali coast (020430Z November DMSP visible imagery). (Imagery downloaded from SPIDR).



TROPICAL CYCLONE 06B

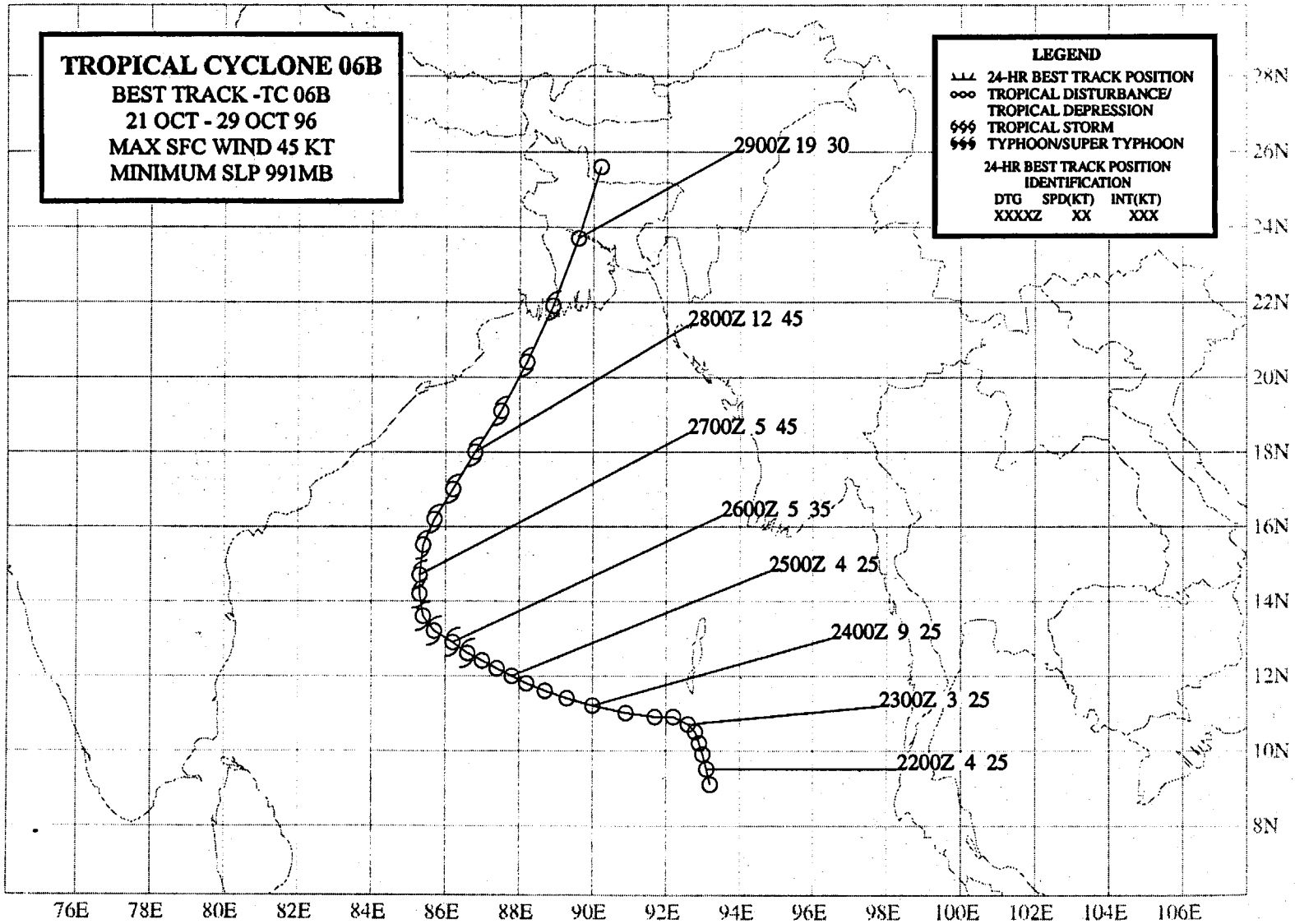
BEST TRACK -TC 06B
21 OCT - 29 OCT 96
MAX SFC WIND 45 KT
MINIMUM SLP 991MB

LEGEND

- 24-HR BEST TRACK POSITION
- TROPICAL DISTURBANCE/
TROPICAL DEPRESSION
- ⊖ TROPICAL STORM
- ⊖⊖ TYPHOON/SUPER TYPHOON

24-HR BEST TRACK POSITION
IDENTIFICATION

DTG	SPD(KT)	INT(KT)
XXXXZ	XX	XXX



TROPICAL CYCLONE 06B

The area of poorly organized convection that became Tropical Cyclone 06B (TC 06B) was detected south of the Andaman Islands and first mentioned on the 211800Z October Significant Tropical Weather Advisory. The tropical disturbance was under the influence of strong upper-level easterly wind shear, which resulted in the low-level circulation center being exposed to the east of the deep convection. JTWC issued the first of three TCFAs at 220930Z as the shear appeared to weaken. The anticipated development was delayed, however, and the TCFA was reissued at 230730Z, and again at 240600Z. The convection did finally become better organized and JTWC issued the first warning valid at 250600Z. After recurvature on 27 October, the cyclone accelerated to the northeast. TC 06B made landfall on the heavily populated delta region of West Bengal India near the Bangladesh border at 281800Z (See Figure 3-06B-1). The final warning was issued, valid at 290000Z, as the filling cyclone moved further inland. Heavy rains associated with TC 06B caused flooding, which immobilized much of metropolitan Calcutta. A 9-foot (3-m) storm surge inundated low lying coastal areas in Bangladesh where reports indicated that 14 people were killed, over 2000 people were injured, and 100 fishermen were missing.

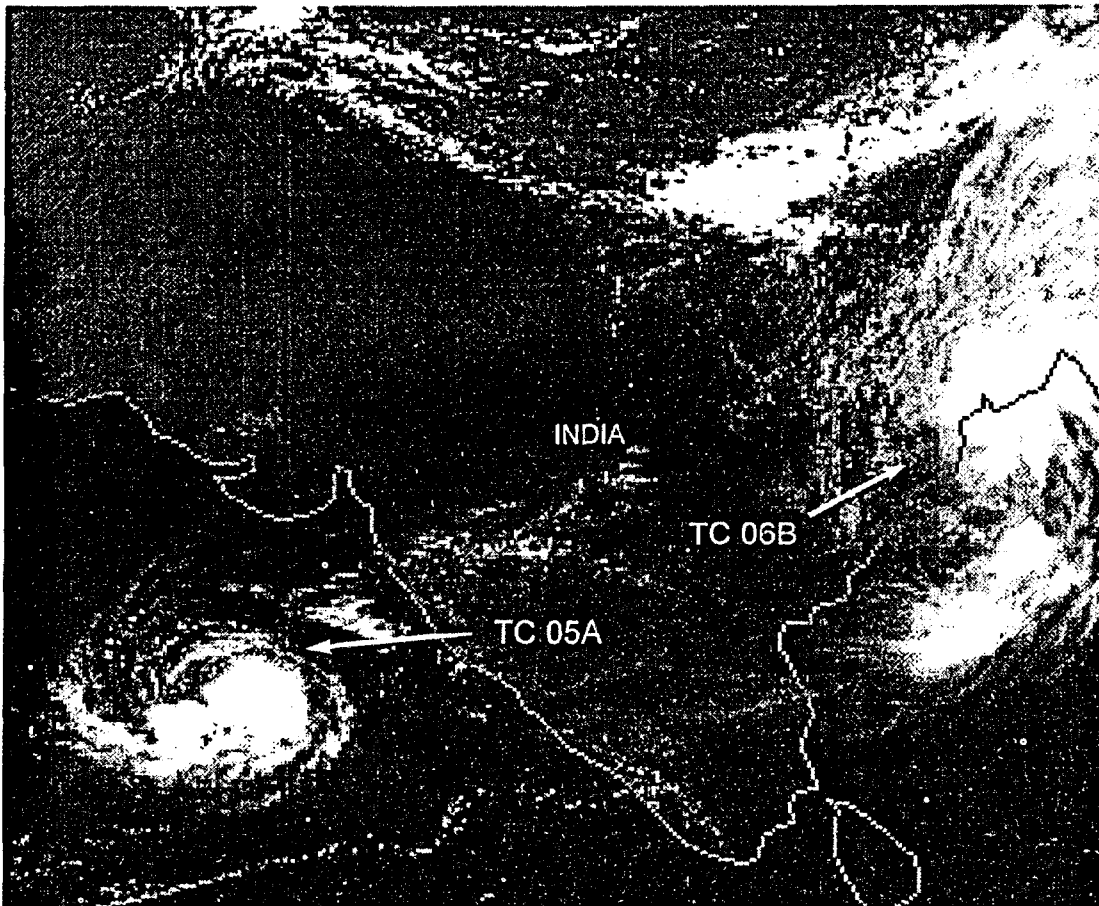


Figure 3-06B-1 TC 06B (upper right) just after making landfall. TC 05A is seen to the west of the India subcontinent (280350Z October visible DMSP imagery).

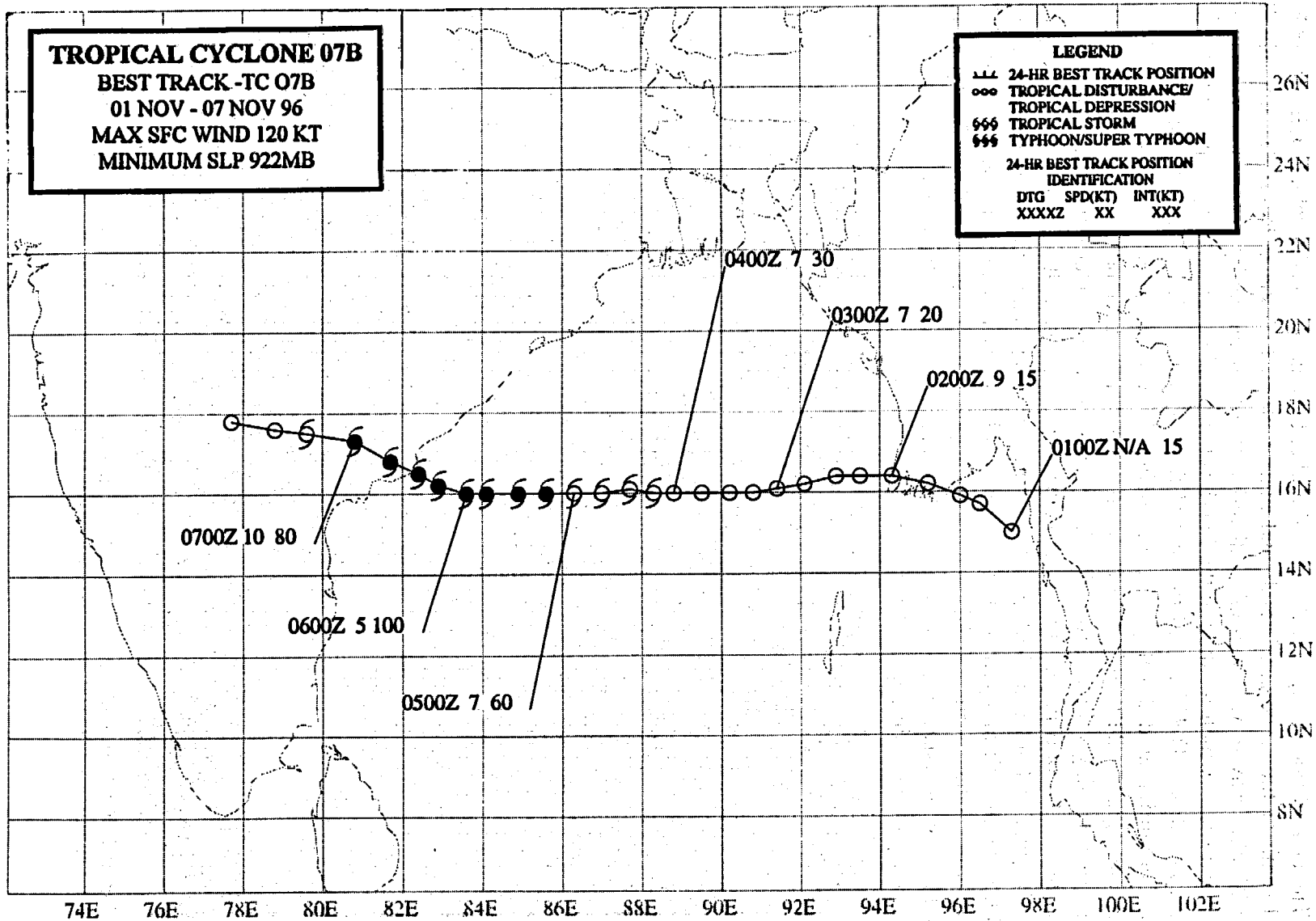
TROPICAL CYCLONE 07B

BEST TRACK - TC 07B
01 NOV - 07 NOV 96
MAX SFC WIND 120 KT
MINIMUM SLP 922MB

LEGEND

- 24-HR BEST TRACK POSITION
- ooo TROPICAL DISTURBANCE/
TROPICAL DEPRESSION
- 666 TROPICAL STORM
- 666 TYPHOON/SUPER TYPHOON

24-HR BEST TRACK POSITION
IDENTIFICATION
DTG SPD(KT) INT(KT)
XXXXZ XX XXX



TROPICAL CYCLONE 07B

As the remnants of TD 43W dissipated over the rugged Malay peninsula, new convection was noted in the Andaman Sea and first mentioned on the 011800Z November Significant Tropical Weather Advisory. Improved convective organization led to the issuance of a TCFA at 030730Z, followed by the initial warning on TC 07B, valid at 031200Z. The system tracked steadily westward under the influence of deep easterly steering flow. Intensification was more rapid than the normal one-T-number per day, and continued until TC 07B peaked at 120 kt (62 m/sec) just before landfall (Figure 3-07B-1) at 061200Z. The development of the wind field associated with this cyclone was evident in the microwave imagery provided by FNMOC on the MISTIC system. After crossing the coast near Kakinada (240 nm (445 km) north-northeast of Madras) at 061300Z, TC 07B weakened as it continued inland. JTWC issued the final warning valid at 070600Z. The cyclone's impact in the coastal areas was significant, and more than 1,000 deaths were attributed to TC 07B. Of these fatalities, 42 passengers were lost when a ferry sank during the storm. More than 1,000 fisherman were reported missing at sea. TC 07B was also responsible for widespread flooding, the destruction of at least 10,000 homes, and the loss of hundreds of thousands of acres of rice crop. More than 250 villages were reported under water and many coastal communities were inundated by 12-foot-high waves. Worst hit was the coastal city of Kakinada where the cyclone dumped 8.8 inches (226 mm) of rain.

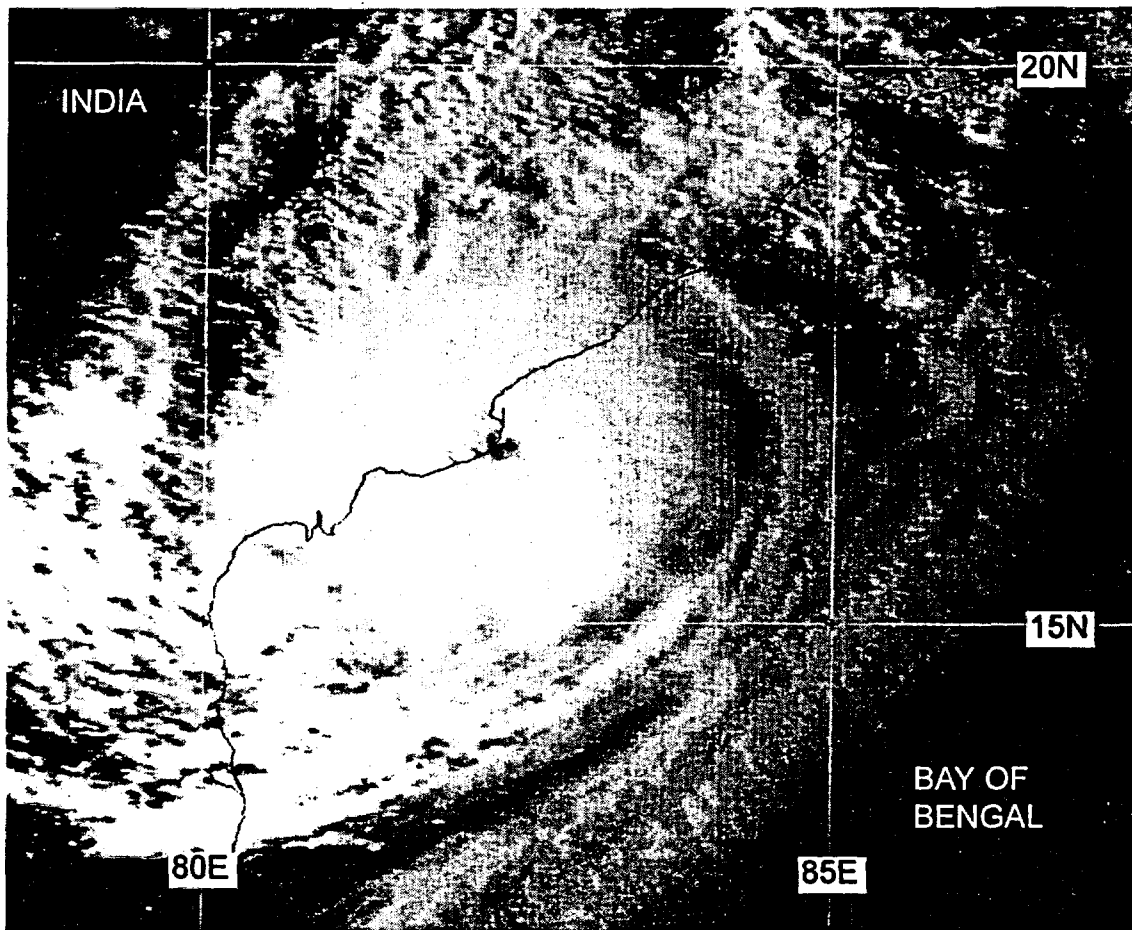


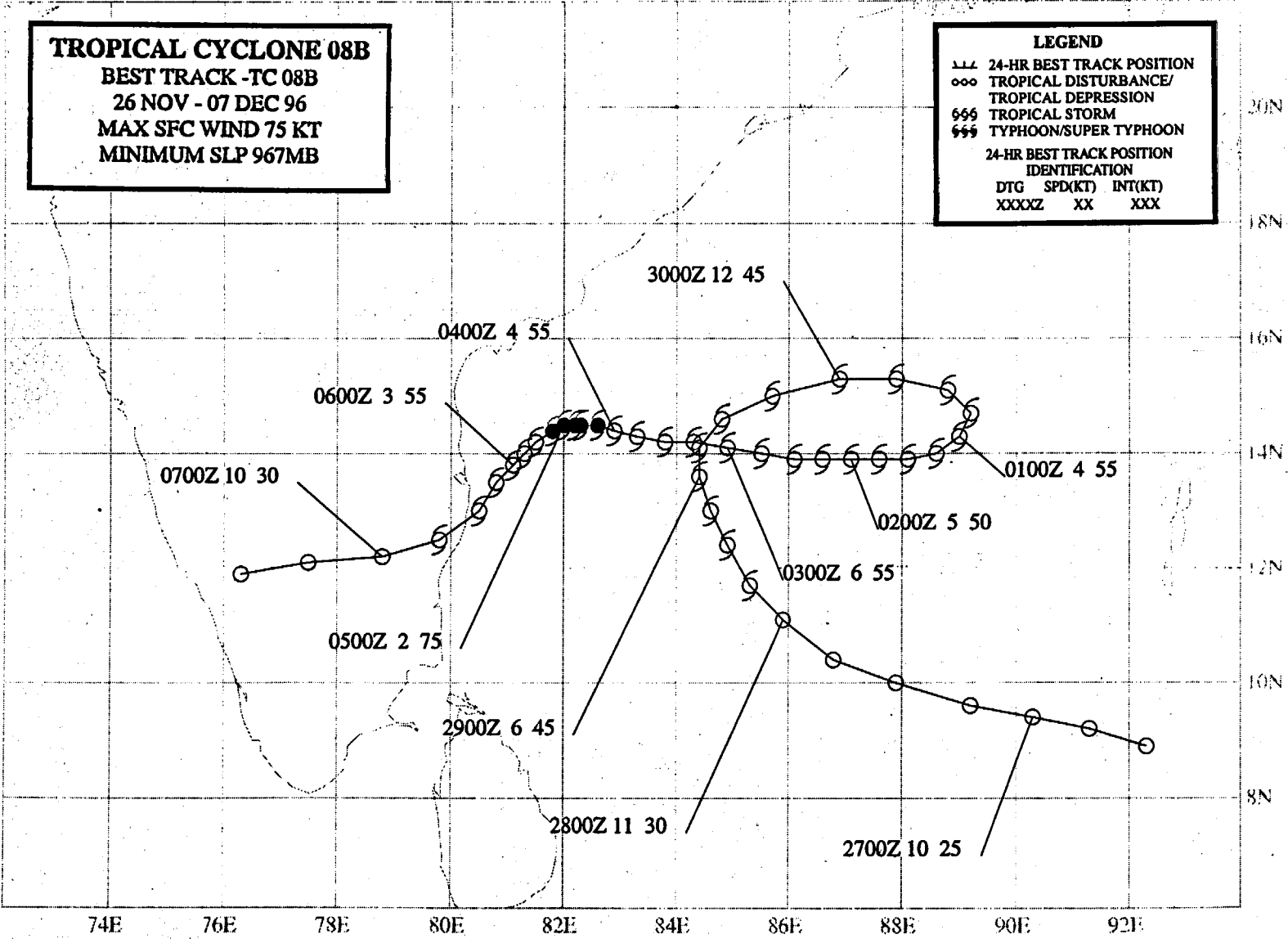
Figure 3-07B-1 TC 07B at peak intensity of 120 kt (62 m/sec)(061024Z November visible GMS imagery).

TROPICAL CYCLONE 08B
BEST TRACK - TC 08B
26 NOV - 07 DEC 96
MAX SFC WIND 75 KT
MINIMUM SLP 967MB

LEGEND

--- 24-HR BEST TRACK POSITION
 ooo TROPICAL DISTURBANCE/
 TROPICAL DEPRESSION
 666 TROPICAL STORM
 666 TYPHOON/SUPER TYPHOON

24-HR BEST TRACK POSITION
 IDENTIFICATION
 DTG SPD(KT) INT(KT)
 XXXXZ XX XXX



236

TROPICAL CYCLONE 08B

I. HIGHLIGHTS

Tropical Cyclone 08B (TC 08B) was unusual for three reasons: 8 days in warning, a 4-day loop, and erratic southwestward movement along the coast of India. Hundreds of lives were probably spared because TC 08B weakened before making landfall.

II. TRACK AND INTENSITY

TC 08B formed in the monsoon trough just south of the Andaman Islands. The persistence of an area of poorly organized convection over a well developed low-level circulation resulted in JTWC's first mention of the tropical disturbance on the 261800Z November Significant Tropical Weather Advisory. As the system slowly developed, JTWC issued the first TCFA at 270130Z. However, a second TCFA was required at 272230Z to reposition the alert area to the west. An increase in overall organization and intensity prompted JTWC to issue the first warning valid at 280600Z. Although TC 08B's initial track was to the west-northwest, the cyclone started a large clockwise loop on 29 November that took four days to complete. Early on 04 December, the system slowed and peaked at 75 kt (39 m/sec). As the cyclone approached the eastern periphery of the blocking high in the low to middle levels over India, strong 50-kt (26 m/sec) upper-level southeasterly winds appeared (Figure 3-08B-1). These features resulted in a track change to the southwest, and increased vertical wind shear weakened the cyclone. By the end of 05 December, the upper and lower levels of the cyclone had become decoupled. The convection was displaced to the northwest and the LLCC moved to the southwest. At 061500Z, TC 08B moved ashore near Pondicherry, about 60 nm (110 KM) south of Madras. The final warning was issued, valid at 061800Z, as the system dissipated over southwestern India.

III. DISCUSSION

a. *Longevity*

An investigation of Bay of Bengal cyclones since 1972 indicates that no other looping tropical cyclone has taken four days to complete its looping motion. Also, the 8-day period of warning is considered very long, as the average period in warning for Bay of Bengal cyclones is less than four days. Longer warning periods have been noted for cyclones that form in the Bay and move westward in to the Arabian Sea before dissipating.

b. *NOGAPS performance*

With regard to TC 08B's change of track to the southwest near the coast of India, NOGAPS correctly anticipated the movement as early as 02 December — three days before it actually occurred.

IV. IMPACT

Because TC 08B weakened over water before making landfall, the death toll was very low, 7. There were no reports of significant damage.

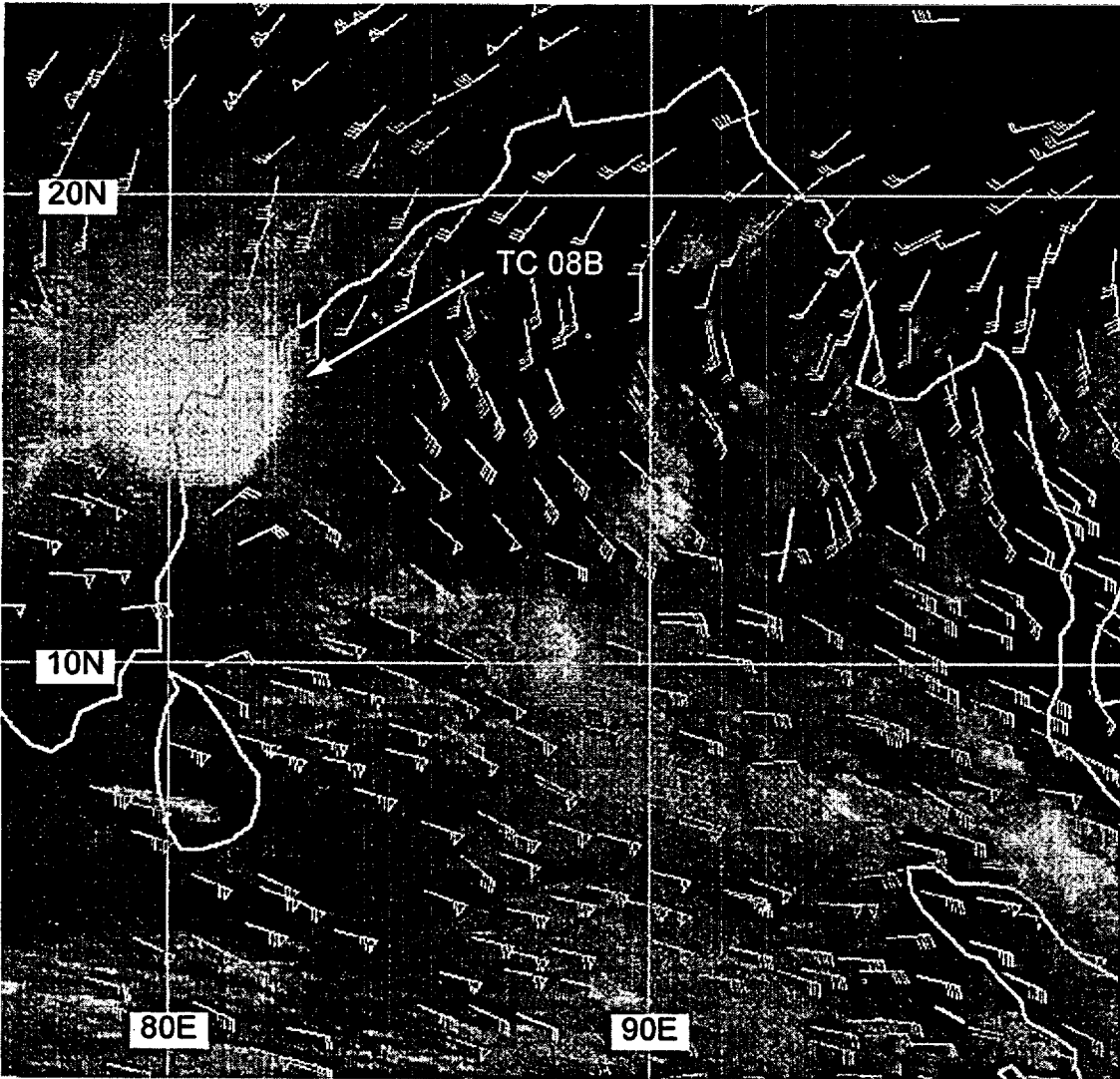


Figure 3-08B-1 Water vapor imagery and upper-level cloud-track winds reveal strong southeasterly winds impinging upon TC 08B (041132Z December water vapor GMS imagery).